Classical and Quantum Aspects of Near-Horizon Physics

Surojit Dalui

A thesis
submitted for the degree of

Doctor of Philosophy

Supervisor

Dr. Bibhas Ranjan Majhi

Department of Physics
Indian Institute of Technology Guwahati
Guwahati - 781039, Assam, India

Classical and Quantum Aspects of Near-Horizon Physics

A thesis submitted by

SUROJIT DALUI

SUPERVISOR: **DR. BIBHAS RANJAN MAJHI**

Department of Physics
INDIAN INSTITUTE OF TECHNOLOGY GUWAHATI

A thesis submitted to Indian Institute of Technology Guwahati in accordance with the requirements of the degree of DOCTOR OF PHILOSOPHY in the Department of Physics.

JANUARY 10, 2023

To my parents - *for everything.*
To my sister - *for being the pillar of my life.*
To my teachers - *for helping me to reach this far.*
To my friends - *for believing in me.*

STATEMENT

Surojit Dalui
Roll No. 176121013
Department of Physics
IIT Guwahati
Guwahati, India

I hereby declare that works presented in the thesis entitled "**Classical and Quantum Aspects of Near-Horizon Physics**" has been carried out by me under the supervision of Dr. Bibhas Ranjan Majhi at the Department of Physics, Indian Institute of Technology Guwahati, India. The thesis has not been submitted anywhere else for any degree. Works presented in the thesis are all my own unless referenced to the contrary in the thesis.

Surojit Dalui

Date: January 10, 2023

DISCLAIMER

The bibliography included in this thesis is, by no means complete but contains the ones which are consulted thoroughly by me. I apologize for inadvertently missing out some of the research papers, review articles and other scientific documents pertaining to the focus of this thesis which should also have been cited.

– Surojit Dalui

CERTIFICATE

Dr. Bibhas Ranjan Majhi
Associate Professor
Department of Physics
Indian Institute of Technology Guwahati
Guwahati, India
email:bibhas.majhi@iitg.ac.in

It is certified that the work contained in the thesis entitled **"Classical and Quantum Aspects of Near-Horizon Physics"** by Mr. Surojit Dalui (Roll No - 176121013), a Ph.D. student in the Department of Physics, Indian Institute of Technology Guwahati is carried out under my supervision and has not been submitted elsewhere for the award of any other degree.

Dr. Bibhas Ranjan Majhi

Date: January 10, 2023

LIST OF PUBLICATIONS

1⋆. **Presence of horizon makes particle motion chaotic**
Surojit Dalui, Bibhas Ranjan Majhi and Pankaj Mishra
Phys. Lett. B ***788****, 486 (2019)* [arXiv:1803.06527 [gr-qc]].

2. **How robust is the indistinguishability between quantum fluctuation seen from noninertial frame and real thermal bath**
Chandramouli Chowdhury, Susmita Das, **Surojit Dalui** and Bibhas Ranjan Majhi
Phys. Rev. D ***99****, no.4, 045021 (2019)* [arXiv:1902.06900 [gr-qc]].

3. **Conformal Vacuum and Fluctuation-Dissipation in de-Sitter Universe and Black Hole Spacetimes**
Ashmita Das, **Surojit Dalui**, Chandramouli Chowdhury and Bibhas Ranjan Majhi
Phys. Rev. D ***100****, no.8, 085002 (2019)* [arXiv:1902.03735 [gr-qc]].

4⋆. **Role of acceleration in inducing chaotic fluctuations in particle dynamics**
Surojit Dalui, Bibhas Ranjan Majhi and Pankaj Mishra
Int. J. Mod. Phys. A ***35****, no.18, 2050081 (2020)* [arXiv:1904.11760 [gr-qc]].

5⋆. **Horizon induces instability locally and creates quantum thermality**
Surojit Dalui, Bibhas Ranjan Majhi and Pankaj Mishra
Phys. Rev. D ***102****, no.4, 044006 (2020)* [arXiv:1910.07989 [gr-qc]].

6⋆. **Near horizon local instability and quantum thermality**
Surojit Dalui and Bibhas Ranjan Majhi
Phys. Rev. D ***102*** *no.12, 124047 (2020)* [arXiv:2007.14312 [gr-qc]].

7⋆. **Horizon thermalization of Kerr black hole through local instability**
Surojit Dalui and Bibhas Ranjan Majhi
Phys. Lett. B ***826*** *(2022), 136899* [arXiv:2103.11613 [gr-qc]].

8⋆. **Thermal nature of a generic null surface**
Surojit Dalui, Bibhas Ranjan Majhi and Thanu Padmanabhan
Phys. Rev. D ***104*** *(2021) no.12, 124080* [arXiv:2110.12665 [gr-qc]].

9. **GUP Effects on Chaotic Motion Near Schwarzschild Black Hole Horizon**
Avijit Bera, **Surojit Dalui**, Subir Ghosh and Elias C. Vagenas
Phys. Lett. B ***829*** *(2022), 137033* [arXiv:2109.00330 [gr-qc]].

Note: ⋆ marked publications are included in the thesis.

WORKS PRESENTED IN THE CONFERENCES

1. Presented a poster titled **"Presence of horizon makes particle motion chaotic"**, at *30th meeting of Indian Association for General Relativity and Gravitation (IAGRG)*, at BITS Pilani Hyderabad campus during $3rd - 5th$ January, 2019.

2. Presented a poster titled **"Presence of horizon makes particle motion chaotic"**, at *YITP Asian-Pacific Winter School and Workshop on Gravitation and Cosmology*, at YITP, Kyoto, Japan during $11th - 15th$ February, 2019.

3. Presented a poster titled **"Horizon induces instability and creates quantum thermality"**, at *IISER Mohali* during $10th - 13th$ December, 2019.

4. Presented a poster titled **"Near horizon local Hamiltonian that explains the thermality of horizon"**, at *31st meeting of Indian Association for General Relativity and Gravitation (IAGRG)* through online mode during $19th - 20th$ December, 2020.

5. Presented a poster titled **"A tale of two phenomena: Instability and Thermality, in the near horizon region"**, at the international conference named "Regular black holes in quantum gravity and beyond: from theory to shadow observations" through online mode during $18th - 21st$ October, 2021.

6. Delivered a talk, titled **"A tale of two phenomena: Instability and Thermality, in the near horizon region"**, organized by the Department of Mathematics, BITS Pilani, Hyderabad campus during $26th - 28th$ October, 2021.

7. Delivered a talk, titled **"A tale of two phenomena: Instability and Thermality, in the near horizon region"**, at *32nd meeting of Indian Association for General Relativity and Gravitation (IAGRG)* organized by the Department of Physics, Indian Institute of Science and Research (IISER) Kolkata during $19th - 21st$ December, 2022.

ACKNOWLEDGEMENTS

"But it's not the destination that matters in the end. It's the journey along the way. And I have had one amazing journey."
– Rachel A. Marks.

A doctoral thesis is often described as a solitary endeavour; however, reaching the verge of my PhD life, when I look back, the extensive list that follows definitely proves the opposite. I feel grateful towards several people, who stayed with me over this wonderful journey.

First and foremost, I express my deepest gratitude to the most important person without whom this would not have been possible at all, my supervisor Dr. Bibhas Ranjan Majhi, for all the guidance and support throughout my PhD journey. He is one of the most intriguing person I have ever encountered in my life who had more insight about me than myself. He knows the art of bringing out the best in a student. I can still clearly recall feeling lost and bewildered, and I owe him a great deal for helping me realise my actual potential. His expertise, commitment to his work, and example of a well-balanced life as a researcher have always inspired me. Most importantly, he gave me every freedom to span my research interest, explore challenging things and work as an individual with new collaborations. From him, I take many gifts, parts of him that I will carry with me for the years to come. Examples of these are his appreciation for detail and precision, his passion for science, his genuine concern for his students and his endurance in times of adversity. I consider myself a wiser man than when I started, and that is a blessing that few can grant.

I am grateful to my doctoral committee members - Dr. Debaprasad Maity, Dr. Sayan Chakrabarti and Dr. Pankaj Kumar Mishra for their valuable suggestions during the yearly assessments of my research work. I have learned a lot from these two pioneers, Debu Sir and Sayan Sir, during the discussions in the gravity journal club. However, I would like to convey a special thanks to Pankaj Sir for his endurance in helping me to develop the numerical codes during the initial years of my PhD when I was an amateur

in coding. I can recall the times writing those codes with him in his office at odd hours, jumping for delight every time we got the correct solution. I am truly grateful to these people as they were intended to support me whenever required.

I would like to thank the instructors who taught us during the PhD coursework. I appreciate the excellent teaching provided by Prof. Padma K Padmanabhan, Prof. Pravat Kumar Giri, Prof. Girish Sampath Setlur, Dr. Meduri C Kumar and Dr. Udit Raha.

The past and current heads of the physics department, Prof. P Poulose, Prof. Subhradip Ghosh, and Prof. Perumal Alagarsamy, thank you for your support. I want to express my gratitude to all of the technical support personnel, academic, and non-academic members of the department who assisted me in different ways throughout my research period.

I would like to thank my other collaborators and co-authors. Thanks to Dr. Pankaj Kumar Mishra again. I gratefully acknowledge the contributions of Dr. Ashmita Das, Chandramouli Chowdhury, Sushmita Das, Avijit Bera, Prof. Subir Ghosh, Prof. Elias C. Vagenas and the late Prof. Thanu Padmanabhan. It was because of them that I got the opportunity to work on various problems and in the process acquired a great extent of knowledge and experience.

I am specially thankful to my former and present group members cum friends Krishnakanta Da, Mousumi Di, Subhajit Da, Sumit, Dipankar, Subhankar, Gopal Da and Soumya Da for our stimulating intellectual exchanges (including our arguments on philosophy, society, and politics!).

Also, during my PhD, I have learned a great deal of things from Charu sir, Sovan sir, Soumitra sir and Subhaditya sir. Special thanks to Charu sir, for giving me the opportunity to perform the teaching assistantship under his supervision, where I learned the true meaning of excellent teaching. I also recall our intriguing conversation about music during our violin lessons, when we exchanged many ideas.

For being a part of my PhD journey, I would like to thank my fellow batch mates and dear friends Sanket, Riajul, Arghyajit, Samit, Pronoy, Tathagata, Nasim, Subrata, Devender, Devabrat, Madhurima, Ipsita, Roni, and Shilpi. Meeting these amazing people has been a true pleasure. I acknowledge every bit of your help during this voyage.

I was blessed with some of the great seniors on this campus. I am extremely grateful to Rakesh Da, Rajesh Da, Aritra Da, Sayan Da, Anirban Da, Sayandeep Da, Subhajit Da, Ambarish Da, Soumya Da, Bichitra Da, Pulak Da, Abhisek Da, Sujit Da, Kallol Da, Ramiz Da, Basabendu Da and Krishnanjan Da with whom I exchanged many valuable thoughts on physics and non-physics topics. It has been a real pleasure to meet these wonderful people, and I am really thankful to every one of you for being a part of this

journey. In the days ahead in my life, I'll treasure every piece of advice you give me.

I would like to recognize some of my dear juniors, Swarup, Mrinal, Sourav, Sahabub, Golam, Mandira, Sudeshna, Partha, Roson, Monu, Samprit, Soumen, Gargi, Shantanu, Seshadri, Lipika, Debabrata, Chinmoy, Dipankar, Avishek, Suresh and Niloy for their immense support, respect and love. I am also very fortunate to have some special juniors cum brothers, Kushal and Atanu, who have supported me no matter what during the darkest hours of my life.

I would like to convey my special thanks to my football teammates Sumit Da (captain!), Karuna Da, Roson, Subrata, Sahabub, Sourav, Arghyajit, Bibhas Sir and many more. I still recall the day we lost the final match at PFL, but we won many more things on that memorable day!

My life during this voyage has been made cherishable and interesting by some colourful and memorable hostel mates to whom I would like to express my heartiest feelings. I am indebted to Sanket, Anjishnu, Anindya, Aritra, Arin, Santanu, Alik, Jyotirmoy, Avirup and Argha for making my hostel feel like home. I recall the extremely difficult circumstances we faced while being imprisoned in our rooms during the global pandemic. However, I was lucky enough to have these people around me who taught me that friendship has the strength to overcome any challenging situation.

During the times of the global pandemic, we have witnessed numerous difficult scenarios. As a result, I must thank everyone who is battling COVID-19. We shall overcome this together. On this note, I would like to thank Kakati Da and Tarzaan Da for delivering essential supplies during the days of complete lockdown amidst global pandemic. Thanks to both of you.

I would want to express my gratitude to a few of my close friends, including Rahul, Sudipta, Ayaz, Bidyut, Abinash, Avdhesh, Satyendra, Pravi, and Vandana, who I have known since I started my master's programme. I am fortunate to still have these folks in my life who are willing to listen to my continual nagging.

I would like to thank some special friends from my college days to this date who are very close to my heart, including Rajarshi, Pradip, Arindam, Sovon, Prasun, Jyotirmoy and Arnab.

The list will be incomplete if I don't mention my childhood friends, the other two 'Musketeers' of our group, Avik and Niladri. We have grown up together, and they have been constant friends throughout my life.

I owe my deepest gratitude to my sister Surovi Dalui who has been the pillar throughout my entire life. Her continual care, encouragement and support have helped me to

reach this far. I appreciate your compassion and consider myself extremely lucky to have you in my life.

Finally, the persons without whom none of this would have any meaning, are my parents. I would like to convey my sincere respect to Satyajit Dalui and Sabita Dalui for their sacrifices, unconditional love for me as well as their unwavering support throughout my whole life. Life is meaningless without my father's poor jokes and my mother's cooking!

On an ending note, I just want to say one thing, *I am indebted to the IITG campus, to Guwahati, to Assam, to North-East, for everything, for every single thing.*

– Surojit

FEAR

"It is said that before entering the sea
a river trembles with fear.

She looks back at the path she has traveled,
from the peaks of the mountains,
the long winding road crossing forests and villages.

And in front of her,
she sees an ocean so vast,
that to enter
there seems nothing more than to disappear forever.

But there is no other way.
The river can not go back.

Nobody can go back.
To go back is impossible in existance.

The river needs to take the risk
of entering the ocean
because only then will fear disappear,
because that's where the river will know
it's not about disappearing into the ocean,
but of becoming the ocean."

– *Khalil Gibran*

Abstract

In recent years, researchers' attention has been sparked by the thermal and geometrical characteristics of black hole horizons as well as their intimate relationship with the dynamics of particle motion surrounding them. Because of this, research into near-horizon physics has received a lot of interest recently. Over time, systems have begun to exhibit some intriguing behaviours whenever they come under the dominance of this mysterious one-way membrane, according to scientists. One of these traits is the appearance of *chaotic dynamics* in a system in the vicinity of the horizon. It has been found that the influence of horizon on a system can introduce chaos within the system. Research on chaos in the presence of horizons has been ongoing for a long time, but the reason for this special feature of the horizon is still not apparent. Similarly, it is crucial to take into account in this context why all horizons (whether static or stationary) express the same phenomenological quality.

Contrarily, the idea of black hole thermodynamics has been around for a while and is based on an analogy between the laws governing black holes and those governing typical thermodynamical systems. However, no one has ever really addressed why these thermodynamical quantities are connected to the horizon. In actuality, we still don't fully understand the underlying physical process that generates temperature in the horizon system. For instance, the kinetic theory of gases explains that the temperature of a gas contained in a cylinder is caused by the kinetic energy of the gas particles. However, it is unknown at this time whether a similar mechanism will operate in the scenario of a horizon. As a result, it is also unknown which microscopic degrees of freedom (MDOF) are in charge of such a property. Despite numerous tries, there are currently no conclusive explanations.

Therefore, in the present thesis, for the first time, we have tried to provide a unified reason for both the characteristics of horizon, i.e. the reason for chaotic influence on a system and the underlying possible reason for the thermal behaviour of it and have tried to find out if there is any connection between them. We begin the thesis with a thorough explanation of the characteristics of classical black holes. After the introductory part we introduce the first part where we present some classical results for a system that is located in the vicinity region of an event horizon. Interestingly, we find that the system begins to exhibit chaotic behaviour as soon as it is exposed to the horizon's influence. In the second part we try to figure out why a system in the near horizon area behaves in such a chaotic manner. In the third part we study the quantum consequences of the results we obtained in the classical scale in the near horizon region. We find

that the near-horizon instability may be a reason for the chaotic situation and also the thermal behaviour of the horizon. In the fourth part we apply the same formalism to more generalised backgrounds in order to better grasp the core reason for thermality in those circumstances. Finally, the thesis is concluded with a brief discussion of our conclusions and potential future applications.

Table of Contents

List of Figures

Figure **Page**

CHAPTER 1

INTRODUCTION

It was the year 1905, and it was Einstein's enchanted year. He authored three seminal publications in that year on light quanta [1], Brownian motion [2], and the foundations of the Special Theory of Relativity [3]. Each one alters one's perspective on how to describe a physical phenomena. Einstein's masterwork, on the other hand, was yet to be discovered. Following his work on the Special Theory of Relativity, Einstein continued to work on gravity, pondering how to formulate it in a relativistically invariant manner. It took Einstein around ten years to achieve the peak, and after many tries and errors, he presented the world with the *General Theory of Relativity* (GR) in 1915 [4]. It is widely regarded as one of the greatest intellectual achievements of all time, a stunning theory derived entirely from pure thinking and capable of describing every element of gravitational physics ever seen. This theory turned one hundred years old in 2015, and it is currently regarded as one of the most amazing physics ideas ever developed in human history. Einstein's inherent idea was *the (local) equivalence of gravitation and inertia* which is widely known as the *Einstein Equivalence Principle*. It led him to the conclusion that, unlike the other natural forces, gravity is best characterised and understood as the manifestation of *geometry and curvature of space-time*. This profound realisation tilted the world of theoretical physics and has had an earnest impact on the physics community still today.

1.1 It Starts With One Thing: Gravity

"Why do we fall? – Because of Gravity!"

Gravity is one of the four fundamental forces in nature. It is the gravity that shapes the large scale structure of the universe, but strangely, it is the weakest among the four categories of forces. People have recognised Newton's theory of gravitation as a viable theory to describe the gravitational force for more than two centuries since it successfully describes the motion of celestial objects. However, Newton's theory had significant limitations, such as failing to explain Mercury's perihelion precession and failing to explain why gravity enters the picture between two objects that are far apart in the absence of any form of medium. However, until Einstein's theory of general relativity (GR) in 1915, it was widely considered as the most acceptable theory for explaining the motion of objects under the effect of gravity. This theory, based on *Riemannian geometry*, was not only staggering with respect to that time's perspective but also remained to be equally fascinating in recent times. It describes gravity from the perspective of geometry itself. Time also has a coordinate status, in this theory, and thus the notion of the space-time was coined. According to this theory, the curvature of the space-time is dependent on the matter content of the space-time. This connection is evident from the Einstein's famous field equations, in natural units $c = 1 = \hbar$ which is

$$G_{\mu\nu} \equiv R_{\mu\nu} - \frac{1}{2} R g_{\mu\nu} = 8\pi G T_{\mu\nu}, \tag{1.1}$$

where, $T_{\mu\nu}$ denotes the energy-momentum tensor for matter, $g_{\mu\nu}$ denotes the metric tensor and $R_{\mu\nu}$ is the Ricci tensor obtained from the Riemann curvature tensor, both of which can be obtained from the metric tensor. Apart from repeating Newtonian gravity's results, general relativity's aesthetic appeal resides in its bold predictions - *gravitational red-shift, the bending of light, gravitational lensing, modification of the precession angle of orbits and so on* [5–13]. General relativity gave an explanation for the perihilion change of planet Mercury's orbit in the same year, 1915, which was beyond the realm of Newtonian gravity and is considered as general relativity's first success. Soon after, Arthur Eddington and Frank Dyson carried out a renowned experiment during a solar eclipse in 1919 [9]. Their observations of the deflection of sunlight during the solar eclipse were consistent with the general theory of relativity, which made this theory famous overnight. This incident paved the path to the realisation of the enormous prospect of this newfound understandings. The recent discovery of gravitational waves from black

hole mergers [14, 15] is another noteworthy accomplishment of this theory which came after a century of the advent of the theory.

On the other hand, there is quantum field theory (QFT) [16–18] which is the other pillar of modern physics besides GR. Quantum field theory is a topic which combines the concepts of classical field theory, special theory of relativity and quantum mechanics to explain the physical dynamics of subatomic particles. In quantum field theory, particles are described by the underlying field excitations. While this theory is very successful in describing a lot of phenomena, it is plagued with divergences coming from the perturbative calculations when an interaction is included in the system. In order to tackle these divergences, different renormalisation techniques were developed later on. One of the breakthroughs in quantum field theory appeared in 1970 [19], through the development of gauge theory, when it was shown that all the standard model particles and forces could be incorporated into a single field theory. However, the most perplexing quest of amalgamation of the general theory of relativity with quantum field theory remains unsettled, which leads to emerging a new topic, known as *quantum gravity*.

One of the most enthralling problems of modern physics is the venture to get a complete theory of quantum gravity [20]. The exact stumbling block lies in providing a quantum mechanical description of gravity, which is itself a classical theory, to begin with as described by Einstein's general theory of relativity [21–23]. The hunt for a proper quantum theory of gravity also emanates from the urge to understand the high energy characteristics of quantum fields, which is again connected to the short distance constitution of the spacetime. It is already known that the other three fundamental forces of nature, namely electromagnetism, weak and strong force have their successful explanations in quantum field theory but the inclusion of gravity in the single field theory has remained a challenge till now. In this regard, *string theory* [24–26] has emerged as one of the most popular candidates to include gravity in this league. For the past few years string theory has provided a significant development in this direction. On the other hand, *loop quantum gravity* (LQG) [27–34] which is basically a background independent quantum theory has joined in this context. The prime focus of loop quantum gravity is to provide a quantisation procedure based on Einstein's geometric formulation rather than considering gravity as a force. It is noteworthy that in both these theories, the concept of minimum length scale has been introduced [35, 36]. It should be mentioned that other than these non-perturbative approaches there are also very successful perturbative approaches in the form of *effective field theories* [37, 38]. These perturbative approaches comprise of the quantum field theory in curved space-times [39–43], also known as

the *semi-classical quantum gravity*. In these semi-classical approaches, the quantum fields are considered to propagate in a classical background geometry. This manifests an extension of the flat space-time theory to the curved space-time, that can be treated locally as flat space-time. Some of the celebrated predictions of quantum field theory in curved space-time are particle creation from black hole space-times [43–67] and in time-dependent space-times. The remarkable outcome that using a semi-classical approach, back holes can radiate particles with a thermal spectrum is known as Hawking effect [68]. We will discuss more about Hawking effect in the later part of this thesis but before that let us take a tour to see how gravity behaves in some special space-time regions.

1.2 Black Hole: The Invisible Monster

"Black holes are where God is divided by zero."– Steven Wright

Since the arrival of the general theory of relativity and even with its complicated non-linear field equation, several attempts have been made to understand the closed-form solution of Einstein's field equation. In the year 1916, after a few months after Einstein's discovery, Karl Schwarzschild [69] presented the world with a non-trivial exact solution of Einstein's vacuum field equations for a point mass, known as the Schwarzschild solution. Around the same time as Schwarzschild, Johannes Droste [70] arrived at the same solution independently. In the same year, Hans Reissner [71] generalized the Schwarzschild solution and found that these are the solutions of Einstein-Maxwell equations having electrically charged objects. Later, Gunnar Nordatröm [72] independently arrived at the same solution, which is now known as the famous Reissner-Nordström metric. After that, many scientists contributed to the solution of this problem (Eddington 1924 [73]; Lemaitre 1933 [74]; Einstein and Rosen 1935 [75]) before the final solution was acquired (Synge 1950 [76]; Finkelstein 1958 [77]; Fronsdal 1959 [78]; Kruskal 1960 [79]; Szekeres 1960 [80]; Novikov 1963 [81], 1964 [82]). The major lesson learned during this study is that the space-time manifold with the metric representing the gravitational field may have global features that differ from the Minkowski space-time. Those global features lead to the peculiar singularities of Einstein equation which are known as *"black holes"* (BH). A fascinating space-time region where gravity is so strong that nothing-not even the light-can escape. We shall talk more about black holes and its features in the later part but before that let us wrap off the history first. In the scenario of a black hole, such global features are connected with its topology and the

causal structure. Though a solution for a non-rotating black hole has been known for quite a long time, in 1963, Roy Kerr [83] discovered a solution of the Einstein equation, describing the gravitational field of a stationary rotating black hole. A principle feature of the Kerr solution is the *dragging into rotation effect*, induced by the rotation of the black hole. Since its theoretical prediction to the present day detection [84–87] of over a hundred years of profuse journey, those solutions fascinate physicists because of their unparalleled curiousness, which are yet to be unveiled. The existence of essential singularities is one such exotic property which are still difficult to apprehend completely. However, gradually physicists acknowledge the fact that GR is still a bit away for being the complete descriptive theory of gravity. In 1958, David Finkelstein identified that the very existence of such singularity comes with another exotic character; constitute with a hypothetical surface called *horizon*, from which nothing can come out, even the light. John Archibald Wheeler named these peculiar object as *'black hole'* and the research on black holes became one of the most active fields of research till now. The recent discoveries of gravitational waves [88–91] from the binary black holes merger in 2015 and the first-ever image of black hole produced by *Event Horizon Telescope* collaboration [84] in 2019, have ended the long-standing debate over the existence of black holes in reality.

Now, keeping aside the history, let us talk about these singularities, i.e. black holes, for a moment. A crucial distinction of GR from Newtonian gravity is that the *"action at a distance"* is replaced by a built-in causality structure in Einstein's theory. The initial value formulation of GR splits the *ten Einstein equations* into *six evolution equations* and *four constraint equations* [21]. The first four equations are made up of a set of hyperbolic quasilinear equations that evolve the initial conditions over time. On a Cauchy space-like surface, the latter equations constraint the appropriate initial data. As a result, the causality structure resembles the light-cone structure of special relativity locally. However, because space-time is dynamical, the Cauchy development of smooth geometry and matter trapped on a space-like surface may lead to a singularity as a result of some catastrophic event, such as the gravitational collapse of a massive body or a high-energy collision. For timelike or null geodesics, and diverging scenarios for geometric invariants generated with the metric curvature, this singularity means that space-time is geodesically incomplete. As shown by the theorems of Penrose and Hawking [92] that singularities indeed make an appearance in Einstein's theory. Their principle statement is that the theory of GR collapses for curvatures of the order of the Planck scale, which disclose the requirement of the quantum description of space-time. The physical

significance of GR is dependent on the *Cosmic Censorship* [93] protective mechanism against singularities, which asserts that *no naked singularities can exists*. Singularities resulting from realistic matter may only occur behind a surface, known as a *event horizon*, from which no information can reach an observer on the outside of it. A black hole is a type of object that exists within the event horizon. To put it another way, a black hole is the region of space-time with an asymptotic conformal structure that does not reside in the causal past of future null infinity for space-times . Its boundary in the full space-time manifold is called the future event horizon.

The formation of black holes as a result of the gravitational collapse of enormous objects has long been investigated. It has been investigated analytically as well as numerically (we recommend seeing the reviews [94] and [95]). Numerical analysis has recently been used to the generation of black holes by high-energy collisions [96]. An event horizon is created using semi-realistic materials in accordance with cosmic censorship. It has also been demonstrated that no matter is required for the formation of a BH, since the focusing of incoming gravitational waves may suffice [94]. According to the hoop conjecture [97], a BH will arise whenever a given enough quantity of energy is confined in a sufficiently small region of space. The astonishing truth is that, regardless of the characteristics of the initial matter distribution, space-time settles down to a unique stationary black hole solution. Stationary BH solution can be *static, axially symmetric or both* [92]. The metric in static space-time case is regarded as stationary and invariant under time reversal symmetry. Therefore, it is to be noted that all static space-times are stationary. In addition to the Schwarzschild black hole, there also exist other stationary black hole solutions which are *Reissner-Nordström* [71, 72], *Kerr* [83] and *Kerr-Newman* solutions [98]. The static, spherically symmetric and electrically charged solution represents the Reissner-Nordström BH. Whereas, the rotating ones represent Kerr and Kerr-Newman solutions, but the latter one is the electrically charged.

Among all the BH solutions Kerr-Newman case is considered to be the most general one. Besides this, other solutions are assessed as the special cases. Here one theorem is worth to mention known as the reputed *uniqueness theorems*, which undertake the fact that the properties of a stationary BH can be notably explained by just three parameters of the Kerr-Newman BH which are *the mass M, the electric charge Q* and *the angular momentum J* [99]. It was Wheeler who humorously introduced the statement that *"black holes have no hair"* [100]. Later on, many authors proposed the proof of the uniqueness theorem in a long chain of theorems. Hawking stepped first among them when he manifested the fact that the topology of any stationary BH is spherical in nature [92]. It

is also applicable for both electrically neutral and charged BH solutions. Later Israel, analyzed the static solutions where he found that any topologically spherical vacuum solution is requisite to represent the Schwarzschild BH solution [101]. In accordance with *Carter-Robinson theorem*, all stationary, axisymmetric spherical vacuum solutions can be recognized by just two parameters M and J [102, 103]. Thus, those solutions belong to the Kerr family, whereas an analogous result holds for Kerr-Newman BHs [104]. Now, the noteworthy point is all the properties of a stationary BH are explained by its mass, charge and angular momentum as no other classical field can form around a BH [105, 106].

However, the fascinating part is that in the process of gravitational collapse, BHs overlook all other properties of its matter except the mass, the electric charge and the angular momentum. On a similar note, a somehow similar phenomenon is observed in case of a thermodynamic system of ordinary matter - when a thermodynamical system reaches an equilibrium situation with its surroundings, and the properties of the system can be described by some macroscopic quantities only. Since the thermodynamical properties of a system can be explained by the four laws of thermodynamics, in the same way one might expect similar laws for stationary BHs as well, and there are theorems that explain the thermodynamic properties of a BH. These theorems are known as the *four laws of black hole mechanics* which were formulated by Hawking, Bardeen and Carter in the early '70s [107, 108]. Now, let us dig into that topic.

1.3 Black Holes Are Not So Black After All

"If you feel you are in a black hole, don't give up: there is a way out!"
– Stephen Hawking

1.3.1 The Quartet Laws of Black Hole Thermodynamics

The laws of BH mechanics involve an important quantity known as the *surface gravity* (κ)[1]. It is that quantity which basically represents the limiting value of the force exerted from the asymptotic infinity with the aim to hold a unit test mass on the horizon. Grasping these concepts and with the proper implication one can express the laws of BH mechanics which are as follows:

[1]For general definition of the surface gravity, please see [109]

- ***The Zeroth law:*** *This law suggests that the surface gravity κ is constant on the horizon of a stationary BH.*
  With the closer look one can see that this theorem bears a resemblance with the zeroth law of thermodynamics and it provides us an logical objective to expect that the temperature of a stationary BH is proportional to κ. Therefore, in a certain sense, the surface gravity seems to play the part of the temperature of the BH. However, an important consequence of the zeroth law is that the stationary black holes can be of two types: extremal black holes for which the surface gravity vanishes ($\kappa = 0$) and a non-extremal black holes with bifurcate horizons.

- ***The First law:*** *Black holes satisfy the following equation*

$$\delta M = \frac{1}{8\pi}\kappa\ \delta A + \Omega_{\rm BH}\ \delta J_{\rm BH} + \Phi_{\rm BH}\ \delta Q, \tag{1.2}$$

  where M is the mass, A is the area of the horizon, J is the angular momentum, Q is the charge and $\Omega_{\rm BH}$ and $\Phi_{\rm BH}$ are the angular velocity and the electrostatic potential respectively. Thus, in essence, the first law simply asserts that the mass energy is conserved. On a comparison of this theorem with the first law of thermodynamics, one can see that the area of the horizon (A) has a similar role as entropy in thermodynamics and the surface gravity κ is analogous to the temperature of the system. Although the original derivation [108] was done for stationary perturbations, later, it was generalized for non-stationary perturbations also [110, 111].

- ***The Second law:*** *This theorem suggests that if the Cosmic Censorship Conjecture holds and $R_{\mu\nu}k^\mu k^\nu \geq 0$ for all null k^μ, then*

$$\delta A \geq 0 \tag{1.3}$$

  in any classical process.
  This theorem is often termed as *Hawking's area law of black holes*. Now, the area of the horizon (A) can be expressed in terms of the so-called irreducible mass $M_{\rm ir}$ which is:

$$A = 16\pi\ M_{\rm ir}^2. \tag{1.4}$$

  The irreducible mass, in turns, has the form

$$M_{\rm ir} = \frac{1}{2}\sqrt{\left(M + \sqrt{M^2 - a^2 - Q^2}\right)^2 + a^2}, \tag{1.5}$$

where $a = J/M$ is the angular momentum per unit mass. Therefore, the present theorem can be presented alternatively as

$$\delta M_{\rm ir} \geq 0. \tag{1.6}$$

Therefore the above equation sets an upper limit for energy extraction from a rotating BH. Using the so-called Penrose process, it is possible to extract energy from a rotating BH (For further details, we recommend Ref. [112]). Furthermore, this theorem has at least two significant consequences. Firstly, it imposes a restriction on the amount of energy that can radiate away in BH collisions. Secondly, this theorem forbids the bifurcation of a BH because bifurcation would give rise to a contradiction between the area law and the conservation of energy. We will talk more about this law in the later parts of this chapter, but before that, let us see what the third law has to say.

- ***The Third law:*** *Now, this theorem suggests that by any physical process it is impossible to reach at* $\kappa = 0$.
  Once again, one can visualise that this theorem has an obvious association to thermodynamics. It is strikingly analogous to the third law of thermodynamics that suggests that by any means of physical process it is impossible to reach at $T = 0$. Since only the extremal BHs can have zero surface gravity, this theorem implies that a non-extremal BH cannot transform into an extremal BH.

Initially, people thought that the four laws of BH mechanics were just analogous to the four laws of thermodynamics without any inherent physical meaning of it. But, at the time when Hawking showed the world that when quantum mechanics comes into the picture, BH indeed has a temperature and has an intimate connection with the thermodynamics and he transformed this analogy into identity. Hawking [68, 113] revealed that when the quantum effects are taken into consideration, black holes can radiate. Later, this radiation was famously known as *Hawking radiation* which we shall discuss in the next part.

1.3.2 Hawking Radiation: Where There is Quantum Mechanics, There Is a Way to Cross the Horizon

The story begins with Hawking's publication on area theorem and Bekenstein proposed the idea that the area of the event horizon of a BH basically quantifies its entropy. More

specifically, Bekenstein [114, 115] put forward that the entropy of a BH is, in SI units,

$$S = \gamma \frac{k_B c^3}{\hbar G} A, \tag{1.7}$$

where γ is a constant. However, from the concept of information theory and using Shanon's entropy, he was able to predict a certain value of γ, namely $\frac{\ln 2}{8\pi}$, which later turned out to be incorrect. However, Bekenstein's idea inspired Hawking. Incorporating the quantum field theoretical treatment in curved space-time, he was able to re-express the correct value of this constant to be one-quarter [68]. Hence, in SI units, the BH entropy turns out to be

$$S = \frac{1}{4} \frac{k_B c^3}{\hbar G} A. \tag{1.8}$$

This outcome is famously known as the *Bekenstein-Hawking entropy law* for BHs.

The entropy of a BH is manifested by the process of radiation, which occurs at the event horizon of the BH. The original idea of Hawking was based on the properties of quantum field theory in curved space-time, and it was one of the pioneering results of this theory. In essence, he considered the behaviour of the vacuum states of a massless Klein-Gordon field where the field was transported from the past null infinity to the future null infinity near the event horizon of a collapsing Schwarzschild BH. By explicit computation of the Bogoliubov coefficients it turned out that the vacuum states at asymptotic past are different from the ones at asymptotic future (see [116] and [43] for detailed calculation of Bogoliubov coefficients) which was quite a surprise. As a consequence of that, an observer at the future null infinity observes a flux of particles emitting out from the immediate vicinity region of the event horizon of the BH. The expectation value for the number of particles emitting out of the BH with angular frequency ω agrees with the Planck distribution for the blackbody radiation at the *Hawking temperature* in SI units

$$T_H = \frac{\hbar c^3}{8\pi G k_B M}, \tag{1.9}$$

and in terms of the surface gravity, κ the above equation turns out to be

$$T_H = \frac{\hbar \kappa}{2\pi c k_B} \, . \tag{1.10}$$

This above temperature directly leads to the Bekenstein-Hawking entropy presented in Eq. (1.8). These results also developed the fact that this temperature is independent on the details if the gravitational collapse and therefore, one might expect that this result holds for eternal black holes as well.

The phenomenon of BH radiation is somewhat baffling topic since BHs are defined by *"regions of no escape"*. Due to this some heuristic explanations have been put forward by many authors for the origin of the radiation. The most renowned one is obviously by Hawking himself. His core idea was that the spontaneous pair production process in the vicinity region of the event horizon furnishes a mechanism for the radiation. In case of a normal situations, a virtual particle-anti-particle pair annihilates itself very rapidly after their emergence. However, it is possible that in the near horizon region, the members of the virtual pair become separated by the existence of the horizon such that the annihilation process is prevented. In that case, one member of that pair escapes away from the BH with positive energy which contributes in the Hawking radiation, while the other one having the negative energy is swallowed by the BH itself. Hence, the observer situated outside the horizon notices a flux of quanta with positive energy which seems to come out of the BH.

After Hawking's original work, there have been various semi-classical approaches of the Hawking effect with different physical assumptions. In the year 1977, Hawking and his student G. Gibbons [117, 118] developed an approach based on the method of analytical continuation to a Euclidean section which is basically the Wick rotation method. Particularly, they computed the action for the gravitational field on the complexified space-time. The analytic continuation $t \to i\tau$ of the BH metric was performed and the periodicity of τ is chosen for the removal of the conical singularity. Interestingly, the purely imaginary values of the action gives a contribution to the partition function for a grand canonical ensemble at Hawking temperature (Eq. (1.10)) and the periodicity of the complexified time (τ) around the horizon is identified as the inverse of the Hawking temperature. Using this idea, they were able to show that the entropy associated with the black hole metric is exactly equal to the expression of Eq. (1.8). At the same time, Christensen and Fulling [119] were able to obtain the expectation value of each term of the stress-energy tensor by exploiting the structure of trace anomaly, which eventually led to Hawking flux. They particularly constructed different regularisation methods to obtain the anomaly coefficient values of the conformally coupled scalar field. Using this information regarding the trace of the renormalised stress tensor they showed that the Hawking radiation for BHs is consistent with the covariantly conserved stress-tensor whose expectation value is well behaved on the horizon. Later S. Robinson and F. Wilczek [120–122] put forward a novel technique to compute the Hawking flux from a BH. Their technique was basically established on the basis of gauge and gravitational anomalies. Their key point was that the physics near the horizon of a (3+1) dimensional static

black hole can be represented using an infinite collection of (1+1) dimensional fields where each of them is propagating in the space-time metric given by "$t-r''$ section of the entire space-time metric. Considering this interpretation they imposed the constraint that outgoing modes vanish in the near the horizon region as a boundary condition. Also, in the vicinity region of the horizon the ingoing modes does not affect any physical phenomenon outside the horizon as the region inside the horizon is causally disconnected from the exterior. Hence, this theory acquires a definite chirality which possesses both gauge and gravitational anomaly [123]. But, it becomes anomaly free when one considers the contribution from the ingoing modes which are though classically irrelevant. As a result of that a restriction is being imposed on the structure of the stress-energy tensor which is eventually responsible for the Hawking radiation [120]. Later Banerjee and Kulkarni [124–126] introduced a more conceptually concise method (covariant expression for anomaly including the covariant boundary conditions) to obtain the Hawking flux. Further approaches on this topic may be found in the following papers [127–129].

However, there are numerous probable explanations for Hawking radiation, the most notable of which being the *tunneling effect* through the event horizon. A semi-classical technique of modelling Hawking radiation as a tunneling phenomenon was proposed in the 1990s [130] and received a lot of interest in the physics community [54, 130–189]. The method of producing the electron-positron pair under a constant electric field is quite similar to this concept. The main idea is that the phenomena of pair creation occurs within a BH's event horizon. The ingoing mode is one of the pair's production members, while the outgoing mode is the other. Now, the theory proposes that by starting just inside the event horizon and going all the way to infinity, the outgoing can adopt trajectories that are classically forbidden. The question now is: *how does this outgoing mode pass the horizon barrier?* The picture suggests that, this mode effectively moves out due to a tunneling process caused by the shrinking of the horizon. As a result, the departing particle's action becomes complex, and the tunnelling amplitude is determined by the imaginary component of that action. Incoming particles, on the other hand, present a different picture. The ingoing particle's action is real, just as any particle is allowed to fall inside the horizon classically. It is also worth noting that the $(t-r)$ component of the total metric dominates near-horizon physics, with tunnelling occurring exclusively in the radial direction. As a result, in the near horizon area, all of the angular portion may be ignored, and the solution of the field equation corresponds to the angular quantum number $l=0$, i.e. solely for the s-wave [130–132].

As a result, the basic essence of tunneling is based on the computation of the imag-

inary component of the action for the process of s-wave emission beyond the horizon, which on the other hand is connected to the Boltzmann factor for emission at Hawking temperature. The tunnelling probability for the classically prohibited route of the s-wave coming from inside to outside the horizon may be calculated using the WKB approximation which lands us to the following form

$$\Gamma \propto \exp(2\ \mathrm{Im}S)\ . \tag{1.11}$$

Here S is the classical action of the trajectory to leading order in $\hbar$ (where $\hbar = 1$ here). The Hawking temperature may now be recovered at linear order by extending the action in terms of particle energy. In particular, with $2S = \beta E + O(E^2)$, one gets

$$\Gamma \sim \exp(-2S) \simeq \exp(-\beta E) \tag{1.12}$$

where the higher order energy terms have been neglected. The higher order terms represent a self-interaction effect deriving from energy conservation [54, 131]; nonetheless, the extension to linear order is all that is necessary to determine the temperature expression. The the above expression is basically the regular Boltzmann factor for a particle of having energy E. Here β is the inverse temperature of the horizon. Now, as the concept of tunneling appears into the picture therefore, it reveals that Hawking effect is a quantum mechanical phenomenon and the presence of horizon is obligatory for this purpose.

Now, coming back to the calculation of the imaginary part of the action, there are two different methods in literature. The first one is by *radial null geodesic method* which was first introduced by Parikh and Wilczeck [54] followed from the work of Kraus and Wilczek [130–132] and the other method is the *Hamilton-Jacobi (HJ) method* introduced by Srinivasan et al [140–143]. After that, a lot of researchers [151, 181, 186, 188–197] used the radial null geodesic method as well as HJ technique extensively in order to find out the Hawking temperature for different space-time scenarios. However, several issues and facets have been discussed extensively in these papers [147, 148, 160–162, 198–207]. Here, we shall give a very short review on both of these methods whereas one can find the detailing of these methods in these extensive literature [54, 140–142, 146–149, 151, 158, 160–162, 165, 181, 186, 188–207] which will give the readers some new insights and explications.

The elimination of the apparent singularity at the event horizon, which is settled by going to the Painleve coordinates [208], is the first stage in the radial null geodesic approach. The next part consists of the consideration of a null s-wave which is emitted from the black hole. When the entire action is examined in depth [130–132], it can be

shown that the imaginary term is the only portion of the action that contributes to tunnelling. The imaginary portion of the action may then be calculated using Hamilton's equations of motion and knowledge of null geodesics. The tunneling probability of the null s-wave coming from inside to outside of the horizon is then computed using the WKB approximation, which illustrates the relationship with the Boltzmann factor for the emission at Hawking temperature.

The HJ technique, on the other hand, considers an emitted scalar particle while discarding its self-gravitation and assuming that its action fulfils the relativistic Hamilton-Jacobi equation. As a result, based on the knowledge of the metric's symmetries, one examines an acceptable ansatz for the action's form. This method is persuaded by applying the WKB approximation to the Klein-Gordon equation. The modes involved in this situation are also related to the angular quantum number $l = 0$, which is the s-wave. The benefit of this technique is that it may be applied to any coordinate system because the ansatz is based solely on the symmetry of space-time. By applying the WKB approximation to other wave equations, such as the Dirac equation for spin-1/2 fermions, this technique may be used to other types of particles than scalar particles. In chapter 5, we will explicitly apply this approach in our context to get the temperature of our system.

In an effort to comprehend the underlying physics of the Hawking effect, Unruh [209] uncovered another phenomena, known as the Unruh effect. The fundamental concept of Unruh effect relies on the *equivalence principle:* by selecting a uniformly accelerated frame, one can ignore the locally gravitational effect and the observers who have different conceptions of positive and negative frequency modes will differ to each other on the particle content of their respective vacuum states. More specifically, in this case, there are two observers: the Rindler observer, which is uniformly accelerated, and the inertial observer, which is located in Minkowski space-time. The Minkowski space-time seems to have a horizon in the eyes of the Rindler observer. Interestingly, the Minkowski vacuum would appear to an inertial observer to be absolutely empty, while a Rindler observer would find particles in that vacuum. Furthermore, a thorough calculation reveals that the emission spectra are equal to the spectra of a black body with the temperature

$$T_U = \frac{\hbar a}{2\pi} \tag{1.13}$$

where a denotes the acceleration of a Rindler observer. With $a \to \kappa$, the temperature is clearly similar to that of Hawking. Therefore, the similarity between these two effects are vividly discernible. Both these effects are associated with horizon. The Unruh effect is related with the Rindler horizon while the Hawking effect is tied to the event horizon

of a black hole.

1.4 The Unfinished Story of Black Hole Radiation

There are various repercussions of Hawking radiation. The temperature of a black hole increases as its mass decreases, as shown by Eq. (1.9), implying that smaller black holes are hotter than larger ones. Furthermore, as a black hole radiates, it loses mass and grows hotter and hotter, implying that the black hole's specific heat is negative. Because the black hole loses mass throughout the radiation process, it finally evaporates. The last phases of black hole evaporation are unknown, as existing theories are likely to fail when the black hole's mass reaches on the order of *Planck mass* $m_{\mathrm{Pl}} = \sqrt{\hbar c/G} \sim 10^{-8}$ kg. The phenomenon of black hole evaporation has always been a source of consternation among physicists. When one tries to generalise the conclusions found at the semi-classical level, the most basic aspect of quantum physics, namely unitary evolution, appears to be violated [68]. As previously stated, Hawking demonstrated that the evaporation of the black hole is essentially the radiation of positive energy, flux of the particle obeying the distribution of the thermal spectrum with respect to an asymptotic observer, and a flux of particles of negative energy inserting into the black hole and decreasing its mass when the quantum effect is included in the derivation. Therefore, the mass lost by the black hole appears in the form of energy of thermal radiation. This process may describe the thermodynamic picture of the black hole but it contradicts the standard unitary quantum mechanics [210]. The flux of the outgoing particles received by the asymptotic observer, remain entangled with the ingoing flux. As a result of that, the subsequent Hawking radiation is thermal which is due to the fact that the modes that penetrated the horizon are traced over. The BH shrinks and loses its mass as a result of this process, which is manifested in the form of Hawking radiation. The conceptual unease develops, however, when the black hole totally disappears as a result of this action, resulting in an apparent paradox. In the end, the departing particle has nothing with which to maintain their entanglement; nonetheless, they stay in a mixed state since the entanglement with the inner modes was not explicitly severed during the evaporation process. This is essentially the polar opposite of unitary quantum evolution.

There is also the issue of the information content of the stuff that collapsed to produce the black hole, as well as the matter that falls into the black hole. The no-hair theorem [112] states that aside from mass, charge, and angular momentum, no further information can be collected by an observer on the horizon's edge. As a result,

all knowledge about that stuff that crossed the horizon barrier would wind up in the singularity and be obliterated. As a result, it appears that information about the original state of matter (other than mass, charge, and angular momentum) that falls behind the horizon is not encoded in the Hawking radiation and is therefore unavailable to the asymptotic observer. This circumstance appears to need a non-unitary development [211].

There are several ideas in the literature to address the *Information paradox*. An initial resolution originates that this semi-classical Hawking process can not be trusted all the way to the complete evaporation of BH. This works only when the black hole is large enough; as it becomes smaller, the quantum aspect of gravity begins to dominate the entire idea, and the semi-classical concept must collapse. As a result, one can expect corrections to the semi-classical description that makes it non-thermal. Those non-thermal corrections can keep some information. The authors of [210] have shown that all of these adjustments are sub-dominant in character and that none of them can render the unitary theory. There have been some recommendations that a complete adjustment to the unitary quantum theory itself be made in order for it to be included into non-unitary processes [212]. However, using some conceptual considerations, such changes to the quantum unitary theory have been proposed [213, 214]. These non-unitary theories, on the other hand, may be relevant to particular physical circumstances [215] in which the predictions differ from the usual unitary theory, restricting the models.

1.5 Black Hole Entropy: So Where Do We Stand Now?

In addition to Hawking's original concept, there exist other procedures to the Hawking radiation. Gibbons and Hawking [117, 118, 216] established the path integral technique, which is the most well-known. Feynman pioneered path-integral quantization as an alternative to canonical quantization in non-relativistic quantum physics [217]. The extension of this approach might potentially be used to quantify the gravitational field. The path integrals for gravity, on the other hand, are exceedingly difficult to analyse. If one restricts himself to the semi-classical approximation, in which space-time is treated as a rigid background, the first order approximation reproduces the Bekenstein-Hawking entropy law (Eq. (1.8)). The clear advantage of the path-integral method is that the black hole's thermal characteristics are solely geometrical in origin, not attributable to the behaviour of quantized matter in the neighbourhood of the event horizon. This implies that entropy and temperature can be regarded as intrinsic features of gravity. There are

various more derivations of the Hawking effect that are based on significantly different physical assumptions than the path-integral method (we recommend this Ref. [55] for a review). The fact that multiple opinions on the Hawking radiation exist shows that our existing methodologies cannot fully comprehend the genesis of black hole radiation.

The Bekenstein-Hawking entropy law has a number of significant implications. First and foremost, since in natural units

$$\delta S = \frac{1}{4}\delta A, \tag{1.14}$$

the first law of back hole mechanics, i.e. Eq. (1.2) can be written as

$$\delta M = T_{\rm H}\,\delta S_{\rm BH} + \Omega_{\rm BH}\,\delta J_{\rm BH} + \Phi_{\rm BH}\,\delta Q. \tag{1.15}$$

Due to this substitution the equation emerges with a dramatic change as this equation describes now *thermodynamics* rather than the mechanics of a black hole. Hence this equation is usually termed as the *first law of black hole thermodynamics*.

Second, when the black hole emits radiation, its mass and the region of its event horizon shrink. This, incidentally, violates the second law of BH mechanics, as well as the second law of thermodynamics. Bekenstein, on the other hand, proposed a solution to this perplexing dilemma. He argued that, while the black hole's entropy decreases, the overall entropy $S_{\rm tot} = S_{\rm ext} + S_{\rm BH}$, where $S_{\rm ext}$ is the entropy of the exterior space-time region, is a non-decreasing function of time in any space-time in any process [114, 218]. To put it another way,

$$\delta S_{\rm tot} \geq 0 \quad \text{in any process.} \tag{1.16}$$

The above statement is known as the *generalized second law of thermodynamics*.

However, the most essential consequence of black hole entropy is its statistical interpretation, at least from the perspective of quantum gravity: Because a black hole's entropy is $S = \frac{1}{4}\frac{k_{\rm B}c^3}{\hbar G}A$, we anticipate it to have $\exp\frac{1}{4}\frac{c^3}{\hbar G}A$ microstates corresponding to its macrostate. In comparison to the three classical degrees of freedom anticipated by the no-hair theorems, a macroscopic hole possesses an immense number of quantum-mechanical degrees of freedom. The presence of these microstates poses a plethora of fascinating questions. Are these degrees of freedom linked to the quantized matter fields on a background geometry, or do they correlate to the quantum states of the collapsing matter inside the black hole? Is it feasible that the concept of black hole entropy comes from this? Could the concept of black hole entropy be derived from the microscopic structure of space-time itself?

1.6 The Need to Explain the Thermality of Black Hole: But how?

1.6.1 Instability and thermality: The Inescapable Connection

The inquiries listed above illustrate that, despite the fact that back hole thermodynamics has been studied for a long time, there are still some compelling reasons to pursue it further, as we have done in our thesis. One method is to dig out the inherent characteristics of space-time in the vicinity region of an event horizon. Analysing the near horizon physics has gained significant attention in recent time because over the time physicists have seen systems start showing some fascinating behaviours whenever it reaches under the ascendancy of this mystifying one-way membrane. One such characteristics is the manifestation of *chaotic dynamics* in a system in the near horizon region. When a system is influenced by horizon, it has been discovered that it can create chaos into the system [219–224]. A similar situation was explored in a recent paper [225] in the case of string surrounding charged black brane. Chaos in the presence of a horizon has been researched extensively throughout history, but the explanation for this unique aspect of the horizon has yet to be fully understood. Similarly, why all horizons (static or stationary) convey the same phenomenological characteristic is an important point to consider in this context. People have attempted to explain the chaotic dynamics of the horizon in the quantum domain as well, since the inquiry has not been restricted to the classical scale. The behaviour of some quantum operator's out-of-time-order correlator (OTOC) is used to investigate quantum chaos events [226, 227]. The hallmark of quantum measure of chaos [226, 227] is the distinctive exponential growth of OTOC in certain instances.

However, one important element to remember is that anytime we talk about chaos, there must be certain instability characteristics in the system that characterise its chaotic nature. This is referred to as the Lyapunov exponent [228]. Things have become highly fascinating as a result of a new discovery on the upper bound of the Lyapunov exponent anticipated in the Sachdev-Ye-Kitaev (SYK) model [226]. In the classical model, it was discovered in [220] that the radial velocity of the particle rises exponentially in the near-horizon region for any static or stationary black hole. In this scenario, the upper bound of the instability factor is theoretically compatible with that of the SYK model. This has also been proven statistically. The upper bound on the Lyapunov exponent is defined in all of these scenarios by the black hole's surface gravity. This upper bound is dependent on the temperature [226, 229], as it is well known that surface gravity is connected

to Hawking temperature [68, 113]. The upper bound of the Lyapunov exponent may be proven in an experimentally realisable configuration using a trapped-ion approach, according to a recent research [230].

In fact, there is some evidence that there is a link between the system's instability and its associated quantum thermality. M. Srednicki's initial study [231] proposed that a chaotic system inherently integrates thermal behaviour. At a similar vein, Morita [232] recently proposed that an unstable classical mode with a fixed Lyapunov exponent cannot have zero temperature in the quantum scale. An inverse harmonic oscillator (IHO) is one of the most well-studied unstable systems in this field. The IHO produces instability at the classical level, and researchers discovered that quantum temperature can result from it, which is dictated by the instability factor. This analysis is remarkable which shows that the derived temperature is a pure quantum consequence, and hence vanishes in the classical limit. All of these studies point to a tight relationship between instability and pure quantum temperature. More exactly, this classical instability can be a cause of a system's pure quantum temperature.

The findings of Bekenstein [114] and Hawking [68, 113] demonstrate that the black hole horizon shows thermodynamic phenomenon and the temperature associated with the horizon, interestingly, is an observer-dependent variable that is also a pure quantum entity. However, black hole thermodynamics is a long-standing concept which originates through an analogy between the laws of black holes and those of usual thermodynamical systems, but the reason why these thermodynamical quantities are associated with horizon has never been discussed properly anywhere. The horizon temperature, interestingly, is an observer-dependent variable that is also a pure quantum entity. Therefore, one of the primary thrusts since the start of this thermal idea of horizon has been to find an appropriate microscopic cause of the aforementioned black hole thermodynamics. There are various efforts, each with its own set of strengths and flaws, and none of them is complete. We would like to talk about one of the major difficulties in this sector. Despite the fact that a thermodynamical parameter such as temperature fits neatly with the horizon, the issue remains: *what is the source of this temperature?* For example, it is known from the kinetic theory of gases that the kinetic energy of the gas particles is the source of the temperature of a gas contained in a cylinder. However, whether a similar mechanism will be applied in case of a horizon or not is yet to be known. Consequently, which microscopic degrees of freedom (MDOF) is responsible for such a feature is not known either. Though people have tried several attempts, there have been no concrete explanations until now.

In the present thesis we aim to investigate this option for the first time to explain the presence of horizon temperature in light of previous and new data in the context of a relationship between classical instability and quantum thermality. We believe it can be a useful tool in explaining this. In this regard, we would like to point out that in some works, IHO has appeared in the black hole system [220, 232, 233]. For example, Hashimoto et al [220] shown that if one analyses the maxima of a field potential in black hole space-time, the effective motion of a particle is equivalent to that in an IHO potential. Later, Morita [232] and Hegde et al [233] separately shown that such an IHO causes temperature to rise under quantization that is proportional to the system's instability factor. In a completely different context [234, 235], it was discovered that when a particle scattering phenomena is studied in a black hole space-time in the presence of a localised shock wave, the effective scattering Hamiltonian is that of IHO, which also occurs in the quantum domain. The prospect of instability in the form of IHO for a black hole background, which imparts thermality to the system, is evident in all of the papers described above. Furthermore, this characteristic is local since it appears in a very narrow region surrounding a certain point – either the potential maximum [220] or the site of the shock wave [235]. As a result, none of these assessments are directly related to the horizon. To put it another way, no observations have been made near the location of the horizon. Given that temperature is a horizon attribute, this should emerge entirely from the survey around this one-way membrane. That is why the primary goal of this thesis is to determine whether there is any instability near the horizon and, if so, whether that instability is linked to the chaotic dynamics of a system or has any relationship with the horizon temperature at the quantum scale.

In a nutshell, the goal of the current thesis is to first investigate how systems behave in the region near the horizon, and by researching these features, we attempt to provide some answers to open concerns about horizons. The entire thesis consists of four parts, excluding introduction and conclusion. The first chapter introduces some well-known results of black hole physics. Many of the issues discussed there are not directly connected with the main subjects of this thesis, but their purpose is to offer an extensive introduction to the properties of classical black holes - especially for the readers who are not experts of general relativity. In the latter half of the introductory chapter we raise some open questions regarding black hole thermodynamics and wrap off the chapter with some motivations behind the thesis. Now, comes Part I which includes chapter two and three in which we present some classical results for a system that is located in the vicinity region of an event horizon. Interestingly, we find that the system

begins to exhibit chaotic behaviour as soon as it is exposed to the horizon's influence. Part II contains only one chapter (chapter four), in which we try to figure out why a system in the near horizon area behaves in such a chaotic manner. All computations are done in the classical scale until Part II. Part III, which consists of one chapter (chapter five), is devoted to studying the quantum consequences of the near-horizon *local* instability, and the chapter concludes with our proposed conjecture regarding the relationship between instability and thermality of a system in the near horizon region. Part IV is divided into two chapters (chapters six and seven) in which we apply the same formalism to more generalised backgrounds (Kerr and GNC space-time) in order to better grasp the core reason for thermality in those circumstances. We present a brief conclusion and future directions for our findings in chapter eight.

1.7 Chapter-wise overview: Outline of the thesis

The results discussed in this thesis are based on the works in [236–241]. In this section, we have summarized the research guidelines of the thesis as follows,

Chapter 2 :

What happens to a system when it approaches very near to an event horizon? One of the remarkable properties of the horizon, according to many experts, is its impact on integrable systems, which causes the system to become chaotic. For distinct black hole systems where the particle is deemed massive or charged or spinning, a lot of work has been done in this direction. The dilemma with the massless particle, on the other hand, has yet to be addressed. The study of massless particles that follow null geodesics has long been interesting because they cause the Hawking radiation. As a result, in this chapter, we begin our calculations by looking at the motion of a *massless* and *chargeless* particle extremely close to the event horizon. It demonstrates that the radial motion is exponentially increasing, implying that when an integrable system is subjected to the impact of the horizon, chaos can be induced in the particle motion. This is being confirmed by investigating the Poincaré sections of the trajectories with the insertion of a harmonic trap to confine the particle's motion in the near-horizon region. Two scenarios have been investigated: (a) *any static, spherically symmetric black hole (SSS BH)* and, (b) spacetime represents a *stationary, axisymmetric black hole (e.g., Kerr metric)*. In both circumstances, we discovered that our system does not exceed the upper limit of a black hole system's largest Lyapunov exponent value, i.e. the horizon's surface gravity. We have also demonstrated the appearance of chaos by analysing the Power Spectral Density (PSD) of the system which basically gives us the information of the route to chaos.

Chapter 3:

We learned in the previous chapter that when an event horizon exists, a system begins to exhibit chaotic behaviour in the near-horizon region. As a result, the continuing hypothesis that *the presence of a horizon may produce chaos in an integrable system* is studied further in this chapter from the perspective of a uniformly accelerated frame. We create a model that consists of a massless and chargeless particle trapped in a harmonic oscillator in a uniformly accelerated frame (namely Rindler observer). Here the Rindler frame provides a Killing horizon without any intrinsic curvature to the system. This

distinguishes the current findings from the earlier research. We discover that the motion of a particle caught in harmonic potential systematically shifts from periodic to chaotic for certain values of system characteristics (such as acceleration and particle energy). This means that the mere presence of a horizon, rather than the inherent curvature (i.e. gravitational influence) in the background, is enough to cause chaos in the particle's motion. This current investigation further illuminate and balustrade our conjecture.

Chapter 4:

After finding out the chaotic behaviour in a system near the horizon, our next aim was to explore the underlying explanation behind this intriguing feature of the horizon. Therefore, for the first time in this chapter, we have attempted to provide a cohesive explanation for such a remarkable characteristics of the horizon. The near horizon Hamiltonian in Painleve coordinates of a chargeless and massless particle, at the leading order, is $H \sim xp$ type in the presence of any horizon, whether static or stationary, where p is the canonical momentum and x is its conjugate position of particle. For the appearance of this Hamiltonian the equations of motion suggest that the radial coordinate or the radial momentum diverges when the particle resides very near to the horizon and introducing instability into the system. Not only that, we also find out another set of coordinates, the Eddington-Finkelstein (EF) coordinates, in which the particle's motion along the null trajectory is equally unstable in the near horizon domain. When the particle is following the outgoing null route in those precise EF coordinates, we find that the observer associated with the EF frame measures the radial momentum of the particle as $p \sim e^{-\kappa t}$ where t is the EF time coordinate and the corresponding Hamiltonian of the system comes out to be of xp structure again. Therefore, as in the near horizon limit, i.e. $t \to -\infty$ the radial momentum diverges and indicates the presence of instability just like the case of Painleve coordinate system. Hence, it suggests that although the instability is observer independent for our particle motion, the particular form of the Hamiltonian is observer dependent. The observer associated with this specific frame of the particle, either in Painleve or in EF coordinates will see this form of the near horizon Hamiltonian.

Chapter 5:

In the last chapter we found that the particular structure of the Hamiltonian (xp kind) is responsible for the unavoidable instability provided by the horizon on the particle's

motion at classical level. Following this classical picture we next proceed for the quantum calculation in the present chapter. We find out that our observer either in Painleve coordinates or in EF coordinates, predict the automatic appearance of thermality as result of this aforesaid instability. We investigate this fact using different quantum approaches (tunneling mechanism, detector response method and by calculating the Density of States of the xp Hamiltonian) in order to establish our previous conjecture, in a more robust way. In every case, the temperature found out to be that given by the Hawking. Therefore now, under the present investigation, we reframe this conjecture as – *the presence of instability in the near horizon region is the mechanism for providing the temperature to the horizon as seen by a particular class of observers.*

Chapter 6:

In this chapter, the validity of our already proposed conjecture – *horizon creates a local instability which acts as the source of the quantum temperature of black hole* – is being tested here for Kerr black hole. In the earlier chapters this has been explicitly shown for spherically symmetric static black hole. The more realistic situation like Kerr spacetime, being stationary and axisymmetric, is a non-trivial example to analyze. We show that for a chargeless massless particle, the near horizon radial motion in Kerr spacetime, like SSS BH, can be locally unstable. The radial contribution in the corresponding Hamiltonian is $\sim xp$ kind once more. Finally we show that the horizon thermalization can be explained through this Hamiltonian when one does a semi-classical analysis. It again confirms that near horizon instability is liable for its own temperature and moreover generalizes the validity of our conjectured mechanism for the black hole horizon thermalization.

Chapter 7:

Dynamical properties of a generic null surface are known to have a thermodynamic interpretation. Such an interpretation is completely based on an analogy between the usual law of thermodynamics and structure of gravitational field equation on the surface. In this chapter we materialise this analogy and show that assigning a temperature on the null surface for a local observer is indeed physically relevant. We find that for a local frame, chosen as outgoing massless chargeless particle (or field mode), perceives a "*local unstable Hamiltonian*" very near to the surface. Due to this it has finite quantum probability to escape through acausal null path which is given by Maxwell-Boltzmann like distribution, thereby providing a temperature on the surface. In the previous chap-

ters, the connection between instability and thermality was established only in specific cases containing horizons. Here we generalise the same for a generic null hypersurface. Therefore, we feel that the present discussion may unfold the deeper reason for having the thermodynamical quantities of not only horizon but also for any generic null surface at the quantum level.

Chapter 8:

We dedicate this final chapter of our thesis for the possible extensions of the results discussed in the thesis as well as a list of new problems that can be done in the future. Also we have highlighted several important conclusions related to our work.

From the next chapter onwards, we have the detail analysis of the thesis. Each chapter of the thesis contains several appendices that are added at the end of the respective chapters. Here we shall use geometrized unit where, $c = G = k_{\mathrm{B}} = 1$. Here c is the velocity of light, G is Newtonian constant of gravitation, k_B is Boltzmann constant etc. Here we will consider the signature of the Lorentzian metric to be $(-,+,+,+)$.

Part I

Horizon: The nest of chaos

CHAPTER 2

CHAOS NEAR EVENT HORIZON

2.1 Introduction and Motivation

An event horizon; such a mysterious boundary in our universe beyond which events cannot influence classically an outside observer. The event horizon is like a one-way membrane; objects can go in from outside to inside but not the other way round; even light cannot escape from it. In 1958, David Finkelstein employed General Relativity to introduce a definition of a black hole event horizon as a boundary beyond which events of any kind cannot influence an outside observer. Therefore, it is that utterly mystifying region around the black holes whose characteristics are yet to be fully understood by physicists. The coupling of general relativity and quantum field theory is one of the main tools which has shown that it can lead us to yield an explanation of several phenomena of a black hole. Theoretically, black holes are the solutions of Einstein's equations of motion defined by the region from which nothing can escape classically. The recent discovery of LIGO [88] confirms that black holes are no longer a theoretical concept; rather, they indeed have the existence in the universe. Till today, researchers are devoting a lot of attention not only to understand the physics of black holes but also the kind of phenomena that they induce around themselves both at the astrophysical and the quantum level. In that sense, the study of near horizon physics conveys its importance in various ways as it can resolve many mysteries regarding the properties of black holes.

The close connection between the geometrical properties of the space-time horizon

and the dynamics of particle motion near it has always been one of the prime topics for researchers. People have understood that this relation may lead to demystify many properties of the horizon at the classical as well as at the quantum level. Recently, a quantum mechanical treatment explores the fact that the presence of the Killing horizon makes the particle motion Brownian when seen from an accelerated frame [242]. However, in this chapter, we try to understand how the motion of a particle behaves when it approaches very near to the black hole horizon (which is an event horizon). This investigation will be performed completely in a classical way. In the classical picture, a considerable amount of studies has been done in this direction. Many researchers have observed that *one of the fascinating characteristics of the horizon is its influence on the integrable systems, and it turns the system into a chaotic one.* In the classical picture this has been established successfully in [220, 243–252]. These calculations are performed mainly based on either Newtonian approximation [244, 245] or effective potential technique [243, 246–248, 251]. Moreover, black hole system is either spinning [251] or magnetized [252] with the massive, charged or spinning test particles [249, 250]. There is a recent analysis [220] that considers the effect of Schwarzschild black hole on a massive test particle in the presence of harmonic potentials as a perturbation. To make sure that the particle does not enter into the horizon, an extra potential has been added to the system. It has been observed in all cases that the motion of the particle is chaotic in nature. Therefore, an ample amount of work has been done in this direction, but *the situation with the massless particle has not been addressed so far.* The study of massless particles which follow the null geodesics has always been an important and interesting topic for discussion. It is observed that the null geodesic is responsible for the Hawking radiation [68, 113] of the particles from the horizon (see [54, 170, 171] for understanding the Hawking radiation as tunneling). Therefore, it may be worth mentioning that the radiated particles, after escaping from the horizon barrier, exhibit chaotic behaviour in their motion due to the influence of the horizon as well as other external perturbations due to the presence of various objects in the universe. This implies that *the horizon not only radiates (Hawking radiation), it also infuses chaos*. Of course, this is not a conclusive statement, rather a suggestive one. In order to get more insight into this, one needs to investigate more, maybe in the quantum mechanical way.

Now, whenever we talk about chaos, that one particular quantity comes into the picture which is known as Lyapunov exponent. This is a quantity which basically quantifies the rate of separation of infinitely close trajectories for a dynamical system. There has been a sporadic attempt to understand the behaviour of Lyapunov exponent for the case

of null trajectories of a particle [219], but this does not give a complete understanding of the situation. However, in the context of horizon the value of the Lyapunov exponent also has an upper bound. Interestingly, the bound can be shown to be given by $\lambda_L \leq \kappa$, where κ is the surface gravity of the black hole [226] (it is the acceleration of a particle, measured by an asymptotic distance observer, which is very near to the horizon). The bound has been by analysing the out-of-order correlator of some observables in the Sachdev-Ye-Kitaev (SYK) model. Recently in [220] this bound has been predicted for a massive particle in a completely different analysis. This shows that the bound is very much universal in nature. However, this does not give a complete understanding of the situation in the near horizon region. Till now, this has been a thriving area of research since the last few years as we know that the interaction of light with gravity is quite non-trivial in nature. After having these discussions, we now turn our focus to the main analysis.

In the following sections we shall start with analysing the trajectories of a massless and chargeless particle in a very near-horizon region of a SSS BH. We shall study the Poincare sections of the particle trajectories, the maximal Lyapunov exponent value and PSD diagrams and shall try to understand the effect of the horizon on this integrable system. Next, we shall study the same analyses in the near horizon region for a stationary axisymmetric (Kerr) BH and shall try to investigate the in-depth implications of rotation parameters into the system.

2.2 Static spherically symmetric black hole

Consider a static, spherically symmetric black hole background, given by

$$ds^2 = -f(r)dt^2 + \frac{dr^2}{f(r)} + r^2 d\Omega^2 \,, \tag{2.1}$$

where the horizon $r = r_H$ is determined by $f(r = r_H) = 0$ and $d\Omega^2 = (d\theta^2 + \sin^2\theta d\phi^2)$. It has a coordinate singularity at this position. To remove this let us adopt the Painleve coordinate transformation [54, 208]:

$$dt \to dt - \frac{\sqrt{1-f(r)}}{f(r)} dr \,. \tag{2.2}$$

Under this transformation, the above metric takes the following form:

$$ds^2 = -f(r)dt^2 + 2\sqrt{1-f(r)}\,dtdr + dr^2 + r^2 d\Omega^2 \,. \tag{2.3}$$

It has a timelike Killing vector $\chi^a = (1,0,0,0)$ and the energy of a particle, moving under this background, is given by $E = -\chi^a p_a = -p_t$, where $p_a = (p_t, p_r, p_\theta, p_\phi)$ is the four momentum vector. Our aim in the following is to find this energy in terms of other components of momentum. To find it, we take help of the covariant form of the dispersion relation $g^{ab}p_a p_b = -m^2$, with m, mass of the particle. Expanding this under the background (2.3), we obtain

$$E^2 + 2\sqrt{1-f(r)}\; p_r E - \left(f(r)p_r^2 + \frac{p_\theta^2}{r^2}\right) = m^2 \;, \tag{2.4}$$

where, only the radial and θ directions motion have been considered, i.e., the particle is moving only along the radial and the θ directions. For a massless particle, solution of the above equation (2.4) with $m = 0$ gives the energy. It is found that it has two values:

$$E = -\sqrt{1-f(r)}\; p_r \pm \sqrt{p_r^2 + \frac{p_\theta^2}{r^2}} \;. \tag{2.5}$$

The positive sign denotes the energy for the outgoing particle, while the other sign is for the ingoing particle. In this paper, we will be mainly interested in investigating the dynamics of the outgoing particles; therefore, throughout the discussions, only the positive sign will be considered.

Next aim is to find the trajectory of the particle. It will be computed from the Hamilton's equations of motion. Before that concentrate for the moment only on the *very near horizon radial motion*. The equation of it (taking $p_\theta = 0$) for the energy (2.5) is $\dot{r} = \partial E/\partial p_r = -\sqrt{1-f(r)} + 1$. Make an expansion of $f(r)$ near the horizon as

$$f(r) \simeq 2\kappa(r - r_H) \;, \tag{2.6}$$

where we have retained only the first-order term. Here $\kappa = f'(r_H)/2$ is the surface gravity of the black hole. Substitution of this in $\dot{r}$ equation leads to

$$\dot{r} \simeq \kappa(r - r_H) \;. \tag{2.7}$$

The solution is $r = r_H + C r_H e^{\kappa\lambda}$, where C is the integration constant and λ is the parameter with respect to which the derivative is taken, i.e., $\dot{} \equiv \frac{d}{d\lambda}$. The equation of the radial momentum in the near-horizon region becomes (considering only the leading order terms)

$$\dot{p_r} \simeq -\kappa p_r \tag{2.8}$$

which then leads to the solution $p_r \sim e^{-\kappa\lambda}$. Therefore, either r or p_r shows the exponential growth with the increase of the affine parameter $|\lambda|$ depending on the sign of λ. Here, we

consider λ to be positive. This implies the exponential growth of radial motion, which can be attributed to the appearance of chaos in an integrable system when it comes to the influence of the horizon. This can be expected as in GR, even a photon can have unstable circular motion, which is not expected in Newtonian approximation [253]. Note that the actual trajectories which will be evaluated and investigated later part of the paper are highly non-linear in four-dimensional phase space. We shall show explicitly that this is indeed the case by keeping this particle in a harmonic potential and allowing it to move along the θ direction as well. In this situation, it may be worth pointing out that the Lyapunov coefficient (λ_L) is bounded as [226]:

$$\lambda_L \leq \kappa \tag{2.9}$$

where the maximum Lyapunov exponent value if defined as

$$\lambda_{L,max} = \lim_{\lambda\to\infty} \frac{1}{\lambda} \ln\left[\frac{\delta r(\lambda)}{\delta r(0)}\right] \tag{2.10}$$

and $\delta r(\lambda)$ represents the separation between two infinitesimal close trajectories at time parameter λ. As we are considering the null paths, notion of "time" parameter is not so obvious like the case of timelike geodesics. Proper time can not be used as a valid parameter since it vanishes along the null path. In this case the four momentum $p^a = dx^a/d\lambda$ is chosen in such a way that the parameter λ turns out to be affine one (see analysis around Eq. (3.62) of [253]). The momentum components, appeared in Eq. (2.4), are defined in this way. Since p^a is a tensor, the parameter λ needs to be a scalar and hence it does not change under coordinate transformation. So the Lyapunov exponent defined here does not has any coordinate dependence. Now, if one considers the quantum nature of the black hole, then it has a temperature, given by the Hawking expression $T = \hbar\kappa/2\pi$. In that case, the above bound reduces to a very well known form $\lambda_L \leq 2\pi T/\hbar$. This was first mentioned in [226] for the SYK model.

There is a very interesting connection with the above radial null geodesic (2.7) with the Hawking effect in the context of tunneling mechanism [54, 170, 171]. It must be noted that precisely this path has been used to find the tunneling probability from the horizon for the outgoing particles. One finds that this is non-zero and leads to Hawking radiation with the temperature mentioned above. Therefore, after escaping from the horizon, the radiated particles may exhibit chaotic motion due to the influence of the horizon as well as the perturbation induced by the presence of other objects in the universe. Hence the current analysis implies that the horizon not only radiates it also makes the radiation chaotic.

With this, let us now confirm if the presence of the horizon really creates chaos in the system. For that we consider two harmonic potentials $(1/2)K_r(r-r_c)^2$ and $(1/2)K_\theta(y-y_c)^2$ along r and θ directions, respectively. Now, one thing is worth to mention here that in our discussion, we are not considering the massless particle to be a harmonic oscillator itself. Rather we assume that particle is trapped under a hramonic potential. This situation is not new. Such a theory has been studied earlier in various cases; e.g. propagation of optical beam with harmonoic potential [254], relativistic massless harmonic oscillator [255]. Here $y = r_H\theta$, K_r and K_θ are spring constants while r_c and y_c are the equilibrium positions of these two harmonic potentials. The massless particle is initially under these potentials. Now, this system is kept under the influence of the black hole horizon as well. Our aim is to investigate the collective impact of the horizon on this integrable system, particularly the nature of the particle trajectories. This type of model was initially suggested in [220] for massive particle. Here we choose the form of black hole metric $f(r)$ as (2.6). Now, if the particle moves under the influence of these potentials under the background (2.3) then the total energy of this particle is

$$E = -\sqrt{1-f(r)}\; p_r + \sqrt{p_r^2 + \frac{p_\theta^2}{r^2}} + \frac{1}{2}K_r(r-r_c)^2 + \frac{1}{2}K_\theta(y-y_c)^2 \tag{2.11}$$

and correspondingly, the equations of motion will have the form as

$$\dot{r} = \frac{\partial E}{\partial p_r} = -\sqrt{1-f(r)} + \frac{p_r}{\sqrt{p_r^2 + \frac{p_\theta^2}{r^2}}}\,; \tag{2.12}$$

$$\dot{p}_r = -\frac{\partial E}{\partial r} = -\frac{f'(r)}{2\sqrt{1-f(r)}}p_r + \frac{p_\theta^2/r^3}{\sqrt{p_r^2 + p_\theta^2/r^2}} - K_r(r-r_c)\,; \tag{2.13}$$

$$\dot{\theta} = \frac{\partial E}{\partial p_\theta} = \frac{p_\theta/r^2}{\sqrt{p_r^2 + p_\theta^2/r^2}}\,; \tag{2.14}$$

$$\dot{p}_\theta = -\frac{\partial E}{\partial \theta} = -K_\theta r_H(y-y_c)\,. \tag{2.15}$$

In the above, the interaction between the harmonic potentials and the black hole space-time has been taken as very weak so that this can be ignored compared to the other terms in (2.11). These are the main equations which we will use to study the motion of the particle numerically.

2.3 Kerr black hole

After having the discussion on the effect of the SSS black hole on the particle in this section, we investigate the effect of rotation of the black hole on the overall dynamics of the system. For this, we can proceed in a similar way as we did for SSS. The Kerr metric in dragging Painleve coordinate is given in [151]. Due to the large size of the equations, the metric and the trajectories for this case have been provided in Appendix 2.A. It may be noted that here also if one concentrates only on the radial trajectories, it is given by (setting $\theta = 0$ and $p_\theta = 0$ in eq. (2.A.11) of Appendix 2.A)

$$\begin{aligned}\dot{r} &= 1 - \sqrt{\frac{a^2 r + 2r_H^3 - r r_H^2}{r_H(a^2 + r_H^2)}} \\ &= 1 - \sqrt{1 - 2\kappa(r - r_H)} \simeq \kappa(r - r_H)\,,\end{aligned} \tag{2.16}$$

where,

$$\kappa = (r_H^2 - a^2)/(2r_H(r_H^2 + a^2)). \tag{2.17}$$

Note that in this case also we are getting the same radial equation in the near horizon limit. So again, the same solution. As a result of this, the Lyapunov coefficient bound would be given by (2.9). Therefore we can see that the rotating black hole also appears to infuse chaotic fluctuations in the motion of particles. In the next section, we will ascertain this observation by numerically solving the full set of dynamical equations and will also investigate the detailed influence of the rotation on the chaotic dynamics of the particles.

Before going to the numerical analysis, it is very useful to check if any other external potential (like due to the backreaction of the different fields on the space-time) can affect the bound (2.9) on the Lyapunov exponent. For that, suppose we consider an arbitrary potential which is a function of radial coordinate only, i.e. $V(r)$. This assumption is very much convenient for more realistic potentials, made by some other fields condensation with a back reaction to the gravity metric one usually encounters. As for example, in the case of scalar fields, the potential near to the horizon is of the form $\ln(x/C_0)$, while, for electrostatic case, it is proportional to x [220], where $x = r - r_H$ and C_0 is a positive constant. Under these circumstances, the equations of motions for SSS case will be given by (2.12) – (2.15) with harmonic term in (2.13) will be replaced by $(-dV/dr)$. With this, we find that there will be no contribution of the potential term in the Eq. (2.15). Now to understand the behaviour of radial motion, as earlier, we need to concentrate only on the radial equation by setting $p_\theta = 0$. Since we are using the massless condition, it can be

noted that although the equation corresponding to $\dot{p_r}$ will be affected by the term like $dV(r)/dr$, the equation of $\dot{r}$ (Eq. (2.12)) will not get affected as it is independent of p_r. Hence the motion along the radial direction will remain unaffected by introducing any arbitrary potential of the form $V(r)$. Therefore the solution of $\dot{r}$ will always be given by that of Eq. (2.7), and correspondingly the Lyapunov exponent is bounded by the surface gravity κ. However, for the massive particle mass factor will appear in the equation of $\dot{r}$ and the form of $V(r)$ will affect the motion in the radial direction as it will not be independent of p_r. As a result, the solution of $\dot{r}$ will get changed and then this change will certainly appear in the bound of λ. These particular features have been explicitly discussed in [220]. Therefore overall, we find that the addition of any radial potential will not affect the upper bound of the Lyapunov coefficient for massless particles. Arguing on the similar line, one can check that addition of the above mentioned potential $V(r)$ will also not affect the bound of Lyapunov exponent in the case of Kerr Black Hole (See equations (2.A.11) – (2.A.14)).

2.4 Numerical Analysis

The last section was mainly dedicated to show that there is some instability in the radial trajectory of the particles whenever the system comes under the influence of the horizon. However, this claim will be more firm if we can show the presence of chaos numerically. Therefore, the present section will be more focused on the numerical sides of our analysis. The first pivot of our analysis will be the study of the Poincaré sections of the system. In the later part, our main focus will be on studying the Lyapunov exponents and Power spectral density (PSD) of the system.

2.4.1 Poincaré sections

In the present numerical analysis, we shall particularly concentrate on the study of Poincaré maps or Poincaré sections. Poincaré map is defined as the intersection of a periodic orbit in the state space of a continuous dynamical system with a lower-dimensional subspace. The essential idea of these maps, or rather these sections, is to boil down the way we represent a dynamical system. However, the system has to have some certain properties for this, namely to return to some region in its state space from time to time. This is fulfilled if the system is periodic, but it also works with chaotic dynamics. Here, in this case, to draw the Poincaré map, we adopt the polar plane ($\theta = 0$) as a Poincaré section and plot the points on (r, p_r) plane when the particle crosses the Poincaré section with $p_\theta > 0$. If the motion is not chaotic, the plotted points will form a closed curve in the two-dimensional $(r - p_r)$ plane. The reason for that is that a regular orbit will move on a torus in the phase space, and the curve is the cross-section of the torus. Now, if the orbit is chaotic, some of these tori will be broken, and the Poincaré map does not consist of a set of closed curves, but the points will be distributed randomly in the allowed region. Hence, from the distribution of the points, we can judge whether the motion is chaotic or not.

Now, in the last section, we analytically showed that the presence of black hole horizon induces the exponential growth of the radial trajectory of the particles, which indicated the chaotic behaviour for both SSS and Kerr black holes. In this section we ascertain the claim by analyzing the Poincaré section of the system obtained by solving the dynamical equations of motion for SSS (Eqs. 2.12-2.15) and Kerr (see Eqs. (2.A.11)–(2.A.14) of Appendix 2.A) black holes. First, we present Poincaré sections for the SSS black hole and then those for the Kerr black hole in which we systematically analyse the effects of the rotation parameter on the chaotic fluctuations.

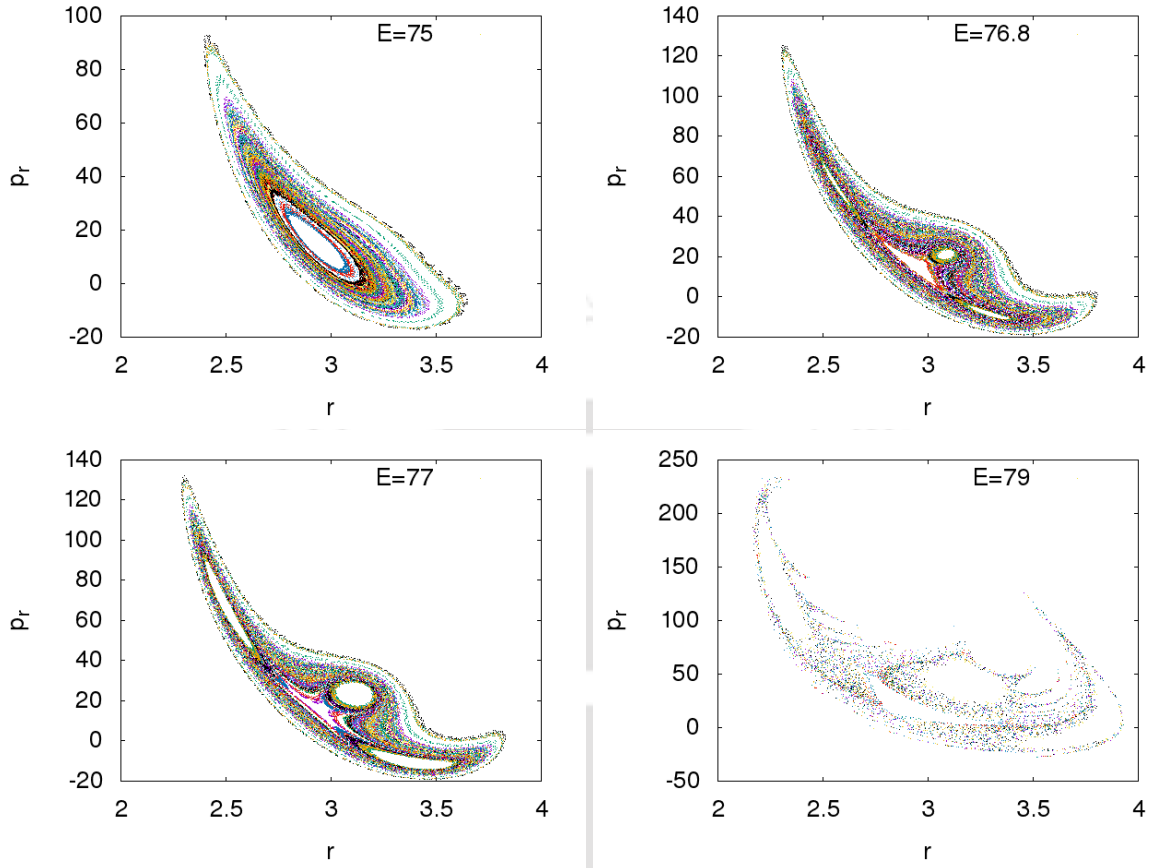

Figure 2.1: (Color online) The Poincaré sections in the (r, p_r) plane with $\theta = 0$ and $p_\theta > 0$ at different energies for the SSS black hole. The energies are $E = 75$, $E = 76.8$, $E = 77$, and $E = 79$. The other parameters are $r_H = 2.0$, $\kappa = 0.25$, $r_c = 3.2$, $\theta_c = 0$, $K_r = 100$ and $K_\theta = 25$. For large energy the KAM Tori break and the entire region gets filled with the scattered points indicating the presence of chaos.

For SSS black hole model, the dynamical equations (Eqs. 2.12-2.15) are numerically solved using the fourth order Runge-Kutta scheme with fixed $d\lambda = 10^{-3}$. For present study we have considered $K_r = 100$, $K_\theta = 25$, $r_H = 2$, $\kappa = 0.25$, $r_c = 3.2$ and $\theta_c = 0$. The variables r, θ, and p_r are initialized with the random numbers and p_θ is obtained from Eq.(2.11) for a fixed energy E.

In Fig. 2.1 we show the Poincaré section of the particle trajectory (for SSS type black hole) projected over the (r,p_r) plane for different energies. The section is defined by the condition $p_\theta > 0$ and $\theta = 0$. We have considered the energies $E = 75, 76.8, 77,$ and 79 as indicated in the plots. For low energy $E = 75$ the Poincaré section exhibits the regular KAM (Kolmogorov-Arnold-Moser) tori [256] and the corresponding orbit is mainly confined near the center of the harmonic potential ($r_c = 3.2$). Different colors

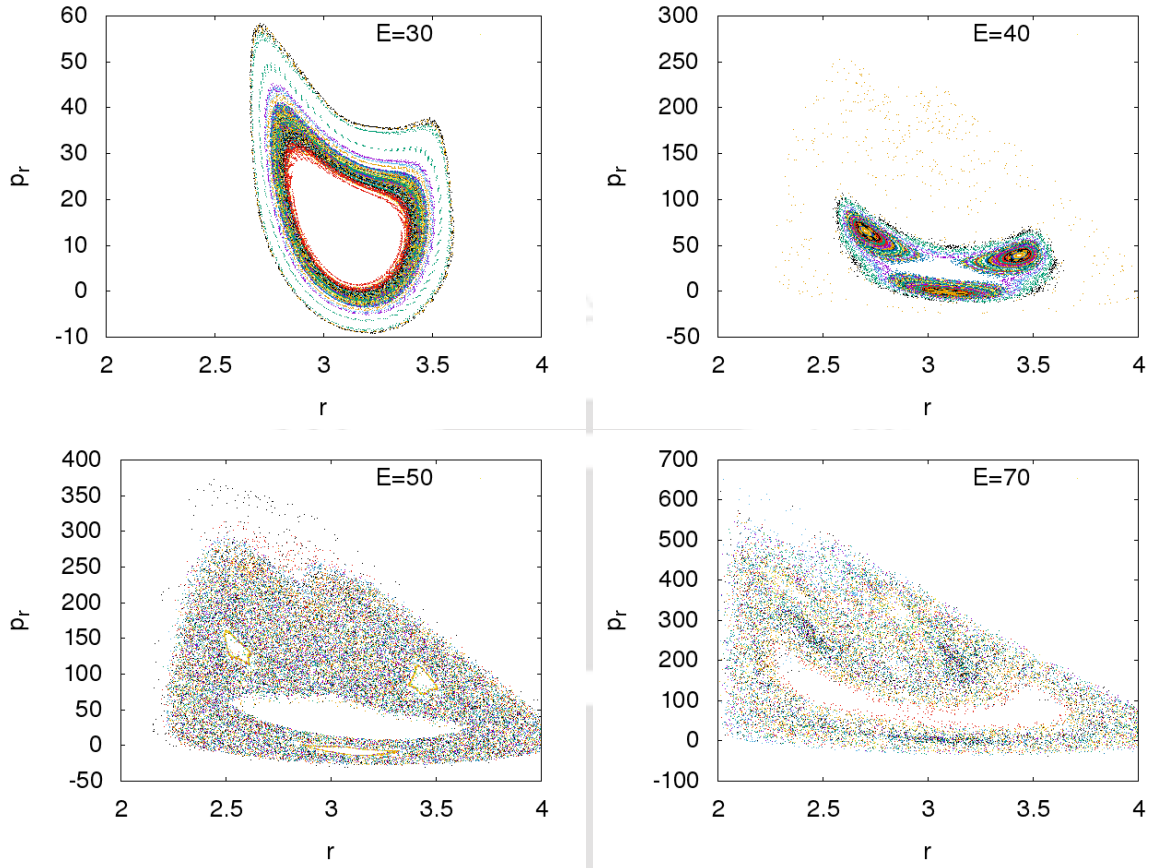

Figure 2.2: (Color online) The Poincaré sections in the (r, p_r) plane with $\theta = 0$ and $p_\theta > 0$ for different energy for the Kerr black hole model at fixed rotation parameter $a = 0.9$. The energies are $E = 30$, $E = 40$, $E = 50$, and $E = 70$. The other parameters are same as in Fig. 2.1. For large energy the KAM Tori break and the entire region is filled with the scattered points indicating the chaotic trajectory of the particles.

in the figures indicate the trajectory of the particles for different initial conditions. As the total energy of the system is increased, the trajectory approaches near the black hole horizon ($r_H = 2$); as a consequence of this, KAM tori starts getting distorted and appeared to be pinched, as shown in the figure for E=76.8 and E=77. Further increase in the energy ($E = 79$) results in the complete breaking of regular Tori and the appearance of scattered points in the plane. This feature of the Poincaré section supports the chaotic nature of the particle trajectory near the horizon, as shown in the last section. Due to the presence of the horizon, we have some upper bound on the energy. At present, increasing the energy further above $E = 79$, we find that during time evolution, r becomes less than the position of the horizon ($r_H = 2$) that brings numerical instability in our calculation.

In order to see the effect of the rotation of the black hole on the particle dynamics

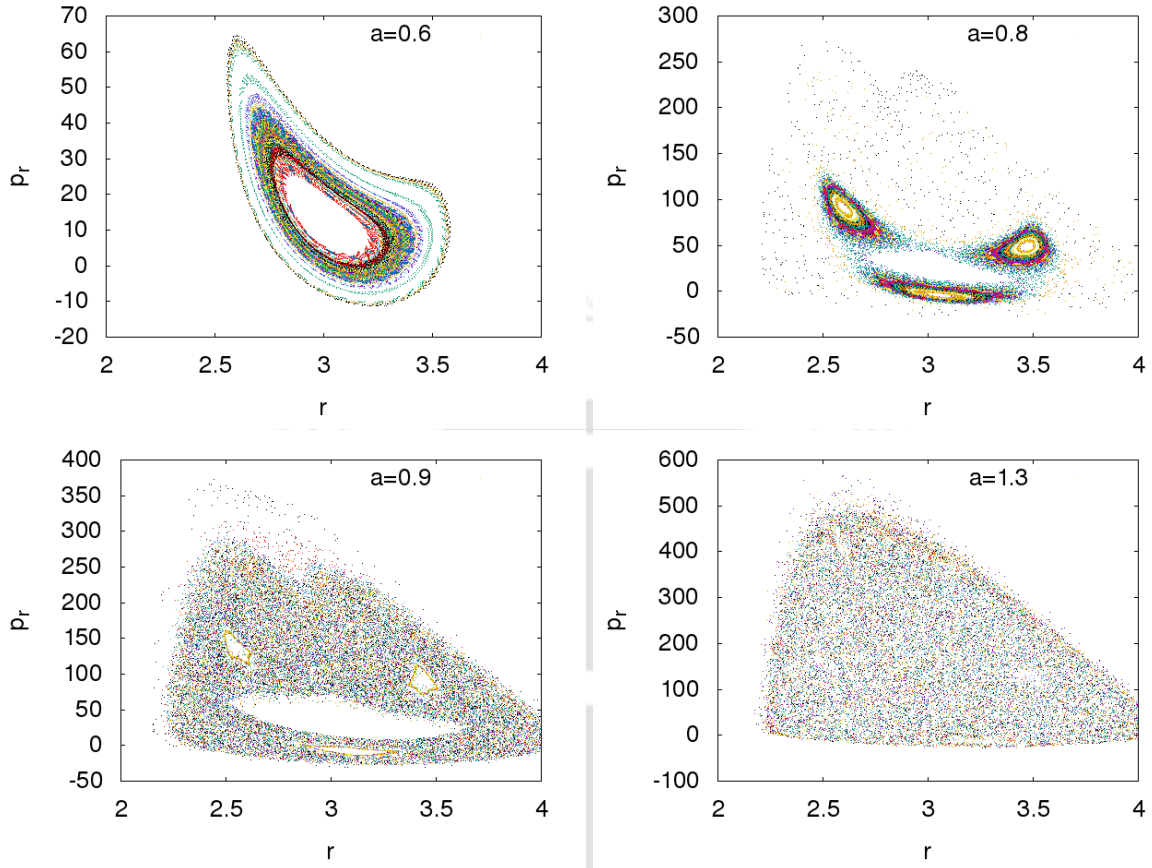

Figure 2.3: (Color online) The Poincaré sections in the $(r,\ p_r)$ plane with $\theta = 0$ and $p_\theta > 0$ for fixed energy E=50 with different rotation parameter a. The rotation parameter $a = 0.6$, $a = 0.8$, $a = 0.9$, and $a = 1.3$, respectively from the top to the bottom. The other parameters are $r_H = 2.0$, and $K_r = 100$ and $K_\theta = 25$. Increase in the rotation induces the chaos in the dynamics of the particles.

next we consider the Kerr black hole model. The corresponding dynamical equations (see Eqs. (2.A.11)–(2.A.14) of Appendix 2.A) are solved using the Runge-Kutta fourth-order. The initial conditions are chosen in a similar line as discussed for the SSS model. In Fig. 2.2 we show the Poincaré sections for different energies with fixed rotation parameter $a = 0.9$. All the other parameters are considered the same as the SSS model. We observe a similar feature of the KAM tori upon the increase of energy for the Kerr black hole as we observed for the SSS model. The regular KAM tori appeared at low energy $E = 30$ gets squeezed along with the appearance of some region filled with the scattered points as the energy is increased to $E = 40$. At high energy ($E = 50, 70$), as the surface of the trajectory approaches near the horizon, there is a complete breaking of these tori which is quite evident with the filling of the region with the random points.

Interestingly here, we obtain that the chaotic nature appears at relatively lower energy than those obtained with the SSS black hole. This particular feature suggests that the rotation of the black hole may introduce more chaotic fluctuations in the trajectories of the particles approaching towards the horizon. We confirm this by analysing the nature of the particle trajectory by changing the rotation parameter a for fixed energy $E = 50$. In Fig. 2.3 we plot the Poincaré section in the plane (r, p_r) for different rotation parameters $a = 0.6, 0.8, 0.9$, and 1.3 at fixed energy $E = 50$. We clearly find that the increase in a introduces chaotic fluctuations in the trajectories, and at very high rotation $a = 0.9, 1.3$, the trajectory becomes fully chaotic. The nature of the appearance of chaos in the system upon an increase in the a for fixed energy appears to be the same as those obtained while increasing the energy for fixed $a = 0.9$ (see Fig. 2.2).

So far, our numerical calculation is based on the near horizon approximated metric. This has been done as we are interested in investigating the influence of the horizon on particle dynamics when it is very near to the horizon. In this region, we must have $r - r_H < r_H$. It may be noted that the condition is well incorporated in the simulations as all the data points in the figures are confined within such a range. In a similar context, the same type of approximation has also been taken recently in [220]. Here we emphasise that the use of near horizon approximation has nothing to do with the appearance of chaotic behaviour in the system. To confirm this fact, we also perform the same numerical analysis without any approximation in the metric coefficients (please see Appendix 2.B). The Poincare sections (see Figures 2.9 and 2.10) again show similar behaviour. Hence the appearance of the chaotic nature of the particle motion in the presence of the horizon is an inevitable fact.

2.4.2 Lyapunov exponents

In literature the Lyapunov exponent of a dynamical system is defined as the quantity that characterizes the rate of separation of infinitesimally close trajectories [257]. In phase space if we consider two trajectories with initial separation δx_0, the rate of divergence within the linearized approximation is given by

$$|\delta x(\lambda)| \approx e^{\lambda_L \lambda} |\delta x_0| \tag{2.18}$$

where λ_L is the Lyapunov exponent and the maximum Lyapunov exponent is defined in Eq. (2.10). In this situation, it may be worth to point out that the value of the Lyapunov exponent has an upper bound which was first mentioned in [226] for the SYK model. For

our system the Lyapunov exponent (λ_L) is bounded by

$$\lambda_L \leq \kappa \ , \tag{2.19}$$

where κ is the surface gravity of the black hole as we mentioned earlier. We shall explicitly show in chapter 4 about this bound using Monodromy matrix. Now, in order to justify this upper bound for our system, we present the numerically computed Lyapunov exponents for different cases. We have adopted the standard algorithm to compute the largest Lyapunov exponent, which is related to the rate of separation of the trajectories for two nearby points [257]. We consider the energy $E = 78$ for the SSS type black hole for which we obtain the full chaotic behaviour of the motion of the particle. Figure 2.4 shows the time variation of the largest Lyapunov coefficient at energy $E = 78$. The Lyapunov exponent settles to a positive value (~ 0.04) which supports the chaotic nature of the particle motion. In addition, the value is well below the upper bound $\kappa (= 0.25)$.

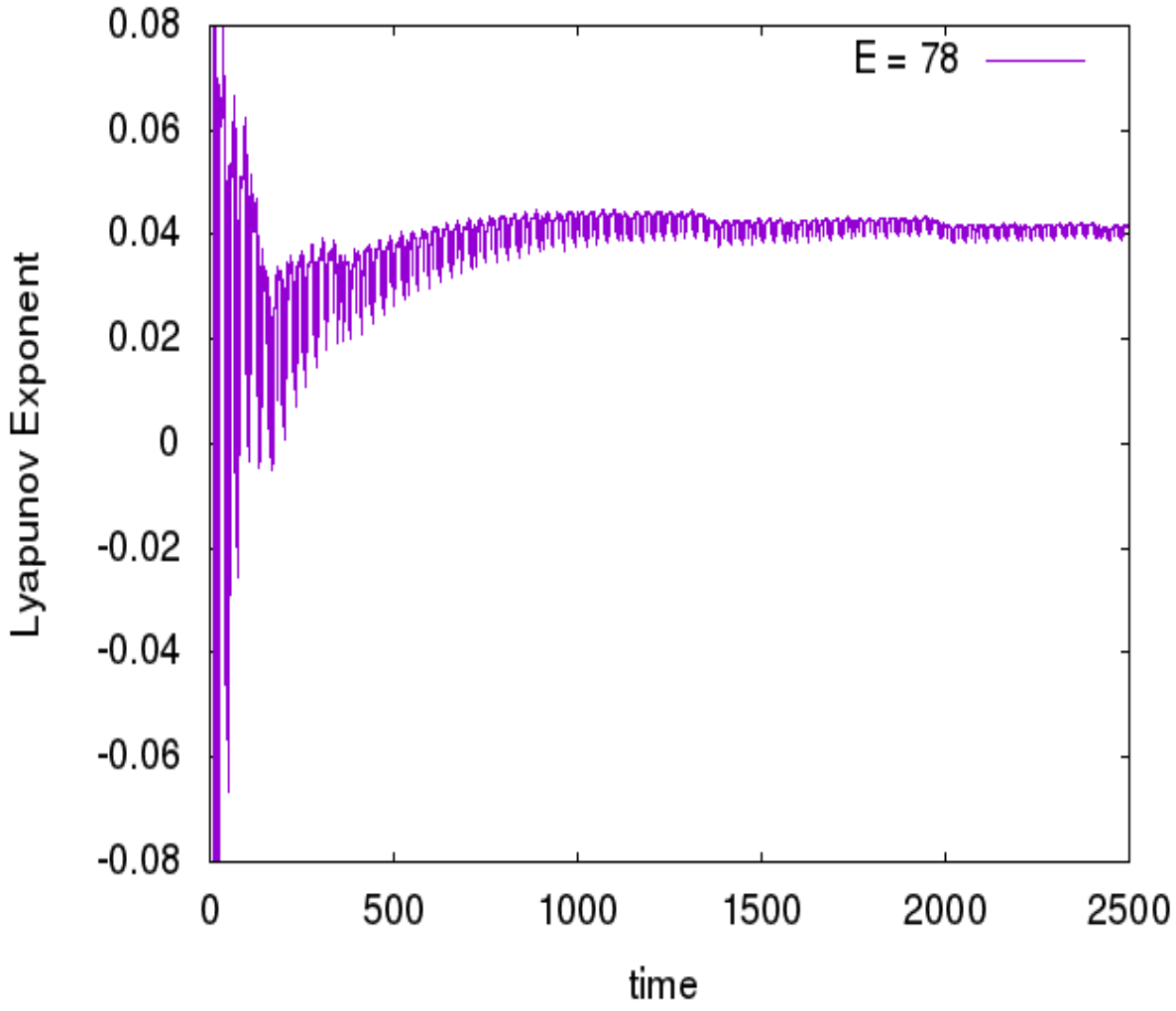

Figure 2.4: (Color online) Largest Lyapunov exponent for the SSS black hole at the energy value $E = 78$. The exponent settles at positive value ~ 0.04.

In the case of the Kerr black hole, the upper bound on the Lyapunov exponent depends on the rotation parameter (see Eq. (2.17)). In Fig. 2.5 we show the time evolution of the largest Lyapunov exponent corresponding to the particle trajectory for Kerr black hole for different rotation parameter ($a = 0.6, 0.8, 0.9, 1.3$). Interestingly we observe that the steady-state Lyapunov exponent increases on an increase of the rotation parameter that supports our observation that the rotation of the black hole induces more chaotic fluctuations in the motion of the particles. In addition, we find that the obtained value of the Lyapunov exponents for different values of the a is much lower than the corresponding upper bound (see Eq. (2.17)) where the upper bounds for different values of a are

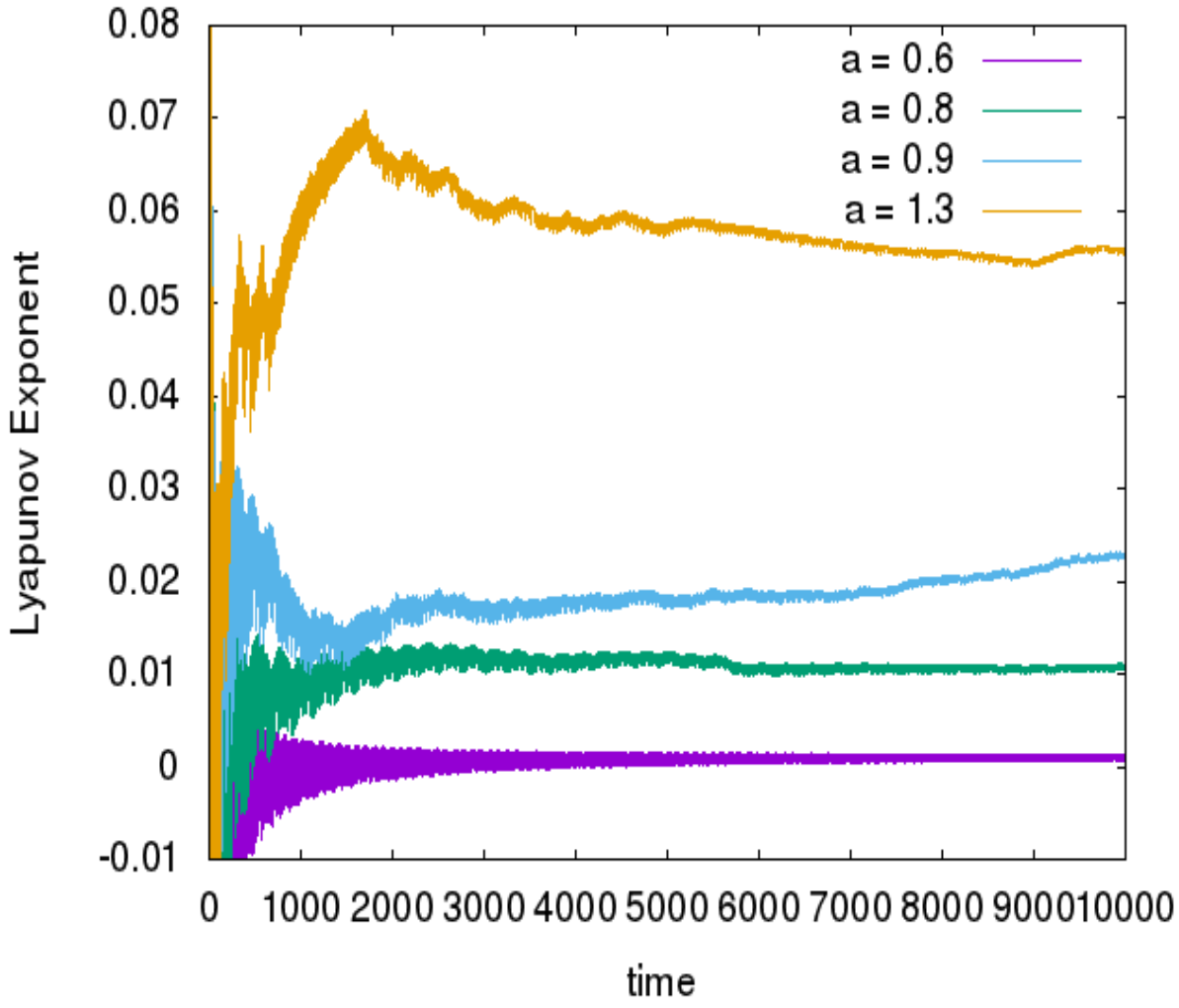

Figure 2.5: (Color online) Largest Lyapunov exponents for the Kerr black hole for different values of the rotation parameter $a = 0.6, 0.8, 0.9$ and 1.3 at constant energy $E = 50$. The exponents increases on increase of a.

given below (here $r_H = 2$):

- for $a = 0.6$ we have $\kappa = 0.299$,
- for $a = 0.8$ we have $\kappa = 0.345$,
- for $a = 0.9$ we have $\kappa = 0.377$,
- and for $a = 1.3$ we have $\kappa = 0.615$.

2.4.3 Power Spectral Density (PSD)

To get a deeper understanding about the dynamical behavior of our composite system whenever it comes under the influence of the horizon, we systematically investigate the evolution of the radial coordinate, $r(\lambda)$ with respect to the affine parameter (λ). To get an extensive idea of the trajectory of the system and the deeper understanding of the onset chaotic behavior of the system, the power spectral density (PSD) is analyzed which is defined as [258],

$$\text{PSD} = \frac{1}{2\pi\mathcal{N}}|r(\mathcal{N}, f, \Delta\lambda)|^2 \,, \tag{2.20}$$

where $r(\mathcal{N}, f, \Delta\lambda)$ is the discrete Fourier transform of $r(\lambda)$ evaluated at $\lambda = k\,\Delta\lambda$ ($k = 0, 1, ..., \mathcal{N}$ and $\mathcal{N}$ is the length of the discrete affine parameter series).

One crucial fact is worth mentioning here that PSD associated with regular dynamics is recognizable as simple sharp line spectra at some fundamental frequencies of the system and simple sharp lines of their lower order combinations and overtones. These persist with increasing time parameter (λ in this case). However, PSD associated with chaotic dynamics are notoriously grassy and erratic, having many incompletely separated peaks with no obvious pattern of central frequencies and amplitudes. Specific peaks do not persist for arbitrary large time parameter, and increasing time parameter sufficiently causes peak to split into two or more subpeaks. Moreover, the PSD of chaotic dynamical systems is found to exhibit an exponential decay which is one of the most distinguishable characteristics of identifying any chaotic system.

Now, in this section our particular interest is to investigate how the radial coordinate ($r(\lambda)$) of the particle motion changes with the change of the total energy of the composite system (E) by studying PSD. First, we shall study the case of SSS horizon where our aim is to look for the dynamical changes into our composite system when it comes very near to the SSS horizon. We have already obtained that as we increase the value of the total energy of the composite system, it starts to come under the influence of horizon. Therefore, in order to see how the dynamics of our composite system changes when it comes under the influence of the horizon, we start increasing the value of the total energy of the system (E). Next, we shall study PSD in the Kerr spacetime in order to see how the dynamics of the system changes with the change of the total energy and with the change of the rotation parameter.

Now, we have the expression of the total energy of our composite system (Eq. (2.11)). Next, in the background of static spherically symmetric space-times we plot the figures of PSD (Fig. 2.6) for different values of energy (E).

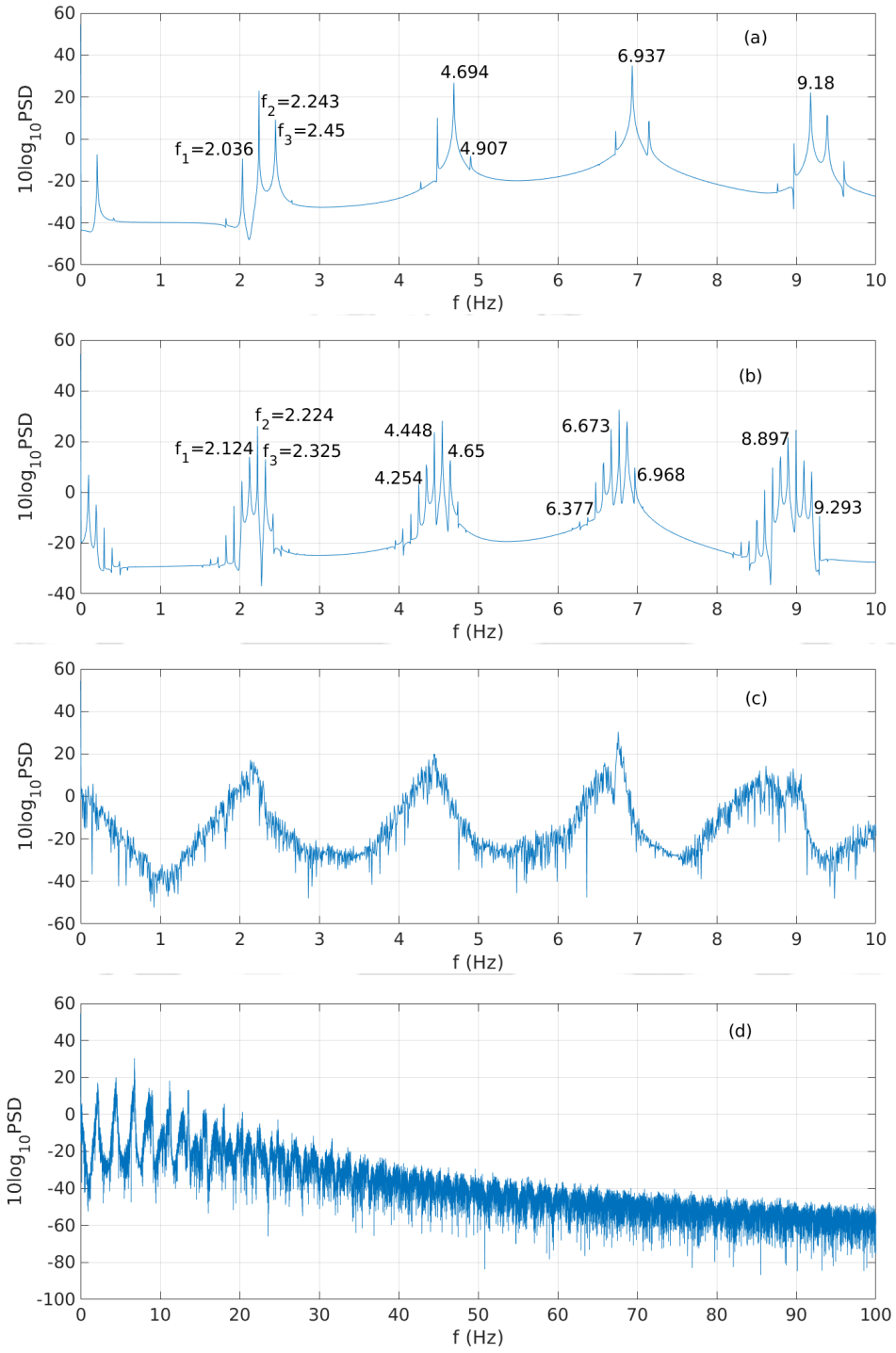

Figure 2.6: (Color online) PSD for the SSS black hole at different values of energies with $\theta = 0, p_\theta > 0, K_r = 100, K_\theta = 25, r_c = 3.2, \theta_c = 0, \kappa = 0.25, r_H = 2.0$. The enrgies are $(a)E = 75, (b)E = 77, (c)E = 78.5$. Upto $E = 75$, only f_1, f_2 and f_3 and their harmonics are present but for higher values of energy i.e from $E = 77$ onwards more frequencies start populating the spectrum. At $E = 78.5$, the highly population of frequency spectrum and the exponential decay indicate (d) the onset of chaos.

Now, let us discuss in a more detailed manner in order to see what happens when the total energy of the system (E) is changed. We have the equations of motion of the particle (2.12-2.15), and after solving these equations numerically, we plot the PSD diagrams using (2.11) for different values of the total energy of the system ($E = 75,\ 76.8,\ 77$ and 79). The values of the other parameters are set as before (mentioned in Section 2.4.1). Now in Fig. 2.6 we see for low energy value of the total energy of the system ($E = 75$) the system contains only three frequencies and their harmonics (see Fig. 2.6(a)). As we found in the earlier section that for the lower value of the energy $E = 75$, the Poincaré sections are periodic in nature, which means the effect of the horizon is yet to appear into the system. The appearance of PSD peak at $f_2 \simeq 2.243$ is the fundamental frequency, and the other frequencies at 4.694, 6.937 and 9.18 are the harmonics of that fundamental frequency. The appearance of other frequencies of oscillations, i.e. $f_1,\ f_2$ etc., in the evolution of $r(\lambda)$, indicates our system is quasi-periodic in nature. As we further increase the value of E, we see that more frequencies near $f_1,\ f_2$ and f_3 start getting populated (see Fig. 2.6(b) and 2.6(c)). At the higher value of the energy, i.e. at $E = 78.5$ PSD shows a fully populated pattern over the frequency range and interestingly, there is an exponential decaying nature of it which is the distinguishing character of the onset of chaos. Thus for $E = 78.5$, the evolution of $r(\lambda)$ displays the chaotic behaviour of the particle dynamics in the near-horizon region. Hence, we obtain a series of transitions in the dynamics of our system, namely from periodic to quasi-periodic and finally to chaotic dynamics, as the total energy of the system (E) is increased. Therefore, it results in a quasi-periodic route to chaos.

Similarly, we have also studied the PSD for the Kerr case (see Fig. 2.7 and Fig. 2.8). We have already found the equations of motion of the particle (Eq. (2.A.11) - Eq. (2.A.14)) in the Kerr background. Now, in Fig. 2.7 we see that for the lower energy value of the total energy of the system ($E = 30$), the system has some quasi-periodic nature. However, as we go for the higher values of the system energy (for $E = 60,\ 70$), PSD diagrams show a fully populated pattern over the frequency range and the exponential decaying nature, which is the distinguished character of the onset of chaos as we mentioned earlier. We have already learned that the increment in the system energy represents that our probed particle is approaching the horizon. Therefore, the increment in the population of the frequencies in the PSD diagram with the increment in the energy value suggests that as our system approaches the horizon, it results from a quasi-periodic nature to a chaotic nature.

Next, we have studied the effect of the rotation parameter (a) in the particle motion near the horizon region in Fig. 2.8 through analysing PSD. We can see from the Fig. 2.8 that for the lower value of the rotation parameter (for $a = 0.6$) the system retains its quasi-periodic nature. However, as we increase the values of a, more frequencies start appearing into the PSD (for $a = 0.8$) and for large values of the rotation parameter ($a = 0.9$ and 1.3) the PSD diagrams become highly populated in the frequency range and the exponential decaying nature is also visible. Therefore, it infers that as the rotation parameter increases in the Kerr spacetime, the system turns its nature from a quasi-periodic to chaotic nature.

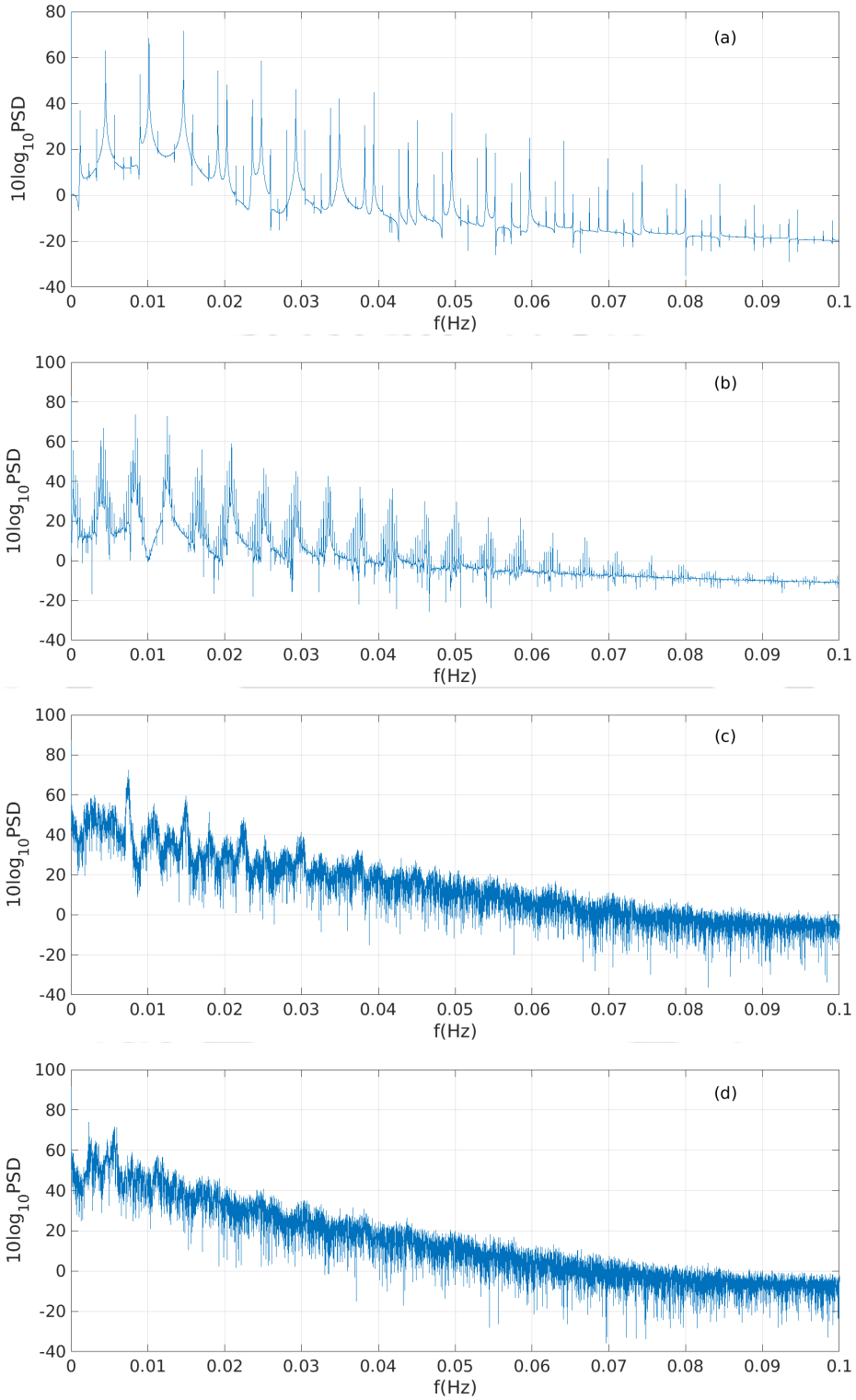

Figure 2.7: PSD for Kerr black hole at different values of energy at fixed rotation parameter $a = 0.9$. The energies are $(a)E = 30, (b)E = 40, (c)E = 50$ and $(d)70$. One can clearly see as the value of energy increases more frequencies start populating the spectrum. The highly population of frequency spectrum and the exponential decay ((c) and (d)) indicate the onset of chaos.

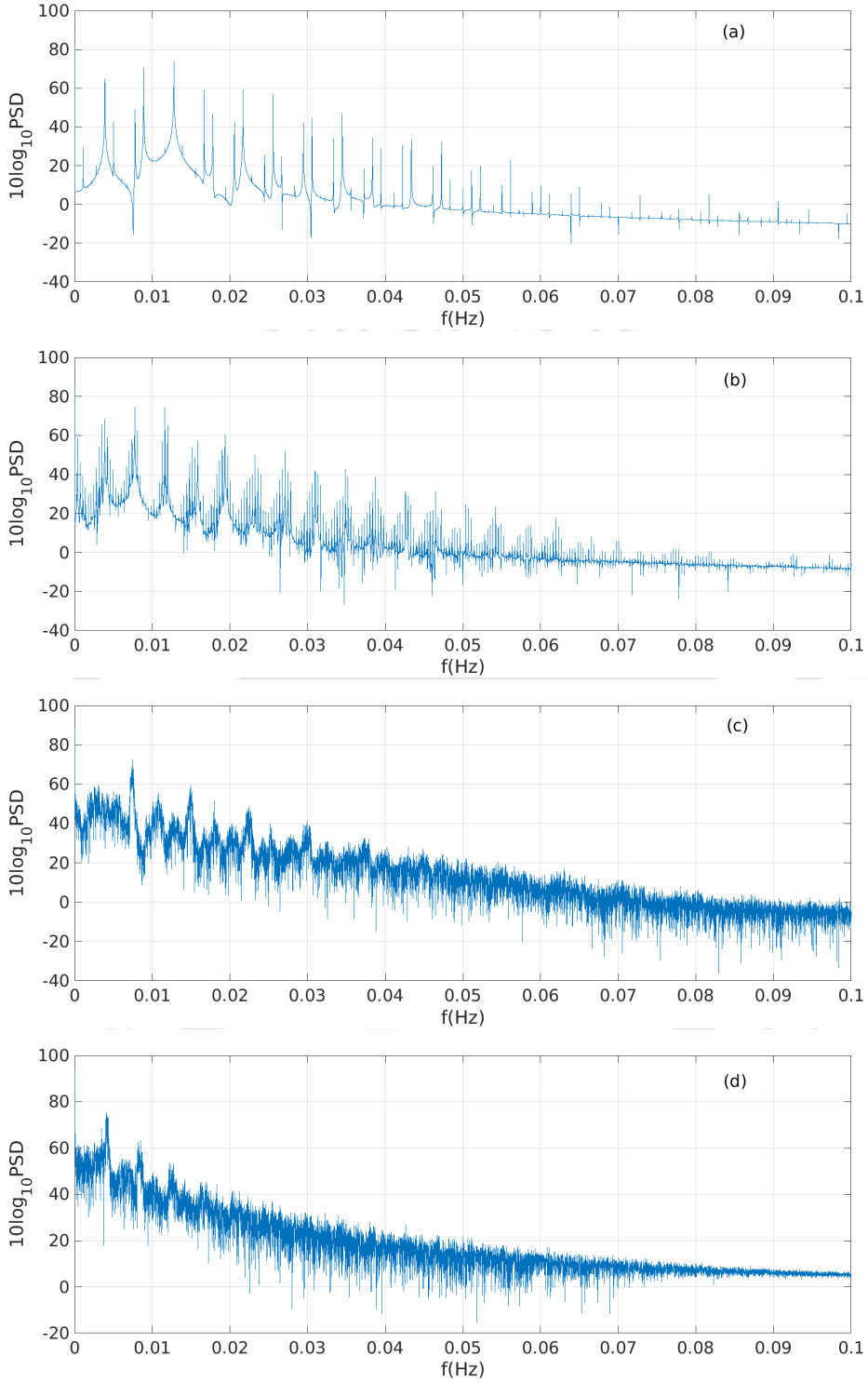

Figure 2.8: PSD for Kerr black hole at different values of rotation parameters for a fixed value of energy $E = 50$. The rotation parameter values are $(a)a = 0.6$, $(b)a = 0.8$, $(c)a = 0.9$ and $(d)1.3$. One can clearly see as the value of the rotation parameter increases more frequencies start populating the spectrum. The highly population of frequency spectrum and the exponential decay ((c) and (d)) indicate the onset of chaos.

2.5 Summary and Discussions

In this chapter, we have studied the implications of the influence of an event horizon on an integrable system when the system comes under the influence of the horizon. The whole study has been done in the classical picture. Now, let us briefly discuss and summarise our findings in this section.

The trajectories of a massless and chargeless particle in a very near horizon region have been studied. The theoretical analysis showed that the radial motion is an exponentially increasing function of the time parameter. This indicates that the horizon may influence chaotic behaviour in the motion of a particle in an integrable system when it interacts with the horizon of a black hole. Carefully investigating the situation in the presence of harmonic potential, it has been observed that this is indeed the case. We found that the trajectories of the particle trapped in a Harmonic potential which is an integrable system, becomes chaotic in nature after a certain value of the energy of the system. Here both SSS and Kerr black holes cases have been investigated. For the SSS case, the chaos occurs at a particular energy range. Note that our SSS metric is not necessarily restricted to Schwarzschild space-time; rather it incorporates all candidates of this type. Therefore even the SSS analysis is much more general than the earlier ones. Interestingly, we observed that the rotation parameter induces more chaos in the particle motion.

Overall we find that although the dynamics of a particle is integrable in the presence of SSS and Kerr black hole, the addition of harmonic perturbation leads generation of chaos in the system. This is consistent with the KAM theory, which states that the non-linear perturbation in the integrable dynamical system results in the generation of the chaos [256]. There are several examples reported earlier in support of this claim; like the addition of non-linear perturbation in Henon-Heiles potential leads to chaotic behaviour of the system at high energy [259], the appearance of chaos in double pendulum (Hamiltonian) for large oscillation [260] (also see [261] for a discussion in this direction). In our case, for small perturbation, i.e., when the harmonic term is small, we observe a regular tori. These tori break and convert into the scattered points as the energy of the system increases, which indicate an increase in the harmonic perturbation that makes the system chaotic. The same characteristics we also obtained by studying PSD for different values of the energy of the system, which results in a quasi-periodic route to chaos.

In a similar way, one can treat the presence of the black hole like a perturbation for

the particle trapped in the harmonic potential. Again the integrability of the harmonic particle is lost due to the presence of the black hole. The feature of the non-integrability in the dynamics of the particle that arises due to the addition of the harmonic potential (as the perturbation) to the particle energy in the presence of the black hole has been reported in [220] recently. This was done for a massive particle. Here we investigated for the massless one.

In this calculation, the outgoing path is taken to be the geodesics for a zero mass particle for which the radial direction is the null geodesic. This particular path plays an important role in investigating the Hawking radiation as tunnelling phenomenon [54, 171]. It reveals that the horizon not only radiates quantum mechanically but also can influence the trajectories of the particles when they are very near to the horizon where the perturbation can come from the other objects in the universe. If this is the case, then it may be possible that the radiated particles may follow chaotic motion after being escaped from the horizon barrier. Note that due to the complexity of the problem here, we have not been able to provide any rigorous analytical calculations to support the claim. To be more sure about the detailed nature of the effect of the horizon on the chaotic fluctuation, we need to investigate more on this. Also, it must be mentioned that our analysis is completely classical in nature. Probably a systematic calculation based on quantum mechanics may unravel more information about the chaotic behavior of the particles in black hole space-time.

Before concluding, we also mention that in this chapter, the influence of horizon on an integrable system has been investigated. Here for simplicity, the integrable system has been chosen as a massless and chargeless particle trapped in harmonic potentials. Then we allowed it to interact with the horizon of a black hole. The underlying idea is exactly in the spirit of the foundations of equilibrium statistical mechanics. In this subject, we always allow our system, which is under investigation, to interact with other systems (a finite system for microcanonical ensemble and a heat reservoir for canonical ensemble), either thermally or mechanically. In general, it has been assumed that the interaction Hamiltonian is very small (i.e. a weak interaction between the two systems), and hence the total energy of the composite system is the sum of the energies of the individual systems. At the equilibrium, the question is asked as: What is the probability of finding the system, under investigation, having an energy between E to $E+\delta E$ for Microcanonical ensemble while for a canonical ensemble, what is the probability of finding the system in a particular microstate We all know that this information actually encodes the full macroscopic description of the system in terms of a number of accessible

microstates in Microcanonical ensemble or partition function in Canonical ensemble. In this chapter, we are also investigating in the same fashion. We allowed one integrable system to interact with the black hole horizon and investigated the trajectories of a particle in the system. The energy of the composite system is taken as the sum of the energies of the individual system, ignoring the interaction; i.e. any influence of the harmonic potentials on the space-time has not been taken into account. Within this scenario, we found that the composite influence can make particle motion chaotic in nature. Of course, if the interaction is not negligible, then this also has to be taken into account. We leave this for the future.

Appendices

2.A Trajectories in Kerr spacetime

In the Painleve coordinate transformation the Kerr metric can be written in this form [151]:

$$d\hat{s}^2 = -f dt^2 + g dr^2 + 2h dt dr + k d\theta^2 \tag{2.A.1}$$

where,

$$f = \frac{\bigtriangleup \Sigma}{(r^2+a^2)^2 - \Delta a^2 \sin^2\theta} \; ; \tag{2.A.2}$$

$$g = \frac{\Sigma}{r^2+a^2} \; ; \tag{2.A.3}$$

$$h = \frac{\sqrt{2Mr(r^2+a^2)}\Sigma}{(r^2+a^2)^2 - \Delta a^2 \sin^2\theta} \; ; \tag{2.A.4}$$

$$k = \Sigma = r^2 + a^2\cos^2\theta \; , \tag{2.A.5}$$

and $\Delta = r^2 + a^2 - 2Mr$. M is the mass and $a = J/M$ is the angular momentum per unit mass. We call it as rotation parameter. The event horizon is given by $\Delta = 0$. It leads to the location of horizon as

$$r_H = M + \sqrt{M^2 - a^2} \; . \tag{2.A.6}$$

Using $p_a p^a = 0$ and identifying the energy of the massless particle as $E = -p_t$, we find the energy of the particle which is moving through the two harmonic potentials in the above background can be calculated as:

$$E = -\frac{h}{g}p_r + \sqrt{\frac{h^2}{g^2}p_r^2 + \frac{f}{g}p_r^2 + (\frac{1}{k}\frac{fg+h^2}{g})p_\theta^2} + \frac{1}{2}K_r(r-r_c)^2 + \frac{1}{2}K_\theta(y-y_c)^2 \; . \tag{2.A.7}$$

Now since we are interested near to the horizon, expanding $f(r)$ upto the first order one obtains

$$\begin{aligned} f(r) = f(r_H) + (r-r_H)f'(r_H) \quad = \quad & -\frac{a^2\sin^2\theta}{r_H^2 + a^2\cos^2\theta} \\ & + \frac{r_H^4 - a^4\cos^2\theta + r_H^2 a^2 \sin^2\theta}{r_H(r_H^2 + a^2\cos^2\theta)^2}(r-r_H) \; . \end{aligned} \tag{2.A.8}$$

Using this and replacing all the variables in Eq. (2.A.7) the energy turns out to be,

$$E = X - \frac{p_r Y(a^2+r^2)}{2\Sigma} + \frac{1}{2}(y-y_c)^2 K_\theta + \frac{1}{2}(r-r_c)^2 K_r \; , \tag{2.A.9}$$

where

$$X = \sqrt{\frac{p_\theta^2 + p_r^2(a^2+r^2)}{\Sigma}} \; ;$$
$$Y = \sqrt{\frac{(a^2+r_H^2)(a^2+2r^2+a^2\cos 2\theta)(a^2 r - 2(r-2r_H)r_H^2 + a^2 r\cos 2\theta)}{r_H(a^2+r^2)(r_H^2+a^2\cos^2\theta)^2}} \; . \quad (2.A.10)$$

Now the equation of motions are

$$\dot{r} = -\frac{(a^2+r^2)(XY-2p_r)}{2X\Sigma} \; , \quad (2.A.11)$$

$$\begin{aligned} \dot{p_r} \;=\; & -K_r(r-r_c) - \Big[-\frac{r(2X\Sigma - p_r Y(a^2+r^2))}{\Sigma^2} + \frac{1}{4Y\Sigma}\{4rX + \frac{2rp_r^2 - 2rX^2}{X} - 2rYp_r \\ & - p_r(a^2+r^2)(\frac{Y^2\xi}{r\xi+4r_H^3} + \frac{4rY^2}{a^2+2r^2+a^2\cos 2\theta} - 2rY^2)\}\Big] \; , \end{aligned} \quad (2.A.12)$$

$$\dot{p_\theta} = -\Big[\frac{a^2 X\sin 2\theta}{2\Sigma} - \frac{a^2 Y p_r(a^2+r^2)\sin 2\theta}{2\Sigma^2} - \frac{Z}{2r_H\Sigma Y\zeta^3}\Big] - (y-y_c)r_H K_\theta \quad (2.A.13)$$

and

$$\dot{\theta} = \frac{p_\theta}{X\Sigma} \; , \quad (2.A.14)$$

where

$$\begin{aligned} Z &= a^2 p_r^2 (r-r_H)^2(a^2+r_H^2)\Big(a^2(r+2r_H)(1+\cos 2\theta) - 2r_H^2(3r+2r_H)\Big)\sin 2\theta \; ; \\ \zeta &= r_H^2 + a^2\cos^2\theta \; ; \\ \xi &= a^2 - 2r_H^2 + a^2\cos 2\theta \; . \end{aligned} \quad (2.A.15)$$

These equations have been used to study the motion of the particle numerically.

2.B Presence of chaos without near horizon approximation of metric coefficients

Here, for clarity, we present the appearance of chaos without the near horizon approximation of the metric coefficients. For simplicity, a specific SSS has been chosen, which is the Schwarzschild black hole. The Kerr case is also being discussed. This analysis confirms the fact that the horizon in the space-time indeed induces chaotic behaviour in particle dynamics which is not an artefact of the use of truncated form (i.e. near horizon form of metric coefficient), as we did in our main analysis.

2.B.1 Schwarzschild black hole

For the case of Schwarschild spacetime the energy of the particle is given by (2.20) and the equations of motions are (2.12) – (2.15) with $f(r) = 1 - 2M/r$. Here M is the mass of the black hole. Similar to earlier, we again show the Poincare section in (p_r, r) plane.

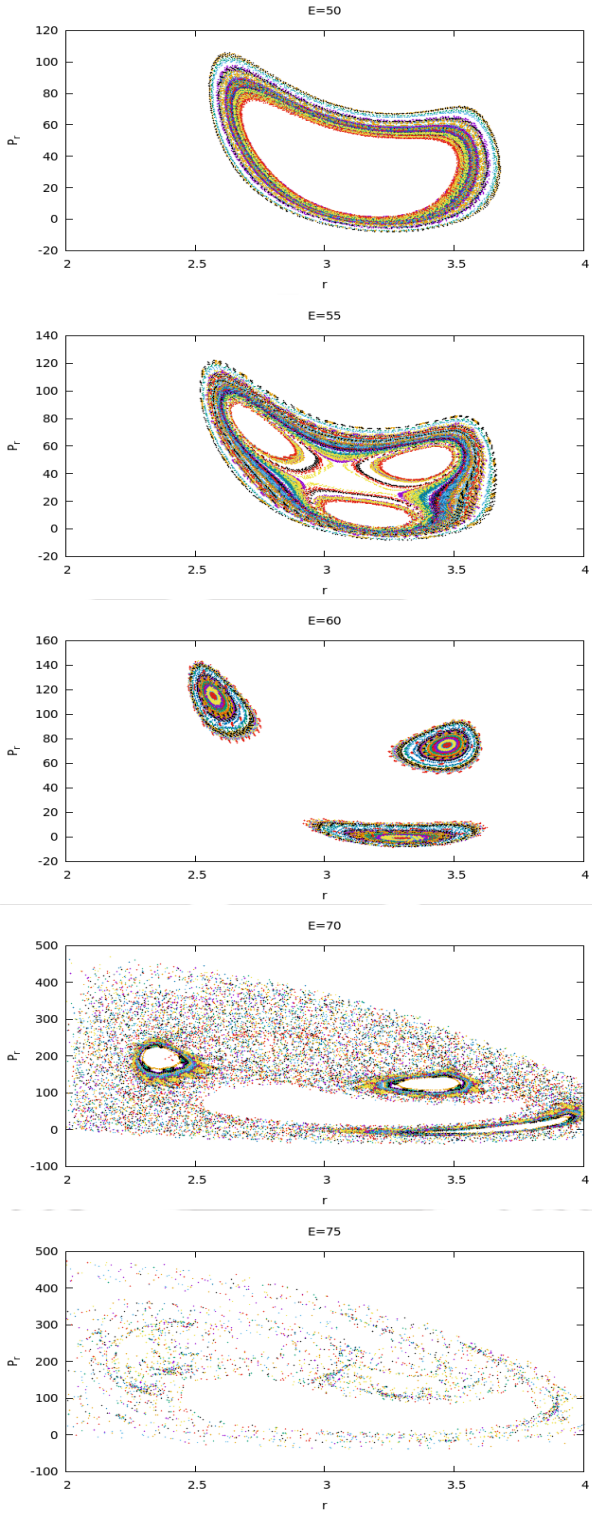

Figure 2.9: (Color online) The Poincaré sections in the (r, p_r) plane with $\theta = 0$ and $p_\theta > 0$ at different energies for the Schwarzschild black hole. The energies are $E = 50$, $E = 55$, $E = 60$, $E = 70$, and $E = 75$. The other parameters are $r_H = 2.0$, $M = 1.0$, $r_c = 3.2$, $\theta_c = 0$, $K_r = 100$, and $K_\theta = 25$. For large energy the KAM Tori break and the entire region gets filled with the scattered points indicating the presence of chaos.

Figure 2.9 clearly shows the presence of chaos in the system after a particular value of energy.

2.B.2 Kerr black hole

Below in Fig 2.10 we show the appearance of chaos in the system in the case of Kerr black hole without the near horizon approximation.

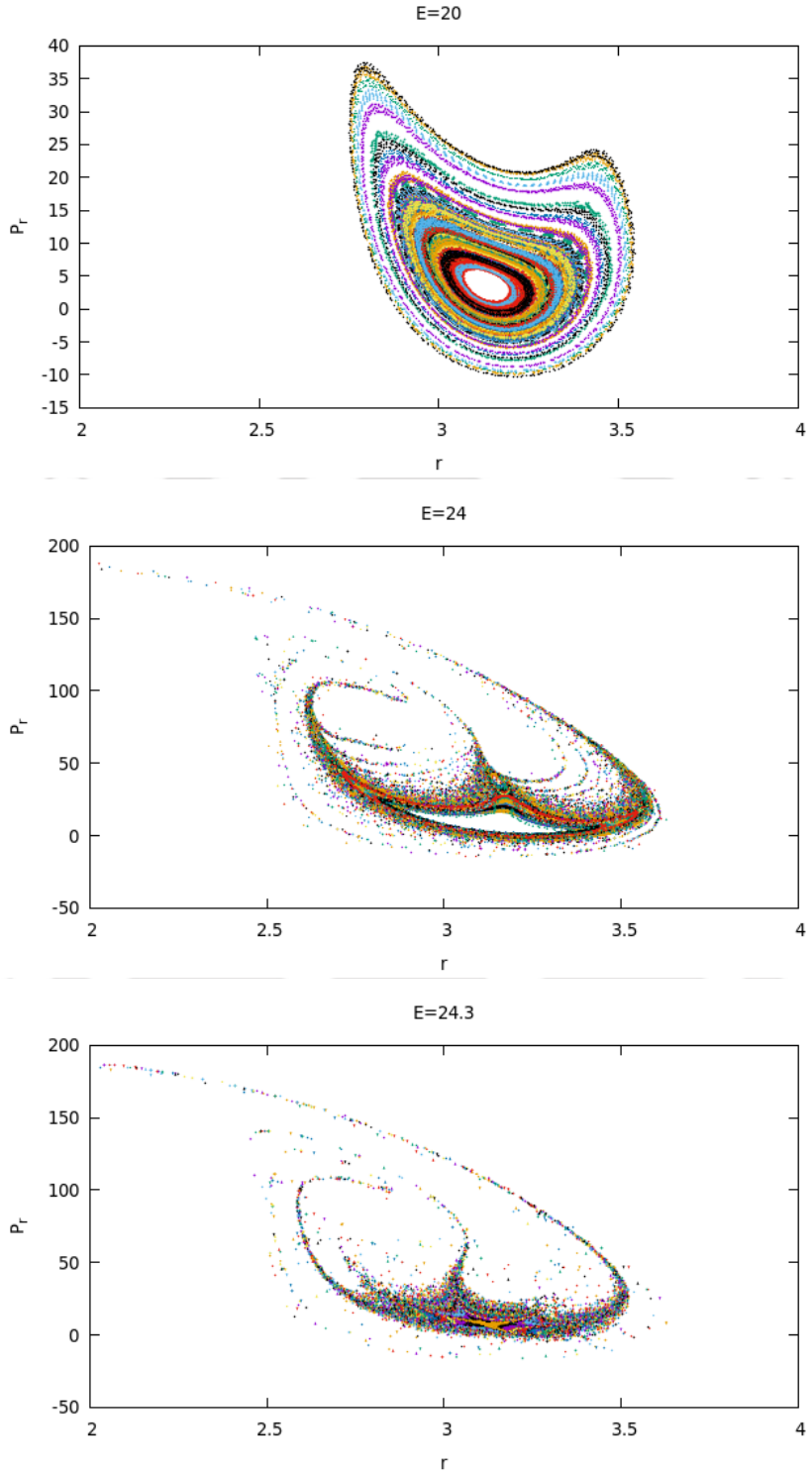

Figure 2.10: (Color online) The Poincaré sections in the $(r,\ p_r)$ plane with $\theta = 0$ and $p_\theta > 0$ for different energy for the Kerr black hole model at fixed rotation parameter $a = 0.7$. The energies are $E = 20$, $E = 24$ and $E = 24.3$. The other parameters are same as in Fig. 2.9. For large energy the KAM Tori break and the entire region is filled with the scattered points indicating the chaotic trajectory of the particles.

CHAPTER 3

CHAOS NEAR RINDLER HORIZON

3.1 Introduction and Motivation

Till now, we have been mesmerised by the fact that an event horizon can induce chaos in a system whenever it reaches under the influence of it. We are also aware of the fact that this mysterious one-way membrane arises as the solution of gravitational equations of motion [262]. The typical examples are Schwarzschild black hole which has *event horizon*, the *de-Sitter horizon* which emerges when the spacetime has a finite boundary at the asymptotic region, *etc.*. These arise in the purely curved background. Interestingly, even in Minkowski spacetime, we have the *Rindler horizon* which is an observer (uniformly accelerated) dependent non-compact horizon. There is a particular reason we shall instigate the Rindler horizon and its fascinating near-horizon characteristics, but before that, let us set up some background about the importance of the present chapter in the context of near-horizon physics.

As we mentioned earlier that in the last few decades, near horizon physics, at classical as well as at quantum level, has been the active area of research [220, 221, 243–252]. In recent time there have been many attempts to study the particle dynamics in presence of event horizon for different kinds of black hole systems where the black hole is either static spherically symmetric [244, 246] or rotating [249] or magnetized [252]. The test particles considered in those cases are either massive, charged, and spinning [250, 251] or the massless ones (discussed in [236] and in the previous chapter). All the analysis done in those cases are performed at the classical level [243, 246–248, 251] and the observed

results show that the motion of the test particles become chaotic in nature. There has also been an attempt to understand the behaviour of Lyapunov exponent for the case of null trajectories of a particle [219]. Another interesting observation has been made in [263], where the authors studied the motion of a test particle in the field of two fixed centres described by Einstein-Maxwell-Dilaton theory. They showed that the transition between regular to chaotic motion is possible as the dilation coupling is varied. In the quantum regime also the influence of horizon on the particle dynamics has been studied. It has been observed that the particle's motion, detected in the Minkowski vacuum by Rindler detector, is Brownian type [242]. A recent analysis in de-Sitter spacetime, from the perspective of quantum field theory, also demonstrated that the produced particle seen from the co-moving observer in conformal vacuum exhibits Brownian type of motion [264].

Moreover, at the classical level it was explored the fact that the regular motion of a system can be chaotic when it experiences the presence of horizon which we have already learned in the previous chapter. This has been tested so far for a massive as well as massless particle in the backgrounds of static spherically symmetric (SSS) as well as Kerr spacetime [220, 236]. In particular, our previous analysis (in chapter 2) has been done for the system in which a particle is trapped in two-dimensional harmonic potential under the background of SSS and Kerr spacetimes. We observed that the harmonic motion can get affected and that may lead to chaos in certain range of parameters of the composite system. In this regard, it must be noted that *all the previous analyses are done for an intrinsically curved background*, except in [220] where the Rindler case has been investigated for a massive particle. So in these cases, the motion of the particle got affected not only by horizon, but also by the curvature of the space-time as well as its own mass.

On the basis of these works mentioned above, a further spontaneous and interesting question in this context that arises is: *what would be the role of only horizon on the overall behavior of the particle motion which lacks the presence of any intrinsic curvature in the spacetime?* So far we observed in different analysis that presence of only horizon captures important features in the system. One of the well known facts is at the quantum level the Rindler horizon is associated with temperature and entropy [209], which is similar to the Hawking effect [113] in black hole case. Although, the later one contains intrinsic curvature, the former does not. Therefore by taking one step further in this chapter we are interested to address the unique role of horizon into the particle motion at the classical level. Other than going into the complexities of curved spacetime, one can

think much more simplified geometry, where a horizon appears naturally and analyze the particle trajectories in order to get the role of horizon. So here we exploit that liberty and consider the well known Rindler spacetime which is merely a flat spacetime (as it is an uniformly accelerated frame in the Minkowski spacetime and the metric is constructed by using the suitable coordinate transformations). Our objective is to focus on the unique implications of the horizon and to see how its presence leaves an imprint into the particle motion. In this regard, we would like to mention that the Rindler spacetime is an interesting choice as *these scenarios can be built up experimentally*. Moreover, if chaos emerges into the particle dynamics again then the claim addressed in the previous chapter that – *the presence of horizon is enough to make the particle motion chaotic* – will be further balustraded.

Motivated by such interesting possibilities, here we consider a chargeless and massless particle trapped under the influence of two-dimensional harmonic potential in the Rindler frame. Here the harmonic trap direction is one along the Rindler x-direction (when the accelerated frame is moving parallel to the Minkowski X axis), and the other one is moving along one of the transverse directions. The particle confined into the harmonic potential in the uniform accelerated frame will also feel the effect of the Rindler horizon. This type of model clearly fulfils our purpose of the present investigation, as the Rindler frame does not have a real curvature effect.

In this regard, it must be mentioned that the analytical calculations only for the motion of an outgoing particle along the x-direction show that position along this particular direction grows exponentially with time when it is situated very near to the horizon. This is certainly the signature that the system can experience chaos. Performing the numerical analysis for the above mentioned model and analyzing the Poincaré sections of the particle trajectories we confirm that chaos is inevitable for certain range of parameters. Another interesting result which is found is that the upper bound of the Lyapunov exponent is the acceleration of the particle which is consistent with the conjectured bound predicted by the SYK model [226].

The present chapter will be dedicated to investigate the further validity of the ongoing conjecture that *the presence of the horizon may induce chaos in an integrable system,* from the perspective of a uniformly accelerated frame. Particularly, we build up a model which consists of a particle (massless and chargeless) trapped in harmonic oscillator in a uniformly accelerated frame (namely Rindler observer). Here the Rindler frame provides a Killing horizon without any intrinsic curvature to the system. This makes the present observation different from the previous studies done in our earlier chapter. Now, let us

start our discussion by defining the path of the massless particle in the near horizon region of a Rindler frame.

3.2 Rindler frame and equations of motion

The frame of a uniformly accelerated observer is given by the Rindler metric. In $(1+3)$ dimensions it is of the form:

$$ds^2 = -2ax\,dt^2 + \frac{dx^2}{2ax} + dy^2 + dz^2\ . \tag{3.1}$$

The location of the Rindler horizon is $x = 0$ and a is the value of the acceleration. To remove the coordinate singularity at $x = 0$, we apply the Painleve coordinate transformation [54, 208]

$$dt \to dt - \frac{\sqrt{1-2ax}}{2ax}dx\ , \tag{3.2}$$

which transforms the metric as

$$ds^2 = -2ax\,dt^2 + 2\sqrt{1-2ax}\,dtdx + dx^2 + dy^2 + dz^2\ . \tag{3.3}$$

The energy of a particle with respect to this frame can be determined by the inherent timelike Killing vector $\chi^a = (1,0,0,0)$ of this spacetime. It is identified as $E = -\chi^a p_a = -p_t$, where $p_a = (p_t, p_x, p_y, p_z)$ is the four momentum of the particle.

Below, we want to mention the reasons for applying Painleve coordinate transformation.

- In this chapter, the motive is to study the dynamics of a massless and chargeless particle in a uniformly accelerated frame and the effect of the Killing horizon on its motion. In order to do so, we confined the particle very near to the horizon so that the effect of horizon is maximum. Accordingly all the calculation will be done in the near horizon approximation. In this scenario, the form of the metric (3.1) which has a coordinate singularity at $x = 0$ is not a good choice. So one needs to choose a different coordinate system where such coordinate singularity does not appear. Also one must be careful that the non-singular coordinates should be such that the corresponding observer can see the horizon as one way membrane. This is because in our case the motion of the test particle should be affected by it. Therefore, although Kruskal coordinates system does not have the singularity problem, the corresponding observer can not feel the horizon. So such system is ruled out. On the other hand Painleve coordinate system has no such problem. It is

free of coordinate singularity as well as the observer can see the horizon as one way membrane. This is also the reason for using the Painleve coordinates in discussing Hawking effect by tunneling mechanism in the null geodesic approach (see Ref. [54]).

- Another important feature of Painleve coordinate transformation is that the component form of the timelike Killing vector which defines the horizon as well as energy of the particle, remains identical to that in original Schwarzschild like coordinates. Initially, the metric (3.1) has the timelike Killing vector $K^a = (1,0,0,0)$ and the component form of this remains same in Painleve also: $\chi^a = (1,0,0,0)$. This can be checked by using the tensorial transformation of a vector under coordinate transformations. This helps us to define energy in terms of only time component of four-momentum in both the coordinate systems. For instance in Schwarzschild like coordinates it is given by $E = -K^a p_a = -p_t$ where t is Schwarzschild time coordinate; while this is again given by only time component of momentum: $E = -\chi^a p_a = -p_t$ where t is the Painleve time. Therefore calculations do not get complecated.

To find the expression for energy E in terms of the space components of momentum, we shall use the standard dispersion relation $g^{ab}p_a p_b = -m^2$ where m is the mass of the particle. Under the background metric (3.3), it is expanded as

$$E^2 + 2\sqrt{1-2ax}\ p_x E - \left(2ax\ p_x^2 + p_y^2\right) = m^2\ , \tag{3.4}$$

where, we have considered only the motion of the particle along x and y directions. This particular choice is taken for simplicity by keeping in mind the minimum dimensions required to demonstrate our particular goal. The solution of the above equation will lead to the expression for energy, which turns out to be

$$E = -\sqrt{1-2ax}\ p_x \pm \sqrt{p_x^2 + p_y^2 + m^2}\ . \tag{3.5}$$

In the above, positive sign refers to the outgoing trajectories, while negative sign signifies ingoing trajectories. Since ingoing particles are trapped inside the horizon and on the other hand we are interested to investigate the system when it is very near, but outside the horizon, we shall concentrate only on the outgoing ones (positive sign of the above equation).

Before proceeding to the main goal, we want to investigate the behaviour of particle trajectories qualitatively when it is under influence of only the Rindler horizon. For simplicity, we consider the particle to be massless; i.e. $m = 0$. If one concentrates only

on the motion along x direction (i.e. for constant values of y and z), then the rate of x variation is given by

$$\dot{x} = \frac{\partial E}{\partial p_x} = -\sqrt{1-2ax} + 1 \, . \tag{3.6}$$

Now if the particle is very near to the horizon such that $2ax < 1$, then the above Eq.(3.6) reduces to

$$\dot{x} \simeq ax \, . \tag{3.7}$$

In the above Eqs. (3.6-3.7), the parameter with respect to which the derivative has been defined is some affine parameter, say λ. It should be such that the four momentum of the massless particle is defined by $p^a = dx^a/d\lambda$ which satisfies $p^a \nabla_a p^b = 0$. This is the usual prescription to define the parameter in the case of a null-like path $x^a = x^a(\lambda)$. Remember that λ is similar to proper time for a timelike geodesic. The solution of the above equation is

$$x = \frac{1}{a} e^{a\lambda} \, . \tag{3.8}$$

This solution implies the exponential growth of position coordinate along the x direction which signifies possible induction of chaos in an integrable system when it comes under the influence of Rindler horizon. We shall show explicitly in the later part of the chapter that if this massless particle is kept in a harmonic potential in the accelerated frame, the motion of the particle in the composite system becomes chaotic for certain values of the parameters, like total energy of the system (E) and the acceleration (a) of the frame.

In order to fulfil our claim now let us concentrate on the equations of motion and see what happens when the influence of horizon comes into play. For that we consider two dimensional harmonic potential in accelerated frame which have the nature $(1/2)K_x(x - x_c)^2$ and $(1/2)K_y(y - y_c)^2$ along Rindler x and y directions, respectively. Here K_x and K_y are the spring constants while x_c and y_c are the equilibrium positions of these two harmonic potentials. Our goal is to discover the fact about the collective impact of horizon on this integrable system. In particular we want to inspect thoroughly in order to determine how the nature of the particle trajectory gets changed or influenced by the presence of Rindler horizon.

We begin our calculation by obtaining the total energy of the composite system when our massless test particle moves in the background Eq. (3.3) under the influence of these two harmonic potentials. So the total energy of the system turns out to be (considering

only the outgoing paths)

$$E = -\sqrt{1-2ax}\; p_x + \sqrt{p_x^2+p_y^2} + \frac{1}{2}K_x(x-x_c)^2 + \frac{1}{2}K_y(y-y_c)^2 \,, \tag{3.9}$$

and correspondingly, the equations of motion will be

$$\dot{x} = \frac{\partial E}{\partial p_x} = -\sqrt{1-2ax} + \frac{p_x}{\sqrt{p_x^2+p_y^2}} \,; \tag{3.10}$$

$$\dot{p_x} = -\frac{\partial E}{\partial x} = -\frac{a}{\sqrt{1-2ax}} p_x - K_x(x-x_c) \,; \tag{3.11}$$

$$\dot{y} = \frac{\partial E}{\partial p_y} = \frac{p_y}{\sqrt{p_x^2+p_y^2}} \,; \tag{3.12}$$

$$\dot{p_y} = -\frac{\partial E}{\partial y} = -K_y(y-y_c) \,. \tag{3.13}$$

In the next section of the chapter we will examine these equations with the help of numerical analysis in order to study the motion of the particle. Here we would like to mention that the interaction between the horizon and the harmonic potentials are taken to be so small that one can ignore that term compared to the other terms. Hence, as pointed out in the previous chapter the total energy of the composite system, in the above, has been taken as the sum of the gravitational and harmonic potentials parts.

3.3 Numerical analysis

To illustrate that the presence of horizon is the origin of chaos, this section will be dedicated to analyze the particle motion numerically. In the previous section we analytically showed that the particle's position along the x direction grows exponentially when the particle is confined very near to the horizon. This particular feature, we invoked, as the possible induction of chaos in an integrable system. In order to confirm our claim we will analyze the Poincaré sections and the power spectral densities of our model (harmonic oscillator in an uniformly accelerated frame), obtained by solving the dynamical equations of motion (Eqs. (3.10)-(3.13)). This will give us the glimpse about the change in the dynamics of the particle trajectory. First we will present the Poincaré sections of our composite system. In the upcoming subsections we will present power spectral density and Lyapunov exponent and show how our dynamical system becomes chaotic for some particular values of parameters, like acceleration (a) and energy (E).

3.3.1 Poincare sections

The results for the Poincaré sections of the particle trajectory are shown in Fig. 3.1 and Fig. 3.2. In Fig. 3.1 the Poincaré sections are projected over the (x, p_x) plane for different values of accelerations but for a particular value of energy (E). Whereas, in Fig. 3.2 the Poincaré sections are plotted for different values of energies (E) while the acceleration (a) of the system remains constant.

The dynamical equations are solved (Eqs. (3.10)-(3.13)) numerically using the fourth order Runge-Kutta method with fixed $d\lambda = 5 \times 10^{-3}$. The other parameters we have chosen are $K_x = 26.75$, $K_y = 26.75$, $x_c = 1.1$ and $y_c = 1.0$. The variables x, y and p_x are initialized with the random numbers and p_y is obtained from Eq. (3.9) for a fixed values of E and a. The sections are the slice defined by $y = 1.0$ and $p_y > 0$. In Fig. 3.1, the Poincare sections are plotted for different values of $a = 0.20, 0.27, 0.295$ and 0.35 while the energy is fixed at $E = 24.0$ as indicated in the plots. In Fig. 3.2, we have considered the energies $E = 20, 22, 24$ and 24.2 while the value of a is fixed at 0.35. For different initial conditions the different trajectories of the particle are indicated by different colors in the figures.

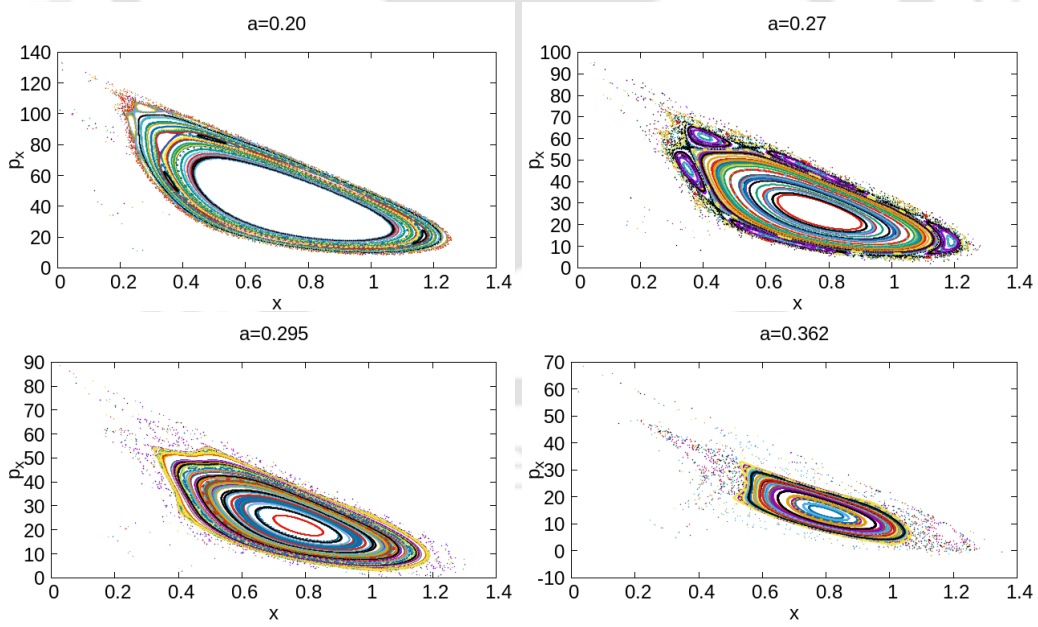

Figure 3.1: (Color online) The Poincaré sections in the (x, p_x) plane with $y = 1.0$ and $p_y > 0$ at different values of acceleration of the system for fixed energy ($E = 24.0$). The values of accelerations are $a = 0.20, 0.27, 0.295$ and 0.362. The other parameters are $K_x = 26.75, K_y = 26.75$, $x_c = 1.1$ and $y_c = 1.0$. For large value of acceleration the KAM Tori break and the scattered points emerge which indicates the onset of chaotic dynamics.

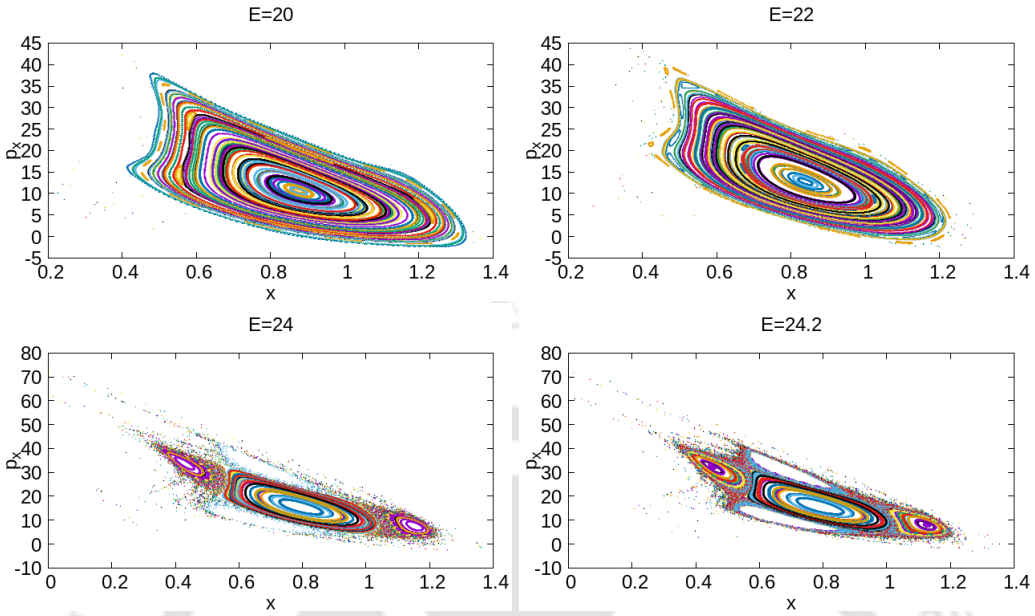

Figure 3.2: (Color online) The Poincaré sections in the (x, p_x) plane with $y = 1.0$ and $p_y > 0$ at different values of energy of the system but for fixed acceleration ($a = 0.35$). The energies are $E = 20, 22, 24$ and 24.2. The other parameters are $K_x = 26.75, K_y = 26.75, x_c = 1.1$ and $y_c = 1.0$. For large value of energy the KAM Tori break and the regions filled with scattered points which indicates the presence of chaotic motion in the particle dynamics.

Now let us investigate these two sets of figures in more careful way. First we explore the effect of acceleration on the particle dynamics. For low value of acceleration $a = 0.20$ the display of regular KAM (Kolmogorov-Arnold-Moser) tori [256] (see Fig. 3.1) reveals the fact that the particle trajectory is regular. As we increase the value of a the trajectories start getting deformed and breaking into small tori. Note that the effect is more pronounced for the orbits which are closer to the horizon. There always have been some regions of regular tori in the figures instead of the fully chaotic region where all the points should be scattered. However, in the present study we could not get the fully developed chaos as we find that the orbits are quite sensitive to the parameters i.e a and E. On further change in those parameters lead to the unbounded situations.

It is noted here that as we increase a, more and more regular tori are broken and correspondingly the chaotic nature of the system appears. This can be attributed to the effects of horizon on the orbit of the particle. The reason can be described in a qualitative way. The relation between the Minkowski coordinates (T, X) and Rindler coordinates

(t,x), for the uniformly accelerated observer on the right wedge, are

$$aT = \sqrt{2ax}\sinh(at);\quad aX = \sqrt{2ax}\cosh(at)\,. \tag{3.14}$$

So the trajectory of the accelerated observer is

$$X^2 - T^2 = \frac{2x}{a}\,, \tag{3.15}$$

which is hyperbolic in nature for a constant x. Now since a is the proper acceleration (as measured by the Rindler frame), the path of the Rindler observer in terms of its own coordinate is $(2x)/a = 1/a^2$; i.e. $x = 1/(2a)$ = constant. So different value of a corresponds to different accelerated observer. It shows that if we increase the value of a, the frame will be more close to the horizon $x = 0$ and the particle will get more effect of the horizon. Hence the instability in the motion of the particle along x will increase according to (3.8). This causes breaking of the orbit when it approaches towards the horizon. That's why we here obtained more breaking of tori as we increase the acceleration.

We obtain from Fig. 3.2 that for low energy $E = 20$ the Poincaré section exhibits the regular KAM tori [256]. As the total energy of the system gets increased the volume of the phase space increases and the trajectory of the particle approaches nearer to the Rindler horizon. As soon as the particle moves nearer to the horizon the trajectories start getting distorted into their structure which can be clearly seen from the Fig. 3.2. The appearance of the scattered points in the outer most regions as we increase the total energy of the system indicates the presence of chaos into the system. The value of energy is chosen in such a way that the particle come close enough to the horizon but not fall into it. Finally we mention that if the particle is massive, the situation does not change. This has been confirmed numerically in Appendix 3.A.

3.3.2 Power Spectral Density

In order to have an instinctual idea about the dynamical behavior of our composite system in an accelerated frame and to understand the collective impact of horizon in the particle trajectories, we systematically investigate the evolution of the position coordinate, $x(\lambda)$ with respect to the affine parameter (which plays the role of time for the massless particle). To get an extensive idea of the trajectory of the system and the deeper understanding of the onset chaotic behavior of the system, the power spectral density (PSD) is analyzed which we have discussed in the previous chapter for the case of static spherically symmetric (SSS) black hole. Now, PSD is defined as [258],

$$\text{PSD} = \frac{1}{2\pi\mathcal{N}}|x(\mathcal{N},f,\Delta\lambda)|^2\,, \tag{3.16}$$

where $x(\mathcal{N}, f, \Delta\lambda)$ is the discrete Fourier transform of $x(\lambda)$ evaluated at $\lambda = k\,\Delta\lambda$ ($k = 0, 1, ..., \mathcal{N}$ and $\mathcal{N}$ is the length of the discrete affine parameter series).

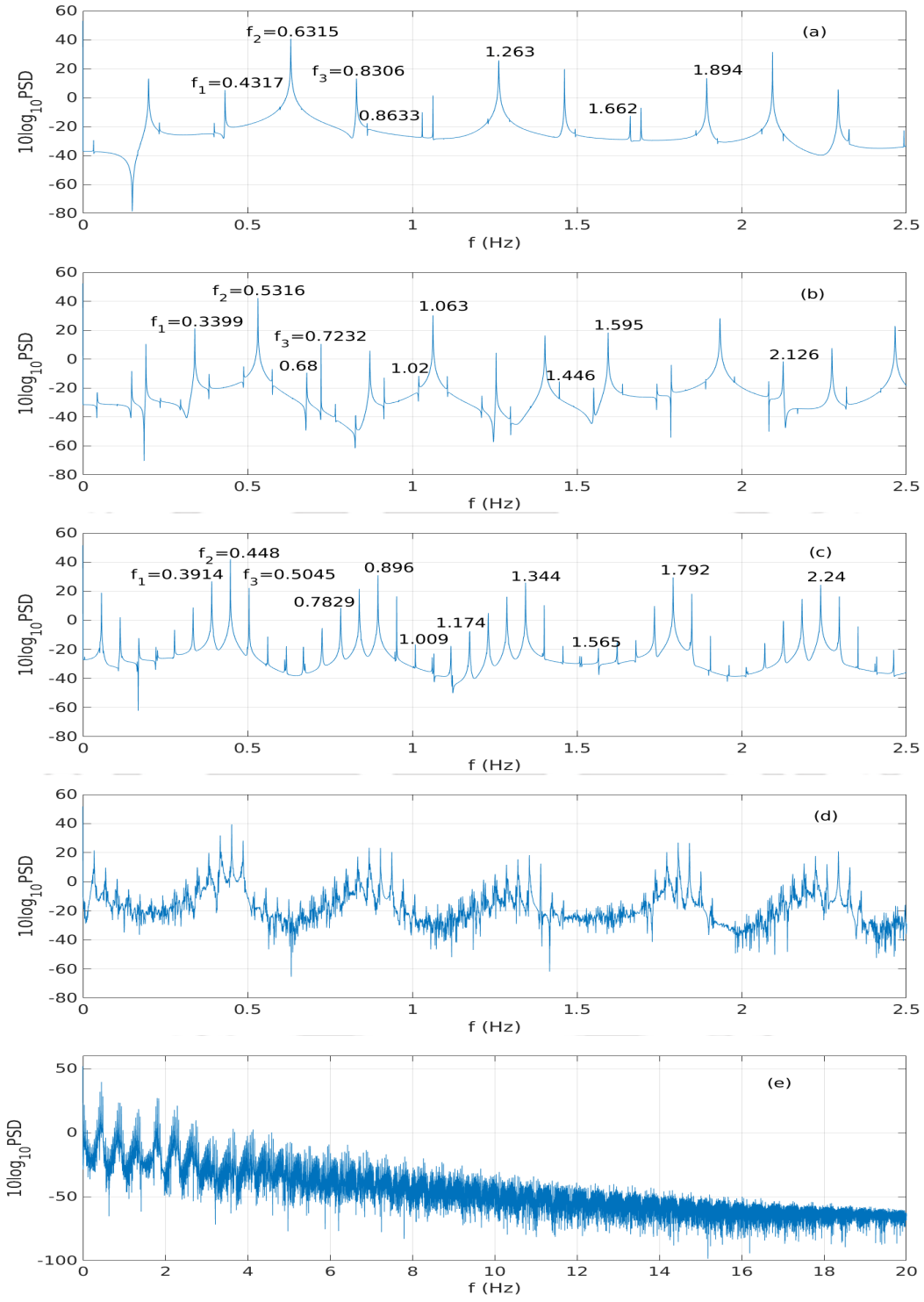

Figure 3.3: (Color online) PSD for $a = 0.35$, $y = 1.0$, $p_y > 0$, $K_x = 26.75$, $K_y = 26.75$, $x_c = 1.1$, $y_c = 1.0$ and for different values of the total energy of the system E, namely $(a)E = 20, (b)E = 22, (c)E = 24, (d)E = 24.2$. Upto $E = 22$, only f_1, f_2 and f_3 and their harmonics are present but for higher values of energy i.e from $E = 24$ onwards more frequencies start populating the spectrum. At $E = 24.2$, the highly population of frequency spectrum which indicates the onset of chaos (see Fig. 3.3(e)).

Let us see what happens when the total energy of the system (E) is changed. In Fig. 3.3 we show PSD for the case when the acceleration is fixed ($a = 0.35$) and E is varied ($E = 20, 22, 24$ and 24.2). As we found from the previous section that for lower value of energy $E = 20$ the Poincaré sections are periodic in nature, that means the effect of horizon has not appeared into system yet. This feature is seen from Fig. 3.3(a) where the PSD diagram is plotted for energy $E = 20$ but only a few number of peaks appear into the plot. The appearance of PSD peak at $f_2 \simeq 0.6315$ is the fundamental frequency and other frequencies at $1.263, 1.894$ and 2.493 are the harmonics of that fundamental frequency. The appearance of other frequencies i.e f_1, f_3 etc, indicates the involvement of other frequencies of oscillations in the time evolution of $x(\lambda)$, which is a signature of the quasi-periodic nature of the system. With further increase in the value of E, we find that more frequencies near f_1, f_2 and f_3 start getting populated (see Fig. 3.3(b) and Fig. 3.3(c)). Finally for high value of energy, i.e., $E = 24.2$, PSD shows fully populated pattern over the frequency range (see Fig. 3.3(d)). That is the distinguishing character of the onset of chaos. Interestingly this has an exponential decaying character. The similar trend of PSD was also obtained in the case of the chaotic region of fluid motion [265]. In this case also, like ours, the chaos is temporal one. It may possible that such exponential decay of PSD (which is completely a phenomenological feature) is a very general nature for a system when it is in chaotic regime. But it needs further investigation which is beyond the scope this present chapter. Thus for $E = 24.2$, the observed a periodic time evolution of $x(\lambda)$ displays chaotic behaviour for the particle dynamics in presence of horizon.

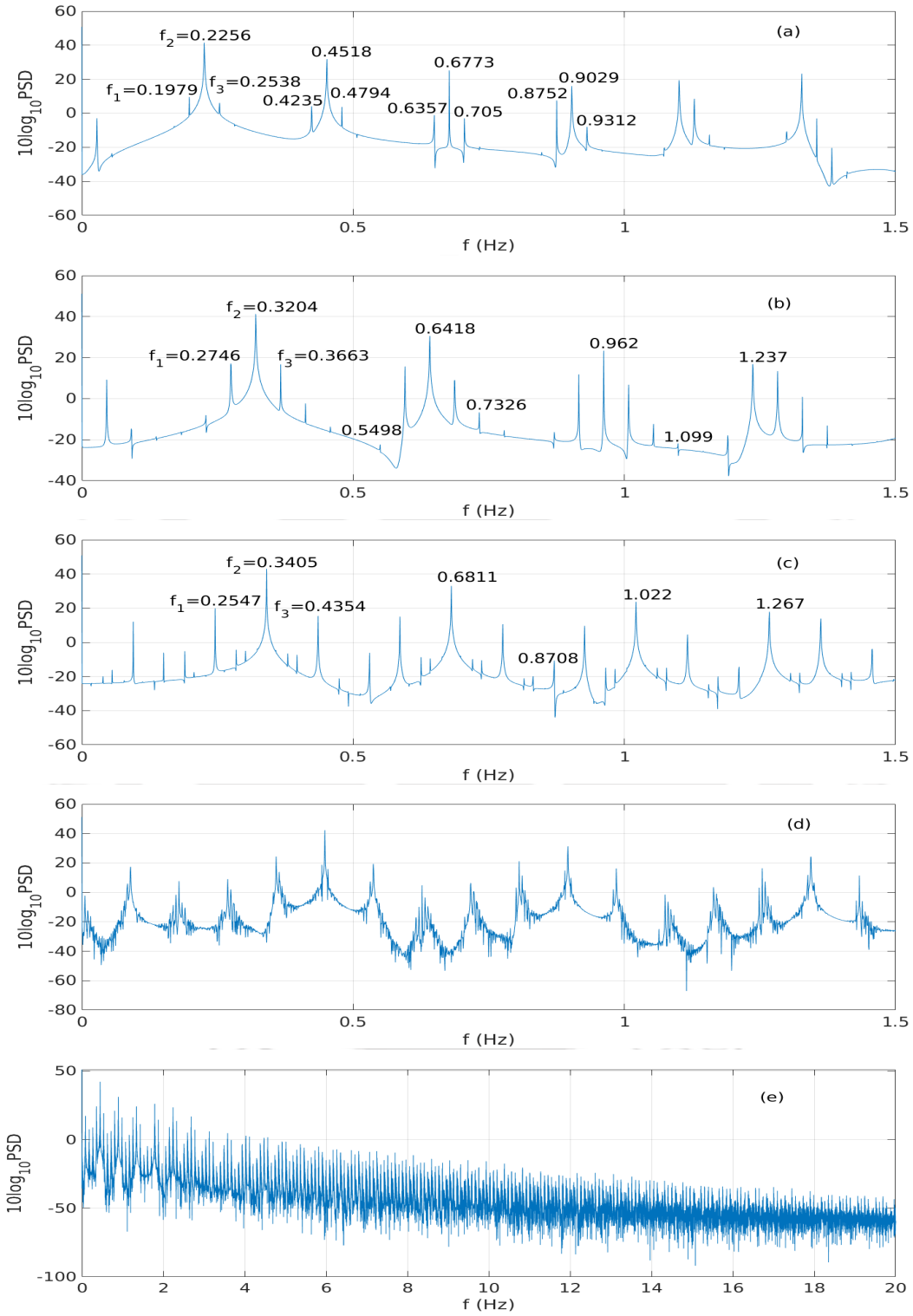

Figure 3.4: (Color online) PSD for $E = 24, y = 1.0, p_y > 0, K_x = 26.75, K_y = 26.75, x_c = 1.1, y_c = 1.0$ and for different values of accelerations a, namely $(a)a = 0.20, (b)a = 0.27, (c)a = 0.295, (d)a = 0.35$. Upto $a = 0.27$, only f_1, f_2 and f_3 and their harmonics are present. From $a = 0.295$ onwards more frequencies start populating the spectrum. At $a = 0.362$, the frequencies are highly populated (see Fig.3.4(e) which indicates the onset of chaos.

Next we plot the PSD diagrams for different values of the acceleration (a = 0.20, 0.27, 0.295 and 0.362) of the system for a fixed value of energy $E = 24.0$ (see Fig. 3.4). For lower value of the particle acceleration i.e at $a = 0.20$ the PSD (Fig. 3.4(a)) shows the presence of only three frequencies, which are $f_1 = 0.1979, f_2 = 0.2256, f_3 = 0.2538$ and their harmonics. While for larger values of a that is at $a = 0.27$ (Fig. 3.4(b)) and at $a = 0.295$ (Fig. 3.4(c)) the frequencies f_1, f_2 andf_3 start getting shifted and other frequencies near f_1, f_2 andf_3 start getting populated like the previous case. Finally, for very large value of $a = 0.362$ (Fig. 3.4(d)) where the interaction between the harmonic potential and the horizon is very large, we found that the PSD diagrams are fully populated with again an exponential decay over the entire frequency region which basically shows the distinguishing feature of the onset of chaos. Hence we obtain a series of transitions in the dynamics of our composite system, namely, from periodic to quasi-periodic and finally to chaotic dynamics as the total energy of the system (E) or the acceleration of the particle (a) is increased. Thus both the cases result in *quasi-periodic route to chaos*.

3.3.3 Lyapunov exponent

In literature Lyapunov exponent is a quantity that quantifies the instability into the system by measuring the rate of separation of infinitesimally close trajectories of a dynamical system [257] (for definition please see the section 2.4.2 and Eq. (2.10) in the previous chapter). Now, the value of the Lyapunov exponent has an upper bound which was first mentioned in [226] for the SYK model. For our system the Lyapunov exponent (λ_L) is bounded by

$$\lambda_L \leq a \ , \tag{3.17}$$

where a is the acceleration of the Rindler frame. This is apparent from the near horizon solution (3.8) for x. Now at the quantum level, the accelerated frame will feel the Unruh temperature $T = \hbar a/2\pi$ (see [209]) and hence the above inequality can be expressed as $\lambda_L \leq (2\pi T)/\hbar$, which is exactly identical to what was obtained for SYK model [226]. In this regard we here mention some recent studies on the bound on Lyapunov exponents in the context of black holes. In [222] authors have studied the minimal length effects on the chaotic motion of a massive particle near the black hole horizon where they have shown that the corresponding Lyapunov exponent is greater than that in the usual case with the absence of the minimal length using the Hamilton-Jacobi method. People have also shown that the bound on the Lyapunov exponent can be violated by a

large number of black holes including the RN-dS black holes or black holes in Einstein-Maxwell-Dilaton, Einstein-Born-Infeld and Einstein-Gauss-Bonnet-Maxwell gravities [266]. Another interesting work [223] where the author performed a systematic study of the maximum Lyapunov exponent values for the motion of classical closed strings in Anti-de Sitter black hole geometries with spherical, planar and hyperbolic horizons. The analytical estimation from the linearized variational equations predict the Lyapunov exponent value modified as $\lambda_L \approx 2\pi T n$, where n is the winding number of the string.

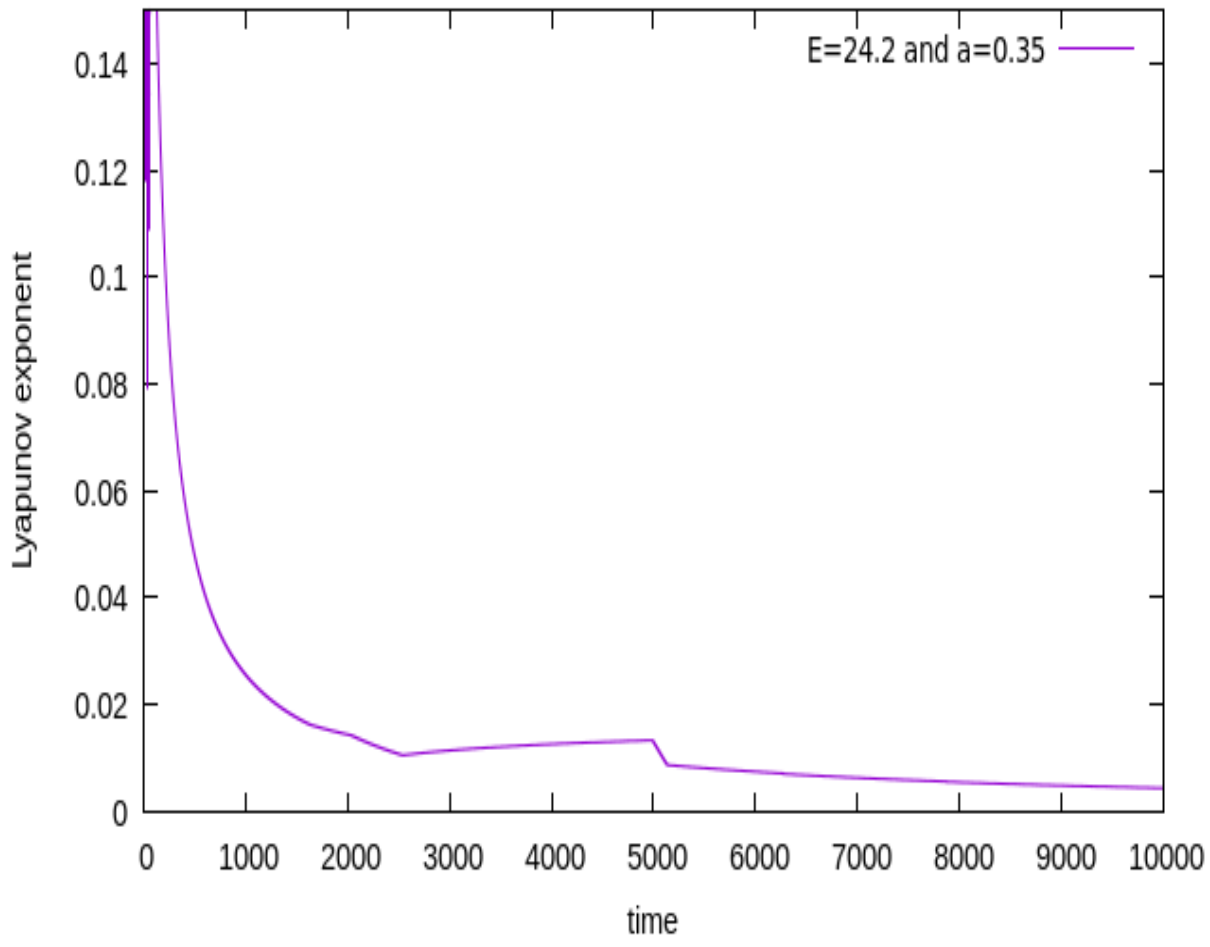

Figure 3.5: (Color online) Largest Lyapunov exponent for the particle in accelerated frame at the energy value $E = 24.2$ and the acceleration $a = 0.35$. The exponent settles at positive value ~ 0.01 which is lower than the upper bound (0.35).

We present our numerical analysis on Lyapunov exponents for different cases in order to show our proposition is reasonable. We have plotted the largest Lyapunov exponent for two cases. First, we consider the energy $E = 24.2$ and $a = 0.35$ (see Fig. 3.5) and secondly,

we have plotted for $E = 24.0$ and $a = 0.362$ (see Fig. 3.6). For both the cases we obtained the chaotic behaviour in the particle dynamics. In both the figures (Fig. 3.5 and Fig. 3.6) it is observed that the Lyapunov exponent settle to positive values (~ 0.01 and ~ 0.02 respectively) which suggests the chaotic motion of the particle. Since we observed that the obtained values of the Lyapunov exponents for both the cases are lower than the bounds (0.35 and 0.362 respectively), it is consistent with our claim.

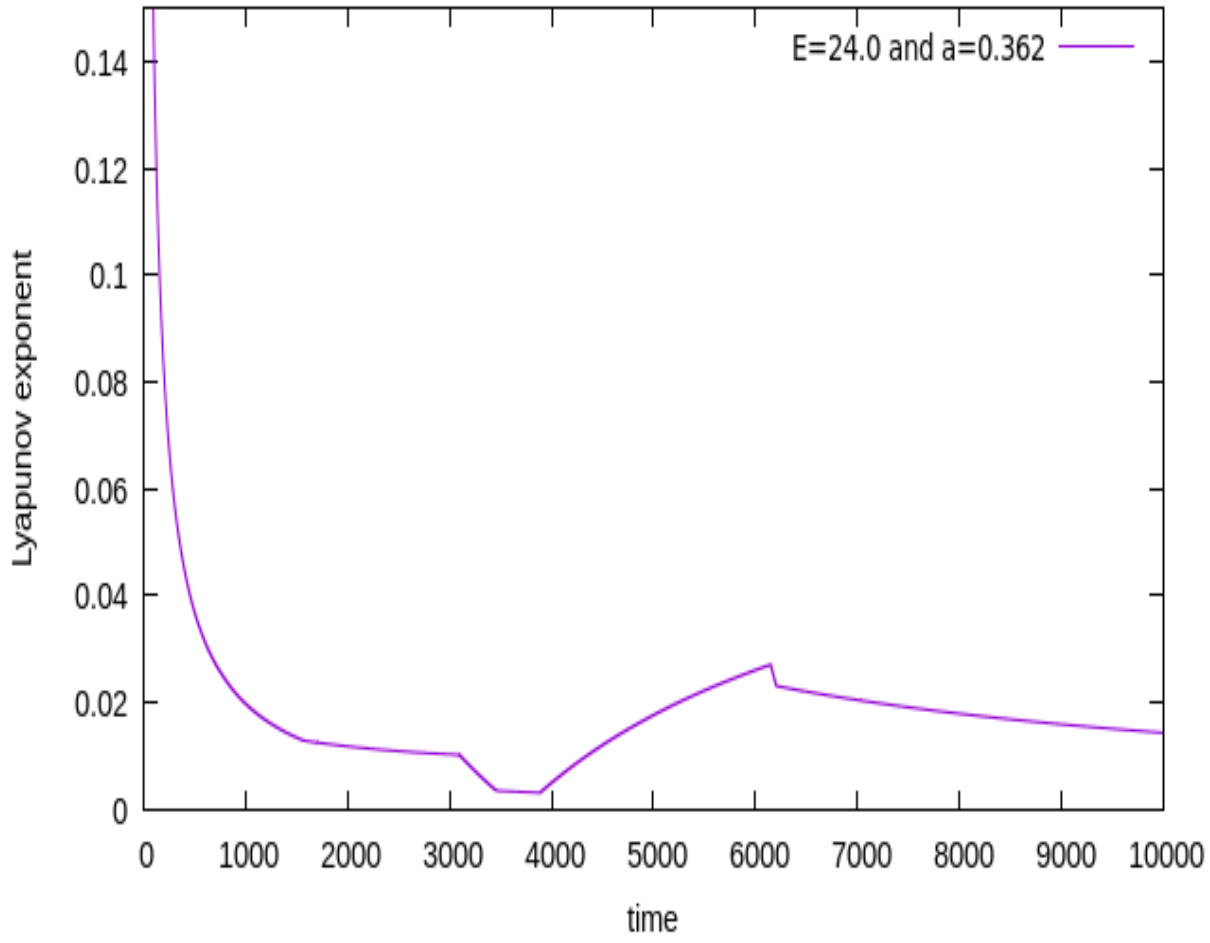

Figure 3.6: (Color online) Largest Lyapunov exponent for the particle in accelerated frame at the energy value $E = 24$ and the acceleration $a = 0.362$. The exponent settles at positive value ~ 0.02 which is lower than the upper bound (0.362).

3.4 Summary and Discussions

In this chapter we have studied the motion of a massless and chargeless particle in an accelerated frame in the flat spacetime background. First we derived the equations of motion of the outgoing particle trajectories and found that the position coordinate along a particular direction increases exponentially with the time parameter which gives us the indication that may be the horizon is influencing the chaotic fluctuation in the particle's motion. Next our aim was to trap the particle near the horizon and study its dynamical behaviour. For this purpose we introduced an external harmonic potential in the accelerated frame and derived the equations of motion from the Hamiltonian of the whole composite system. The whole phenomena are seen by a comoving observer. After solving these equations numerically and analyzing the Poincaré sections and the PSD diagrams we ascertain our claim that chaos can be indeed induced in the particle dynamics by just influence of a horizon.

So it appears that a harmonic oscillator in the Rindler frame lost its periodicity with respect to the comoving observer as it approaches nearer to the horizon. This is consistent with the well known KAM theory. According of which, if an integrable system having the number of degrees of freedom (say n) greater than three, it loses its stability with the application of a small perturbation into the system [267]. Now our system has $n = 4$ degrees of freedom (namely, x, p_x, y, p_y) and that means a general small perturbation can lead our system to instability which is happening for our case. Here if we think the interaction with the horizon as a perturbation then as the perturbation gets increased (due to increase in E and a) the periodic motion of the harmonic oscillator initially decomposes into a number of tori. Further increase in the parameters (E and a) leads to the instability in some of the regular tori that results them breaking into several small tori. It signifies that our harmonic oscillator initially started with a fundamental frequency but later due to the increment in the perturbation the fundamental frequency decomposes and a number of other frequencies show up into the system which is the characteristics of the onset of chaos. Now from the expression of the Hamiltonian of the system we can say that the first term of Eq. (3.9) will act as the perturbation in the system and the other two terms in Eq. (3.9) will form the integrable system of harmonic oscillator in two dimensions. The only source of this perturbation term is the acceleration of the system itself. That means if an harmonic oscillator is moving in two dimensions in a constant accelerated frame, for a comoving observer it would appear that the acceleration itself perturbed the system rigorously and as a result the harmonic

oscillator loses its fundamental frequency and for large perturbation it shows chaotic behavior.

Chaos in the coupled harmonic oscillators (as for an example, double pendulum) system in the flat space time for inertial observer is generally observed due to the presence of the nonlinear coupling [256]. The coupling is independent of the state of the inertial observer. So chaos appears in the system even the velocity of the inertial observer is set to zero. Here, as a precautionary note for the readers, we would like to mention that in our system the coupling between the oscillators appears owing to the presence of the accelerated observer only, which in turn provides a Killing horizon. The coupling among the oscillators are happening through their interaction with this horizon. In absence of the acceleration, the coupling between the oscillator vanishes and that will lead to the disappearance of the chaos from the system. So one needs to be careful while comparing the chaos that appears in our model to those appear in the system of coupled harmonic oscillators for inertial observer.

We also found that the chaos of the particle probing the Rindler horizon has a universal upper bound on the Lyapunov exponent. In this regard, it may be mentioned that the upper bound is given by the acceleration of the particle and it is independent of the external potentials which prevents the particles falling into the horizon (for details on the potential independent nature, see [220]). This upper bound conjecture of the Lyapunov exponent coincides with the prediction of the SYK model, argumented by Maldacena, Shenkar and Stanford [226].

From this analysis it is apparent that an integrable system when comes under the influence of horizon, it's dynamics can be chaotic. Since in the present case, the horizon is part of the flat background (vanishing Riemann curvature), the conjecture – horizon makes system chaotic – is further balustrade as the curvature does not play much role. This has been further elaborated by studying the route to chaos for our present model and the model with harmonic oscillator in static spherically symmetric (SSS) black hole. We observed that they are similar in nature (see the Fig. 2.6 in section 2.4.3 for the PSD of SSS case).

The present analysis is well consistent with the equivalence principle as only horizon is responsible for similar chaotic dynamics in both the setups: accelerated frame and black hole spacetime. In this regard we further want to point out a possible parallel description between the thermality in an accelerated frame (known as Unruh effect [209]) and that for a static observer in black hole spacetime (familiar as Hawking effect [113]). It is well known that both the temperature expressions are identical with the

identification of the acceleration parameter as the surface gravity for black hole. Similar situation again arises here also. It is noticeable that the maximum value of Lyapunov exponent is given by proper acceleration of the frame (see Eq. (3.17)). Whereas, it was already mentioned in the previous chapter that the same for black hole case is given by the surface gravity. So the existing map between acceleration and surface gravity at the quantum level also appears here, but at the classical level.

Furthermore, we hope that as our model composed of simple accelerated frame and harmonic oscillator, an experimental setup may be designed to test this possibility. In addition we point out that in the present context the Rindler spacetime was investigated in [220] for a massive particle in original Rindler coordinates. The bound was obtained same as ours (3.17). Here we worked out for a chargeless and massless particle and the Rindler background has been taken in Painleave coordinates. Interestingly, in both analysis the bound on λ_L is identical and independent of the mass of the particle. This certainly provides an universal feature of horizon as mass of the particle does not play any role on this bound. In this sense, the current analysis is different from the earlier discussions [220, 243–252] (as they either used curved background or massive particle or both simultaneously in their analysis). In this chapter we used massless particle and also investigated the nature of power spectrum density which gives the information on the nature of *route to chaos* when one changes the system parameters. This has not been attempted in earlier analysis. In appendix 3.A we also give the PSD for the massive particle in Rindler frame. We found that route to chaos for both massless and massive is similar in nature – frequency spectrum gets populated as one increases energy or acceleration. This again shows that the horizon actually can make system chaotic while the mass of the particle is not so important.

Let us now summarize what are the information we can have from the study of PSD of our system.

- Study of PSD helps to understand the actual appearance of chaos in a system by analyzing the population of the spectrum with the change of macroscopic parameters of the system.

- Here we studied the motion of massless as well as massive particle in a Rindler frame. In both cases, after analyzing PSDs, we observed that the nature of onset of chaos into the system is similar. Interestingly, the system with massive and massless particle exhibit same route to chaos which in the present case we identified as quasi-periodic route to chaos. Increase of same parameters (e.g. energy and

acceleration) for both the situations, frequency spectra get populated. So we infer that the horizon actually induces chaos to the system, while mass of the particle is not so important.

- At the stage of maximum chaos, the PSDs show an exponential decay in all cases. Although as of now this is completely a phenomenological feature, but it may be possible that such nature is a very general one for any temporal chaos in a system. This statement is just a prediction rather than a concrete one.

The scenario in this context is quite clear that in presence of horizon a system starts showing chaotic fluctuations. Numerical studies also indicate in that direction. However, the major question one can ask in this picture that what might be the particular reason for these chaotic fluctuations in the near horizon, whether it is an event horizon or a Rindler one. We end this chapter by putting forward this question, and in the next chapter, our prime motive will be to hunt down its answer.

Appendices

3.A Presence of chaos in an accelerated frame for a massive particle

The expression of the total energy of the composite system for a massive test particle moving in the background (2.3) under the influence of the two harmonic oscillators is

$$E = -\sqrt{1-2ax}\; p_x + \sqrt{p_x^2+p_y^2+m^2} + \frac{1}{2}K_x(x-x_c)^2 + \frac{1}{2}K_y(y-y_c)^2 \,, \quad (3.A.1)$$

and the corresponding equations of motion are

$$\dot{x} = \frac{\partial E}{\partial p_x} = -\sqrt{1-2ax} + \frac{p_x}{\sqrt{p_x^2+p_y^2+m^2}} \,; \quad (3.A.2)$$

$$\dot{p_x} = -\frac{\partial E}{\partial x} = -\frac{a}{\sqrt{1-2ax}}p_x - K_x(x-x_c) \,; \quad (3.A.3)$$

$$\dot{y} = \frac{\partial E}{\partial p_y} = \frac{p_y}{\sqrt{p_x^2+p_y^2+m^2}} \,; \quad (3.A.4)$$

$$\dot{p_y} = -\frac{\partial E}{\partial y} = -K_y(y-y_c) \,. \quad (3.A.5)$$

3.A.1 Poincaré sections for constant total energy of the system

Here we present the Poincaré sections for a massive particle moving with an acceleration in flat spcaetime for a fixed energy value of the system ($E = 24.0$). The dynamical equations (Eqs. (3.A.2)-(3.A.5)) are solved numerically using the fourth order Runge-Kutta method with fixed $d\lambda = 5 \times 10^{-3}$. The mass of the particle is chosen $m = 1$. The other parameters are kept same as mentioned in the section 3.3. The analysis confirms that in presence of horizon with the increase in the particle acceleration the motion of the massive particle becomes chaotic (see Fig. 3.7) just like the earlier case i.e for the massless particle.

3.A.2 Poincaré sections for constant acceleration of the system

In this part we present the Poincaré sections for the massive particle confined in a two dimensional harmonic potential moving with a fixed acceleration ($a = 0.35$) in flat spcaetime but for different values of energy of the system. The numerical simulations are done in the similar process as earlier keeping all the values of the parameters same.

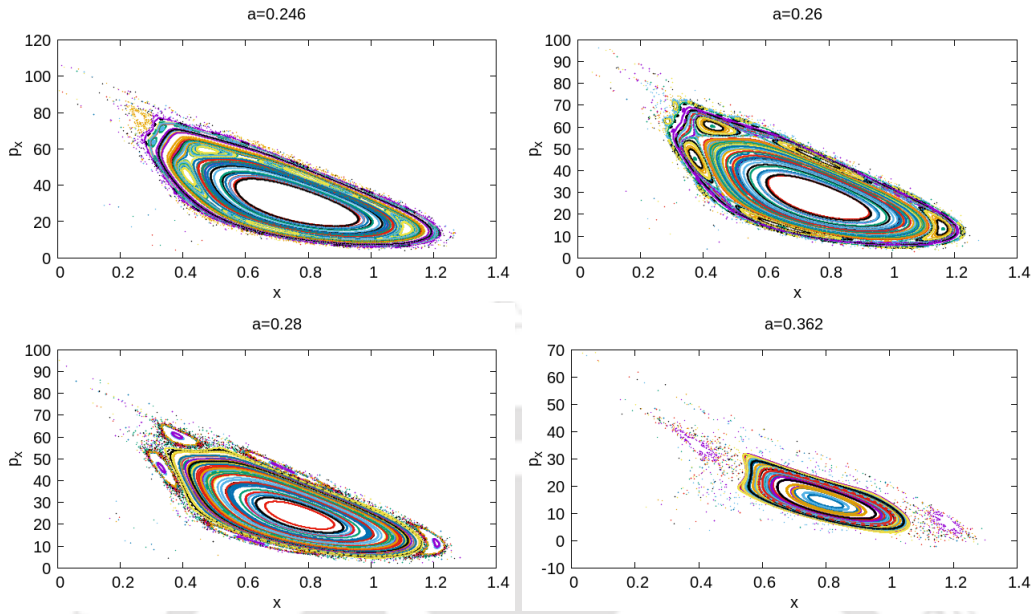

Figure 3.7: (Color online) The Poincaré sections in the (x, p_x) plane with $y = 1.0$ and $p_y > 0$ at different values of acceleration of the system with mass $m = 1$ for fixed energy ($E = 24.0$). The values of accelerations are $a = 0.246, 0.26, 0.28$ and 0.362. The other parameters are $K_x = 26.75, K_y = 26.75, x_c = 1.1$ and $y_c = 1.0$. For large value of acceleration the KAM Tori break and the scattered points emerge which indicates the onset of chaotic dynamics.

The analysis shows us that in presence of horizon with the increase in the total energy of the composite system the motion of the massive particle becomes chaotic which is quite evident from the following figures (see Fig. 3.8).

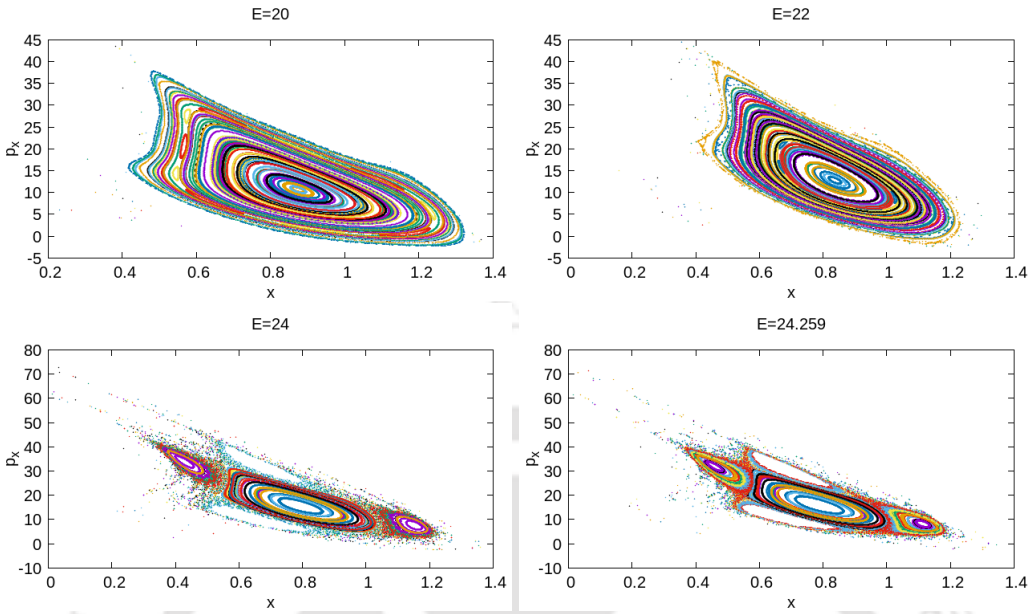

Figure 3.8: (Color online) The Poincaré sections in the (x, p_x) plane with $y = 1.0$ and $p_y > 0$ at different values of energy of the system with mass $m = 1$ but for fixed acceleration ($a = 0.35$). The energies are $E = 20, 22, 24$ and 24.259. The other parameters are $K_x = 26.75$, $K_y = 26.75$, $x_c = 1.1$ and $y_c = 1.0$. For large value of energy the KAM Tori starts breaking and the scattered points begin to appear which indicates the presence of chaotic motion in the particle dynamics.

3.A.3 PSD for a massive particle for constant total energy of the system

In this part we present the PSD diagrams for the massive particle confined in a two dimensional harmonic potential moving with a constant total energy of the system ($E = 24$) in flat spcaetime but for different values of accelerations. The numerical simulations are done in the similar process as described earlier (see 3.3.2) keeping all the values of the parameters same. The analysis shows us that in presence of horizon with the increase in the acceleration of the system, the motion of the massive particle becomes chaotic which is clearly observed as the frequencies start populating the spectrum. From the following figures (see Fig. 3.9) it can be seen for high values of accelerations the frequencies are highly populated which indicates the beginning of the chaotic fluctuations into the system.

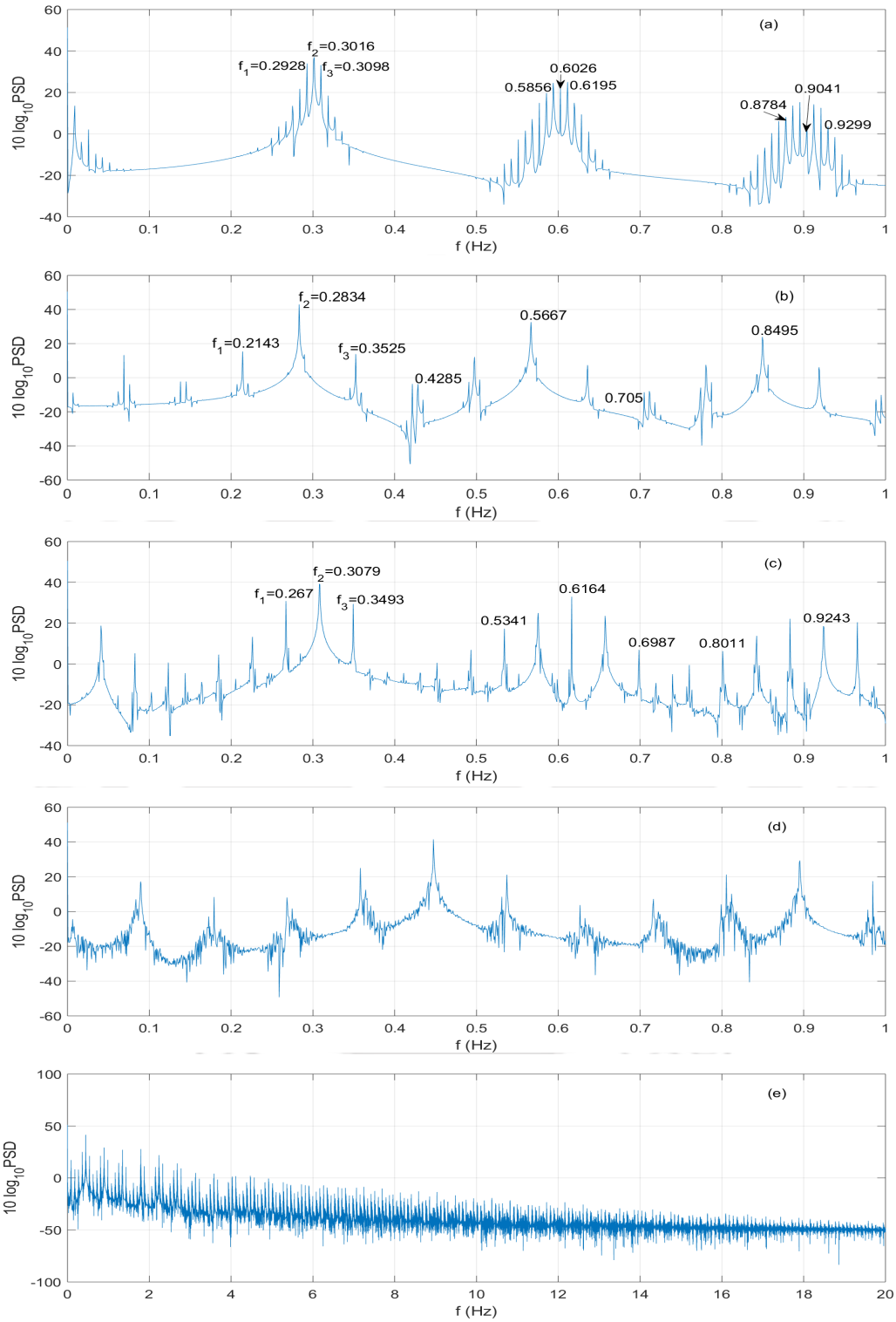

Figure 3.9: (Color online) PSD for a massive particle with mass $m = 1, E = 24, y = 1.0, p_y > 0, K_x = 26.75, K_y = 26.75, x_c = 1.1, y_c = 1.0$ and for different values of accelerations a, namely $(a) a = 0.246, (b) a = 0.26, (c) a = 0.28, (d) a = 0.362$. From the figure it can be seen that from $a = 0.28$ onwards more frequencies start populating the spectrum. At $a = 0.362$, the frequencies are highly populated (see Fig.3.9(e) which indicates the onset of chaos.

3.A.4 PSD for a massive particle for constant acceleration of the system

Here we present the PSD diagrams for the massive particle confined in a two dimensional harmonic potential which is moving with a constant acceleration (a = 0.35) in flat spacetime but for different values of the total energy of the system. The numerical simulations are done in the similar process as earlier keeping all the values of the other parameters same. This analysis shows us that in presence of horizon with the increase in the total energy of the system, the motion of the massive particle becomes chaotic and it is observed as the frequencies start populating the spectrum as the value of the total energy goes higher. From the following figures (see Fig. 3.10) it can be seen for high value of the energy (Fig. 3.10(e)) the frequencies are highly populated which indicates the beginning of the chaotic fluctuations into the system.

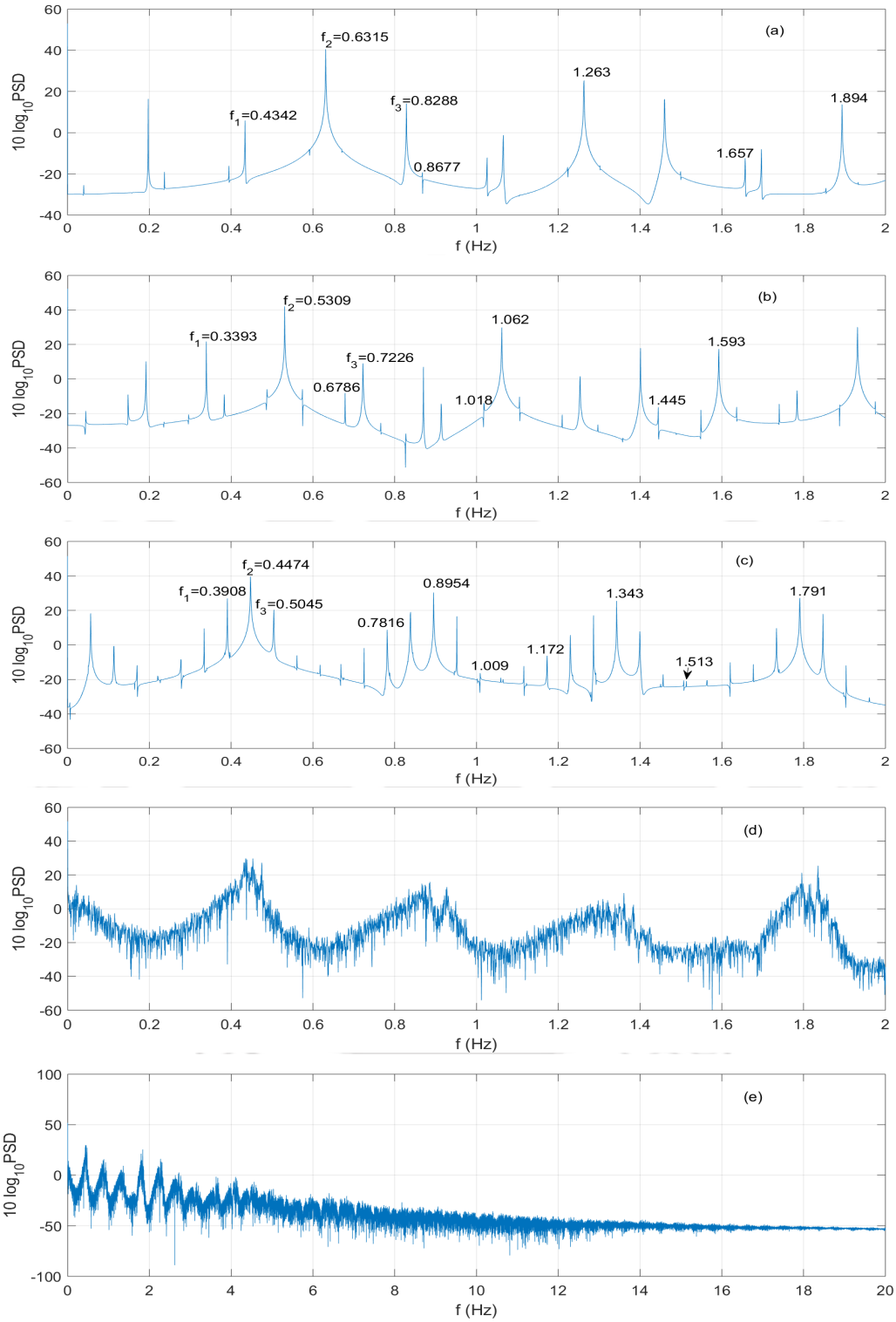

Figure 3.10: (Color online) PSD for a massive particle with mass $m = 1, a = 0.35, y = 1.0, p_y > 0, K_x = 26.75, K_y = 26.75, x_c = 1.1, y_c = 1.0$ and for different values of energies E, namely $(a)E = 20, (b)E = 22, (c)E = 24, (d)E = 24.259$. From the figure it can be seen that from $E = 24$ onwards more frequencies start populating the spectrum. At $E = 24.259$, the frequencies are highly populated (see Fig.3.10(e) which indicates the onset of chaos.

3.A.5 Lyapunov exponent for massive particle

In this section we present our numerical analysis on Lyapunov exponents just like the earlier one (see 3.3.3) but for the massive particle with mass $m = 1$. We have plotted the largest Lyapunov exponent for two cases. First, we consider the energy $E = 24.259$ and $a = 0.35$ (see Fig. 3.11) and secondly, we have plotted for $E = 24.0$ and $a = 0.362$ (see Fig. 3.12). For both the cases we obtained the chaotic behaviour in the particle dynamics. In both the figures (Fig. 3.11 and Fig. 3.12) it is observed that the Lyapunov exponent settle to positive values (~ 0.007 and ~ 0.033 respectively) which suggests the chaotic motion of the particle. Since we observed that the obtained values of the Lyapunov exponents for both the cases are lower than the upper bounds (0.35 and 0.362 respectively), it is consistent with our claim for the massive case also.

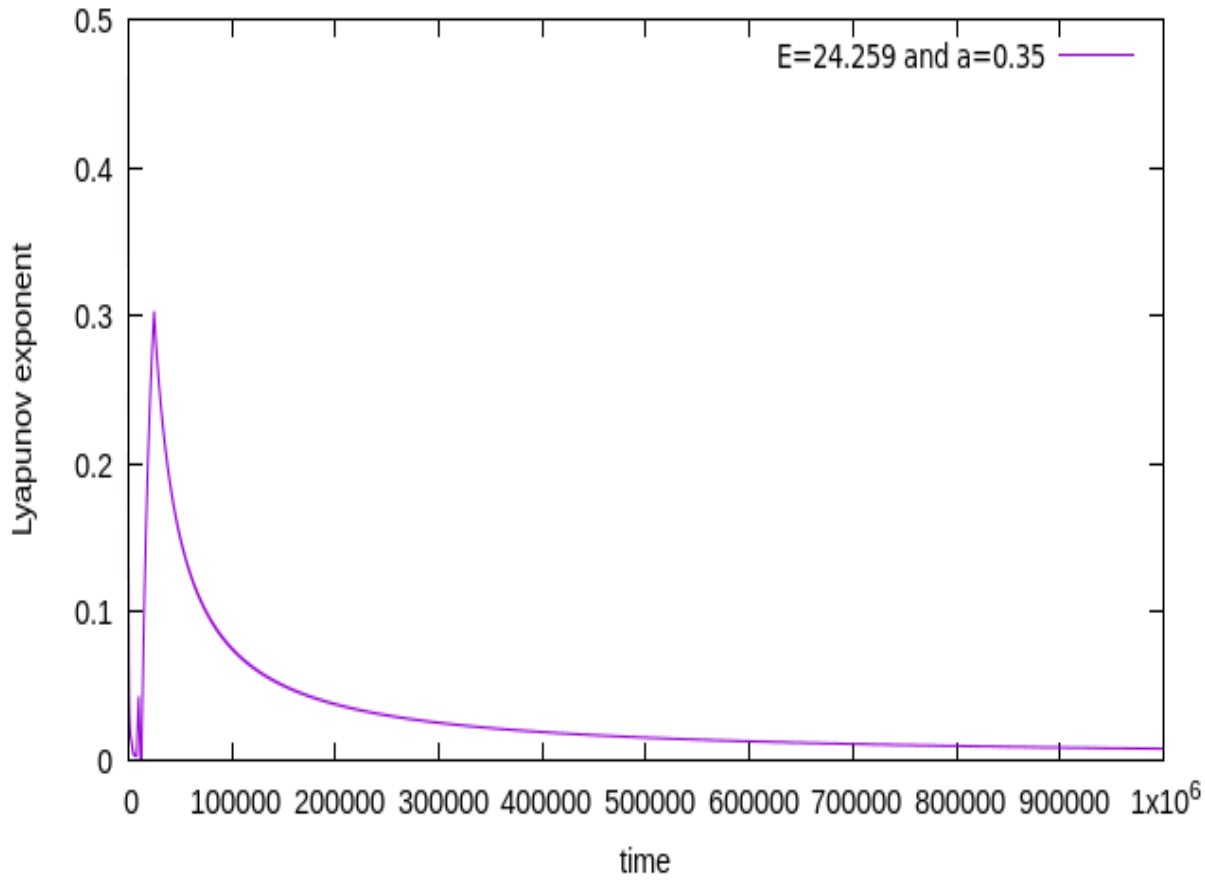

Figure 3.11: (Color online) Largest Lyapunov exponent for the particle in accelerated frame at the energy value $E = 24.259$ and the acceleration $a = 0.35$. The exponent settles at positive value ~ 0.007 which is lower than the upper bound (0.35).

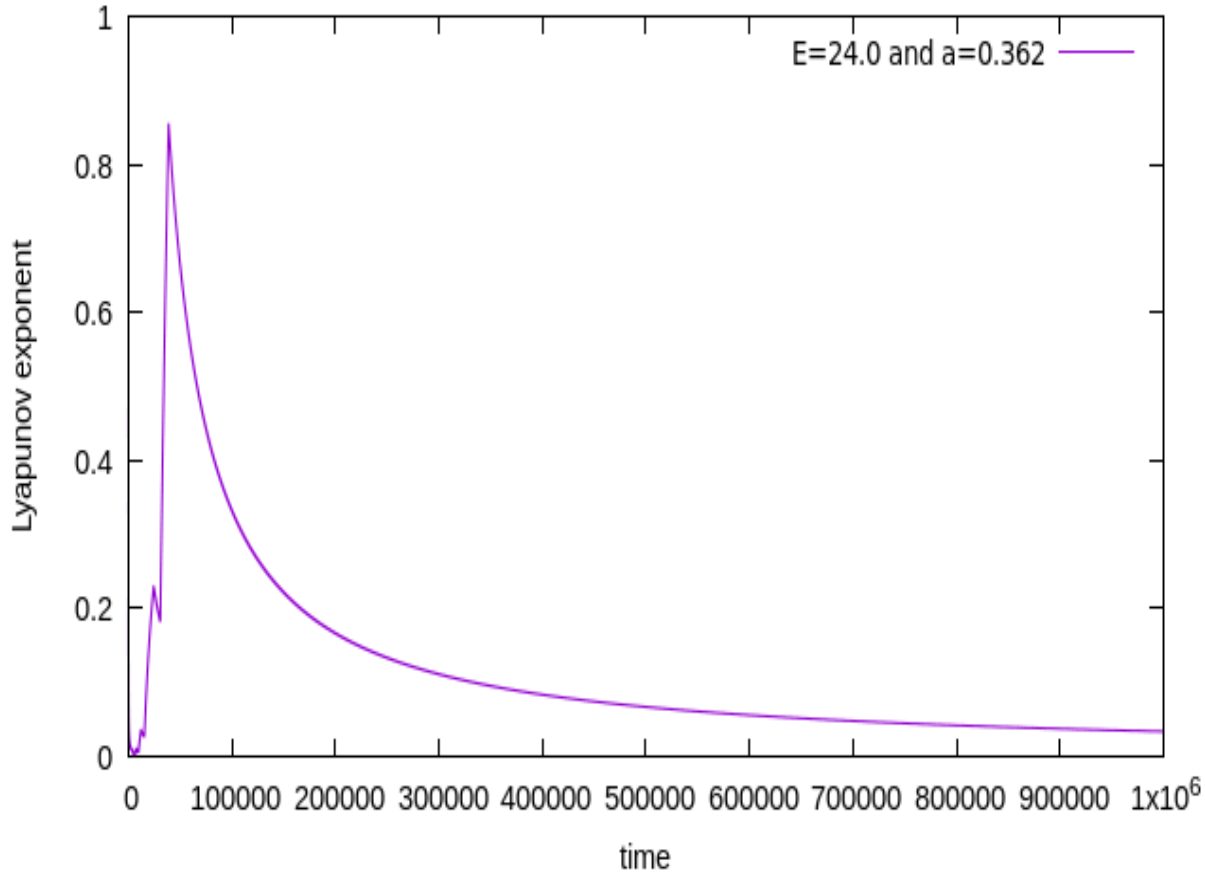

Figure 3.12: (Color online) Largest Lyapunov exponent for the particle in accelerated frame at the energy value $E = 24$ and the acceleration $a = 0.362$. The exponent settles at positive value ~ 0.033 which is lower than the upper bound (0.362).

Part II

Classical scale: Instability

CHAPTER 4

IS NEAR HORIZON LOCAL INSTABILITY THE MAIN REASON FOR CHAOS?

4.1 Introduction and Motivation

Mathematicians usually say *it is very tough to define chaos, but it is easy to "recognize it when you see it."* However, the most challenging part is to find out the reason behind it. In the past two chapters (chapter 2 and chapter 3), we have been fascinated with the fact that a one-way membrane, i.e. the horizon, may create chaotic fluctuations in a system whenever the system comes under the influence of it. An ample amount of studies has been done regarding this [219–224, 236, 237]. Depending upon the values of the available parameters (like the energy of the particle, the mass of the black hole, etc.) the horizon induces chaos into the integrable systems. In a recent work [225], a similar thing has been discussed in the case of string around charged black brane. In the previous two chapters (chapter 2 and chapter 3), we have seen that in the case of static, stationary or in case of a Rindler horizon, an integrable system like a massless particle trapped in a harmonic potential shows chaotic dynamics for particular values of the parameters and when it is under the influence of the horizon. Therefore, an essential spontaneous question one may ask on this note is why the horizons classically give this phenomenological feature in its local territory region. In history, chaotic dynamics in the presence of the horizon have been extensively studied, but the reason behind this fascinating feature of the horizon is yet to be completely

understood. Hence, here comes the most challenging part of finding out the answer to that.

The investigation has not been limited in the classical scale only, and people have tried to expound the chaotic dynamics of the horizon in the quantum regime as well. The phenomena of quantum chaos are mainly examined by the behaviour of the out-of-time-order correlator (OTOC) of some quantum operator [226, 227]. The characteristic exponential growth of OTOC in those cases is the signature of quantum measure of chaos [226, 227].

However, one crucial noticeable point is that, whenever we mention about chaos, there must be some instability factors associated with the system which characterises its chaotic feature. This is known as Lyapunov exponent (LE) (see [228] for a detailed discussion). One recent discovery on the upper bound of the Lyapunov exponent predicted in Sachdev-Ye-Kitaev (SYK) model [226], has made things very interesting. In the previous chapters (chapter 2 and chapter 3) we have already seen for the static (e.g. Schwarzschild spacetime) as well as for the stationary (e.g. Kerr spacetime) BHs, the radial motion of the particle grows exponentially in the near horizon region and the upper bound on the LE is determined by the surface gravity of them whereas for the Rindler case it is determined by the value of the acceleration of the system. Therefore, the upper bound of the instability factor, in this case, theoretically comes out to be consistent with that of the SYK model. This has been verified numerically as well [1]. However, the universality of having the surface gravity as the upper bound of the LE for all the cases is not so obvious and, as far as we know the reason behind it has not been discussed anywhere. Therefore, finding out a concrete explanation for such feature will be the main theme of this chapter.

In the following calculations, we try to study the system from the Hamiltonian perspective in the near horizon region and try to explore some of the features of that system Hamiltonian which may help us describe the appearance of the chaotic fluctuations in the near-horizon region. Now, let us dig into it.

[1]There are few cases [266, 268], which indeed shows the violation of the bound in Lyapunov exponent. This is either due to considering the unstable equilibrium position of the particle motion far from the horizon [266] or due to the inclusion of the quantum correction in the particle motion, provided by the generalised uncertainty principle [268]. Here we shall consider the analysis very near to the horizon. Moreover, in a practical situation, later corrections are very small compared to the original value.

4.2 Near horizon Hamiltonian in the Painleve coordinates

Consider a static spherically symmetric (SSS) BH. Since we are interested in physics near the horizon, in order to remove the coordinate singularity at the horizon, we shall work with the SSS metric in Painleve coordinates expressed in chapter 2 (see Eq. (2.3) in chapter 2). In principle, near horizon physics can be studied in any well behaved coordinates around the horizon, like those found in [269]. But here we adopted Painleve coordinates as it is being extensively used from very early days to study horizon properties. Note that we are interested in the near horizon physics. Here we consider only the radial motion of the particle. The same has already been used in several occasions to study the near horizon physics, like in investigation of Hawking effect using gravitational anomalies [120, 121, 124, 128, 173, 175] as well as tunneling formalism [54, 172–174] (see also [270, 271] for some recent works). In this case considering only the radial motion of the particle, we can obtain the form of the Hamiltonian as:

$$H = p_r \left[1 - \sqrt{1 - 2\kappa(r - r_H)}\right] , \tag{4.1}$$

where κ is the surface gravity of the black hole, p_r is radial momentum corresponding to radial coordinate r and r_H is the location of horizon. Details can be seen in the earlier chapter (chapter 2) where we considered a composite system where the massless and the chargeless particle was trapped in a harmonic potential. However, in the present scenario we have constructed the Hamiltonian simply considering the massless particle residing near a SSS BH with the exclusion of the harmonic potential. Just to mention, the same expression of the Hamiltonian can also be obtained for Kerr case by considering only $\theta = 0$ and ϕ fixed trajectories, with

$$\kappa = \frac{r_H^2 - a^2}{2r_H(r_H^2 + a^2)} , \tag{4.2}$$

where a is the angular momentum per unit mass. For Kerr case, at this point the outer region of ergosphere and event horizon coincides and hence no ambiguity will arise. Details are given in chapter 2. However, a more general situation will be addressed later in chapter 7. So for stationary black hole here the above argument is very restrictive. Since we are interested near to the horizon, expanding (4.1) upto the first order one obtains

$$H \simeq \kappa x p , \tag{4.3}$$

where $x \equiv (r - r_H)$ and $p_r \equiv p$. The same Hamiltonian can also be obtained for the particle motion in the near to Killing horizon regime in a Rindler frame (chapter 3). It shows a possible inherent property of the horizon, as long as near horizon dynamics of the massless particle is concerned [2]. Note that, this one is of the Berry-Keating type $H \sim xp$ [273], which provides instability into the motion of the particle dynamics. We shall focus on this in the next section.

4.2.1 Local Instability in the classical regime

We immediately see that the system, represented by (4.3), has a hyperbolic point at $x = 0$ and at $p = 0$ which induces the instability into the particle's motion in the radial direction. This is of course there only in the vicinity of horizon. Therefore, we call this as *"local instability"*. The Hamilton's equations of motion are

$$\dot{x} = \kappa x, \quad \dot{p} = -\kappa p \ , \tag{4.4}$$

where the dot refers to the derivative with respect to the *affine parameter*, say λ, which parametrises the path. The solutions are are

$$x(\lambda) = x(0)e^{\kappa\lambda}; \ \ p(\lambda) = p(0)e^{-\kappa\lambda} \ . \tag{4.5}$$

The above Eq. (4.5) shows that the radial motion is unstable for the choice of a positive affine parameter in the near horizon region [3]. In chapter 2 we obtained the similar radial equation of motion for the massless particle in the near horizon region of a SSS and a Kerr BH. Not only that in chapter 3 we have also seen that the particle motion becomes unstable in a similar way near the Killing horizon in the Rindler case. Therefore, this result implies the fact that the growth of the radial coordinate may be the possible reason for instability and inducing chaos in an integrable system and this peculiar xp Hamilton is responsible for that.

Now, let us study what is happening to the trajectories in the near horizon region. In order to see the time (λ here) evolution of the neighbouring trajectories, consider a trajectory (say l^{th}) which starts at phase space position (x_A, p_A) at λ_A and ends at (x_B, p_B) after one period $T_l = \lambda_B - \lambda_A$. We are interested to examine the effect when one

[2] The Hamiltonian, corresponding to the surface part of Einstein-Hilbert action, has similar structure with respect to particular choice of canonical conjugate variables [272]

[3] However, it can be shown that the instability can be present in the radial momentum coordinate also on the choice of affine parameter. In the next section 4.3 we shall show the that this is indeed the case.

changes the initial position and momentum slightly, say $(\delta x_A, \delta p_A)$. Use of (4.5) leads to the relation between the separations for $T_l > 0$ as

$$\begin{bmatrix} \delta x_B \\ \delta p_B \end{bmatrix} = \underbrace{\begin{bmatrix} e^{\kappa T_l} & 0 \\ 0 & e^{-\kappa T_l} \end{bmatrix}}_{M_{BA}} \begin{bmatrix} \delta x_A \\ \delta p_A \end{bmatrix} . \tag{4.6}$$

The above matrix M_{BA} is known as the Monodromy matrix [274]. We mention that only the classical periodic trajectories are important here and they contribute to the density of states at the quantum level [274]. Consequently, (4.6) yields the homogeneous instability, represented by calculating the largest instability factor (IF) [228]:

$$\lambda_{L,max} = \lim_{T_l \to \infty} \frac{1}{T_l} \ln \left[\frac{\delta x_B}{\delta x_A} \right] = \kappa > 0 . \tag{4.7}$$

Usually the positive instability factor is associated with chaos in the system.

We saw that the near horizon trajectories are the one which diverge exponentially. It explains why any integrable system must be affected when it reaches very near to the horizon. In particular, this local instability may influence chaotic dynamics to a system when it comes very near to the horizon for some particular values of available parameters. Such an event is consistent with the Kolmogorov–Arnold–Moser (KAM) theory [256]. This can be a probable explanation for getting chaotic behaviour in the earlier numerical analysis which we have done in the previous chapter 2 where a particle is trapped in potential like harmonic one, kept under the BH background. Moreover, such a thing is happening irrespective of the consideration of spacetime. The universal property of the spacetimes is - all of them should contain a horizon. In addition, the presence of any intrinsic curvature of the spacetime is not crucial; only the existence of horizon alone is enough to make the motion of the particle chaotic. As for example, particle dynamics on Rindler metric in harmonic trap also exhibits chaotic behaviour as we have seen in chapter 3. This feature of horizons is due to the fact that the leading order particle Hamiltonian, near horizon, is inherently $H \sim xp$, which provides the local unstable trajectories in the particle motion.

However, based on these facts mentioned above, there are certain remaining issues which are needed to be addressed. They are as follows.

- Is there any other set of observers other than Painleve, which also predicts a similar instability?
- Are all these features in general observer-dependent, or some are not so?

- Can the instability be addressed without going to Hamiltonian (or equivalently Lagrangian) analysis?
- Is it possible to construct Hamiltonian of the system just by the knowledge of the nature of instability in the near horizon regime? This will elaborate on the active role of xp type Hamiltonian in this system.

In the remaining sections of this Chapter, we shall try to elaborate on these issues. However, we shall explicitly try to address these features for those observers who can feel the existence of the horizon. Notably, there exists another set of such coordinates known as Eddington-Finkelstein (EF) coordinates. Hence, we shall try to analyse the issues mentioned earlier in EF coordinates for a probed massless particle residing in the near-horizon region of a SSS BH. First, let us define that coordinate system and the path of the outgoing massless particle in the near-horizon region. We start in the following way.

4.3 Outgoing path of massless particle in Eddington-Finkelstein (EF) coordinates

Massless particle follows null-like trajectories and therefore the tangent to the path must be null-like. To identify those, for simplicity, we consider a static spherically symmetric black hole (SSSBH) metric in Schwarzschild coordinates (t_s, r, θ, ϕ) as

$$ds^2 = -f(r)dt_s^2 + \frac{1}{f(r)}dr^2 + h(r)(d\theta^2 + \sin^2\theta d\phi^2). \tag{4.8}$$

Usually in $(1+3)$ dimensions $h(r) = r^2$, but we kept this as a general function of radial coordinate for our future purpose. The above coordinate system is singular at the event horizon $\mathscr{H}$, which corresponds to $f(r_H) = 0$. Since we shall confine our investigation in the near horizon regime, the above singularity is not desired to exist in the choice of coordinates. Moreover, we want the particle to follow the outgoing null trajectory. For this purpose, Kruskal-Szekeres (KS) coordinates (U, V, θ, ϕ) in the null-null form will be relevant ones. Since the paths will be outgoing ones, we consider the particle propagates along the normal to U = constant surface, where

$$U = \pm\exp(-\kappa u) + 1\ . \tag{4.9}$$

(Following the discussion in Section 2.5 of [275], we here choose the above convention). Since the normal to null surface is tangent to it as well, the particle will propagate

along this U = constant surface if the tangent to it's path be this null normal. For the above choice, the event horizon $r = r_H$ is located at $U = 1$. Here κ is the surface gravity defined by $\kappa = f'(r_H)/2$. The $+(-)$ sign stands for the coordinate is defined outside (inside) the event horizon. For the present purpose, only the $+$ sign will be considered as our test particle resides outside the horizon. In the above, u is known as the Eddington-Finkelstein (EF) outgoing null coordinate. There is also EF ingoing null coordinate v. Both of them are related to Schwarzschild coordinates by the relations $u = t_s - r_*$ and $v = t_s + r_*$, respectively with the tortoise coordinate r_* is defined as

$$dr_* = \frac{dr}{f(r)} \ . \tag{4.10}$$

The KS coordinates cover the whole spacetime and, therefore, very much adopted to freely falling observer. In order to realize the presence of the horizon by the particle and to confine it outside black hole, the null trajectories will be viewed from a different coordinate system, defined only outside the horizon. For that purpose, we adopt a new set of EF coordinates (t, r, θ, ϕ) where t is related to old coordinates as

$$t = v - r = t_s + r_* - r \ , \tag{4.11}$$

where r_* is taken to be valid outside the horizon. Since t_s and r are timelike and spacelike in the $r > r_H$ region, these new coordinates are properly suited for this region only. The metric (4.8), in these, takes the following form:

$$ds^2 \ = \ -f(r)dt^2 + 2\Big(1 - f(r)\Big)dtdr + \Big(2 - f(r)\Big)dr^2 + h(r)\Big(d\theta^2 + \sin^2\theta d\phi^2\Big) \ . \tag{4.12}$$

Considering that the observer is in this frame, we shall calculate all our physical quantity in these coordinates. So now, our next task is to calculate the normal to U = constant surface, which describes the path of the massless particle. Since the observer is in the new EF frame, we need to transform the normal vector in these coordinates. This will give the form of the trajectory of the massless particle with respect to our desire observer.

The normal vector to U = constant (say, K) surface is determined by $l_a = e^{\rho}\nabla_a U$, where ρ is some scalar field on this. For the moment value of K can be *any* constant. But since we are interested in near horizon region, at the end, whenever necessary, the limit $U = K \to 1$ will be taken to achieve our final goal. With this we find the following components of l^a on any U = constant surface in (t, r, θ, ϕ) coordinates as

$$l^a = -\kappa e^{[\rho - \kappa(t - 2r_* + r)]}\left(1 - \frac{2}{f(r)}, -1, 0, 0\right) \ . \tag{4.13}$$

Let us now choose ρ in such a way that $l^t = 1$. Then we obtain the contravariant components of the tangent to particle trajectory as

$$l^a = \left(1, \frac{f(r)}{2-f(r)}, 0, 0\right) . \tag{4.14}$$

Consequently the covariant components are

$$l_a = \left(\frac{f(r)}{f(r)-2}, 1, 0, 0\right) . \tag{4.15}$$

One can check that on the horizon $\mathscr{H}$ the components reduces to $l^a \overset{\mathscr{H}}{=} (1,0,0,0)$, which has the same normalization as that of the timelike Killing vector for this spacetime. This motivated the purpose of above choice for ρ.

Now the integral curves $x^a(\mu) = (t, r, \theta, \phi)$ of l^a, characterized by

$$\frac{dx^a(\mu)}{d\mu} = l^a(x(\mu)) , \tag{4.16}$$

where μ is the parameter which fixes the particle position at a particular moment, lead to the outgoing null trajectory of our massless particle along any U = constant surface. Note that the angular components of l^a vanishes and so *the particle will have motion only along the radial direction*. In the upcoming section we shall study these trajectories in the near horizon regime, i.e. in the limit $U \to 1$ (or equivalently $f(r) \to 0$).

4.3.1 Radial behaviour in the near horizon region

So far, we found the path of our test particle, given by the integral curve (4.16) of the tangent vector (4.14). We are now in a position to investigate the behaviour of this curve in the vicinity of the horizon. Since it has been observed that (4.14) does not have any angular component, the particle will perform only the radial motion. Therefore, our local analysis will give the nature of the radial coordinate of the particle.

Since the components of tangent vector l^a is given by (4.14) and $x^a = (t, r, \theta, \phi)$, the time component of (4.16) yields

$$\frac{dt}{d\mu} = 1 \Rightarrow \mu = t . \tag{4.17}$$

Then the radial component of (4.16) leads to

$$\frac{dr}{dt} = \frac{f(r)}{2-f(r)} . \tag{4.18}$$

The solution of this will give us the behaviour of the particle trajectory in the radial direction. Since we are interested in the neighbourhood region of the horizon, the metric

coefficient $f(r)$ can be taken as the leading term of the Taylor series expansion of it around $r = r_H$:

$$f(r) \simeq 2\kappa(r - r_H) \ . \tag{4.19}$$

Substituting this in (4.18) and then keeping upto the relevant leading order ($\mathcal{O}(r - r_H)$), we obtain

$$\begin{aligned} \frac{dr}{dt} &\simeq \frac{2\kappa(r - r_H)}{2 - 2\kappa(r - r_H)} \\ &\simeq \kappa(r - r_H) \ . \end{aligned} \tag{4.20}$$

The solution of it is

$$r - r_H = \frac{1}{\kappa} e^{\kappa t} \ . \tag{4.21}$$

Later we shall show that the effective Hamiltonian corresponding to (4.21) is given by (4.3) and hence the corresponding momentum will have the form of $p \sim e^{-\kappa t}$. Now, as our probed particle resides very near ot the horizon, so, in the limit of $t \to -\infty$, the radial momentum diverges, i.e. $p_r \to \infty$. Therefore, it suggests the fact that our test particle experiences instability in the presence of the horizon. We shall elaborate this towards the end of the present subsection.

As this instability in the radial motion is experienced by the particle as long as it is situated very near to the horizon, we call this *local* instability. The similar feature we also obtained in the painleve coordinates also which we mentioned in the previous section (see Eq. (4.5)). Not only that we have also seen this feature in the previous two chapters (chapter 2 and chapter 3) for the case of SSS and Kerr BH and for the Rindler case also. However, this instability lies only in the vicinity region of the horizon and therefore, for the rest of the chapter, we shall call this as just instability without the explicit mention that it is locally applicable. But keep in mind that whenever such is stated, this is always in a local sense.

Before going into the discussion of the consequences of this local instability, we will show that the above can also be realised in an alternative way. We know the expansion parameter of the congruence of geodesics Θ, which is defined as

$$\Theta = q^{ab} \nabla_a l_b \ , \tag{4.22}$$

where q_{ab} is the transverse part of the metric g_{ab}, defined as

$$q_{ab} = g_{ab} + l_a n_b + l_b n_a \ . \tag{4.23}$$

Here n_a is an auxiliary null vector field which satisfies $l^a n_a = -1$. Therefore, using the non-affinely parametrised geodesic equation defined in Appendix 4.A (see Eq. (4.A.1.1)) and using (4.23) and (4.22), the parameter Θ can be expressed in terms of l^a and $\tilde{\kappa}$ as

$$\begin{aligned} \Theta &= \nabla_a l^a - \tilde{\kappa} \\ &= \frac{1}{\sqrt{-g}} \partial_a (\sqrt{-g}\, l^a) - \tilde{\kappa} \ , \end{aligned} \tag{4.24}$$

where g is the determinant of the metric.

Now, the expansion parameter of the null geodesic congruence (Θ) encodes the information about the behaviour of geodesics – how the distance between two neighbouring paths changes. Therefore, it is instructive to investigate this parameter in the present context. Below we shall use the value of Θ, calculated in Appendix 4.A, to obtain the behaviour of radial direction in the vicinity of the horizon. We shall come back to this quantity again in the next section.

Now, for the metric (4.12) we can write from Eq. (4.24)

$$\partial_r l^r = \Theta - \frac{h'(r)}{h(r)} l^r + \tilde{\kappa} \ , \tag{4.25}$$

where prime indicates the derivative with respective to the r coordinate. Notice that, in the near horizon regime the expression (4.A.2.2) for Θ implies that the expansion parameter is of the order $(r - r_H)$. Similarly, (4.14) shows l^r is also $\mathcal{O}(r - r_H)$ in this approximation. On the other hand Eq. (4.A.1.18) shows that $\tilde{\kappa} = \kappa + \mathcal{O}(r - r_H)$. Therefore, in the limit $r \to r_H$, keeping only the leading order terms in Eq. (4.25) we obtain

$$\partial_r l^r = \kappa \ . \tag{4.26}$$

Now using the fact that $l^r = dr/dt$, the solution of the above comes out to be $r = (1/\kappa)e^{\kappa t} + C$ where C is an integration constant. Since, for $r \to r_H$ (i.e. $r_* \to -\infty$) implies $t \to -\infty$, one obtains $C = r_H$. Therefore we have the same solution (4.21). Also note that very near to the horizon ($t \to -\infty$), the radial momentum p_r diverges as we have mentioned earlier. This is the indication of instability near the horizon.

We now make a comment for the same in $(1+1)$ dimension static black hole case. This is needed as later in some situations we shall consider this lower-dimensional case for the simplicity of the calculation. For (1+1) dimensional case i.e. considering the $(t-r)$ sector of metric (4.12), one can readily show that time and radial components of l^a are given by those given in (4.14). Therefore, one again finds the same radial behaviour as obtained in (4.21). Also, as here Θ vanishes and the determinant of the metric is $g = -1$,

the definition for expansion parameter (4.24) reduces to Eq. (4.26). Hence one finds (4.21) again, and so the existence of the instability in the particle motion in the near horizon region persists in this case as well. This indicates that the present instability is completely due to the influence of the horizon in spacetime, not specific to the number of spacetime dimensions.

4.3.2 A covariant realisation of local instability

We found that the radial motion is unstable in nature in the very near to the horizon. In this regard, it is natural to ask – what happens to the family of these null geodesics in this region? Whether this congruence of geodesics also faces a similar instability due to the horizon. Moreover, in the last section we mentioned that the expansion parameter Θ can be an important quantity to illuminate our main investigation. Particularly as it measures the separation between the two nearby geodesics, it will be interesting to see how this separation changes with time. Thus we shall have a more concrete idea of instability, provided by the horizon. Therefore, the present section will be dedicated to examining the evaluation of Θ for null geodesics in the nearby region of the horizon. The most promising way is to start with the Raychaudhuri's equation for null congruence [276]. Since it is in the covariant form, we expect that the evaluation character of Θ, obtained from this, in contrary to the earlier section, may provide a covariant description of our aforesaid instability.

Raychaudhuri equation for null geodesics is [276]

$$\frac{d\Theta}{d\mu} = \tilde{\kappa}\Theta - \frac{1}{2}\Theta^2 - \sigma_{ab}\sigma^{ab} + \omega_{ab}\omega^{ab} - R_{ab}l^a l^b \ . \tag{4.27}$$

Here we shall study this equation in the near horizon of our SSSBH spacetime (4.12). All the quantities are defined with respect to the null vector (4.14). Let us now examine each of the terms on the right hand side of the above equation. These are all calculated in Appendix 4.A. We found that the shear parameter $\sigma_{ab} = 0$ (see Eq. (4.A.3.4)) and since l_a is hypersurface orthonormal, we must have the rotation parameter $\omega_{ab} = 0$ as well. Next note that in the near horizon region $\Theta \sim \mathcal{O}(r - r_H)$ (see Eq. (4.A.2.2)), whereas as mentioned in the last section, $\tilde{\kappa} = \kappa + \mathcal{O}(r - r_H)$. The evaluation of the term $R_{ab}l^a l^b$ for metric (4.12) yields

$$R_{ab}l^a l^b = \frac{f^2(r)\left(h'^2(r) - 2h(r)h''(r)\right)}{2(f(r)-2)^2 h^2(r)} \ . \tag{4.28}$$

Now, for the value of $h(r) = r^2$ the above term vanishes. Therefore, keeping the leading order terms, i.e. $\mathcal{O}(r - r_H)$ terms in the right hand side of Eq. (4.27) one obtains

$$\frac{d\Theta}{d\mu} = \kappa\Theta \, . \tag{4.29}$$

Performing the integration of the above equation we obtain the form of the expansion parameter as

$$\Theta = \kappa e^{\kappa\mu} \, . \tag{4.30}$$

Therefore we can see that in the near horizon region the expansion parameter of the geodesic congruences is exponentially increasing as μ increases. We will demonstrate how this expansion parameter feature suggests that the particle's radial motion is unstable in the vicinity of the horizon. Additionally, when one obtains the Θ value in this structure, it automatically denotes that the particle's geodesic motion is unstable in the near-horizon region.

This analysis not only indicates the presence of local instability for the particle motion but also provides a covariant description and realisation of this phenomenon. Since Θ is a scalar quantity, we now understand that for this particular particle motion, the aforesaid *instability is an observer independent feature of horizon*.

We now show that from Eq. (4.30) the explicit form of unstable nature in radial motion can be evaluated. In our EF coordinates we identified $\mu = t$ (see Eq. (4.17)). One can check that at the horizon (i.e. $t \to -\infty$), Θ vanishes, which implies that the above solution correctly satisfies the required boundary condition. The value of Θ for our metric (4.12) is given by (4.A.2.2). In the near horizon regime, at the leading order, it comes out to be

$$\Theta \simeq \frac{2\kappa}{r_H}(r - r_H) \, , \tag{4.31}$$

where we have used $h(r) = r^2 \to r_H^2$ and $h'(r) = 2r \to 2r_H$. Substitution of this in the solution (4.30) yields $r - r_H \simeq (r_H/2)e^{\kappa t}$. Thus again, we found the similar unstable nature in the radial direction. It must be mentioned that for the trajectory given by the tangent vector (4.14) *although the instability is an observer-independent feature, this particular radial character with time is related to EF observer*. This is a very crucial observation in this analysis.

4.3.3 Near horizon instability: Hamiltonian analysis

So far, without using any formal prescription, like Lagrangian or Hamiltonian analysis, we have been able to show the appearance of local instability on the radial motion of

a massless particle in the vicinity of the horizon. This feature has been shown earlier in the earlier section (4.2.1) of the present chapter using the Hamiltonian analysis in Painleve coordinates for the metric. It was shown that the near horizon Hamiltonian takes the form $\sim xp$, where $x = r - r_H$ and p is the radial momentum. In the present section, we are using a new EF coordinates and found that here also, a similar feature is appearing in radial motion even in this new coordinates. Therefore, it would be interesting to see whether a Hamiltonian prescription can be built out in our present analysis. More importantly, we are interested in investigating the possibility of finding out the Hamiltonian of our system using the obtained radial feature in the earlier sections. If so, then whether it is again similar to xp. In this section, we shall first find the Hamiltonian from our earlier findings on the radial trajectory and then verify this by deriving the same using dispersion relation for the massless particle on the background (4.12). This obtained structure of Hamiltonian will be very important for the later purpose of our analysis.

4.3.3.1 Hamiltonian from trajectories

The near horizon radial motion is driven by Eq. (4.21). Therefore use of Hamilton's equation of motion $\dot{x} = \partial H/\partial p$ implies

$$\frac{\partial H}{\partial p} = \kappa x \ , \tag{4.32}$$

where $x \equiv r - r_H$. Solution of this is given by $H = \kappa xp + f_1(x)$, where $f_1(x)$ is an arbitrary function of radial coordinate. This can be fixed by using the information that the corresponding Lagrangian must vanish as we are dealing with massless free particle. The Lagrangian for this solution comes out to be

$$L = p\dot{x} - H = -f_1(x) \ . \tag{4.33}$$

So to make it vanish, we must choose $f_1(x) = 0$. Thus we find that the Hamiltonian in the near horizon regime is given by

$$H = \kappa xp \ . \tag{4.34}$$

We now verify this below by direct evaluation of Hamiltonian from the dispersion relation. This method has been adopted in the earlier chapter 2, but for the Painleve coordinates. Therefore, the momentum is given by $p \sim e^{-\kappa t}$. Now, from here also one can see as for a given energy the radial momentum p diverges as $x \to 0$. The limit $x \to 0$ is basically

equivalent to $t \to -\infty$, i.e. our test particle is approaching towards the horizon. We have already witnessed this momentum divergence in our earlier discussion and here also we confirm it again in the limit of $x \to 0$. This indicates again the fact our massless particle feels the presence of "*local instability*" in the vicinity region of the horizon.

4.3.3.2 Hamiltonian from dispersion relation

We again start with the static spherically symmetric metric written in EF coordinates (4.12) which has a timelike Killing vector $\chi'^a = (1,0,0,0)$ and the energy of a particle moving under this background is given by $E = -\chi'^a p_a = -p_t$, where p_a is the four momentum whose components are $p_a = (p_t, p_r, 0, 0)$. The angular components are chosen to be zero as for our choice of path there is only radial motion (see Eq. (4.14)). Using the covariant form of the dispersion relation $g^{ab}p_a p_b = 0$ for massless particle, we obtain the equation of the energy in terms of the radial component of the momentum as

$$(f(r)-2)E^2 - 2(1-f(r))Ep_r + f(r)p_r^2 = 0\ . \tag{4.35}$$

It is found that the energy has two solutions:

$$E = \frac{(f(r)-1)p_r \mp p_r}{2-f(r)}\ , \tag{4.36}$$

where the positive sign for the outgoing particle and the negative sign for the ingoing one. With the near horizon approximation i.e. for $f(r)$ given in Eq. (4.19), we obtain the expression for the energy of the outgoing particle (i.e. taking the $+ve$ sign solution) as

$$\begin{aligned} E &= \frac{(f(r)-1)p_r + p_r}{2-f(r)} \\ &= \frac{\kappa(r-r_H)p_r}{1-\kappa(r-r_H)} \\ &\simeq \kappa(r-r_H)p_r + \mathcal{O}(r-r_H)^2\ . \end{aligned} \tag{4.37}$$

Since we are interested near to the horizon, taking up to the first-order one obtains the expression of the Hamiltonian for the outgoing particle as (4.34) [4], with $p_r \equiv p$.

So we observed that the nature of Hamiltonian, like in Painleve coordinates (4.3), is $\sim xp$ even in EF coordinates. As we have already mentioned in the Painleve coordinate

[4]It may be mentioned that this type of Hamiltonian is somehow very common feature of the gravitational system. It appears in different situations in the presence of gravity. At the thermodynamic level, the surface part of the Einstein-Hilbert action yields xp type Hamiltonian [272]. Also similar observation has been noticed for the dynamics of super-translational parameter in the context of asymptotic symmetry of a null surface [277].

(section 4.2) that this Hamiltonian is inherently unstable in nature, having the hyperbolic points at $x = 0$ and $p = 0$, which induces the instability into the particle's motion. Similarly, the equations of motion corresponding the Hamiltonian are same as we have obtained earlier (see Eq. (4.5)). It immediately shows us again that at the classical level, the radial motion of the massless particle is unstable in the vicinity of the horizon, which we have already shown in different approaches in the previous sections.

4.4 Summary and Discussions

We shall end this classical discussion with the following comment. In the previous chapters (chapter 2 and chapter 3) we have already seen that horizon induces chaos in a system whenever the system comes under the influence of it. Not only that, for a very long time through various approaches, people have seen this phenomena [219–224, 236, 237] and notably this is common to any black hole spacetime. To follow up the real cause of this universal feature was the main theme of this chapter. To find out the concrete reason we argued that the instability may be the main cause of it. In section 4.2 the static spherically symmetric black hole, Rindler case and very restrictive trajectories for Kerr black hole have been explored in Painleve coordinates. It is observed that such is due to the appearance of xp type Hamiltonian for a near horizon motion of a particle. On the basis of this investigation a further spontaneous question one may ask if there is any other set of observers other than Painleve where the same phenomena can be observed. More precisely whether this feature is observer dependent or not.

Therefore, in the later section 4.3 we investigated the whole phenomena in a more extensive way. We find that there is another set of coordinates, namely the Eddington-Finkelstein (EF) coordinates, in which the motion of the particle along the null trajectory also faces the instability in the near horizon region. Moreover, such instability is very much there for any observer when the particle is following the outgoing null path in that particular EF coordinates. It implies that *the observed near horizon instability of the particle motion is an observer-independent phenomenon for this particular motion of the particle*. Notably, again the instability factor is given by the surface gravity of the black hole. Next, we find that the observer associated with the EF frame measures the radial motion as $r \sim e^{\kappa t}$ where r and t are the EF radial and time coordinates, and radial momentum as $p \sim e^{-\kappa t}$ respectively. The corresponding Hamiltonian comes out to be in xp structure again similar to the Painleve case. It suggests that although the instability is observer independent for our particle motion, the particular form of the Hamiltonian is

observer dependent. The observer associated with this specific frame, either in Painleve or in EF coordinates will see this form of the near horizon Hamiltonian.

Following this classical picture, our next aim is to know whether such local instability in the near horizon region have any observable outcomes or not. In order to realise that quantum aspects of this instability will be addressed in the next chapter. Our main objective will be to study the aforesaid instability at the quantum scale using various possible ways to extract more knowledge about its consequences in the near horizon region.

Appendix

4.A Evaluation of $\tilde{\kappa}$, Θ and σ_{ab} for the null vector (4.14) in the background (4.12)

4.A.1 Non-affinity coefficient $\tilde{\kappa}$

Consider the null normal vector field l_a of any null hypersurface generates a null geodesic congruence. The non-affinely parametrised geodesic equation is given by

$$l^b \nabla_b l_a = \tilde{\kappa} l_a \ , \tag{4.A.1.1}$$

where $\tilde{\kappa}$ is called the non-affinity coefficient. In order to find $\tilde{\kappa}$ for the geodesic curves, given by (4.14), first we need to compute the gradient of the null normal ($\nabla_b l_a$). We have already computed the components of l_a in Section (4.3) (see Eq. (4.15)). Therefore, the components of $\nabla_b l_a$ in EF coordinates are obtained for the metric (4.12) as

$$\nabla_b l_a = \begin{pmatrix} \frac{1}{2}\frac{f(r)f'(r)}{f(r)-2} & \frac{1}{2}\frac{(f(r)-4)f(r)f'(r)}{(f(r)-2)^2} & 0 & 0 \\ \frac{f'(r)}{2} & \frac{1}{2}\frac{(f(r)-4)f'(r)}{f(r)-2} & 0 & 0 \\ 0 & 0 & -\frac{1}{2}\frac{f(r)h'(r)}{f(r)-2} & 0 \\ 0 & 0 & 0 & -\frac{1}{2}\frac{f(r)h'(r)}{f(r)-2}\sin^2\theta \end{pmatrix} . \tag{4.A.1.2}$$

where $\nabla_b l_a = \partial_b l_a - \Gamma^c_{ba} l_c$ and the non-zero components of Christoffel symbols (Γ^c_{ba}) are given below

$$\Gamma^t_{tt} = -\frac{1}{2}(-1+f(r))f'(r) \tag{4.A.1.3}$$

$$\Gamma^t_{rt} = -\frac{1}{2}(-2+f(r))f'(r) \tag{4.A.1.4}$$

$$\Gamma^t_{rr} = -\frac{1}{2}(-3+f(r))f'(r) \tag{4.A.1.5}$$

$$\Gamma^t_{\theta\theta} = \frac{1}{2}(-1+f(r))g'(r) \tag{4.A.1.6}$$

$$\Gamma^t_{\phi\phi} = \frac{1}{2}(-1+f(r))g'(r)\sin^2\theta \tag{4.A.1.7}$$

$$\Gamma^r_{tt} = \frac{1}{2}f(r)f'(r) \tag{4.A.1.8}$$

$$\Gamma^r_{rt} = \frac{1}{2}(-1+f(r))f'(r) \tag{4.A.1.9}$$

$$\Gamma^r_{rr} = \frac{1}{2}(-2+f(r))f'(r) \tag{4.A.1.10}$$

$$\Gamma^r_{\theta\theta} = -\frac{1}{2}f(r)g'(r) \tag{4.A.1.11}$$

$$\Gamma^r_{\phi\phi} = -\frac{1}{2}f(r)g'(r)\sin^2\theta \tag{4.A.1.12}$$

$$\Gamma^\theta_{\theta r} = -\frac{1}{2}\frac{g'(r)}{g(r)} \tag{4.A.1.13}$$

$$\Gamma^\theta_{\phi\phi} = -\cos\theta\sin\theta \tag{4.A.1.14}$$

$$\Gamma^\phi_{\phi r} = \frac{1}{2}\frac{g'(r)}{g(r)} \tag{4.A.1.15}$$

$$\Gamma^\phi_{\phi\theta} = \cot\theta \tag{4.A.1.16}$$

Now, using the values of the $\nabla_b l_a$ components we obtain

$$l^b\nabla_b l_a = \left(\frac{2f'(r)f(r)}{(f(r)-2)^3}, \frac{2f'(r)}{(f(r)-2)^2}, 0, 0\right). \tag{4.A.1.17}$$

Using the geodesic equation (4.A.1.1) and comparing Eq. (4.A.1.17) with the expression of Eq. (4.15), we deduce the value of $\tilde{\kappa}$ as

$$\tilde{\kappa} = \frac{2f'(r)}{(f(r)-2)^2}. \tag{4.A.1.18}$$

4.A.2 Expansion parameter Θ

The expansion parameter of the congruence of geodesics Θ has already been defined in the subsection 4.3.1 (please see Eq. (4.22)). Since, in this case the determinant of the

metric (4.12) is $g = -h^2(r)\sin^2\theta$ and l^a is given by (4.14), Eq.(4.24) yields

$$\Theta = \frac{1}{h(r)\sin\theta}\partial_r\left[\frac{h(r)f(r)}{2-f(r)}\sin\theta\right] - \tilde{\kappa} \ . \tag{4.A.2.1}$$

Next using (4.A.1.18) in the above we obtain the expression of the expansion parameter

$$\Theta = \frac{h'(r)f(r)}{h(r)(2-f(r))} \ . \tag{4.A.2.2}$$

4.A.3 Shear parameter σ_{ab}

The shear parameter σ_{ab} of the congruence of geodesics is defined as

$$\sigma_{ab} = \frac{1}{2}(b_{ab} + b_{ba} - \Theta q_{ab}) \ , \tag{4.A.3.1}$$

where b_{ab} is the orthogonal component of $\nabla_a l_b$ projected by q_{ab}:

$$b_{ab} = q_a^c q_b^d \nabla_c l_d \ . \tag{4.A.3.2}$$

Now, the induced metric q_{ab} for the space-time metric (4.12) is given by

$$q_{ab} = \begin{pmatrix} 0 & 0 & 0 & 0 \\ 0 & 0 & 0 & 0 \\ 0 & 0 & g(r) & 0 \\ 0 & 0 & 0 & g(r)\sin^2\theta \end{pmatrix} . \tag{4.A.3.3}$$

Therefore, using the induced metric components (q_{ab}) and applying (4.A.1.2) and (4.A.3.2) in (4.A.3.1) one can easily calculate each component of σ_{ab}. This can be readily shown that each term of σ_{ab} vanishes i.e.

$$\sigma_{ab} = 0 \ . \tag{4.A.3.4}$$

Part III

Quantum scale: Thermality

CHAPTER 5

LOCAL INSTABILITY LEADS TO THERMALITY

5.1 Introduction and Motivation

One might have thought that black holes truly are black, but they aren't and there is a reason behind this statement. The intimate connection between gravitational dynamics of the black hole horizon and classical thermodynamics uncovered the fact that black holes possess thermodynamic attributes like entropy [114, 218] and temperature [68, 113, 278]. In the seventies, several remarkable works unveiled the tantalising connection between gravity and thermodynamics. The story starts with the pioneering works by Hawking [68, 113] and Bekenstein [114, 218], which show that black holes have entropy and that is proportional to its horizon surface area. Following the works of others [278–280] thereafter, it led to the fact that for every law of black hole mechanics, a corresponding law of classical thermodynamics also exists, which infers that black holes are to be considered as thermodynamical objects. However, it is claimed that every law of black hole mechanics is an analogy with the conventional law of thermodynamics. Still, the robustness of the analogy comes into the limelight when Hawking [68] revealed the fact that black holes can radiate when quantum effects are taken into consideration. It unveiled a new period where people learned that *black holes are not so black, they radiate.* It led to the fact that the concept of temperature is purely quantum mechanical in the context of black hole horizon. Since then, understanding the thermalisation of the black hole horizon has been one of the central interests among physicists. As we said the concept of black hole thermodynamics [108, 113, 114] is an

idea which originates through an *analogy* between the laws of black holes and those of the usual thermodynamical systems, and it remains same till date. However, the more profound question in this context would be to ask how this thermal nature comes into the picture whenever we talk about horizon. In fact, the underlying physical mechanism which provides temperature to the horizon is still unclear to us. For instance, we can work out the thermodynamics of a system from the underlying theory of statistical mechanics as we know the nature of the microstructure of a solid or gas from its atomic and molecular level. However, in case of spacetime, which microscopic degrees of freedom is responsible for the emergence of temperature into the system in presence of the horizon is not known properly. There are several attempts, and all of them have their own merits and demerits, and also none of them are complete. Here we want to address one of these important issues in this area. Although the thermodynamical parameter like temperature nicely fits with the horizon, the question remains – what is the source of this temperature? *The underlying mechanism in which sources such temperature still is one of the grey areas*. Therefore, the hunt for finding out a concrete explanation for such feature is still under progress.

Hawking [68, 113] had shown that back holes radiate and the radiating photons are thermal in nature, and the temperature for the corresponding radiating particles was predicted as

$$T = \frac{\hbar\kappa}{2\pi} \tag{5.1}$$

where κ is the surface gravity of the black hole. On the other side, the upper bound of the instability factor or rather the Lyapunov exponent (LE) in the context of black hole chaos is given by the surface gravity (κ) of the black hole [226] which we have already seen in the previous three chapters as well (chapter 2, chapter 3 and chapter 4). Since, the maximum value of the instability factor is given by κ and the horizon temperature is also determined by this one, therefore, this upper bound is dependent on the temperature [226, 229]. Interestingly, it leads to a striking fact that there might be some connection between these two phenomena, i.e. instability and thermality. These two characteristics may seem to be different to each other, but their unification may become a strong candidate to answer the long-standing question about the origination of the horizon thermodynamics.

In fact, there are shreds of evidence about the connection between the instability of the system and its corresponding quantum thermality. The original work of M. Srednicki [231] suggested that a chaotic system naturally incorporates thermal behaviour. Recently

Morita [232], in a similar note, suggested that an unstable classical mode, characterised by a fixed value of Lyapunov exponent, cannot have zero temperature in the quantum scale. One of the extensively investigated unstable systems in this direction is an inverse harmonic oscillator (IHO). At the classical level, the IHO provides instability, and people found that quantum temperature can arise from it, which is determined by the instability factor. A notable feature of this analysis is that the obtained temperature is a pure quantum consequence, and so in the classical limit, it does vanish. All these findings indicate that there is a close bond between the instability and the pure quantum temperature. More precisely, this instability at the classical level can be a source of a pure quantum temperature of a system.

Motivated by the earlier and recent observations in the context of connection between the classical instability and quantum thermality, we want to explore in this chapter such a possibility to explain the existence of horizon temperature. We feel that it can be an important tool to explain this. In this connection, we want to mention that there are some works where IHO (which, as we mentioned earlier, provides instability) has appeared in the black hole system [220, 232, 233]. For example, Hashimoto et al [220] have shown that if one considers the analysis around the maxima of a field potential in the black hole spacetime, the effective motion of a particle is that in an IHO potential. Later on, Morita [232] and Hegde et al [233] independently showed that such IHO gives rise to temperature under quantization which is proportional to instability factor of the system. In a completely different context [234, 235] it has been observed that if a particle scattering phenomenon is considered in a black hole spacetime in the presence of localised shock wave, the effective scattering Hamiltonian comes out to be that of IHO, which also gives rise the same in the quantum regime.

The noticeable fact in all these works, mentioned above, is the possibility of the existence of instability in the form of IHO for a black hole background, which provides thermality to the system. In addition, this feature is *local* as it exists in a very small region around a particular point – either around the maxima of the potential [220] or around the location of the shock wave [235]. Hence none of these analyses is directly connected with the horizon. In other words, *the existing observations have not been done around the location of the horizon*. Since we know that the temperature is the property of the horizon, this should arise totally from the investigations around this one-way membrane.

In chapter 2 and in chapter 3 we have seen whenever an integrable system comes under the influence of the horizon it starts showing chaotic dynamics depending upon

the available parameters (like energy of the particle, mass of the black hole etc). In the previous chapter, i.e. in chapter 4, our aim was to find out the reason behind this fascinating feature of the horizon. We learnt from that study that the local instability in the near horizon region may be the reason for that. In particular, we investigated the behaviour of a massless and chargeless particle in the vicinity of the black hole horizon which is moving *only radially outward direction very near to the horizon*. We found out that the near horizon Hamiltonian of the particle, at the leading order in radial distance from the horizon, is $H \sim xp$, where p is the conjugate momentum of position variable x. We showed this explicitly for any static spherically symmetric black hole in both Painlevé and Eddington-Finkelstein coordinates.

Based on these facts, the very first question one may ask is whether this near horizon instability may lead us to the thermal behaviour of the horizon or not. If it does, then the next question is *what is the information we gain about our observer because thermality of the horizon itself is an observer-dependent phenomenon.* Therefore, investigations of these questions and finding a concrete answer will be the central theme of this present chapter.

5.2 Thermality of horizon

In order to find out whether the local instability in the near horizon region leads us to explain the thermal behaviour of the horizon or not, we start our analyses with two well known techniques which are the tunneling formalism and the detector response approach. The first one will lead us to obtain the probability of a particle escaping through the horizon and the later approach will give us the information about the possibility of quantum fluctuations in other observer's vacuum with respect to our observer.

5.2.1 Thermality through tunneling formalism

Classical general relativity has given us the concept that nothing can escape from black hole. However, the quantum probability of escaping from the barrier of the horizon can be different. The previously obtained Hamiltonian in Painlevé (4.3) or in EF coordinates (4.34) are same and it can be used here to find this. The quantum probability of escaping horizon is the main quantity which is found in tunneling formalism to study the Hawking effect (For the underlying concept and details of this method see [54, 140, 173, 174]. Also see [175] for an extensive list of works on tunneling formalism).

The actual idea of the tunneling method consists of one ingoing particle and one outgoing particle. The outgoing particle is allowed to follow classically forbidden trajectories, by starting just behind the horizon. Thus the classical particle action becomes complex and so the principal contribution in the tunneling amplitude comes from the imaginary part of this action for this outgoing particle. However, the action of the ingoing particle must be real, since classically a particle can fall beyond the horizon. It is one of the key points of this mechanism as will be seen later. Since, tunneling is a near horizon theory and it occurs radially, this phenomena is effectively dominated by the two dimensional $(t-r)$ metric. Now, there are two different methods in the literature to calculate the imaginary part of the action: the first one was introduced by Parikh-Wilczek [54] which is the radial null geodesic method and the other one is the Hamilton-Jacobi method (HJ) which was first used by Srinivasan et. al. [140] [1].

The radial null geodesic method considers a null s-wave emitted from the black hole. The only part of the action that contributes an imaginary term is $\int_{r_{in}}^{r_{out}} p_r dr$, where p_r is the momentum of the emitted null s-wave. Then by applying the Hamilton's equation and the knowledge of the null geodesics, the imaginary part of the action is being calculated. Then by using the WKB approximation the tunneling probability for the null s-wave coming from inside to outside the horizon is being calculated, which in turn is related to the Boltzmann factor for the emission of Hawking temperature.

On the other hand the HJ method involves consideration of an emitted scalar particle, ignoring its self-gravitation, and assumes that the action of the particle satisfies the relativistic Hamilton-Jacobi equation. From the symmetries of the metric one chooses an appropriate ansatz for the form of the action. In our following calculations we shall adopt the HJ method within a semi-classical approximation to find the Hawking temperature in the near horizon region.

Now, in order to implement the inherent idea of HJ method to calculate the tunneling probability, first, we need to identify the outgoing and the ingoing particle near the horizon. Then we shall calculate the HJ action for the outgoing and the ingoing particle, respectively, in order to find out the corresponding wave functions of the particles. These wave functions will lead us to obtain the emission and the absorption probability of the outgoing and the ingoing particle, respectively, and finally, their ratio will give us the tunneling probability of the particle. The analysis is semi-classical in nature, and calculation at the vicinity of the horizon is sufficient.

[1] Based on the tunneling idea, using the connections between the coordinates on both sides of the horizon, the same has been done in [173, 174]

We start with the standard ansatz for wave function for a particle as

$$\Psi(x) = \exp\left[-\frac{i}{\hbar}S(x)\right], \tag{5.2}$$

where $S(x)$ is the Hamilton-Jacobi action for the particle, defined as an integration of the momentum p of the particle with respect to the position coordinate x variable:

$$S(x) = \int p dx\ . \tag{5.3}$$

(Here we have considered the above expression for two-dimensional phase space). Now, applying $\hat{p} \equiv -i\hbar\partial/\partial x$ on (5.2) we shall have the momentum eigenvalue as -$\partial S/\partial x$. For the outgoing case we consider the positive momentum eigenvalue, i.e. which leads to have $\partial S/\partial x < 0$. In a similar fashion, for the ingoing one, one must have the negative eigenvalue, i.e. $\partial S/\partial x > 0$. After this identification, we are interested in calculating the emission probability of the outgoing particle while the absorption probability for ingoing one. The ratio of them will give us the required tunneling probability.

The energy of the outgoing particle is given by (4.34). Since $H = E$ is the conserved quantity here, we substitute p in terms of x in (5.3) to find the outgoing action. Also since the emission probability will be our main interest, the limits of the integration must be chosen $x = -\epsilon$ to $x = \epsilon$ where $\epsilon > 0$ (i.e. from just inside the horizon to just outside of it). Thus the "emission" action is given by

$$\begin{aligned} S[\text{Emission}] &= \frac{E}{\kappa}\int_{-\epsilon}^{\epsilon}\frac{dx}{x} \\ &= -\frac{i\pi E}{\kappa} + (\text{real part})\ . \end{aligned} \tag{5.4}$$

In performing the above integration, we noticed that $x = 0$ is the pole of the integrand. Therefore, we need to choose the complex path of the particle in such a way so that the probability of crossing the horizon remains a *physically relevant* quantity. *Physically relevant* quantity means with the choice of a wave function ansatz the probability of the particle to cross the horizon must becomes zero at the limit $\hbar \to 0$. Here, in this case we choose the path in the upper complex plane. If we had chosen the path in the lower complex plane then the probability diverges at the limit $\hbar \to 0$ which implies that probability is not a *physically relevant* quantity in that case. Since the outgoing particle starts from inside the black hole where $x < 0$, we have $\partial S/\partial x < 0$, which is consistent with the definition of the outgoing nature of the trajectory. On the other hand, the "Absorption" action for the ingoing particle will be real as the limits of integration never include the

horizon singularity. This can be checked trivially with the identification of energy for the ingoing particle as $E = -p$ (see Eq. (4.36)). So, the probability of emission turns out to be

$$\begin{aligned} P[\text{Emission}] &\sim \left| e^{-\frac{i}{\hbar} S[\text{Emission}]} \right|^2 \\ &\propto \exp\left(-\frac{2\pi E}{\hbar\kappa}\right). \end{aligned} \tag{5.5}$$

whereas the probability of absorption is $P[\text{Absorption}] = 1$. Hence the tunneling probability is evaluated as

$$\Gamma = \frac{P[\text{Emission}]}{P[\text{Absorption}]} \sim \exp\left(-\frac{2\pi E}{\hbar\kappa}\right). \tag{5.6}$$

Note that the above one is thermal in nature as it has the form of Boltzmann factor. Therefore, the temperature is identified as

$$T = \frac{\hbar\kappa}{2\pi}. \tag{5.7}$$

Now, our probed particle feels this temperature. Since we have considered that the particle and the horizon construct a composite system and if these two subsystems are in thermal equilibrium with each other, then this above expression is also the temperature of the black hole horizon, which exactly matches with the standard Hawking expression [113].

We just observed that the near horizon Hamiltonian (4.34) predicts a finite probability of escaping a particle from the horizon and thereby providing a temperature to the horizon. Since this Hamiltonian shows a local instability, we argue that such instability is responsible for the thermal behaviour of the black hole. From this analysis, we can note that the observer is associated with either Painlev*é* or EF coordinates. But at this point, it is not vivid whose vacuum state is filled with a particle with respect to this frame. It is the well-known limitation of the tunneling approach. This will be illuminated in the next subsection by adopting a different approach.

5.2.2 Identifying our observer: Detector's response approach in EF coordinates

Thermality is an observer dependent phenomenon [116, 209] and vacuum plays an important role in this case. The precise choice of observer and the corresponding choice of vacuum is very important in that sense. Therefore, the aim of our next approach is to identify the observer and the corresponding vacuum state connected to this thermality.

One such popular approach is investigating through the detector's response of a two-level atomic detector, which can give us the clear idea to identify our observer and the vacuum [281–283]. In this section we shall perform the calculations particularly in EF coordinates. The choice of the observer here is the one which is following the path (4.21) in the near horizon regime. The vacuum is chosen to be Boulware vacua, which is defined with respect to the static observer in Schwarzschild coordinates. We will find the transition rate of the atomic detector, which moves along the trajectory (4.21) with respect to this Boulware vacuum. The calculation must be performed very near to the horizon. The particular preference of this vacuum among others like Unruh or Kruskal vacua is due to the fact that Unruh and Kruskal ones are not vacuum with respect to static frame, whereas Boulware is a trivial one. Therefore it is apparent that the present moving frame again finds Unruh and Kruskal vacua as non-trivial one. Hence whether Boulware appears to be non-trivial with respect to our present observer will be an interesting observation (a discussion of defining different vacuum states can be followed from [116]).

Let us consider a two-level atomic detector (say a is the excited level and b is the ground state) is moving along the geodesic (4.21). We consider the massless scalar field Φ under this background and its modes are denoted by u_ν with frequency ν. The modes for the atomic detector (massless) we denote as ψ_ω, where ω is the characteristic frequency. The interaction Hamiltonian between the atomic detector and the field is taken as

$$\hat{H}_{int}(\tau) = Q[(\hat{a}_\nu u_\nu + h.c.)(\hat{\sigma}_\omega \psi_\omega + h.c.)] \,, \tag{5.8}$$

where the operator $\hat{a}_\nu$ is the photon annihilator operator and $\hat{\sigma}_\omega$ is the atomic detector lowering operator. $h.c.$ signifies the hermitian conjugate. Q is the coupling constant which determines the strength of the interaction and τ is the detector's clock time. This type of model was originally considered for this purpose in [284] and later has been subsequently used in [270].

Initially, when there is no photon is detected, the detector stays in the ground state $|b\rangle$ i.e the field is in the Boulware vacuum $|0\rangle$. So the initial state of the whole system is $|0,b\rangle = |0\rangle \otimes |b\rangle$. Now after interaction the detector will go to state $|a\rangle$. Then the transition amplitude of the detector, using the first order perturbation theory, is given by

$$\Gamma_{detect} = -i \int_{\tau_i}^{\tau_f} d\tau \langle 1_\nu, a|\hat{H}_{int}(\tau)|0,b\rangle \,, \tag{5.9}$$

where $|1_\nu\rangle$ is the one particle state of Φ and τ_i and τ_f are the initial and the final clock times of the detector respectively. In this subsection, we have chosen $\hbar = 1$. Therefore,

the probability of excitation of the atomic detector, at the first order, for the interaction Hamiltonian (5.8) turns out to be

$$\begin{aligned} P_{\uparrow} &= Q^2 \Big| \int_{\tau_i}^{\tau_f} d\tau \langle 1_\nu, a | \hat{H}_{int}(\tau) | 0, b \rangle \Big|^2 \\ &= Q^2 \Big| \int_{\tau_i}^{\tau_f} d\tau u_\nu^*(\tau) \psi_\omega^*(\tau) \Big|^2 . \end{aligned} \tag{5.10}$$

This is the working formula and it can be re-expressed in different forms according to the necessities.

Here, for the case where we are dealing with the black hole, we are interested only on the radial trajectories of the atomic detector. Therefore, the variable τ in Eq. (5.10) has to be expressed in terms of the radial coordinate r and the integration limit of r has to be from initial value of r (say r_i) to the final position (say r_f). Under this circumstances, we re-express (5.10) as (for details please see [270]):

$$P_{\uparrow} = Q^2 \Big| \int_{r_i}^{r_f} dr \left(\frac{d\tau}{dr} \right) u_\nu^*(r) \psi_\omega^*(r) \Big|^2 . \tag{5.11}$$

Here re-expressing the detector's path (4.21) as t in terms of radial coordinate we obtain

$$t = \frac{1}{\kappa} \ln \left(\frac{r}{r_H} - 1 \right) + \text{constant} , \tag{5.12}$$

where the constant, irrelevant for the present analysis, is given by $(1/\kappa)\ln(\kappa r_H)$. Next taking[2] $\tau = t$, the positive frequency mode corresponding to the detector is

$$\psi_\omega = e^{-i\omega t} . \tag{5.13}$$

The positive frequency Boulware mode for massless scalar field can be obtained by solving the Klein-Gordon (KG) equation $\Box\Phi = 0$ under the background of (4.8). Near the horizon KG equation reduces to

$$\left[\frac{\partial^2}{\partial t_s^2} - \frac{\partial^2}{\partial r_*^2} \right] \Phi = 0 , \tag{5.14}$$

where in the near horizon limit r_* is given by

$$r_* \simeq \frac{1}{2\kappa} \ln \left(\frac{r}{r_H} - 1 \right) . \tag{5.15}$$

The solutions are $e^{-i\nu(t_s \pm r_*)}$, where the positive sign corresponds to ingoing and the negative sign refers to outgoing modes. Here, our detector is moving in the outward

[2]Since, the path is null-like, we choose t as the affine parameter and therefore it can serve as detector's clock time.

direction and so we will consider the ingoing Boulware mode to investigate the response of the detector. Therefore we choose

$$u_\nu = e^{-i\nu(t_s+r_*)} . \tag{5.16}$$

Hence expressing the integrand of Eq. (5.11) in terms of the radial coordinate and using (5.12), we obtain the probability of transition as

$$P_\uparrow = \frac{Q^2}{\kappa^2}\left|\int_{r_H}^{r_f} d\left(\frac{r}{r_H}\right)\left(\frac{r}{r_H}-1\right)^{\frac{i}{\kappa}(\nu+\omega)-1} e^{i\nu r}\right|^2, \tag{5.17}$$

where the upper limit is taken as position r_f which is situated very near to the horizon. It has to be chosen in such a way that it's value satisfies our near horizon approximation i.e. $\left(\frac{r}{r_H}-1\right) << 1$.

In order to get some convenient look of Eq. (5.17) let us first make change of variable: $(r/r_H)-1 = y$. Then (5.17) reduces to

$$P_\uparrow = \frac{Q^2}{\kappa^2}\left|\int_0^{y_f} dy\; y^{\frac{i}{\kappa}(\omega+\nu)-1} e^{i\nu(y+1)}\right|^2 . \tag{5.18}$$

This can be expressed in terms of lower incomplete Gamma function (See page no. 527 of ref. [285]):

$$P_\uparrow = \frac{Q^2}{\kappa^2}\left|\frac{1}{(-i\nu)^{\frac{i}{\kappa}(\omega+\nu)}}\,\gamma\left(\frac{i}{\kappa}(\omega+\nu), -i\nu y_f\right)\right|^2 . \tag{5.19}$$

But to get a better understanding, here we shall examine it numerically for different values of ω. In order to do that, first we need to make all the variables dimensionless. We choose the following substitutions in Eq. (5.18):

$$r_H\omega = \omega'; \quad r_H\nu = \nu' \quad \text{and} \quad r_H\kappa = \kappa'. \tag{5.20}$$

Then Eq. (5.18) reduces to the following form:

$$P'_\uparrow = \left|\int_0^{y_f} dy\; y^{\frac{i}{\kappa'}(\omega'+\nu')+\epsilon-1} e^{i(\nu'+i\epsilon)(y+1)}\right|^2 . \tag{5.21}$$

where $P'_\uparrow = \frac{\kappa'^2}{Q^2 r_H^2}$ and in the above we have introduced a very small parameter ϵ to make the integration convergent.

Now, we numerically integrate the above expression for different values of ω' and then plot $\nu'^2 P'_\uparrow$ as a function of ν' and the value of y_f is taken as $y_f = 0.1$ in this case. The plot is represented in Fig. (5.1). This shows that the nature of the transition probability

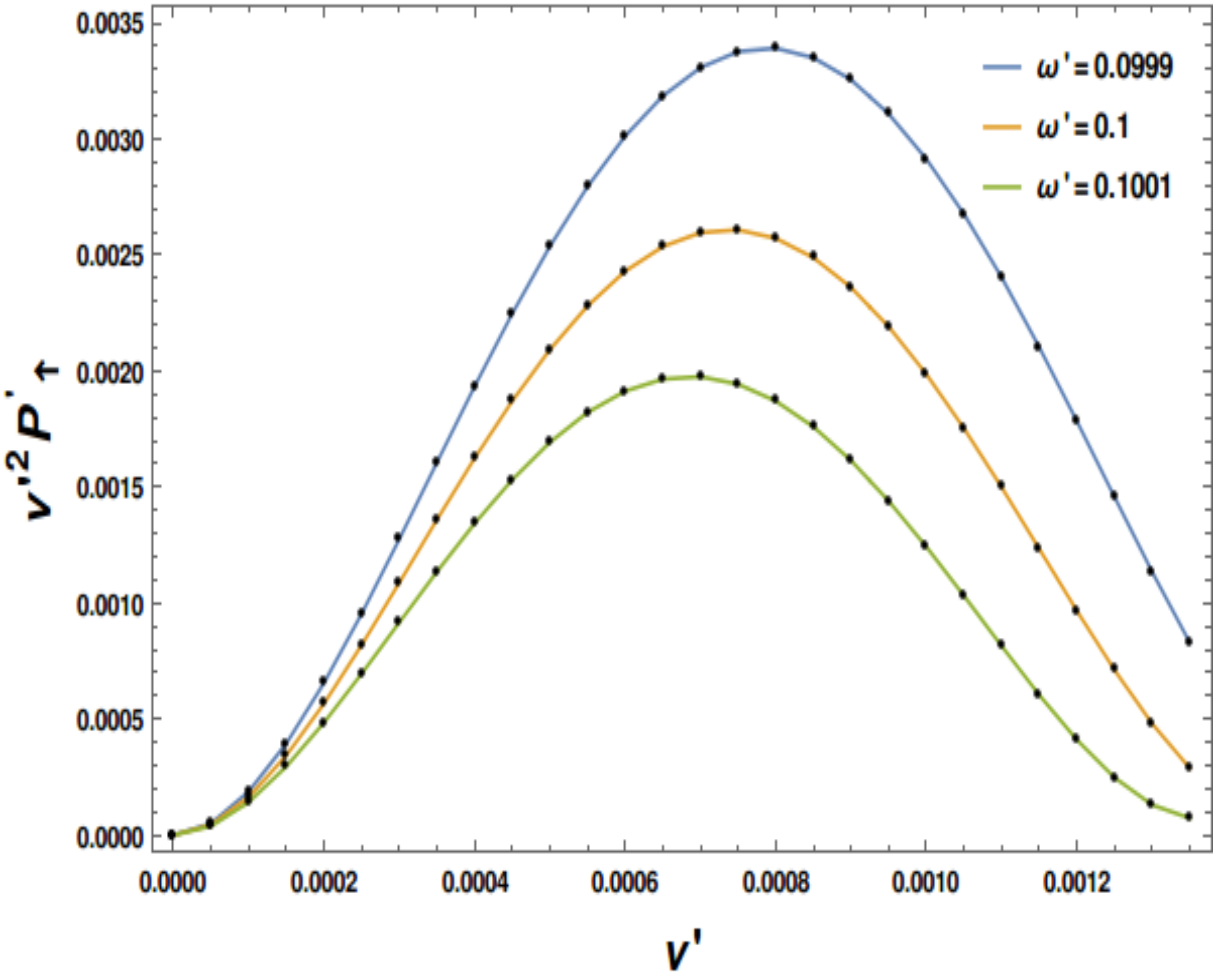

Figure 5.1: Plot of $v'^2 P'_{\uparrow}$ Vs v' for different values of ω'. The choice of the small parameter is $\epsilon = 0.00095$ and $y_f = 0.1$.

of the detector is similar to Planck distribution. So the detector will register particles in the Boulware vacuum when it moves along our local unstable path. Hence with respect to this observer, the vacuum appears to be thermal. As we increase the value of ω', the peak of the curve decreases. It means that for higher values of ω', the probability of detecting particle gets lessened.

In the similar approach one can also derive the expression for probability of detecting an outgoing scalar field mode by an ingoing detector in the near horizon region. It means that the detector is moving very near to the horizon but this time its direction of motion is towards the horizon, just opposite to the previous case. In this case the EF time

coordinate is represented in terms of the outgoing EF coordinates (u,r,θ,ϕ) as

$$t = u + r = t_s - r_* + r \ . \tag{5.22}$$

In the similar approach we can re-express the path of the ingoing detector in a form which leads to t as a function of the radial coordinate (Discussion about the path is given in Eq. (5.A.2.6) in Appendix 5.A.2). For the near horizon approximation using Eq. (5.A.2.3) of the Appendix 5.A.2 we obtain

$$t = -\frac{1}{\kappa}\ln\left(\frac{r}{r_H} - 1\right) + \text{constant} \ . \tag{5.23}$$

Now, proceeding with exactly similar approach like the case of the outgoing detector one can land up to the expression of probability which turns out to be

$$P_{\downarrow} = \frac{Q^2}{\kappa^2}\left|\int_0^{y_f} dy\ y^{-\frac{i}{\kappa}(\omega+\nu)-1} e^{-i\nu(y+1)}\right|^2 , \tag{5.24}$$

and it basically gives the same result as in the case of the outgoing detector (FIG.(5.1)).

Therefore, the outgoing and the ingoing atomic detector, following the null path, detects ingoing and outgoing scalar particle, respectively, in the Boulware vacuum. The Planckian nature of the plots suggests that at the quantum level, the vacuum appears to be thermal. We showed this for near horizon trajectory. For completeness, we also show that our present observer, when moves throughout the whole spacetime, then also it will perceive thermality. This we present in Appendix 5.A for the Schwarzschild black hole where the near horizon approximation is being avoided. To have a complete analytic analysis, the calculation is performed in $(1+1)$ dimensions, and the temperature is identified to be the Hawking expression (5.7).

5.3 xp Hamiltonian and its connection with thermality

In the presence of the horizon, our probed massless particle experiences a xp kind Hamiltonian in the near-horizon region. Also, due to the presence of this xp Hamiltonian, our particle experiences thermality in the vicinity of the horizon. Therefore, it is apparent that this particular Hamiltonian has the inherent characteristics of thermality. So, it is quite evident that thermality will emerge automatically wherever this Hamiltonian appears. This Hamiltonian is related not only to the black hole spacetime but also to the other systems. $H \sim xp$ Hamiltonian has a very tight relationship with the quantum chaos

[286]. Mathematicians also find this Hamiltonian very interesting as this Hamiltonian might be the desired operator that provides a solution to the Hilbert-Pólya conjecture, and this conjecture has an intriguing connection with one of the prominent problems of modern mathematics, i.e. Riemann hypothesis. Thus the particular structure of the Hamiltonian has a wide range of applications from the perspective of mathematics and quantum mechanics as well [286–289]. However, in the following sections, we particularly would like to study the thermal characteristics of xp Hamiltonian. We like to show that this xp Hamiltonian has some inherent thermal nature at the quantum scale through various calculations. The development of the thermal characteristics of this Hamiltonian may explain the thermality of the horizon. In this spirit, we shall construct a few physical models driven by κxp Hamiltonian and show that the thermality naturally emerges in those models. In addition to the models discussed in the main calculations, we also provided another toy model of κxp in which we illustrated its thermal nature using a perturbative method (please see Appendix 5.D).

5.3.1 Thermality through Gutzwiller's formula

In the previous chapter 4 we have already seen that in the near horizon region the our probed massless and chargeless particle experiences a local instability and it turns out that the corresponding Hamiltonian of that particle motion is xp kind (please see Eq. (4.3) of chapter 4) both in Painlevé and in EF coordinates. Apart from the classical perspective, the unique structure of the Hamiltonian xp kind has a great consequence if we turn our attention to the quantum mechanics level. Particularly, we are interested in finding the response of the "local instability" at the quantum level. As this can manufacture instability, the usual quantization rule normally not applicable. In this regard, Gutzwiller's trace formula [274, 290] will be important one.

The density of states $\rho(E)$ for a particular energy E is expressed in terms of Green function $G(q,q',t)$ as [274, 290] (a derivation of this formula is also being presented briefly in Appendix 5.B.1)

$$\begin{aligned}\rho(E) &= -\frac{1}{\pi}\text{Im}(\text{Tr}(G)) \\ &= -\frac{1}{\pi}\text{Im}\left(\int G(q,q,E)dq\right), \end{aligned} \tag{5.25}$$

where q is the coordinate. The trace of the Green function can be evaluated by the

Gutzwiller's trace formula [274](for detailed calculations please see Appendix 5.B.2) :

$$g(E) = \int dq G(q,q,E) \quad = \quad -\frac{i}{\hbar}\sum_l \frac{T_l}{||M_{BA,l} - I||^{\frac{1}{2}}} \exp\left[\frac{i}{\hbar}S_l(E) - i\frac{\mu_l \pi}{2}\right], \tag{5.26}$$

where the summation is over all the classically allowed trajectories. In the above, μ_l is Maslov index for the lth trajectory and $S_l(E)$ is the Jacobi action

$$S_l(q_A, q_B, E) = \int_{q_A}^{q_B} p dq \ , \tag{5.27}$$

calculated between two points q_A and q_B. T_l is the period for the primitive orbit, which means the time needed for one passage and in terms of $S_l(E)$, it can be expressed as

$$T_l = \frac{\partial S_l(E)}{\partial E} \ . \tag{5.28}$$

M_{BA} in the denominator of (5.26) is our monodromy matrix (4.6) and I is the identity matrix. $||\ldots||$ stands for modulus of the determinant. The formula (5.26) is derived in path integral approach with the assumption that Hamiltonian can be expressed as $H = p^2/(2m) + V(x)$ where m is the mass of the particle with momentum p, moving under the potential $V(x)$.

In our present analysis, H is given by (4.3). However, for $H \sim xp$, the trajectories are unbounded in nature. As we have seen from the previous chapter 4 the solutions of the equations of motion for radial trajectory corresponding to are $r \sim e^{\kappa t}$ and $p_r \sim e^{-\kappa t}$. The near horizon limit for both Painlevé and EF cases can be achieved by considering $t \to -\infty$. The interesting part is that at this limit p_r diverges which suggests that the particle feels instability when it resides very near to the horizon. Therefore, the existence of this xp Hamiltonian suggests that there lies a "local instability" region in the vicinity of the horizon.

In addition, here, x is always positive (as the particle is moving outside the horizon), while p can be both positive and negative. To satisfy periodicity condition, Berry-Keating used a particular type of boundary condition on x and p [273], which was later generalized by considering a phase space having fixed boundaries [291]. But till now the most convincing existing prescription is to use a complexified version of H in a new set of canonical variables which leads to a harmonic oscillator (HO) [292] which will be shown in the following calculations.

$H \sim xp$ can be cast in the required form by changing the variables from one canonical set to another [273]:

$$x = \frac{1}{\sqrt{2}}(P - X); \quad p = \frac{1}{\sqrt{2}}(P + X) \ , \tag{5.29}$$

so that one can use (5.26) in our case as well. In these new variables (4.3) becomes

$$H = \frac{\kappa}{2}(P^2 - X^2) \,. \tag{5.30}$$

This implies that (4.3) is simply a canonically rotated inverted harmonic oscillator (IHO). Comparing this with the usual form of Hamiltonian for a IHO: $H_{IHO} = \frac{P^2}{2m} - \frac{1}{2}m\omega^2 X^2$, we found that for our system $m \equiv \frac{1}{\kappa}$ and $\omega \equiv \kappa$.

In order to calculate $S_l(E)$ in (5.26) from (5.27) we will use the following procedure. A direct evaluation shows that the energy eigenvalues are that of HO with a naive substitution of the frequency $\omega \to i\omega_0$ [289, 293, 294]. There after this substitution has been appeared to be very fruitful in the quantum description of the IHO. Since we are also interested to the quantum regime, the same prescription will be followed here. Under $\omega \to i\omega_0$, we have $H_{IHO} \to H_{HO} = \frac{P^2}{2m} + \frac{1}{2}m\omega_0^2 X^2$, which gives periodic motion in phase space. Now with this for a full periodic motion along the l^{th} orbit, (5.27) yields the area in phase space under the curve with energy E_l. This is given by $S_l = (2\pi E_l)/\omega_0$. Therefore the analytic continued action for our system turns out to be

$$S(E_l) = -\frac{2\pi E_l}{i\kappa} \,, \tag{5.31}$$

where we have used $\omega_0 \to -i\omega = -i\kappa$. Consequently, (5.28) yields $T_l = 2i\pi/\kappa$. This particular action (5.31) can also be obtained in a different approach also other than complexifying the frequency part by considering an enclosed path encircling the horizon (for detailed calculations please see Appendix 5.C).

It is well known that the path integration can be interpreted as the partition function when the time coordinate is complexified. The periodicity of complex time is identified as the inverse temperature. Using this idea Hawking showed that by Euclideanising the black hole metric the calculation of the partition function gives us correct expression for the entropy of the horizon. Here the periodicity of complexified time around horizon is identified as the inverse of the Hawking temperature [295]. In our calculation by complexifying the frequency we obtained $T_l = 2i\pi/\kappa$. Interestingly, this value exactly matches with time period what Hawking found by Euclideanising the spacetime. Therefore, we feel that there may be a close connection between Hawking's argument with our complexification of the frequency.

Hence, substitution of this and (5.31) in (5.26) with $T_l \to iT_l$ we find the expression for the density of states as

$$\rho(E) = \frac{1}{\hbar\kappa}\sum_l \frac{1}{\sinh\pi} e^{-\frac{2\pi E_l}{\hbar\kappa}} \cos\frac{\mu_l \pi}{2} \,. \tag{5.32}$$

Here in the denominator, we substituted $||M_{BA,l} - I||^{\frac{1}{2}} = 2\sinh(\kappa T_l/2) \to 2\sinh(i\kappa T_l/2)$ (see Eq. (4.6)). The above one is thermal in nature up-to some factor [3] and the temperature is identified as (5.7) which exactly matches with the standard Hawking expression [113] for black hole. Note that the particular form (5.32) is the characteristic feature of IHO which is an unstable system. It may be pointed that IHO leads to thermal nature at the quantum level has also been reported recently in [232, 233, 277].

The Gutzwiller trace formula, for finding the total density of states (DOS) for an unstable system have two parts. One is the mean part, calculated for the action ($S_l(X_A, X_B, E)$) of vanishing path length; i.e. $|X_B - X_A| \to 0$ and another part corresponds to $|X_B - X_A| \neq 0$ (see section 7.3 and 8.1 of [274] for details), known as the oscillatory part. Berry and Keating [273] showed that in case of xp kind Hamiltonian, the mean part of the counting function $< \mathcal{N} >$ can be calculated for a truncated case and from which the mean part of the DOS can be obtained using $< \rho(E) >= d < \mathcal{N} > /dE$. The asymptotic expression for this comes out to be positive. Our expression (5.32) is oscillatory in nature as it has been obtained for $|X_B - X_A| \neq 0$. This can be both positive and negative, depending on the value of $\cos(\mu_l \pi/2)$. We would like to mention here that negative DOS is not at all surprising for near equilibrium systems. For instance, in literature [296] the negative value of DOS has been reported for quantum system. In [297] it has been explained that DOS can have negative values when one has quasi-probability distribution, like Wigner distribution function, at the quantum level. This is mainly related to the situation when the system is little away from the equilibrium. DOS has a close relation with the Wigner function (see section 8.1.3 of [274]) and it has negative values for states which are not classically allowed. However, these negative values must vanish at the classical limit $\hbar \to 0$. One can check that this is exactly happening for (5.32) as well. It is a pure quantum contribution and vanishes for $\hbar \to 0$, whereas the mean value is always positive. This fact is related to the unstable behaviour of the Hamiltonian. The significance of this, till date, is not well understood.

Now, earlier in the classical analysis we found that the IF has an upper bound: $\lambda_L \leq \kappa$. Therefore (5.7) yields $\lambda_L \leq \frac{2\pi T}{\hbar}$, which was conjectured earlier in SYK model [226]. Consequently, one finds that the temperature of the system is bounded from lower as

$$T \geq \frac{\hbar}{2\pi} \lambda_L \ . \tag{5.33}$$

[3] The expression of DOS in Eq. (5.32) is not *pure thermal* as it consists of some factors. Therefore, we call this expression *thermal up-to some factors*. However, we can identify the temperature of the system from this equation which is basically the Hawking's expression (5.7).

In [221] and in the previous chapters (chapter 2, chapter 3 and chapter 4), the above inequality is obtained by using the classical prediction of the upper bound on LE with the assumption that the horizon has Hawking temperature. This temperature concept was taken as external information. But in the present analysis, we systematically derived this temperature, and so the above relation is now certain rather than prediction. This can also be predicted from the OTOC calculation which for large time t yields $C(t) \sim e^{2\kappa t}$. The OTOC calculation has been done for HO in [227]. This is given by $C(t) \sim \cos^2 \omega_0 t$ (see Eq. (3.4) of [227]). Now a naive substitution of $\omega_0 = -i\kappa$ will lead to that for our case: $C(t) \sim \cosh^2 \kappa t$, which for large t yields $C(t) \sim e^{2\kappa t}$. Similar result has also been obtained for IHO recently in [298] through Loschmidt echo, which is closely connected to OTOC, by a direct calculation. This is the signature of quantum property of chaos which also identifies $\lambda_{L,max} = \kappa$ and provides another way of defining largest IF.

This analysis implies that the "local instability", created by the horizon, may not only induce chaos in a system at the classical level; but also makes the system thermal at the quantum level by a minimum temperature. The unavoidable unstable environment in the near horizon region puts its automatic signature by making a system quantum mechanically thermal. Here one must be careful that, the aforesaid near horizon instability does not mean the particle plus horizon system is chaotic one (see chapter 4). Rather we are saying that this instability may lead to chaos in a system (e.g. particle trapped in a harmonic potential) under some certain circumstances (as we have seen in chapter 2 and chapter 3). Interestingly, the quantum implication of this hyperbolic point is always emergence of temperature at the quantum level.

5.3.2 Thermality through Scattering

Till now, we observed that the horizon provides an unstable potential to the massless particle in its neighbourhood region. Moreover, it causes the particle to feel the black hole as a thermal object. This quantum phenomenon can also be elaborated through a "scattering" model of a particle. The idea is the following. When a particle is moving very near to the horizon, it will feel the influence of the horizon through the local Hamiltonian (4.34). Then the state of the particle will be influenced. The change of wave function can be evaluated by visualising (4.34) as the governing potential for the scattering phenomenon. In order to proceed towards the main purpose first, we need to identify the initial (before scattering) and final (after scattering) energy eigenstates of the system.

As we have mentioned earlier our xp Hamiltonian can be visualised as that for an inverted harmonic oscillator (IHO) in a new set of canonical variables (X, P). The

relation between the old and these new ones are given by Eq. (5.29). Then in the (X,P) diagram, the old (x,p) variables are considered to be as ingoing and outgoing directions, respectively. This is shown in Fig. 5.2.

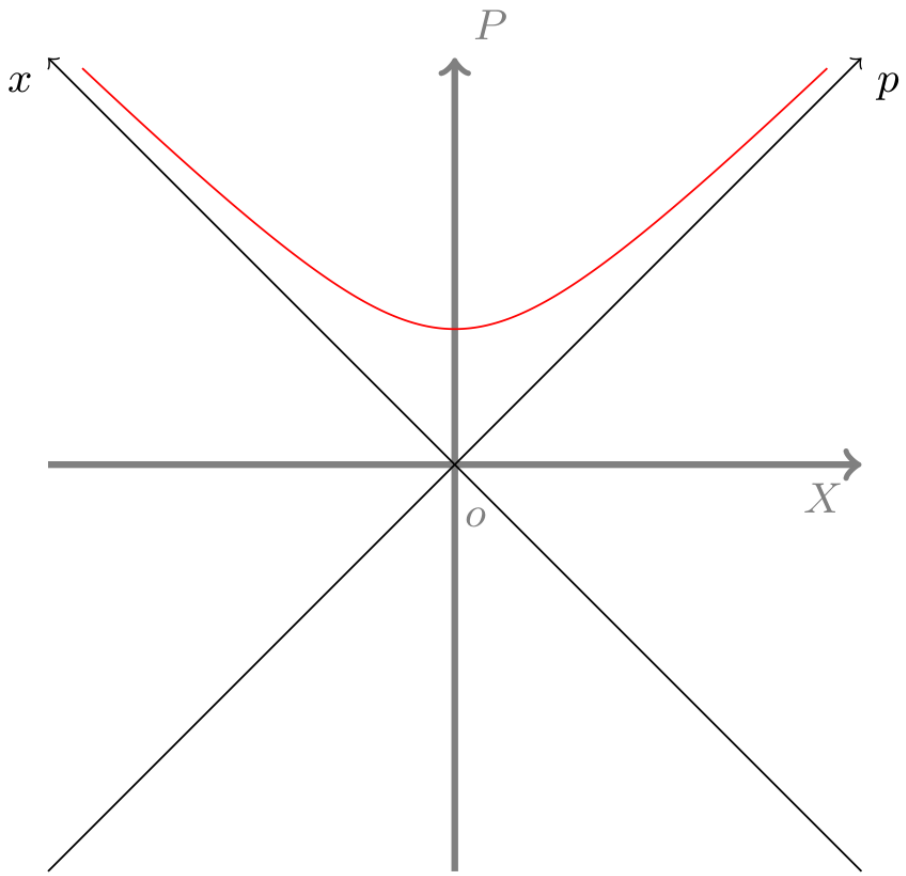

Figure 5.2: $X-P$ diagram: red line represents the trajectory of the particle.

Here the value of x is always positive, therefore the trajectory for $E>0$ in the $X-P$ plane always remains in that quadrant where both p and x are positive definite (see Fig. (5.2)). Since, along x is identified as the ingoing direction, the energy eigenstate in x representation is the initial state of the system. Likewise, p representation energy state is our final state for the system. Therefore our next task is to find the eigenstates for Hamiltonian (4.34) in both representations.

In order to make Hamiltonian (4.34) hermitian, we express this as

$$\hat{H} = \frac{\kappa}{2}[\hat{x}\hat{p} + \hat{p}\hat{x}] \ , \tag{5.34}$$

where the basic commutator is given by $[\hat{x}, \hat{p}] = i\hbar$. Then the inner product between x and p states is

$$\langle x|p\rangle = \frac{1}{\sqrt{2\pi\hbar}} \exp\left(\frac{ixp}{\hbar}\right) . \tag{5.35}$$

To find the initial state, we represent Hamiltonian operator in position representation:

$$\hat{H} = -i\tilde{\gamma}\left[x\frac{\partial}{\partial x} + \frac{1}{2}\right] \ , \tag{5.36}$$

where $\tilde{\gamma} = \hbar\kappa$. With this the initial state with energy E comes out to be

$$\langle x|E\rangle_i = \frac{1}{\sqrt{2\pi\tilde{\gamma}}} \frac{1}{x^{\frac{1}{2}-\frac{iE}{\tilde{\gamma}}}} \quad \text{with} \quad x > 0 \ . \tag{5.37}$$

This is the initial eigenstate with energy E in x-representation.

The final state is determined by expressing the Hamiltonian in momentum representation:

$$\hat{H} = i\tilde{\gamma}\left[p\frac{\partial}{\partial p} + \frac{1}{2}\right] \ . \tag{5.38}$$

Eigenstate with energy E of this operator yields the final state of the system as

$$\langle p|E\rangle_f = \frac{1}{\sqrt{2\pi\tilde{\gamma}}} \frac{1}{p^{\frac{1}{2}+\frac{iE}{\tilde{\gamma}}}} \quad \text{with} \quad p > 0 \ . \tag{5.39}$$

This is the final state in p-representation.

Now we shall find the relation between the final state and initial state. The similar approach has been adopted earlier in [234, 235]. Let us start with the final state in x-representation

$$\begin{aligned} \langle x|E\rangle_f &= \int_{-\infty}^{\infty} dp \langle x|p\rangle\langle p|E\rangle_f \\ &= \frac{1}{2\pi\sqrt{\tilde{\gamma}\hbar}} \int_0^{\infty} dp \ e^{\left(\frac{ix}{\hbar}\right)p} \ p^{\left(-\frac{iE}{\tilde{\gamma}}+\frac{1}{2}\right)-1} . \end{aligned} \tag{5.40}$$

To perform the integration, we use the formula (see page no. 604 of [262] for details)

$$\int_0^{\infty} dx e^{-bx} x^{s-1} = e^{-s\ln b}\Gamma(s) \ , \tag{5.41}$$

with the condition $\mathrm{Re}(b) > 0$ and $\mathrm{Re}(s) > 0$. To satisfy these conditions for integration (5.40), we take $b = -i(x/\hbar) + \epsilon$ and identify $s = -i(E/\tilde{\gamma}) + (1/2)$ with $\epsilon > 0$. At end of the integration we consider the limit $\epsilon \to 0$. This leads to

$$\begin{aligned} \langle x|E\rangle_f &= \frac{\hbar^{-\frac{iE}{\tilde{\gamma}}}}{\sqrt{2\pi}} e^{\frac{i\pi}{4}} e^{\frac{\pi E}{2\tilde{\gamma}}} \Gamma\left(\frac{1}{2} - \frac{iE}{\tilde{\gamma}}\right) \frac{x^{-\frac{1}{2}+\frac{iE}{\tilde{\gamma}}}}{\sqrt{2\pi\tilde{\gamma}}} \\ &= \frac{\hbar^{-\frac{iE}{\tilde{\gamma}}}}{\sqrt{2\pi}} e^{\frac{i\pi}{4}} e^{\frac{\pi E}{2\tilde{\gamma}}} \Gamma\left(\frac{1}{2} - \frac{iE}{\tilde{\gamma}}\right) \langle x|E\rangle_i \ . \end{aligned} \tag{5.42}$$

In the last step (5.37) has been used. So we find the relation between the final energy eigenket $|E\rangle_f$ and the initial one $|E\rangle_i$ as

$$|E\rangle_f = \underbrace{\frac{\hbar^{-\frac{iE}{\tilde{\gamma}}}}{\sqrt{2\pi}} e^{\frac{i\pi}{4}} e^{\frac{\pi E}{2\tilde{\gamma}}} \Gamma\left(\frac{1}{2} - \frac{iE}{\tilde{\gamma}}\right)}_{C_i} |E\rangle_i \ . \tag{5.43}$$

The modulus square of the coefficient (C_i) in the above equation gives the probability of finding the particle in the initial state itself. Therefore, the transition probability for the particle to jump from initial ($|E\rangle_i$) to the final state ($|E\rangle_f$) is

$$P = 1 - |C_i|^2 = \frac{1}{e^{\frac{2\pi E}{\hbar\kappa}} + 1} \ , \tag{5.44}$$

which yields again the thermal nature with temperature is given by (5.7).

Now, it is well known that the scattering phenomenon in black holes can provide the information about the frequency of the QNM (see page no. 397 of [262]). The imaginary part of the frequency is determined by the poles of the Gamma function appearing in Eq. (5.43). It is clear that the poles are at $E_n = -i\tilde{\gamma}(n + 1/2)$ with $n = 0, 1, 2\ldots$. So the imaginary part of frequency is given by $\omega_n = -i\kappa(n + 1/2)$ which matches with the earlier finding [262, 299–301].

In this context, it is worth to mention that the probability expression (Eq. (5.44)), obtained using the scattering process, has an intimate relationship with the probability (Eq. (5.6)) which we got using the tunneling approach in Section 5.2.1. The transition amplitude $\sim \langle x_2| e^{-(i/\hbar)Ht} |x_1\rangle$ (known as propagator), in scattering process, is related to the Feynman's path integral $\sum_{\text{All paths}} \exp\left[(i/\hbar)S\right]$, where S is the classical action. Modulus square of this quantity yields the transition probability, which is (5.44) in the present case. In the semi-classical limit, under saddle point approximation, path integral comes out to be proportional to $e^{(i/\hbar)S}$. Interestingly in tunneling formalism, based on WKB approximation, the ansatz for wave function is given by (5.2) which is similar to

this semi-classical transition amplitude in the scattering process. Therefore it is expected that in the semi-classical regime both the tunneling probability and transition probability must coincide (For details, see chapter 7 of [302]). It is known that this regime is best achieved by taking $\hbar \to 0$ and in this limit one can check that the probability distribution (Eq. (5.44)), keeping only the dominating term, turns out to be

$$P \simeq \exp\left(-\frac{2\pi E}{\hbar\kappa}\right) . \tag{5.45}$$

This is exactly identical to Eq. (5.6) and thereby validating the standard relationship between scattering amplitude and the tunneling probability in the semi-classical limit.

5.4 Summary and Discussions

The reason why horizon is associated with temperature has always been a fascinating question towards the physics community. On the other hand, we have seen in the previous chapters (chapter 2 and chapter 3) that within the theoretical framework we predict the possibility of induction of chaotic behaviour in a system when it is under the influence of the horizon. There is a surge of discussion in this direction. Interestingly, both of these phenomena are characterised by a common horizon quantity, namely the surface gravity. Therefore, it appears that this "apparent interlink" between them may help us to uncover such properties of the horizon. In chapter 4, we predicted that the existence of local instability, created by the horizon in its vicinity region, maybe a possible reason for the chaotic motion. However, in the previous chapters (chapter 2, chapter 3 and chapter 4) the chaos and the instability part we obtained are in the classical picture. Things turn out to be interesting when we enter into the quantum regime and following are the brief discussions about our results in the present chapter.

- In the previous chapter 4 we found that the radial motion of an outgoing massless particle in the Painlevé as well as in the EF coordinates is unstable in the near-horizon region. It is observed that such is due to the appearance of xp type Hamiltonian in the vicinity region of the horizon. After obtaining a clear picture of instability in the classical scale, in the present chapter we targeted quantum calculations in order to see whether this unstable xp kind structure of the near horizon Hamiltonian leads us to visualise the thermal nature of the horizon or not. Therefore, we start our analysis using tunneling approach, where we found that this near horizon Hamiltonian predicts a finite probability of escaping the

particle from the horizon and thereby providing a temperature to the horizon. The expression came out to be as that of Hawking. It confirms our previous claim that the instability created by the horizon in its vicinity region is the possible reason for the thermal behaviour of the horizon at the quantum scale.

- The next approach was the detector response approach in order to get a distinct idea about the relevant vacuum state. In this case, we particularly investigated in EF coordinates. The observer or rather the detector, in this case, is following the same null trajectory in EF coordinate in the near horizon regime, as we mentioned earlier. The vacuum was chosen to be that Boulware vacuum in this case. After evaluating the response function numerically, we have obtained that the transition probability of the detector of detecting a photon in the Boulware vacuum is similar to Planck distribution. It showed that the detector will see the Boulware vacuum as a thermal bath.

- Next, our aim was to show particularly the inherent thermal characteristics of the xp which may appear not only in black hole space time but also in other areas of physics also. We started with by calculating the density of states (DOS) of the system. In this process we particularly used the Gutzwiller's trace formula because usual quantization rule normally not applicable in this case. First, we write down the xp Hamiltonian in another canonically rotated coordinates and it turns out to be the Hamiltonian of an inverse harmonic oscillator. However, the complexified version of the IHO Hamiltonian leads to a harmonic oscillator which helped us to calculate the DOS using Gutzwiller's trace formula. Interestingly, the expression of the DOS turns out to be thermal in nature and the temperature is identified as the Hawking temperature [113].

- The other feature of the unstable potential is, it shows scattering phenomena. Therefore, our next approach was to study the scattering phenomena in the presence of this unstable xp kind near horizon Hamiltonian. Identifying the "in" and "out" states we obtained the transition probability for the particle to jump from the initial to final energy state, which yielded the thermal nature again with the desired Hawking temperature. Moreover, we gained the information about the frequency of the quasinormal modes from this scattering which matches with the earlier findings [262, 299–301].

Now, let us summarise the whole concept starting from the instability and how it leads us

to explain the thermal behaviour of the horizon. In the previous chapter 4, we constructed a model consisting of a probed massless and chargeless particle that was residing in the near-horizon region of a SSS BH. The specific Hamiltonian we obtained in that scenario of xp kind. The noticeable fact of that Hamiltonian is that it turns out to be a Hamiltonian of an IHO in a new set of canonical coordinates, which suggests the fact that the particle experiences a "local instability" in the near-horizon region. This can be realised in other way rounds also. As the particle approaches towards the horizon, i.e. in the limit of $t \to -\infty$, the radial momentum of the particle, i.e. p_r, diverges at the horizon. Due to the presence of this instability at the horizon ($r = r_H$), at the quantum level, we see that the particle escapes the barrier of the horizon through tunneling, forming a complex path. Hence, the singularity at $r = r_H$ not only provides instability in the particle motion but also plays a crucial role in the tunneling formalism. As a consequence of that, we obtain a finite amount tunneling probability of the particle for escaping through the horizon. Furthermore, the expression of the tunneling probability comes out to be of the Boltzmann factor, which is solely due to the xp structure of the Hamiltonian. Ultimately, it leads us to the thermal distribution, which infers the fact that instability is the main reason behind that. Not only that, in Gutzwiller's trace formula, after the quantisation of the DOS, we obtained that the distribution of the energy eigenstates of xp Hamiltonian have thermal behaviour, and we found out that the temperature exactly matches with Hawking's expression. Therefore, it leads us to conjecture that *the local instability created by the horizon in its vicinity region may be the main reason for having the horizon as a thermal object.*

Therefore, a clear recipe has been presented in this chapter about the relationship between instability and thermality in the context of horizon. However, the specific unstable spacetime region is very small, confined only within the neighbourhood of the horizon. Moreover, the way we have studied here is very interesting. Within the various known techniques, the black hole system has been investigated. On this note, we feel that the results, as well as the techniques, introduced here, will not only have a significant impact in the area of black hole physics, but also may uncover several unknown sides of the horizon. Furthermore, the present discussion has been confined within a static, spherically symmetric black hole. The interesting part is to extend it to Kerr and other non-trivial backgrounds which we shall see in the upcoming chapters.

Appendix

5.A Detector's response in $(1+1)$ dimensional Schwarzschild background

In section 5.2.2 we studied the transition probability for an atomic detector, which is interacting with a massless scalar field, moving very close to the horizon. It is found that it will register a particle in the Boulware vacuum. This was done numerically. Here we shall present an analytical approach when the detector is moving throughout the spacetime along our chosen null path, which near to the horizon leads to an unstable trajectory (4.21). The metric will be chosen to be Schwarzschild black hole in $(1+1)$ spacetime dimensions. The two-dimensional case is analytically solvable, and since we will be interested in finding the detected temperature, it is sufficient to consider a two-dimensional situation. Here both ingoing and outgoing detectors will be studied. We shall adopt the previous atomic detector model, and so the working formula for transition probability is given by (5.11).

The Schwarzschild metric in $(1+1)$ dimensional spacetime in Schwarzschild coordinates (t_s, r) is given by

$$ds^2 = -f(r)dt_s^2 + \frac{dr^2}{f(r)}\,, \tag{5.A.1}$$

where $f(r) = \left(1 - \frac{r_H}{r}\right)$. The horizon located at $r_H = 2M$ where M is the mass of the black hole. In the Eddington-Finkelstein coordinates (t, r) the metric transforms into

$$ds^2 = -\left(1 - \frac{r_H}{r}\right)dt^2 + \frac{2r_H}{r}dtdr + \left(1 + \frac{r_H}{r}\right)dr^2\,. \tag{5.A.2}$$

In this case the tortoise coordinate is given by

$$r_* = r + r_H \ln\left(\frac{r}{r_H} - 1\right)\,. \tag{5.A.3}$$

In the following calculation we shall choose the unit such that $\hbar = 1$.

5.A.1 Outgoing detector

The outgoing null path can be determined as earlier. The detector is moving from horizon to radial infinity. In this case the tangent of the path is is determined by the t and r components of (4.14). Therefore the path is found to be the solution of

$$\frac{dr}{dt} = \frac{\frac{r}{r_H} - 1}{\frac{r}{r_H} + 1}\,. \tag{5.A.1.1}$$

Performing the above integration we obtain

$$t = r + 2r_H \ln\left[\frac{r}{r_H} - 1\right] . \tag{5.A.1.2}$$

We have already found the positive frequency mode corresponding to the detector (see Eq. (5.13)). Next, we need to find the positive frequency Boulware mode for the massless scalar field i.e., u_ν, and for that, we need to solve the Klein-Gordon (KG) equation $\Box\phi = 0$ under the background (5.A.2). Since the detector is outgoing, the scalar mode under investigation will be ingoing one. This is given by (5.16). Now, substituting everything in the general form (5.11) (i.e. use (5.A.1.2) and (5.16) along with (5.A.3)) with $\tau = t$ and re-expressing it in terms of the radial coordinate we obtain

$$P_\uparrow = Q^2 \left| \int_{r_H}^{\infty} dr \quad \left(\frac{\frac{r}{r_H}+1}{\frac{r}{r_H}-1}\right) e^{i(2\nu+\omega)r} \left(\frac{r}{r_H} - 1\right)^{2ir_H(\nu+\omega)} \right|^2 . \tag{5.A.1.3}$$

Changing the variable as $(\frac{r}{r_H} - 1) = y$, we find

$$\begin{aligned} P_\uparrow &= Q^2 \left| r_H \int_0^{\infty} dy \left(\frac{y+2}{y}\right) e^{i(2\nu+\omega)r_H(y+1)}\, y^{2ir_H(\nu+\omega)} \right|^2 \\ &= Q^2 |I_{\uparrow 1} + I_{\uparrow 2}|^2 , \end{aligned} \tag{5.A.1.4}$$

where

$$I_{\uparrow 1} = r_H e^{i(2\nu+\omega)r_H} \int_0^{\infty} dy\, y^{2ir_H(\nu+\omega)} e^{i(2\nu+\omega)r_H y} \tag{5.A.1.5}$$

and

$$I_{\uparrow 2} = 2r_H e^{i(2\nu+\omega)r_H} \int_0^{\infty} dy\, y^{2ir_H(\nu+\omega)-1} e^{i(2\nu+\omega)r_H y} . \tag{5.A.1.6}$$

These integrations can be performed using the general formula (5.41) and following the prescription, as performed in section 5.3.2. This leads to

$$\begin{aligned} I_{\uparrow 1} &= r_H e^{i(2\nu+\omega)r_H} \exp\left[-(1 + 2ir_H(\nu+\omega))\left(\ln|(2\nu+\omega)r_H| - \frac{i\pi}{2}\text{sign}[(2\nu+\omega)r_H]\right)\right] \\ &\quad \times \Gamma(1 + 2ir_H(\nu+\omega)) \end{aligned} \tag{5.A.1.7}$$

and

$$\begin{aligned} I_{\uparrow 2} &= 2r_H e^{i(2\nu+\omega)r_H} \exp\left[-2ir_H(\nu+\omega)\left(\ln|(2\nu+\omega)r_H| - \frac{i\pi}{2}\text{sign}[(2\nu+\omega)r_H]\right)\right] \\ &\quad \times \Gamma(2ir_H(\nu+\omega)) . \end{aligned} \tag{5.A.1.8}$$

Substituting them in Eq. (5.A.1.4) and performing the modulus square, we finally obtain the expression for the transition probability as

$$P_{\uparrow} = Q^2 \frac{4\pi r_H \nu^2}{(2\nu+\omega)^2(\nu+\omega)} \times \frac{1}{e^{4\pi r_H(\nu+\omega)}-1} \,. \tag{5.A.1.9}$$

This is thermal in nature up-to some factors and the temperature is identified as

$$T = \frac{1}{4\pi r_H} \,, \tag{5.A.1.10}$$

which is the Hawking expression for Schwarzschild black hole.

5.A.2 Ingoing detector

The detector is now approaching towards the horizon from radial infinity. In this case, the null trajectory is chosen to be along the tangent, which is normal to ingoing null Krushkal-Szekeres coordinate V = constant surface. This is defined by

$$V = \pm \exp(\kappa v) + 1 \,, \tag{5.A.2.1}$$

where $V = 1$ is the horizon. The observer's coordinates are chosen to be outgoing Eddington-Finkelstein coordinates (u,r). Then the EF timelike coordinate (t) is given by Eq. (5.22). In these coordinates (t,r) the metric (5.A.1) takes the following form:

$$ds^2 = -f(r)dt^2 + 2(f(r)-1)dt\,dr + (2-f(r))dr^2 \,. \tag{5.A.2.2}$$

Now as earlier, the tangent to the path is given by

$$l^a = \left(1, \frac{f(r)}{f(r)-2}\right) \,. \tag{5.A.2.3}$$

Correspondingly the covariant components are

$$l_a = \left(\frac{f(r)}{f(r)-2}, -1\right) \,. \tag{5.A.2.4}$$

Therefore again the detector is moving along the radial direction only and the trajectory is determined by

$$\frac{dr}{dt} = \frac{1-\frac{r}{r_H}}{1+\frac{r}{r_H}} \,. \tag{5.A.2.5}$$

Performing the integration in Eq. (5.A.2.5) we obtain the solution of t as

$$t = -r - 2r_H \ln\left[\frac{r}{r_H} - 1\right] \,. \tag{5.A.2.6}$$

Since the detector is ingoing, we shall investigate the outgoing Boulware scalar mode, given by

$$u_\nu = e^{-i\nu(t_s - r_*)} \,. \tag{5.A.2.7}$$

Substituting all these in (5.11) and proceeding in the previous way one finds that the transition probability is same as (5.A.1.3). Therefore the final expression is given by (5.A.1.9). Hence the ingoing detector will register particle in the Boulware vacuum with Hawking temperature (5.A.1.10).

5.B A note on Gutzwiller's trace formula

Density of states (DOS) of a system is defines as

$$\rho(E) = \sum_n \delta(E - E_n) \tag{5.B.1}$$

where δ is the Dirac delta function and the summation runs over all energy eigenvalues of the physical system. We see that the density of states is the derivative of the counting function, $\rho(E) = d\mathcal{N}/dE$. we will link the density of states to the trace of the quantum mechanical Green function, which will be introduced later, and then derive a trace formula, known as the Gutzwiller trace formula [4], to find an expression for the density of states.

5.B.1 The Green's function

We first note that we can write the Dirac delta function as follows

$$\delta(E) = \lim_{\epsilon \to 0} \frac{\epsilon}{\pi} \frac{1}{E^2 + \epsilon^2} \tag{5.B.1.1}$$

Using this expression in (5.B.1), we obtain

$$\begin{aligned} \rho(E) &= \sum_n \lim_{\epsilon \to 0} \frac{\epsilon}{\pi} \frac{1}{(E - E_n)^2 + \epsilon^2} \\ &= -\frac{1}{\pi} \lim_{\epsilon \to 0} \mathrm{Im}\Big(\sum_n \frac{E - E_n - i\epsilon}{(E - E_n)^2 + \epsilon^2} \Big) \\ &= -\frac{1}{\pi} \lim_{\epsilon \to 0} \mathrm{Im}\Big(\sum_n \frac{1}{E - E_n + i\epsilon} \Big) \,. \end{aligned} \tag{5.B.1.2}$$

[4] For detailed calculations, we refer to [274]

If we include the infinitesimal imaginary part $i\epsilon$ into E, and consider the taken limit to be understood in further use of this expression, the statement reduces to

$$\rho(E) = -\frac{1}{\pi}\mathrm{Im}\sum_n \frac{1}{E-E_n} \ . \tag{5.B.1.3}$$

Therefore, in terms of trace of an observable (i.e. Hermitian) operator H of a quantum system, we can write the above form of the DOS as

$$\rho(E) = -\frac{1}{\pi}\mathrm{Im}\left(\mathrm{Tr}\left(\frac{1}{E-H}\right)\right) \ . \tag{5.B.1.4}$$

Now, the quantum mechanical Green's function is given by

$$G(q_A, q_B, E) = \sum_n \frac{\psi_n^*(q_A)\psi_n(q_B)}{E-E_n} \tag{5.B.1.5}$$

Here, the summation runs over all eigenvectors $\psi_n(q)$ of the Hamiltonian of the system. Now we introduce the notation $|q_A\rangle$ for the eigenfunction of the position operator

$$q|q_A\rangle = q_A|q_A\rangle \ . \tag{5.B.1.6}$$

In this notation, we have $\psi_n(q_B) = \langle q_B|\psi_b(q)\rangle$. Therefore, we can rewrite the Green function

$$G(q_A, q_B, E) = \sum_n \langle\psi_n(q)|q_A\rangle \frac{1}{E-E_n}\langle q_B|\psi_n(q)\rangle \ . \tag{5.B.1.7}$$

The position operator is an observable, which implies that the set of eigenfunctions of the operator q is complete. Therefore, we have

$$\int |q\rangle\langle q|dq = I \tag{5.B.1.8}$$

where I denotes the identity operator. In the same way, we have

$$\sum_n |\psi_n\rangle\langle\psi_n| = I \tag{5.B.1.9}$$

Hence, we can write the Green's function as follows

$$\begin{aligned} G(q_A, q_B, E) &= \int \sum_n \langle q_A|q\rangle\langle q|\psi_n\rangle \frac{1}{E-E_n}\langle\psi_n|q'\rangle\langle q'|q_B dq dq' \\ &= \langle q_A|q\rangle\langle q|\sum_n |\psi_n\rangle\langle\psi_n|\frac{1}{E-H}|q'\rangle\langle q'|q_B\rangle dq dq' \\ &= \langle q_A|\frac{1}{E-H}|q_B\rangle \end{aligned} \tag{5.B.1.10}$$

The Green function can thus be seen as the matrix element of the operator $\frac{1}{E-H}$ in the basis of the position eigenvectors. We can now change the expression in (5.B.1.4) into the following expression for the density of states which leads us to Eq. (5.25):

$$\rho(E) = -\frac{1}{\pi}\mathrm{Im}(\mathrm{Tr}(G(E))) = -\frac{1}{\pi}\mathrm{Im}\left(\int G(q,q,E)dq\right) \ . \tag{5.B.1.11}$$

5.B.2 Semi-Classical Green's function and calculation of DOS

In quantum mechanics, the propagator $K(q_A, a_B, t)$ gives the probability density, $|K(q_A, q_B, t)|^2$, for a particle to reach position q_B at time t when starting in position q_A at $t = 0$. For $t \leq 0$, $K(q_A, q_B, t) = 0$. For $t > 0$ it is given by the following expression

$$K(q_A, q_B, t) = \langle q_B | U(t) | q_A \rangle, \tag{5.B.2.1}$$

where $U(t)$ is the time-evolution operator

$$U(t) = e^{-iHt/\hbar} . \tag{5.B.2.2}$$

The time Fourier transform of the propagator is, up to a complex constant, equal to the Green's function

$$G(q_A, q_B, E) = -\frac{i}{\hbar} \int_0^\infty K(q_A, q_B, t) e^{iEt/\hbar} dt . \tag{5.B.2.3}$$

Now, using *Feynman's path integral* approach one can obtain the expression of the propagator as

$$K(q_A, q_B, t) = \int \mathscr{D}(q) \exp\left(\frac{i}{\hbar} \int_0^t L(q, \dot{q}, dt) dt \right) \tag{5.B.2.4}$$

where $\mathscr{D}(q)$ stands for the path integral. To simplify this expression, using the Saddle point approximation one obtains

$$K(q_A, q_B, t) = \left(\frac{1}{2\pi\hbar i} \right)^{d/2} \sum_l |D_{BA,l}|^{1/2} \exp\left(\frac{i}{\hbar} W_{BA,l}(t) - i\frac{\pi\mu_l}{2} \right) \tag{5.B.2.5}$$

where the summation runs over all the classically allowed trajectories from q_A to q_B in time t. We have $|D_{BA}| = \left| -\frac{\partial^2 W_{BA}}{\partial q_B \partial q_A} \right|$ and $W_{BA}(t) = \int_0^t L(q, \dot{q}, t') dt'$. Here, d is the number of dimensions of the system, i.e. the number of generelised coordinates and μ_l is called the Maslov index which is given by

$$\mu_l = \frac{1}{2}[(N-1)d - \alpha_l] \tag{5.B.2.6}$$

where N is the number of divisions of the time interval while going from $0 \to t$ and $\alpha_l = \sum_{j=1}^{(N-1)d} \mathrm{sgn}(\lambda_l^{(j)})$, where λ_l^j are the eigenvalues of $\frac{\partial^2 W_{BA,l}}{\partial q_A \partial q_B}$. Now, using the expression of the semi-classical propagator (Eq. (5.B.2.5)) and putting it into the Eq. (5.B.2.3) one can compute the Green's function

$$\begin{aligned} G(q_A, q_B, E) \quad = -\frac{i}{\hbar} \int_0^\infty \left(\frac{1}{2\pi\hbar i} \right)^{d/2} \sum_l |D_{BA,l}|^{1/2} \exp\Big(\frac{i}{\hbar} [W_{BA,l}(t) + Et] \\ - i\frac{\pi\mu_l}{2} \Big) dt . \end{aligned} \tag{5.B.2.7}$$

Now, if the Hamiltonian is time independent then $H = E$ and we get

$$W_{BA,l} + Et = \int_0^t (L+H)dt' = \int_0^t p_l \dot{q}_l dt' = S_l \tag{5.B.2.8}$$

where S_l is the Hamilton-Jacobi action. Hence,

$$G(q_A, q_B, E) = -\frac{i}{\hbar}\int_0^\infty \left(\frac{1}{2\pi\hbar i}\right)^{d/2} \sum_l |D_{BA,l}|^{1/2} \exp\left(\frac{i}{\hbar}S_l - i\frac{\pi\mu_l}{2}\right) dt \ . \tag{5.B.2.9}$$

After using the saddle point approximation, one gets

$$G(q_A, q_B, E) = -\frac{i}{\hbar}\left(\frac{1}{2\pi\hbar i}\right)^{(d-1)/2} \sum_l |\Delta_{BA,l}|^{1/2} \exp\left(\frac{i}{\hbar}S_l(q_A, q_B, E) - i\frac{\pi\mu_l}{2}\right) \tag{5.B.2.10}$$

where

$$\Delta_{BA,l} = \begin{bmatrix} -\frac{\partial^2 S_l}{\partial q_A \partial q_B} & -\frac{\partial^2 S_l}{\partial q_A \partial E} \\ -\frac{\partial^2 S_l}{\partial E \partial q_B} & -\frac{\partial^2 S_l}{\partial E^2} \end{bmatrix} \ . \tag{5.B.2.11}$$

Finally, the density of states (DOS) is calculated using the expression of the Green function (5.B.2.10) and put it into the formula (5.B.1.11) and using the saddle point approximation, one gets

$$\rho(E) = \frac{1}{\pi\hbar}\sum_l \frac{T_l}{||M_l - I||^{1/2}} \cos\left[\frac{i}{\hbar}S_l(E) - i\frac{\pi\mu_l}{2}\right] \tag{5.B.2.12}$$

where T_l is the period of the primitive orbit and M_l is the Monodromy matrix and I is the identity matrix. This Eq. (5.B.2.12) is the famous Gutzwiller's trace formula for the density of states of a quantum chaotic system.

5.C Finding the action in the near-horizon region

In the present appendix section, we shall show that the action (5.31) can also be obtained in a different way. Since our Hamiltonian (4.34) is valid very near to the horizon, we consider a closed path which encircles the horizon $x = 0$ in a circular trajectory with a very small radius (say $\epsilon \to 0$) as shown in Fig. 5.3.

Actually the path is one which starts just outside the horizon, enters through it and comes back again. So it crosses the singular point $x = 0$ twice. To avoid this a complex path has been chosen and since the relevant contribution comes from the singularity, we have chosen a circular path as shown in Fig. 5.3. The choice of these types of paths

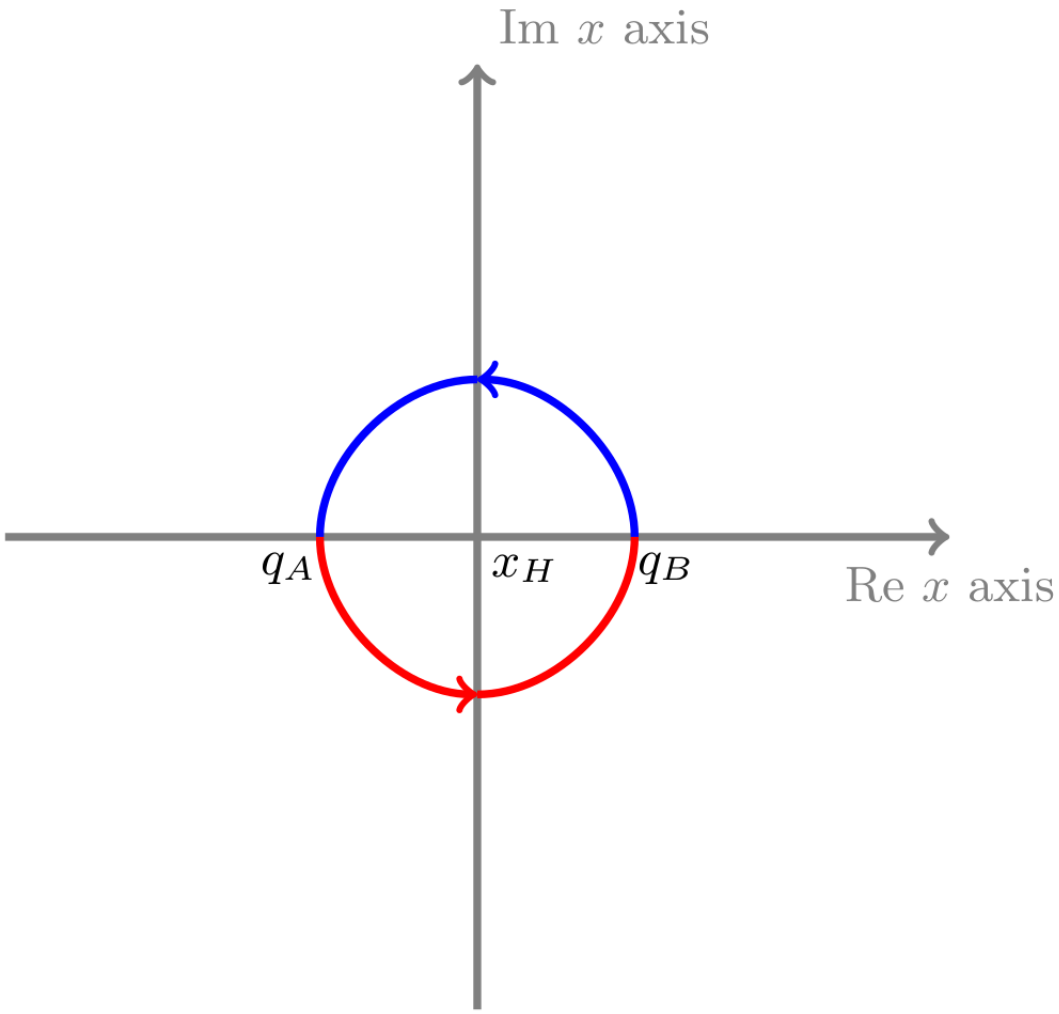

Figure 5.3: The contour diagram across the horizon where the horizon is at x_H

motivated from the semi-classical treatment of Hawking effect in tunneling formalism, similar to what we already discussed in Section 5.2.1. Since the formula (5.26) is semi-classical in nature, we hope that such paths are relevant here as well. With this the action of the particle following the closed path is

$$S_l(E) = \oint p\, dx = \frac{E_l}{\kappa} \oint \frac{dx}{x} \,. \tag{5.C.1}$$

The above closed integration can be divided into two parts:

$$S_l(E) = \frac{E_l}{\kappa} \Big[\underbrace{\int_{q_A}^{q_B} \frac{dx}{x}}_{I_1} + \underbrace{\int_{q_B}^{q_A} \frac{dx}{x}}_{I_2} \Big] \tag{5.C.2}$$

Now, the integration I_1 i.e. when the particle is going from q_A to q_B is evaluated as

$$I_1 = \int_{q_A \to q_B} \frac{dx}{x} = \int_{\pi}^{2\pi} \frac{i\epsilon e^{i\vartheta}}{\epsilon e^{i\vartheta}} d\vartheta = i\pi \ , \tag{5.C.3}$$

where in the above ϵ is chosen to be the radius of the circular path and we substituted $x = \epsilon e^{i\vartheta}$. Similarly, I_2 is evaluated to be

$$I_2 = i\pi \ . \tag{5.C.4}$$

Finally, putting the values of I_1 and I_2 in (5.C.2), we obtain the same expression of the action as in (5.31).

5.D Thermality through a toy model: a perturbative approach

In this appendix section, we visualise the whole system as a following effective quantum mechanical model. We first consider a free massless particle in Minkowski spacetime whose Hamiltonian is given by $H_0 = -p$ (with the choice of unit $c = 1$) which is along the radial ingoing direction. The near horizon Hamiltonian $H \simeq \kappa xp$ is treated as a small interaction of the particle with a potential of this form. So we model the actual system effectively as an interaction picture where a massless particle is interacting with the potential κxp when it is following the trajectory (4.21). So we take the interaction Hamiltonian as

$$\hat{H}_I = \frac{1}{2}\kappa(\hat{x}\hat{p} + \hat{p}\hat{x})\delta(x - \frac{1}{\kappa}e^{\kappa t}) \ . \tag{5.D.1}$$

Dirac-delta function has been introduced in order to make sure that the interaction is occurring only when the particle is moving along the path, given by (4.21). Now, if the particle is a two-level quantum atom, then there is a possibility of transition from one state to another state. Here we want to calculate the probability of transition if the atom is initially in the ground state. So the total Hamiltonian for this quantum system is

$$\hat{H} = \hat{H}_0 + \hat{H}_I \ , \tag{5.D.2}$$

where $\hat{H}_I$ is treated as small compared to $\hat{H}_0$. So the transition amplitude can be evaluated in perturbative way. The unperturbed energy eigen basis are evaluated from $\hat{H}_0 = -\hat{p}$. This will provide the initial and final basis states. These are given by $\psi_i(x) \sim e^{-i\omega_i x}$ and $\psi_f(x) \sim e^{-i\omega_f x}$, respectively (considering $\hbar = 1$ and the velocity of light in free

space $c = 1$). Introducing the transition frequency $\omega = \omega_f - \omega_i$ we write the transition amplitude at the first order perturbation as

$$c_{i\to f} = -i\int_{-\infty}^{\infty} dt\langle f|\hat{H}_I(t)|i\rangle\ e^{i\omega t}\delta(x-\frac{1}{\kappa}e^{\kappa t}) \tag{5.D.3}$$

$$= -\frac{i\kappa}{2}\int_{-\infty}^{\infty} dt\langle f|(\hat{x}\hat{p}+\hat{p}\hat{x})|i\rangle e^{i\omega t}\delta(x-\frac{1}{\kappa}e^{\kappa t}). \tag{5.D.4}$$

Now, let us concentrate on

$$\mathscr{I} = \frac{\kappa}{2}\left(\underbrace{\langle f|\hat{x}\hat{p}|i\rangle\delta(x-\frac{1}{\kappa}e^{\kappa t})}_{\mathscr{I}_1} + \underbrace{\langle f|\hat{p}\hat{x}|i\rangle\delta(x-\frac{1}{\kappa}e^{\kappa t})}_{\mathscr{I}_2}\right). \tag{5.D.5}$$

The first term can be evaluated as follows:

$$\begin{aligned}\mathscr{I}_1 &= \int_{-\infty}^{\infty}\langle f|x\rangle\langle x|\hat{x}\hat{p}|i\rangle\delta(x-\frac{1}{\kappa}e^{\kappa t})dx\\ &= \int_{-\infty}^{\infty}\langle f|x\rangle x\langle x|\hat{p}|i\rangle\delta(x-\frac{1}{\kappa}e^{\kappa t})dx\\ &= \int_{-\infty}^{\infty}\psi_f^*(x)x\left(-i\frac{\partial}{\partial x}\right)\langle x|i\rangle\delta(x-\frac{1}{\kappa}e^{\kappa t})dx\\ &= -i\int_{-\infty}^{\infty}\psi_f^*(x)x\frac{\partial}{\partial x}\psi_i(x)\delta(x-\frac{1}{\kappa}e^{\kappa t})dx\ .\end{aligned} \tag{5.D.6}$$

In the similar approach the other term of Eq. (5.D.5) yields

$$\begin{aligned}\mathscr{I}_2 &= \langle f|\hat{p}\hat{x}|i\rangle\delta(x-\frac{1}{\kappa}e^{\kappa t}) = (\langle i|\hat{x}\hat{p}|f\rangle)^*\delta(x-\frac{1}{\kappa}e^{\kappa t})\\ &= i\int_{-\infty}^{\infty}\psi_i(x)x\frac{\partial}{\partial x}\psi_f^*(x)\delta(x-\frac{1}{\kappa}e^{\kappa t})dx\ .\end{aligned} \tag{5.D.7}$$

Then, using these and substituting the values of ψ_i and ψ_f along with their conjugates in (5.D.5) we obtain

$$\begin{aligned}\mathscr{I} &= \frac{i\kappa}{2}\int_{-\infty}^{\infty}dx\left[e^{-i\omega_i x}(i\omega_f)e^{i\omega_f x} - e^{i\omega_f x}(-i\omega_i)e^{-i\omega_i x}\right]x\delta(x-\frac{1}{\kappa}e^{\kappa t})\\ &= -\frac{\kappa}{2}\int_{-\infty}^{\infty}dx e^{i\omega x}(\omega_f+\omega_i)x\delta(x-\frac{1}{\kappa}e^{\kappa t})\\ &= -\frac{\kappa}{2}(\omega_f+\omega_i)e^{i\frac{\omega}{\kappa}e^{\kappa t}}\frac{1}{\kappa}e^{\kappa t}\ .\end{aligned} \tag{5.D.8}$$

Now, changing the variable $e^{\kappa t} = y$ we have

$$c_{i\to f} = \frac{i(\omega_i+\omega_f)}{2\kappa}\int_0^{\infty} e^{i\frac{\omega}{\kappa}y}y^{\frac{i\omega}{\kappa}}dy\ . \tag{5.D.9}$$

Next, using the formula (5.41) we can perform the integration (see page no. 604 of [262] for details) one finds

$$c_{i\to f}=\frac{i(\omega_i+\omega_f)}{2\kappa}\exp\left[-\left(1+\frac{i\omega}{\kappa}\right)\ln\left|\frac{\omega}{\kappa}\right|+\left(1+\frac{i\omega}{\kappa}\right)\frac{i\pi}{2}\text{sign}\left(\frac{\omega}{\kappa}\right)\right]\Gamma\left(1+\frac{i\omega}{\kappa}\right). \quad (5.D.10)$$

In the above "sign" denotes the sign function. Therefore the probability of transition from $|i\rangle$ to $|f\rangle$ turns out to be

$$|c_{i\to f}|^2=\begin{cases}\frac{\pi(\omega_i+\omega_f)^2}{2\kappa\omega}\frac{1}{e^{\frac{2\pi\omega}{\kappa}}-1}; & \omega>0\\ \frac{\pi(\omega_i+\omega_f)^2}{2\kappa\omega}\frac{e^{\frac{2\pi\omega}{\kappa}}}{e^{\frac{2\pi\omega}{\kappa}}-1}; & \omega<0\end{cases} \quad (5.D.11)$$

In a more compact form we obtain

$$|c_{i\to f}|^2=\frac{\pi(\omega_i+\omega_f)^2}{2\kappa|\omega|}\frac{1}{e^{\frac{2\pi|\omega|}{\kappa}}-1}. \quad (5.D.12)$$

This transition probability is thermal is nature up-to some factors and one identifies the temperature as (5.7).

Now let us give some physical aspects of this perturbation method. The main motive of this approach is to build a quantum mechanical model which mimics the near horizon characteristics. In this case, we have taken the potential to be xp kind, which is basically the near horizon Hamiltonian. Another important point is that we have considered a definite path for the massless particle, which is basically similar to the radial trajectory of a massless particle, which we have shown already in the previous chapter (Sections 4.3.1, 4.3.2, 4.3.3 of chapter 4). Therefore, in a physical sense, this model basically mimics the quantum behavior of the massless particle whenever it comes into the vicinity of the horizon. The non-zero value of the probability whose nature is similar to the Planckian distribution tells us about the thermal behavior in the near-horizon region. Therefore, it can be regarded as an effective approach to show the thermal nature in the near-horizon region.

Part IV

Generalisation to other backgrounds

CHAPTER 6

HORIZON THERMALIZATION OF KERR BLACK HOLE THROUGH LOCAL INSTABILITY

6.1 Introduction and Motivation

Classical black hole physics reveals a set laws of black hole mechanics and that are similar to the laws of thermodynamics. It has already been an established fact that a black hole is a thermodynamical object [68, 108, 113, 114], and it has temperature [68, 113], which is purely a quantum mechanical and observer-dependent quantity. It is also known that the concept of horizon thermalisation originates from the analogy between the laws of black holes and those of the usual thermodynamical systems [108]. However, this analogy is still far away to provide a unified perspective about the core reason for such characteristics of the horizon. In our previous chapter 5, the main goal was to find out the underlying mechanism that furnishes temperature to the horizon, and we shall hunt for the same answer here also but in a different scenario.

In chapter 4 we have shown that through considering a model in the presence of a static spherically symmetric black hole (SSS BH), an outgoing massless and chargeless particle experiences instability in the near horizon region and the Hamiltonian of the system is found to be of $H \sim xp$ kind which is an unstable one. Following that classical picture next in chapter 5 we enter into the quantum regime where we find out some striking insights on the connection between that *local instability* and the horizon thermalisation in the near horizon region. In this context, we would like to mention

some recent developments which also indicate that instability has a close connection with thermality in the context of horizon [232–235, 277, 303–305] [1]. Instability and thermality, these two features may seem different from each other but there lies an important unification between them. In many works [232, 233, 277, 303–305], it has been noted that their intimate relationship has the potential to become one of the leading candidates, which can shed some light on the exact mechanism of horizon thermalisation. As we mentioned earlier, our previous chapters (chapter 4 and chapter 5) have revealed that in the presence of SSS BH, an outgoing massless and chargeless particle experiences instability in the near-horizon region and in the quantum scale. This instability provides temperature into the system, which divulges a noticeable conjecture that *horizon creates a local instability in its vicinity region which acts as the source of the quantum temperature of a black hole*. Within this analysis very recently it has been argued that this conjecture may be supported in a more rigorous picture [304].

However, in those earlier chapters (chapter 4 and chapter 5), the analysis has been restricted only to SSS BH case. Therefore, this conjecture needs to be tested in some realistic situation in order to be more robust. Kerr black hole is one of the prime examples of this kind. Kerr black holes are stationary rotating black holes. Rotating black holes are formed in the gravitational collapse of a massive spinning star, or the collision of a collection of compact objects or stars, and realistic collisions have non-zero angular momentum. Therefore, it is expected that all black holes in nature are rotating ones. So, the Kerr solution has astrophysical relevance, and this study in the near-horizon region of Kerr spacetime will provide us with a much more realistic picture of the explanation of horizon thermalisation.

6.2 Defining the outgoing path of the particle

Like in the earlier chapters (chapter 4 and chapter 5), we start our analysis with a massless and chargeless particle moving under the Kerr spacetime, where the coordinate system adopted here is a generalised version of Eddington-Finkelstein (EF) coordinates to the rotating case. The particle moves along the null normal to the t = constant and r = constant surface.

We start our analysis with the aim of identifying the outgoing trajectory of a massless, chargeless particle in Kerr black hole. This will be the backbone for the main purpose of

[1] Near horizon calculation is sufficient to see particle emission from horizon has also been reported in [306, 307].

the present chapter. The analysis is being followed from Appendix D of [275]. Massless particle follows null-like trajectories and therefore the tangent to the path must be null-like. In Boyer-Lindquist (BL) coordinates $(t_{BL}, r, \theta, \phi_{BL})$, the metric for Kerr black hole is of the form:

$$\begin{aligned} ds^2 = & -\left(1-\frac{2mr}{\rho^2}\right)dt_{BL}^2 - \frac{4mar\sin^2\theta}{\rho^2}dt_{BL}d\phi_{BL} + \frac{\rho^2}{\Delta}dr^2 + \rho^2 d\theta^2 \\ & + \left(r^2+a^2+\frac{2mra^2\sin^2\theta}{\rho^2}\right)\sin^2\theta\, d\phi_{BL}^2 \,, \end{aligned} \tag{6.1}$$

where m and a are mass and angular momentum per unit mass of the black hole, respectively. ρ^2 and Δ are given by

$$\rho^2 = r^2 + a^2\cos^2\theta \quad \text{and} \quad \Delta = r^2 - 2mr + a^2 \,. \tag{6.2}$$

For $a = 0$ the metric reduces to the Schwarzschild metric. However, being a generalization of Schwarzschild coordinates to the rotating case, these coordinates are singular on the event horizon $\mathscr{H}$ which corresponds to $\Delta = 0$. The location of the horizon is then given by

$$r_H = m + \sqrt{m^2 - a^2} \,. \tag{6.3}$$

The metric coefficients are independent of t_{BL} and ϕ_{BL} and thereby respecting time translation invariance and axial symmetry.

Since BL coordinates are not regular at r_H, like our earlier analysis in chapter 4, we adopt here a generalization of Eddington-Finkelstein (EF) coordinates to the rotating case which are regular at the horizon. The spheroidal version of EF coordinates, denoted by (t, r, θ, ϕ), are related to the Boyer Lindquist coordinates $(t_{BL}, r, \theta, \phi_{BL})$ by the following relations:

$$dt = dt_{BL} + \frac{dr}{\frac{r^2+a^2}{2mr} - 1} \,, \tag{6.4}$$

$$d\phi = d\phi_{BL} + \frac{a\, dr}{r^2 - 2mr + a^2} \,. \tag{6.5}$$

The metric in these coordinates turns out to be

$$\begin{aligned} ds^2 = & -\left(1-\frac{2mr}{\rho^2}\right)dt^2 + \frac{4mr}{\rho^2}dt\, dr - \frac{4amr}{\rho^2}\sin^2\theta\, dt d\phi + \left(1+\frac{2mr}{\rho^2}\right)dr^2 \\ & -2a\sin^2\theta\left(1+\frac{2mr}{\rho^2}\right)dr d\phi + \rho^2 d\theta^2 + \left(r^2+a^2+\frac{2a^2mr\sin^2\theta}{\rho^2}\right)\sin^2\theta d\phi^2 \end{aligned} \tag{6.6}$$

Note that all the metric coefficients of the above one are regular at $r = r_H$. Now in order to find the null vector which will be the tangent to our particle path we first find the unit normals to t = constant and r = constant surfaces for the metric (6.6).

Let us consider the foliation of Kerr spacetime by the hypersurfaces Σ_t of the constant Kerr time t. Now, with the application of ADM decomposition (for details please see Appendix 6.A) and comparing the line element (6.6) with Eq. (6.A.10), we obtain the corresponding lapse function

$$N = \frac{\rho}{\sqrt{\rho^2 + 2mr}} \tag{6.7}$$

and the shift vector [275]

$$\beta^a = \left(0, \frac{2mr}{\rho^2 + 2mr}, 0, 0\right), \tag{6.8}$$

$$\beta_a = \left(\frac{4m^2r^2}{\rho^2(\rho^2 + 2mr)}, \frac{2mr}{\rho^2}, 0, -\frac{2amr}{\rho^2}\sin^2\theta\right) \tag{6.9}$$

where a represents the space-time index. The unit timelike normal to Σ_t can be calculated from the values of the lapse function and the shift vector (see Appendix 6.A), which results in

$$n^a = \left(\frac{1}{\rho}\sqrt{\rho^2 + 2mr}, -\frac{2mr}{\rho\sqrt{\rho^2 + 2mr}}, 0, 0\right) \tag{6.10}$$

and the corresponding covariant vector

$$n_a = \left(-\frac{\rho}{\sqrt{\rho^2 + 2mr}}, 0, 0, 0\right). \tag{6.11}$$

Our aim is to calculate the null normal to $\mathscr{H}$. In order to do so our next aim is to calculate the outward (spacelike) unit normal to the 2-surface $\mathscr{S}_t \subset \Sigma_t$ which is defined at $r = \text{const} = r_H$. Its outward (spacelike) unit normal $\mathbf{s}$ lying in Σ_t is obtained as

$$s_a = \left(0, \rho\sqrt{\frac{\rho^2 + 2mr}{A}}, 0, 0\right), \tag{6.12}$$

$$s^a = \left(0, \frac{1}{\rho}\sqrt{\frac{A}{\rho^2 + 2mr}}, 0, \frac{a}{\rho}\sqrt{\frac{\rho^2 + 2mr}{A}}\right). \tag{6.13}$$

where $A = (r^2 + a^2)^2 - (r^2 - 2mr + a^2)a^2\sin^2\theta$.

We then obtain the null normal to $\mathscr{H}$ associated with Kerr slicing $\mathbf{l}$, by inserting the expressions of (6.7), (6.10) and (6.13) into $\mathbf{l} = N(\mathbf{n} + \mathbf{s})$

$$l^a = \left(1, \frac{\sqrt{A} - 2mr}{\rho^2 + 2mr}, 0, \frac{a}{\sqrt{A}}\right). \tag{6.14}$$

It can be checked that on the horizon $\mathscr{H}$ the components reduces to

$$l^a \overset{\mathscr{H}}{=} (1,0,0,a/(2mr_H)) \ . \tag{6.15}$$

Also, one can check that at the limit of $a \to 0$ (6.14) reduces to the expression of the null normal of a Schwarzschild black hole

$$l^a = \left(1, \frac{1-\frac{2m}{r}}{1+\frac{2m}{r}}, 0, 0\right) \ . \tag{6.16}$$

Now, this null normal vector (6.14) an important one as the motion of our massless particle is along l^a. Therefore, the integral curves $x^a(\mu) = (t,r,\theta,\phi)$ of l^a, characterized by

$$\frac{dx^a(\mu)}{d\mu} = l^a(x(\mu)) \ , \tag{6.17}$$

where μ is the parameter which fixes the particle position at a particular moment, leads to the outgoing trajectory of our massless particle along the normal to $\mathscr{H}$.

6.3 Behaviour of trajectory near Kerr horizon

The path of our test particle is given by the integral curves which are expressed in Eq. (6.17). We would like to investigate those trajectories and try to understand how they behave in the near horizon region of the Kerr black hole. Since the components of the normal vector l^a is given by (6.14) and $x^a = (t,r,\theta,\phi)$, the time component of (6.17) yields

$$\frac{dt}{d\mu} = 1 \Rightarrow \mu = t \ . \tag{6.18}$$

Therefore in this analysis the coordinate time t plays the role of the parameter which fixes the moment of particle position.

6.3.1 Behaviour in the radial direction

Since $\mu = t$, the radial motion from (6.17) is determined by

$$\frac{dr}{dt} = \frac{\sqrt{A} - 2mr}{\rho^2 + 2mr} \equiv F(r,\theta) \ . \tag{6.19}$$

Here we denoted the right hand side expression as $F(r,\theta)$ for future convenience. The solution of the above equation will give us the information about the behaviour of the particle trajectory in the radial direction. However, our main interest is to scrutinize the nature of the trajectory in the vicinity of the Kerr horizon. Therefore, we have to

check the behaviour of the solution of Eq. (6.19) taking into account the near horizon approximation. It has already been checked that $F(r_H,\theta)=0$ (see Eq. (6.15)). Therefore, using the Taylor series expansion of $F(r,\theta)$ around $r=r_H$ and considering only the leading order terms we obtain:

$$F(r,\theta)\simeq\kappa(r-r_H)\,, \tag{6.20}$$

where $\kappa=F'(r=r_H,\theta)$ (please see Appendix 6.B and the prime denotes the partial derivative with respect to the radial coordinate r) is identified as the surface gravity of Kerr black hole (see Appendix D.4 of [275]). The value of κ is given by

$$\kappa=\frac{r_H-m}{2mr_H}=\frac{\sqrt{m^2-a^2}}{2m(m+\sqrt{m^2-a^2})}\,. \tag{6.21}$$

Note that κ is a constant (independent of spacetime coordinates) and therefore the leading order term in the expansion of $F(r,\theta)$ (see Eq. (6.20)) is function of radial coordinate only. Since we are interested to this order, denote Eq. (6.20) as $f(r)\simeq\kappa(r-r_H)$. It may be mentioned that κ is the value of non-affinity parameter $\tilde{\kappa}$, calculated at the horizon, which is determined by the non-affinely parameterized null geodesic equation $l^a\nabla_a l_b=\tilde{\kappa}l_b$ for our given (6.14). Therefore keeping upto the relevant leading order (i.e. $\mathcal{O}(r-r_H)$), in the near horizon region Eq. (6.19) reduces to

$$\frac{dr}{dt}\simeq\kappa(r-r_H)\,. \tag{6.22}$$

The solution of it is given by

$$r-r_H=\frac{1}{\kappa}e^{\kappa t}\,, \tag{6.23}$$

which is same as SSS BH case (see Eq. 4.21). In later discussion we will find that the corresponding radial momentum behaves as $p_r\sim e^{-\kappa t}$ and as we have limit $t\to-\infty$ for near horizon, p_r diverges when the particle resides very near to the horizon. This above natures of the radial motion indicates that as long as the particle stays in the vicinity of the horizon, it feels an instability. However, this equation also tells us that this mentioned instability is a “local" feature, not a global one. It is only applicable in the near horizon region. Incidentally, this exact feature has been experimentally verified in a recent investigation [308] on an analog black hole made by photon chip. Moreover it must be noted that the horizon corresponds to $t\to-\infty$ which is consistent to our result $r-r_H=(1/\kappa)e^{\kappa t}$. So within the range $-\infty\leq t<0$ we have $\kappa(r-r_H)<1$ and hence there is no breakdown of our approximation.

6.3.2 Behaviour in the angular direction

Next, let us investigate the particle motion along the angular coordinates. From the obtained path of the test particle, given by the integral curve (6.17) of the null normal vector (6.14) we obtain from the θ component of l^a

$$\frac{d\theta}{dt} = 0 \Rightarrow \theta = \text{constant} \, . \tag{6.24}$$

Therefore, the above equation suggests that the θ coordinate remains constant with respect to time along the trajectory of the particle; i.e. the particle does not have any motion along θ-direction.

The azimuthal component of (6.14) leads us to

$$\frac{d\phi}{dt} = \frac{a}{\sqrt{A}} \, . \tag{6.25}$$

Now, as our interest is in the near horizon region, therefore considering only the leading order term in the above equation we obtain

$$\frac{d\phi}{dt} \simeq \frac{a}{2mr_H} = \Omega_H \, . \tag{6.26}$$

The solution of the above equation is

$$\phi = \Omega_H t \, ; \tag{6.27}$$

i.e. ϕ changes linearly with t along the trajectory as long as the near horizon particle motion is concerned.

The analysis in this section indicates that the motion of the particle in the near horizon regime in the radial direction incorporates a "local" instability, whereas such is absent in the angular directions. In the next section, for this particular motion, we will show the presence of such instability in a coordinate independent way.

6.4 Local instability in geodesic congruence

We have already obtained that there is a local instability in the radial direction of the particle motion in the near horizon region of a Kerr BH. However, in the azimuthal direction this instability is not present. It is always important to give a description of this local instability in a covariant way. The main emphasis is to check whether this instability in the particle motion is an artefact of our chosen coordinate system or this

near horizon instability has any coordinate independent explanation. Moreover, the instability is mainly measured by the exponential nature of separation between the two nearby geodesics. Therefore it is natural to analysis the geodesics deviation equation for our chosen null vector, given by null Raychaudhuri equation, in the near horizon regime. Our main focus hence will be on the expansion parameter Θ, which measures the nature of distance between the geodesics in congruence [276]. Also we will see whether this has any connection to our earlier prediction on radial instability.

The Raychaudhuri equation for null geodesics is [262, 276]

$$\frac{d\Theta}{d\mu} = \tilde{\kappa}\Theta - \frac{1}{2}\Theta^2 - \sigma_{ab}\sigma^{ab} + \omega_{ab}\omega^{ab} - R_{ab}l^a l^b \,, \tag{6.28}$$

where $\tilde{\kappa}$ is the non-affinity coefficient, σ_{ab} is the shear parameter, ω_{ab} is the rotation parameter and R_{ab} is the Ricci tensor. Since our aim is to study this equation in the near horizon region of Kerr spacetime, we will now investigate nature of each terms in the above equation. Note that the quantities are defined with respect to the null vector (6.14) as the motion of our particle is along this vector. Therefore, it is time to examine each of the terms on the right hand side of this equation and try to analyze them. We obtain that although the value of the shear parameter σ_{ab} does not vanish for any arbitrary value of r but on the horizon $r = r_H$ it vanishes, i.e. $\sigma_{ab}(r_H) = 0$ (see [275] for detailed discussion). Therefore, in the near horizon region the leading order term of the shear parameter is

$$\sigma_{ab}(r) \simeq \sigma'_{ab}(r_H)(r - r_H) \,, \tag{6.29}$$

where the higher order terms ($\mathcal{O}(r-r_H)^2$) have been neglected and the prime denotes the derivative with respect to r. We have also found that on the horizon $\Theta \overset{\mathcal{H}}{=} 0$ (please see Appendix 6.C). Therefore, in the near horizon region the leading order term of Θ which contributes in the Raychaudhuri equation is

$$\Theta(r) \simeq \Theta'(r_H)(r - r_H) \,, \tag{6.30}$$

where, as earlier, the higher order terms have been neglected. Whereas for the non-affinity parameter we have $\tilde{\kappa} = \kappa + \mathcal{O}(r - r_H)$. We must also have the rotation parameter $\omega_{ab} = 0$, as l_a is hypersurface orthonormal. On the other hand, since Kerr BH is the solution of vacuum Einstein's field equations, we have $R_{ab} = 0$. Therefore, keeping only the leading order terms, i.e. $\mathcal{O}(r - r_H)$ terms in the right hand side of Eq. (6.28) one obtains

$$\frac{d\Theta}{d\mu} \simeq \kappa\Theta \,. \tag{6.31}$$

Hence the expansion parameter, in the near horizon regime, at the leading order behaves as

$$\Theta \simeq \kappa e^{\kappa\mu} \ . \tag{6.32}$$

So, the above expression suggests that in the near horizon the the geodesic congruence expand exponentially with increase of μ. This is the signature of the presence of instability in the geodesic motion of the particle in the vicinity of the Kerr horizon. As Θ is a scalar quantity and its nature has been extracted from a covariant equation, this above analysis provides a covariant description of our aforesaid local instability as long as particle trajectory is defined by (6.14).

We will now check whether this observation has any direct connection with our radial instability, given by (6.23). The expansion parameter Θ can be expressed in terms of l^a and $\tilde{\kappa}(r,\theta)$ as

$$\Theta = \nabla_a l^a - \tilde{\kappa} \ . \tag{6.33}$$

Now, let us take $\nabla_a l^a = M(r,\theta)$ and in the near horizon region we can expand $M(r,\theta)$ as $M(r,\theta) \simeq \kappa + M'(r_H,\theta)(r-r_H)$, where the prime denotes the derivative with respect to the radial coordinate (a detailed derivation is sketched in Appendix 6.D). Similarly, we can expand $\tilde{\kappa}(r)$ in the near horizon as $\tilde{\kappa}(r,\theta) \simeq \kappa + \tilde{\kappa}'(r_H,\theta)(r-r_H)$. Therefore, putting these values into Eq. (6.33) we obtain the value of expansion parameter in the near horizon region as

$$\Theta = S(r_H,\theta)(r-r_H) \tag{6.34}$$

where $S(r_H,\theta) = \left[M'(r_H,\theta) - \tilde{\kappa}'(r_H,\theta)\right]$ and $S(r_H,\theta) \neq 0$. Now, substituting this value of Θ (6.34) in the solution (6.32) yields $r - r_H \simeq (\kappa/S(r_H,\theta))e^{\kappa t}$. Therefore, the structure of Θ implies that there is instability in the radial motion of the particle which is similar to (6.23) and in this case it is reflected in the radial coordinate solution with the increment of t. With this analysis we conclude that although the local instability is not a coordinate dependent feature for these particular paths, but this specific nature of radial behaviour (6.23) is related to our chosen coordinate system.

6.5 The near horizon Hamiltonian

Let us now proceed to construct the Hamiltonian of the particle which leads to the above observed features in near horizon particle motion. This will be explicitly used later for

the semi-classical analysis of our system.

6.5.1 From the knowledge of trajectory

We have the near horizon radial motion which is given by (6.23). Use of the Hamilton's equation of motion $\dot{r} = \partial H/\partial p_r$ implies

$$\frac{\partial H}{\partial p_r} = \kappa(r - r_H) \,. \tag{6.35}$$

Solution of this is given by

$$H = \kappa(r - r_H)p_r + h_1(r, \theta, p_\theta, \phi, p_\phi) \,. \tag{6.36}$$

where $h_1(r, \theta, p_\theta, \phi, p_\phi)$ is some arbitrary function.

The polar equation of motion of the particle is given by Eq. (6.24). Therefore, use of Hamilton's equation of motion $\dot{\theta} = \partial H/\partial p_\theta$ implies

$$\frac{\partial H}{\partial p_\theta} = 0 \,, \tag{6.37}$$

and the solution of this is given by

$$H = h_2(r, p_r, \theta, \phi, p_\phi) \tag{6.38}$$

where $h_2(r, p_r, \theta, \phi, p_\phi)$ is again an arbitrary function.

The equation of motion along the azimuthal direction is given by Eq. (6.25). Therefore, using again the Hamilton's equation of motion $\dot{\phi} = \partial H/\partial p_\phi$ we obtain

$$\frac{\partial H}{\partial p_\phi} = \Omega_H \,, \tag{6.39}$$

and its solution is given by

$$H = \Omega_H p_\phi + h_3(r, p_r, \theta, p_\theta, \phi) \,, \tag{6.40}$$

where $h_3(r, p_r, \theta, p_\theta, \phi)$ is again some arbitrary function. Therefore, the Hamiltonian of the system becomes

$$H = \kappa(r - r_H)p_r + \Omega_H p_\phi + h(r, \theta, \phi) \,. \tag{6.41}$$

Now, the value of the arbitrary function $h(r)$ can be fixed by using the information that the corresponding Lagrangian must vanish as we are dealing with a massless particle. The Lagrangian for the above Hamiltonian comes out to be

$$L = \sum_i p_i \dot{q}^i - H = -h(r, \theta, \phi) \,. \tag{6.42}$$

Therefore, in order to make it vanish for the massless particle, we must choose $h(r,\theta,\phi) = 0$. Thus we obtain our desired Hamiltonian in the near horizon of the Kerr BH and it is given by

$$H = \kappa(r - r_H)p_r + \Omega_H p_\phi \ . \tag{6.43}$$

Interestingly in this case $H - \Omega_H p_\phi = \kappa(r - r_H)p_r$ has the form of xp, like the SSS black hole as we have seen in our earlier chapter 4, and this is valid only in the near horizon at the leading order in $x = r - r_H$. As the above Hamiltonian is related to the null vector (6.14), which has been constructed from the *outward* timelike and spacelike unit normals, it is related to the *outgoing* trajectory of our particle. Interesting observation is that xp type term is always related to the conserved quantity corresponding to global timelike Killing vector $\xi^a = \xi^a_{(t)} + \Omega_H \xi^a_{(\phi)}$ whose vanishing norm defines the location of the horizon. For instance here the conserved quantity is given by $K = -\xi^a p_a = E - \Omega_H p_\phi$ as $p_t = -E$. It may be noted that the solutions of the equations of motion (for radial trajectory only) corresponding to (6.43) are $r \sim e^{\kappa t}$ and $p_r \sim e^{-\kappa t}$. The near horizon limit is achieved by considering $t \to -\infty$ and interestingly in this limit p_r diverges. Therefore when the particle resides very near to the horizon its motion feels a local instability which reaffirms our earlier demand.

At the end, we aim to the possibility of thermalization of horizon through tunneling of particles through the horizon. In this case Hamiltonians for both outgoing and ingoing are essential. The approach, adopted so far, yields only the outgoing Hamiltonian. In the next section that for ingoing trajectory will be deduced using the dispersion relation among the four-momentum of the particle.

6.5.2 Using dispersion relation

Another way to find out our desired Hamiltonian is from the dispersion relation which relates the four-momentum of our particle. It not only gives the Hamiltonian structure of the outgoing particle but also provides the information about the ingoing one. We start with the Kerr metric written in (t,r,θ,ϕ) coordinates, i.e. Eq. (6.6). The metric (6.6) is clearly stationary and axisymmetric and hence there are two associated Killing vectors: $\xi^a_{(t)} = (1,0,0,0)$ and $\xi^a_{(\phi)} = (0,0,0,1)$. Therefore we have two corresponding conserved quantities for a particle motion: energy $E = -\xi^a_{(t)} p_a = -p_t$ and the angular momentum $L_z = \xi^a_{(\phi)} p_a = p_\phi$ along the rotational axis of the black hole, where p_a is the four momentum whose components are $p_a = (p_t, p_r, p_\theta, p_\phi)$. Now, using the covariant form of the dispersion relation $g^{ab} p_a p_b = 0$ for the massless particle, we obtain the equation of the

energy in terms of the radial and azimuthal components of momenta as

$$g^{tt}E^2 - 2g^{tr}Ep_r + 2g^{r\phi}p_r p_\phi + g^{rr}p_r^2 + g^{\phi\phi}p_\phi^2 = 0 \ , \tag{6.44}$$

where we have substituted $p_t = -E$ and since our particle has no motion along θ (see e.g. Eq. (6.14)) we have used $p_\theta = 0$. The above one yields two solutions of energy:

$$E = \frac{g^{tr}}{g^{tt}}p_r \pm \left[\left(\left(\frac{g^{tr}}{g^{tt}}\right)^2 - \frac{g^{rr}}{g^{tt}}\right)p_r^2 - 2\frac{g^{r\phi}}{g^{tt}}p_r p_\phi - \frac{g^{\phi\phi}}{g^{tt}}p_\phi^2\right]^{\frac{1}{2}} \ , \tag{6.45}$$

where the values of each g^{ab} components are given in Appendix 6.E. Among these two solutions one corresponds to the energy of the outgoing particle and the other solution corresponds to the ingoing one.

Let us now proceed to identify them. First investigate with the negative sign solution of Eq. (6.45). Note that the coefficient of p_r in the first term of Eq. (6.45) is always a negative quantity for the particle outside the horizon (see the values of g^{ab} components in the Appendix 6.E (check Eq. (6.E.2)) whereas the second term (the quantity with the square root) is a positive. On the other hand, since the energy E is positive, the radial momentum p_r is negative in this case. So, it suggests that the energy solution of Eq. (6.45) with the negative sign corresponds to the ingoing particle. Now, putting all the values of g^{ab} components in this solution of energy and considering only the leading order terms in the near horizon region we obtain the energy for the ingoing particle as

$$E = -R_H p_r - \Omega_H p_\phi + C_H \ , \tag{6.46}$$

where $R_H = 4mr_H/(\rho_H^2 + 2mr_H)$ and $\rho_H = \rho(r_H)$ and the value of C_H, which is unimportant for our present analysis, is given in the Appendix 6.E (see Eq. (6.E.4)). From the above expression it is again evident that p_r is negative and thereby confirming again that this energy is for ingoing particle.

Next, we shall investigate the other solution of Eq. (6.45), i.e. the energy value with the positive sign. As we have already obtained the energy solution with the negative sign corresponds to the ingoing particle, therefore consequently we can tell that the energy solution with the positive sign corresponds to the outgoing particle. However, in this case we want to affirm that this energy solution of the outgoing particle exactly matches with the energy solution which we obtained earlier (6.43) with the knowledge of the outgoing particle trajectory (6.19). From the positive energy solution of (6.45), using Hamilton's equation of motion we obtain the radial equation of motion of the outgoing particle which

is

$$\dot{r} = \frac{g^{tr}}{g^{tt}} + \frac{\left[\left(\left(\frac{g^{tr}}{g^{tt}}\right)^2 - \frac{g^{rr}}{g^{tt}}\right)p_r - \frac{g^{r\phi}}{g^{tt}}p_\phi\right]}{E - \frac{g^{tr}}{g^{tt}}p_r} \,. \tag{6.47}$$

Now for our already obtained outgoing radial path, given by (6.19), we want check whether the above yields the energy of the particle as (6.43). Expressing Eq. (6.19) in terms of the g^{ab} one finds (applying the fact $l^a l_a = 0$ and using the expression of l^a, i.e. Eq. (6.14))

$$\dot{r} = \frac{g^{tr}}{g^{tt}} + \sqrt{\left(\frac{g^{tr}}{g^{tt}}\right)^2 - \frac{g^{rr}}{g^{tt}}} \,. \tag{6.48}$$

Substituting the above expression in Eq. (6.47) and solving for E we obtain

$$E = \left[\frac{g^{tr}}{g^{tt}} + \sqrt{\left(\frac{g^{tr}}{g^{tt}}\right)^2 - \frac{g^{rr}}{g^{tt}}}\right]p_r - \frac{\frac{g^{r\phi}}{g^{tt}}}{\sqrt{\left(\frac{g^{tr}}{g^{tt}}\right)^2 - \frac{g^{rr}}{g^{tt}}}}p_\phi \,. \tag{6.49}$$

Now, using the expressions of every g^{ab} component in Eq. (6.49) and taking only the leading order term in the near horizon region we obtain the energy as (6.43). Therefore, we confirm here that the energy solution with positive sign of Eq. (6.49) corresponds to the energy of the outgoing particle.

6.6 Thermalization: Using semi-classical approach (Tunneling method)

We introduced the tunneling mechanism in our previous chapter 5 (see subsection 5.2.1). Through the tunneling approach we will now show that these Hamiltonians are responsible to feel the black hole horizon by the particle as thermal object. As we have already learnt that in this approach the main quantity to be calculated is the tunneling probability which is a ratio between the outgoing and ingoing probability of particle through the horizon (also see [54, 140, 172–175] for the details). We shall follow the same procedure of tunneling mechanism which we have done in our previous chapter 5. We start with the standard ansatz for the wave function for a particle as

$$\Psi(q^\mu) = \exp\left[-\frac{i}{\hbar}S(q^\mu)\right] \,, \tag{6.50}$$

where $S(q^\mu)$ is the Hamilton-Jacobi action for the particle which is defined as an integration of the momentum components p^μ of the particle with respect to the position

coordinates q^μ:

$$S(q^\mu) = \int p_\mu dq^\mu \ . \tag{6.51}$$

Now, applying $\hat{p}_\mu \equiv -i\hbar\partial/\partial q^\mu$ on the wave function we have the outgoing and ingoing trajectories which correspond to $\partial S/\partial q^\mu < 0$ and $\partial S/\partial q^\mu > 0$, respectively. Here we are interested to calculate the emission probability of the outgoing particle while the absorption probability of the ingoing one. The ratio of them will give our required tunneling probability.

Following the same procedure as we have done in chapter 5 (see 5.2.1), first we calculate the emission action of the outgoing particle which comes out to be

$$S[\text{Emission}] = \left(\frac{E - \Omega_H p_\phi}{\kappa}\right)(-i\pi) + \text{Real part} \ . \tag{6.52}$$

Note that for the above one $\partial S/\partial x = (E - \Omega_H p_\phi)/(\kappa x)$ and as inside the horizon $x < 0$, we have $\partial S/\partial x < 0$. Therefore satisfies the outgoing trajectory condition as stated below Eq. (6.51). The “absorption" action for the ingoing particle can be calculated from radial momentum given by (6.46). Since it does not contain any singularity at $x = 0$, one obtains $S[\text{Absorption}] = \text{Real quantity}$. Since for the tunneling probability, the explicit form of the above one is not necessary as long as the final value is real, we do not bother about its actual expression. Therefore, the probability of emission turns out to be

$$P[\text{Emission}] \propto \exp\left[-\frac{2\pi(E - \Omega_H p_\phi)}{\hbar\kappa}\right] , \tag{6.53}$$

whereas the probability of absorption is $P[\text{Absorption}] \sim 1$. Hence the tunneling probability is evaluated as

$$\Gamma = \frac{P[\text{Emission}]}{P[\text{Absorption}]} \sim \exp\left[-\frac{2\pi(E - \Omega_H p_\phi)}{\hbar\kappa}\right] . \tag{6.54}$$

Hence use of the usual argument yields the expression for temperature as

$$T = \frac{\hbar\kappa}{2\pi} \ , \tag{6.55}$$

which is the well known Hawking expression [68, 113] for black hole horizon temperature.

Here we saw that the emission probability, calculated from the Hamiltonian (6.43), is the main for showing the thermality of the horizon. We know that this Hamiltonian, in the locality of the horizon, yields an instability in the radial motion of the particle. This is in favour of our earlier conjecture as we have seen in our previous chapters (chapter

4 and chapter 5), even for more general like an axisymmetric black hole, that horizon creates a local instability in its vicinity which is responsible for its own thermalization as felt by our massless particle.

In the present context, we have shown the appearance of the horizon thermality in the tunneling approach only. There are other approaches where a direct quantum analysis of xp Hamiltonian has been done, and that too led to the thermalization of the horizon, which we already have discussed in our previous chapter 5. Also, in literature, it has been mentioned that xp Hamiltonian (or its inverse harmonic oscillator form) inherently captures thermal character at the quantum level (e.g. see [232–235]). Since this Hamiltonian captures instability as well as thermal property and appeared here due to the presence of the horizon (which are being rigorously shown here), it is then clear that this near horizon instability may be liable for horizon thermalization.

Let us now discuss the reason for proposing such a statement in this context elaborately. In the present scenario, we constructed a model where a probed massless and chargeless particle resides in the near-horizon region of a Kerr BH. The specific Hamiltonian for the outgoing particle we obtain in this case is of xp kind in addition with some rotation part (see Eq. (6.43)). We observed that such a Hamiltonian provides a particle non-zero quantum probability of crossing the horizon. This is the main finding in this analysis to infer that the horizon has a temperature. Now, the noticeable fact about this Hamiltonian is that it can be cast to that of an inverted harmonic oscillator (IHO) in a new set of canonical variables (please see the previous chapter 5 and also see [273]). Furthermore, the IHO potential is unstable in nature. Therefore the test particle here experiences a "local instability" due to the presence of a horizon. This can be realised through the near horizon equations of motion as well. As discussed below Eq. (6.23), the radial momentum diverges as the particle resides in the near-horizon region; i.e. $p_r \to \infty$ as $t \to -\infty$. Also note that p_r diverges at the horizon for a given value of the conserved quantity $H - \Omega p_\phi$ (see Eq. (6.43)). Due to this particular instability at $r = r_H$, we found that the outgoing particle, at the quantum level, tunnels through a complex path. Therefore such singularity, on the one hand, provides instability in the particle motion and, on the other hand, plays a pivotal role in the calculation of the tunneling probability (6.54). We obtain a finite amount of tunneling probability of the particle for crossing the horizon with the correct classical limit (outgoing probability vanishes at $\hbar \to 0$). Moreover, such exponential behaviour of the expression is solely due to xp structure of the Hamiltonian. In general, the time-reversal invariance dictates that the emission probability at a certain time is equal to the absorption probability for

the same time and vice versa. Whereas our result in the present context is not consistent with this. It appears that the probability of emitting out of the particle through the horizon at a certain time is not equal to the probability of absorption into the horizon, resulting in an imbalance in the particle number between the outside and inside the region of the horizon. Furthermore, the exponential nature of the tunneling probability exhibits that the system is thermal in nature. The sole reason for thermality to show up in this calculation is due to the presence of this peculiar singularity at the horizon ($r = r_H$), which originates due to the xp structure of the conserved quantity in the near horizon region. Therefore, it leads us to propose the conjecture that the near horizon local instability shows its presence at the quantum level through the horizon temperature, thereby perceiving the black hole as a thermal object.

6.7 Summary and Discussions

For the past few decades, physicists have been looking for a unified explanation to understand the underlying reason why the horizon is associated with temperature. In this scenario, our present analysis have shown that the possible answer may be hiding behind the classical instability in the near horizon region and its intimate bond with its quantum consequences.

However, in our earlier chapters (chapter 4 and chapter 5), this conjecture has been proposed by investigating only SSS BH scenario. Therefore, in order to attest to the validity of our conjecture, we needed to test it for a more generic class of black holes. Kerr black hole is one of the prime examples of that which is much more realistic than the SSS BH, and have astrophysical relevance. All known stars rotate, and realistic collisions have non-zero angular momentum, therefore, the black holes formed due to the collapse or collision of stars or compact objects are expected to be the rotating ones in nature. Hence, the foremost aim of this work was to test the robustness of the conjecture in a much more realistic picture in order to explain the horizon thermalization.

Like our earlier chapters (chapter 4 and chapter 5), the main focus, in this chapter, was to inspect whether the presence of local instability in the near horizon region is responsible for providing the temperature for a particular set of observer but this time in Kerr spacetime. We finally found that this is indeed the case. Although near horizon instability is an observer independent phenomenon for our chosen null path, the specific feature of the radial motion of the outgoing particle is a coordinate dependent event. The radial contribution in corresponding Hamiltonian of the system comes out to be of xp kind, which is indeed an unstable Hamiltonian. This is where the classical part of the calculation ends. In the quantum regime, using the tunneling approach we obtain that thermality emerges due to that instability and the temperature exactly matches with the Hawking temperature. Therefore, it turns out that the extension of our proposed conjecture is applicable to much more generic black holes also. Hence, the generality of this conjecture is evident here, and thereby providing a prospective to become one of the leading candidates to understand the underlying mystery of the horizon thermalization in the context of black holes. However, whether the generalisation of this proposed conjecture may extend to any generic arbitrary background or not, is one of the interesting questions in this context. We shall aim to find out that particular answer in our next chapter.

Appendix

6.A ADM Decomposition of the Metric

Parametrisation of the space-time adapted to a given choice of the space-time by (constant time) hypersurfaces is done by ADM decomposition [2]. We first assume that the spatial hypersurfaces of this foliation of the space-time are hypersurfaces of constant time (say $t = t_0$) and they are sets of some time function $t(x^a)$,

$$\Sigma_{t_0} = \{x^a : t(x^a) = t_0\}, \tag{6.A.1}$$

with timelike normal vector n^a, $n_a \sim \partial_a t$. We can now introduce coordinates (t, y^i) (where i stands for only space coordinates) on the space-time through a coordinate transformation

$$x^a = x^a(t, y^i) \tag{6.A.2}$$

in the following way:

- Here we specify that for any fixed value of $t = t_0$,

$$x^a_{t_0}(y^i) = x^a(t_0, y^i) \tag{6.A.3}$$

  gives us the embedding of a hypersurface Σ (with coordinates y^i) as the hypersurface Σ_{t_0} in space-time manifold (M),

$$x_{t_0} \; : \; \Sigma \to \Sigma_{t_0} \subset M \; . \tag{6.A.4}$$

- The curves

$$x^a_{y_0}(t) = x^a(t, y^i_0) \tag{6.A.5}$$

  then connect points on different hypersurfaces with the same values of the spatial coordinates $y^i = y^i_0$ and thus provide us with the notion of time evolution from one hypersurface to the next one.

Now, for given $x^a = x^a(t, y^i)$ for some choice of foliation and time-evolution,

$$E^a_i = \left(\frac{\partial x^a}{\partial y^i}\right)_t \tag{6.A.6}$$

[2] For detailed analysis please see [309]

gives us the tangent vectors to the surface Σ_t whereas

$$(\partial_t)^a = \left(\frac{\partial x^a}{\partial t}\right)_y \tag{6.A.7}$$

gives us the components of the time-evolution vector field ∂_t. The curves (6.A.5) may not be normal to the hypersurface. Therefore, in general, ∂_t can be decomposed into a normal and tangential part as

$$(\partial_t)^a = Nn^a + E^a_i \beta^i \ . \tag{6.A.8}$$

The function N and the spatial vector field β^i appeared in the expression are known as the lapse function and the shift vector field respectively. These functions and the vector fields basically parametrise the freedom in the choice of the time-evolution vector. Therefore, we have

$$\begin{aligned} dx^a &= (Nn^a + E^a_i\beta^i)dt + E^a_i dy^i \\ &= Nn^a dt + E^a_i(dy^i + \beta^i dt) \ . \end{aligned} \tag{6.A.9}$$

Plugging this into the line element for the space-time metric and using $g_{ab}n^a n^b = -1$, one obtains

$$ds^2 = g_{ab}dx^a dx^b = -N^2dt^2 + h_{ij}(dy^i + \beta^i dt)(dy^j + \beta^j dt) \ , \tag{6.A.10}$$

where

$$h_{ij} = g_{ab}E^a_i E^b_j \tag{6.A.11}$$

is the induced metric. This is called the ADM decomposition of the metric.

6.B The value of $F'(r=r_H,\theta)$

In Eq. (6.19) we have

$$F(r,\theta) = \frac{\sqrt{A} - 2mr}{\rho^2 + 2mr} \ . \tag{6.B.1}$$

Now, taking the partial derivative of $F(r,\theta)$ at $r = r_H$ we have

$$\begin{aligned} F'(r=r_H,\theta) &= \left[\frac{\frac{\partial}{\partial r}(\sqrt{A}) - 2m}{\rho^2 + 2mr} - \frac{(\sqrt{A} - 2mr)\frac{\partial}{\partial r}(\rho^2 + 2mr)}{(\rho + 2mr)^2}\right]_{r=r_H} \\ &= \frac{\left[\frac{\partial}{\partial r}(\sqrt{A}) - 2m\right]_{r=r_H}}{\rho_H^2 + 2mr_H} \end{aligned} \tag{6.B.2}$$

where $\rho_H^2 = r_H^2 + 2mr_H$ and at $r = r_H$ we have $\sqrt{A} = 2mr_H$ (see 6.15). Now, from the above equation (Eq. (6.B.2)) we have

$$\begin{aligned}
F'(r=r_H,\theta) &= \frac{\frac{1}{4mr_H}[2r(r^2+a^2)+2r\rho^2+2a^2m\sin^2\theta]_{r=r_H}-2m}{\rho_H^2+2mr_H} \\
&= \frac{\frac{1}{4mr_H}[2r_H(r_H^2+a^2)+2r_H\rho_H^2+2a^2m\sin^2\theta]-2m}{\rho_H^2+2mr_H} \\
&= \frac{\frac{1}{4mr_H}[2r_H(2mr_H)+2r_H\rho_H^2+2a^2m\sin^2\theta]-2m}{\rho_H^2+2mr_H} \\
&= \frac{\frac{1}{4mr_H}[2r_H(\rho_H^2+2mr_H)+2a^2m\sin^2\theta]-2m}{\rho_H^2+2mr_H} \\
&= \frac{1}{2m}+\frac{\frac{a^2}{2r_H}\sin^2\theta-2m}{\rho_H^2+2mr_H} \\
&= \frac{1}{2m}+\frac{a^2\sin^2\theta-4mr_H}{2r_H(\rho_H^2+2mr_H)} \\
&= \frac{1}{2m}+\frac{a^2\sin^2\theta-r_H^2-a^2-2mr_H}{2r_H(\rho_H^2+2mr_H)} \\
&= \frac{1}{2m}-\frac{r_H^2+a^2\cos^2\theta+2mr_H}{2r_H(\rho_H^2+2mr_H)} \\
&= \frac{1}{2m}-\frac{\rho_H^2+2mr_H}{2r_H(\rho_H^2+2mr_H)} \\
&= \frac{1}{2m}-\frac{1}{2r_H} \\
&= \frac{1}{2}\left[\frac{1}{m}-\frac{1}{r_H}\right]. \qquad \text{(6.B.3)}
\end{aligned}$$

Now, putting the value of r_H (Eq. (6.3)) in the above equation we obtain $F'(r_H,\theta) = \kappa$ (6.21).

6.C Calculation of the expansion parameter (Θ) on the horizon

We have already defined the expansion parameter (Θ) of the congruence of geodesics in chapter 4 (see 4.24) which is expressed in terms of l^a and $\tilde{\kappa}$ as

$$\begin{aligned}\Theta &= \nabla_a l^a - \tilde{\kappa} \\ &= \frac{1}{\sqrt{-g}}\partial_a(\sqrt{-g}\,l^a) - \tilde{\kappa} \\ &= \frac{1}{\sqrt{-g}}\partial_r(\sqrt{-g}\,l^r) - \tilde{\kappa} \\ &= \frac{1}{\sqrt{-g}}F(r,\theta)(\partial_r\sqrt{-g}) + F'(r,\theta) - \tilde{\kappa}\ . \end{aligned} \tag{6.C.1}$$

Now, at $r = r_H$ we obtain

$$\Theta|_{r=r_H} = \frac{1}{\sqrt{-g}}F(r_H,\theta)(\partial_r\sqrt{-g}) + F'(r_H,\theta) - \kappa\ . \tag{6.C.2}$$

As we already have $F(r_H,\theta) = 0$ and $F'(r_H,\theta) = \kappa$. Therefore, on the horizon ($r = r_H$) the expansion parameter (Θ) turns out to be

$$\Theta|_{r=r_H} = 0\ . \tag{6.C.3}$$

6.D Calculation of $\nabla_a l^a = M(r,\theta)$ in the near horizon region

The null vector is given by (6.14) along which our test particle is moving. Now, expanding $M(r,\theta)$ we find

$$M(r,\theta) = \nabla_a l^a = \frac{1}{\sqrt{-g}}\partial_r\left(\sqrt{-g}\ l^r\right)\ . \tag{6.D.1}$$

Putting the value of l^r and g in the above equation and performing the partial derivative with respect to r we obtain

$$M(r,\theta) = \partial_r F(r,\theta) + \frac{2r}{\rho^2}F(r,\theta)\ , \tag{6.D.2}$$

where $F(r,\theta)$ is already defined earlier, i.e. $F(r,\theta) = (\sqrt{A} - 2mr)/(\rho^2 + 2mr)$ and $F(r_H,\theta) = 0$. Now, using the Taylor series expansion of the function $M(r,\theta)$ in the near horizon region and considering only the leading order terms we obtain

$$M(r,\theta) \simeq M(r_H,\theta) + M'(r_H,\theta)(r - r_H)\ , \tag{6.D.3}$$

where $M(r_H,\theta)=\kappa$ and $M'(r_H,\theta)=\left(\partial_r^2 F(r,\theta)\right)_{r=r_H}+\frac{2r_H}{\rho_H^2}\kappa$ with

$$\begin{aligned}\left(\partial_r^2 F(r,\theta)\right)_{r=r_H} &= \frac{1}{2(\rho_H^2+2mr_H)}\Bigg[\frac{1}{2mr_H}\left(12r_H^2+4a^2-2a^2\sin^2\theta\right)- \\ &\frac{1}{16m^3r_H^3}\left(4r_H(r_H^2+a^2)-2(r_H-m)a\sin^2\theta\right)-\frac{4\kappa(r_H+m)}{\rho_H^2+2mr_H}\Bigg]\,.\end{aligned} \tag{6.D.4}$$

6.E Inverse of metric (6.6) and the value of C_H in Eq. (6.46)

Our massless and chargeless test particle is moving under the background of the metric given by (6.6). Now the determinant of the metric components (6.6) takes a very simple form

$$g=\det(g_{ab})=-\rho^4\sin^2\theta\,, \tag{6.E.1}$$

and the inverse metric takes the form

$$g^{ab}=\begin{pmatrix}-\left(1+\frac{2mr}{\rho^2}\right) & \frac{2mr}{\rho^2} & 0 & 0\\ \frac{2mr}{\rho^2} & \frac{r^2+a^2-2mr}{\rho^2} & 0 & \frac{a}{\rho^2}\\ 0 & 0 & \frac{1}{\rho^2} & 0\\ 0 & \frac{a}{\rho^2} & 0 & \frac{1}{\rho^2\sin^2\theta}\end{pmatrix}. \tag{6.E.2}$$

Now, let us denote $X^2(r,\theta)=\left(\frac{g^{tr}}{g^{tt}}\right)^2-\frac{g^{rr}}{g^{tt}}$, $Y(r,\theta)=\frac{g^{r\phi}}{g^{tt}}$ and $Z(r,\theta)=\frac{g^{\phi\phi}}{g^{tt}}$. Therefore, in terms of these, the energy solution with the negative sign of Eq. (6.45) can be written as

$$\begin{aligned}E &= \frac{g^{tr}}{g^{tt}}p_r-\left[X^2(r,\theta)p_r^2-2Y(r,\theta)p_rp_\phi-Z(r,\theta)p_\phi^2\right]^{\frac{1}{2}} \\ &= \frac{g^{tr}}{g^{tt}}p_r-\left(X(r,\theta)p_r-\frac{Y(r,\theta)}{X(r,\theta)}p_\phi\right)\left[1-\frac{\left(\frac{Y^2(r,\theta)}{X^2(r,\theta)}+Z(r,\theta)\right)p_\phi^2}{\left(X(r,\theta)p_r-\frac{Y(r,\theta)}{X(r,\theta)}p_\phi\right)^2}\right]^{\frac{1}{2}}\,.\end{aligned} \tag{6.E.3}$$

Now, performing the Binomial series expansion of the term under the square root of the above equation we obtain

$$E = \left(\frac{g^{tr}}{g^{tt}} - X(r,\theta)\right)p_r + \frac{Y(r,\theta)}{X(r,\theta)}p_\phi + \underbrace{\left(X(r,\theta)p_r - \frac{Y(r,\theta)}{X(r,\theta)}p_\phi\right)\left[\frac{1}{2}\frac{\left(\frac{Y^2(r,\theta)}{X^2(r,\theta)} + Z(r,\theta)\right)p_\phi^2}{\left(X(r,\theta)p_r - \frac{Y(r,\theta)}{X(r,\theta)}p_\phi\right)^2} + \frac{1}{8}\frac{\left(\frac{Y^2(r,\theta)}{X^2(r,\theta)} + Z(r,\theta)\right)^2 p_\phi^4}{\left(X(r,\theta)p_r - \frac{Y(r,\theta)}{X(r,\theta)}p_\phi\right)^4} + \ldots\right]}_{C(r,\theta)} . \tag{6.E.4}$$

Therefore, considering only the leading order terms in the near horizon region and putting all the values of g^{ab} components we land up to Eq. (6.46) where $C_H = C(r = r_H, \theta)$.

CHAPTER 7

THERMAL NATURE OF A GENERIC NULL SURFACE

7.1 Introduction and motivation

The present chapter will be the eventual part before the conclusion of this thesis, where we shall discuss all of our formalism set up so far in our earlier chapters for a generic background. But, before that, let us set up the backbone of motivation for the present chapter. We have already learned that the close relationship between gravitational dynamics of the black hole horizon and classical thermodynamics uncovered the fact that black holes possess thermodynamic attributes like entropy [114, 218] and temperature [68, 113, 278]. Hawking had shown [68, 113] that the radiating photons are thermal in nature, and the temperature for the corresponding radiating particles was predicted as $T = \hbar\kappa/2\pi$, where κ is the surface gravity of the black hole. Another phenomenon, parallel to Hawking effect, has been predicted theoretically, known as Unruh effect [209]. Such effect can be observed in any local arbitrary gravitational background. To make this perception clearer, we start with the *principle of equivalence* which allows one to construct a local inertial frame around any event in an arbitrary curved spacetime. Given the local inertial frame, one can construct a local Rindler frame, and the observer at rest in the local Rindler frame will perceive a patch of null surface as horizon with a temperature. This result allows us to associate thermodynamical attributions with the null surfaces, which the local Rindler observers perceive as horizons. Such a notable fact leads one to introduce observer-dependent thermodynamic variables [310–313] around any event in spacetime and reinterpret the gravitational field equations

near any null surface in the language of thermodynamics [314] or vis versa [315]. The equality between the field equations on the horizon and the thermodynamic identity has been exhibited for a wide class of models like the cases of stationary axisymmetric horizons and evolving spherically symmetric horizons in Einstein gravity [316], static spherically symmetric horizons [317]. In the Lanczos-Lovelock gravity sector, it has been studied for dynamical apparent horizons [318] and for generic static horizon [319]. Also, in [320], the thermodynamic identity, particularly the Clausius relation, has been established on the Local Causal Horizons using Einstein equation.

Incidentally, one can provide a thermodynamical interpretation of a gravitational field equation either by suitably projecting it on a generic null surface [321–324] or using the diffeomorphism invariance in the near null hypersurface region [325–327]. For instance, Einstein's equation, contracted with null generator and corresponding auxiliary vector, yields a thermodynamical identity of the form $\int_{S_t} d^2x T\delta_{\lambda(k)}s = \delta_{\lambda(k)}E + F\delta\lambda_{(k)}$ [321–324], where symbols have their usual meanings and the variation can be interpreted as the change due to virtual displacement of the null surface along an auxiliary null vector (k), parametrized by the parameter λ (generalization to Lanczos-Lovelock gravity [328] and scalar-tensor theory [329] has been done as well). Therefore, it has been realized that null surfaces which act as one-way membranes to a certain class of observers also possess thermodynamical attributions. This indispensable relation between gravity and thermodynamics led to the idea that *the dynamics of gravity is not fundamental in nature; rather it has emerged from the dynamics of a more fundamental theory*, just like the laws of thermodynamics of a system emerges out from the statistical dynamics of its molecules (see [49] for more details on the concept and aspects of emergent nature of gravity).

However, all these thermodynamical attributions associated with the generic null hypersurface are standing on the platform of complete analogy between the laws of thermodynamics and the structure of the gravitational field equation on the surface. Therefore it is mandatory to provide a clear physical justification in order to call a geometrical quantity on the null surface as a particular thermodynamical entity. To make the concern clear, we point out that Hawking's calculation [68, 113] on the emission spectrum from the black hole horizon clearly indicates the concept of the temperature of the horizon. Similarly, Unruh effect [209] points out the appearance of temperature on the local Rindler horizon. The lack of such robust justification in the case of generic null surface does not give us complete confidence in assigning temperature or entropy on the surface. In the present chapter, our particular aim is to find out the appearance of

temperature without stating any analogical point of view.

It is known that the thermodynamics of a system arises from the underlying statistical theory of microstates. However, in the case of spacetime, which microscopic degrees of freedom is responsible for the emergence of temperature into the system in the presence of the horizon is not known properly. Therefore, the hunt for finding out a concrete explanation for such a feature is still under progress. The general consciousness is - to illuminate the underlying microstructure, it is mandatory to understand the physical mechanism for thermalization of the horizon. In pursuit of achieving to find a unified reason for the origin of horizon thermodynamics, we have already found in the previous chapters (chapter 5 and chapter 6) that the thermal nature of the horizon has some connection with instability in the near-horizon region. In this connection some other works are worth mentioning [231, 232, 304]. At first glance, these two characteristics may seem to be different to each other, but their unification may become a strong candidate to answer the long-standing question about the origination of horizon thermodynamics. It has been shown through considering a model that in the presence of static spherically symmetric (SSS) black hole (chapter 4 and chapter 5) or in case of a Kerr black hole (chapter 6), an outgoing massless and chargeless particle experiences instability in the near-horizon region. In those calculations, it was found that a class of observers see a particle following an outgoing null path, is driven by a Hamiltonian of xp kind for its near horizon motion (chapter 4 and chapter 6). It may be noted that such a Hamiltonian is unstable in nature. Moreover, in the quantum scale, this unstable Hamiltonian provides the temperature into the system, which exactly matches with Hawking's expression. This noticeable fact leads to a conjecture – "*the local instability in the vicinity region of the horizon acts as the source of the temperature of the system*". The noticeable feature of the model is it requires mainly the information of a suitable near horizon null path of the particle, which does not crucially consider the underlying symmetry of the spacetime, like the presence of a timelike Killing vector. Therefore, keeping the above feature in mind, we want to extend the spirit of the aforesaid model in the case of any generic null surface.

7.2 A small introduction to Null Hypersurfaces in GNC coordinates

This chapter intends to investigate the possible thermodynamics properties of an arbitrary null surface. Therefore, our first objective is to describe the neighbourhood region of that null-hypersurface. A preferable choice of coordinate system exists to narrate in this context, known as Gaussian null coordinates (GNC), in analogy with Gaussian normal coordinates. Usually, the Gaussian normal coordinates are constructed by extending the coordinates on a non-null hypersurface to a spacetime neighbourhood using geodesics normal to the surface. However, this construction does not apply to a null surface because the normal geodesics lie itself on it. Therefore, an uniquely defined auxiliary null geodesics are introduced with some certain conditions in order to construct the Gaussian null coordinates, which we shall discuss in the latter part of this section. An elaborate description and detailed discussion on the construction of this coordinate system and how metric is constructed in this coordinate system can be found in [330–333]. Here, in order to keep the clarity of our work, we shall briefly describe some precursory construction of this coordinate system in a more intuitive way.

The primary objective is to construct a coordinate system around any null surface in any spacetime. Consider a smooth null surface N in a four-dimensional spacetime manifold M, where g_{ab} represents the metric on M. We start with a spacelike 2-surface ζ, on N and the coordinates on ζ are introduced as (x^A) for $A = 1,2$, i.e. (x^1, x^2). Now, in order to construct the null surface N using null geodesics, one cannot have these null geodesics lying on the spacelike surface as any vector lies on the spacelike surface has to be spacelike in nature. Therefore, the next coordinate parameter should be introduced in such a way that one must move away from this spacelike surface along any of these null geodesics. Here, we introduce that particular parameter v, not necessarily affine, along the null geodesics increasing in the future direction with the condition $v = 0$ on ζ. Therefore, any point on N in the neighbourhood of ζ can be labelled by the coordinates (v, x^1, x^2), where (x^1, x^2) corresponds to the label given to the null geodesic passing through that point and v is the chosen parameter at that point. The "neighbourhood" corresponds to that sufficiently small region where the geodesics do not cross each other or do not form any caustics. Let us call the future directed vector field tangent to the null geodesics, $\partial/\partial v$, as $\mathbf{l}$. Now, our spacetime is four-dimensional, so it is time for us to introduce the fourth coordinate. With the help of a new set of null geodesics, we can construct the coordinate chart in the surroundings of the null-hypersurface. Introducing

a unique null vector k^a which is situated at each point on the null surface and satisfying these conditions (i) $k^a k_a = 0$, as it is a null vector; (ii) $l^a k_a = -1$ which suggests that k^a sticks out from each point of the null surface instead of lying on the surface; and (iii) $X^a_A k_a = 0$ where $X_A = \partial/\partial x^A$ are the basis vectors correspond to the coordinates (x^1, x^2). The choice of the third condition shows that our auxiliary null vector is uniquely defined. As this vector k^a points out off the null surface, it can be used to go off the null surface. The null geodesics emitted from each point on the null surface in the direction of k^a are labelled by the coordinates (v, x^1, x^2), of that point. We choose a parameter r along this null geodesic and $r = 0$ (we choose again) represents the null surface and $\mathbf{k} = -\partial/\partial r$. Therefore, the chosen affine parameter r can be assigned in the coordinate chart (v, r, x^1, x^2) in the neighbourhood of the null hypersurface means up to the regions where geodesics do not reach a caustic.

After introducing this coordinate system, we shall introduce the metric adapted to this coordinate system in the neighbourhood region of any arbitrary null hypersurface. The construction of this metric has been detailed in [331, 332]. However, we shall recall here some of the essential properties of this metric. The line element adapted in this context takes the following form

$$ds^2 = -2r\alpha dv^2 + 2dvdr - 2r\beta_A dv dx^A + \mu_{AB} dx^A dx^B \ . \tag{7.1}$$

Now, one can see from (7.1) that there are two null surfaces which are at $r = 0$ and at $v =$ constant. Additionally, $r =$ constant where the constant is non-zero represents the time-like surfaces. Besides, the metric components α, β_A and μ_{AB} are the smooth functions of all the coordinates and μ_{AB} is the transverse $(D-2)$-dimensional Riemannian metric on the spacelike surface ζ. We have here a set of null vectors as we mentioned earlier $l^a = (l^v, l^r, l^{x^A}) = (1, 0, \mathbf{0})$ and the unique auxiliary one, i.e. $k^a = (0, -1, \mathbf{0})$. Among these two we can think of l^a as the future-outgoing null vector and k^a as the future-ingoing null vector. The covariant components of these two vectors are $l_a = (-2r\alpha, 1, -r\beta_A)$ and $k_a = (-1, 0, \mathbf{0})$. Therefore, the normal $l_a = \partial_a r$ to the $r = 0$ surface will be a null vector. Moreover this generates the $r = 0$ null surface around which we will do our all analysis.

In order to strengthen the motivation for choosing our desired null hypersurface at $r = 0$, let us first write the static spherically symmetric (SSS) metric in analogous to the GNC form [322]

$$ds^2 = -f(r)dv^2 + 2dvdr + \mu_{AB} dx^A dx^B \ . \tag{7.2}$$

One can see $\beta_A = 0$ in this case comparing it with Eq. (7.1). Now, in the near horizon region we have $f(r) \simeq 2\kappa(r - r_H)$ where $\kappa = f'(r_H)/2$ where the prime denotes the derivative

with respective to r. Therefore, comparing (7.2) with Eq. (7.1) we obtain $\alpha \equiv \kappa$ and the position of the horizon $r = r_H$ is equivalent to the position of the null surface at $r = 0$ in case of GNC metric (7.1). Therefore, in this context the null surface at $r = 0$ is reminiscent to the black hole horizon. In our earlier chapters (chapter 4 and chapter 6) we studied the particle dynamics near the horizon and obtained that particle trajectory becomes unstable near it. Following that essence our objective in this work is to extend this idea in case of any generic null hypersurface and thereby we particularly choose the null surface which is at $r = 0$. The null normal l_a which is at $r = 0$ is given by $l_a = (0, 1, \mathbf{0})$ is the generator of the null surface providing $l^a l_a = 0$ at $r = 0$. Therefore, for our examination in the near null hypersurface region we shall consider the limit $r \to 0$ whenever necessary.

In the present context, our prime aim is to explain how temperature is physically associated with any generic null hypersurface. In order to do so, the first objective is to find out the emission probability of a particle through the null hypersurface. So, we adopt the familiar technique tunneling method [54, 140, 173–175] which we have already introduced in the previous chapters (chapter 5 and chapter 6) (see the section 5.2.1 of chapter 5). We have already known that this formalism predicts the probability of escaping the particle through the null hypersurface. Therefore, to evaluate the tunneling probability first, we need to find out the paths of the particle for both ingoing and outgoing cases. Hence, we acquire the Hamiltonian-Jacobi (HJ) formalism in this case, just like our earlier chapters (chapter 5 and chapter 6), in order to find out the Hamiltonian in the near null hypersurface region for both ingoing and the outgoing cases.

7.3 Hamiltonian: field description

Considering the massless real scalar field ϕ, from the Klein-Gordon (KG) equation $\Box\phi = 0$ under the background of metric (7.1) yields

$$\partial_v\left(\sqrt{\mu}\partial_r\phi\right) + \partial_r\left(\sqrt{\mu}\partial_v\phi\right) + \partial_r\left[\sqrt{\mu}\left(2r\alpha + r^2\beta^2\right)\partial_r\phi\right] + \partial_r\left(\sqrt{\mu}\, r\beta^A\partial_A\phi\right) + \partial_A\left(\sqrt{\mu}\, r\beta^A\partial_r\phi\right) + \partial_A\left(\sqrt{\mu}\,\mu^{AB}\partial_B\phi\right) = 0 \,, \tag{7.3}$$

where μ is the determinant of the induced metric μ_{AB}. Now, we start with the standard ansatz for the scalar field of a particle as (see also [140])

$$\phi = \mathscr{A}(v, r, x^A)e^{-\frac{i}{\hbar}S(v,r,x^A)} \,, \tag{7.4}$$

where $S(v, r, x^A)$ is the HJ action and with respect to the HJ action we define the four-momentum as

$$\frac{\partial S}{\partial x^a} = p_a \,. \tag{7.5}$$

Now, expanding $S(v,r,x^A)$ in the powers of $\hbar$ we find,

$$\begin{aligned} S(v,r,x^A) &= S_0(v,r,x^A)+\hbar S_1(v,r,x^A)+\hbar^2 S_2(v,r,x^A)+.... \\ &= S_0(v,r,x^A)+\sum_i \hbar^i S_i(v,r,x^A)\,, \end{aligned} \tag{7.6}$$

where $i = 1,2,3,....$ The terms from $\mathcal{O}(\hbar)$ onward are treated as the quantum corrections over the semi-classical value S_0. However, our analysis is restricted only upto the semi-classical limit, i.e. $\hbar \to 0$. Therefore, the higher order terms of $\hbar$ can be neglected in the semi-classical limit. At this point, we define $-\partial S_0/\partial v = -p_v = H$, where H is the (semi-classical) Hamiltonian of the system.

Now, the main interest lies in the near $r \to 0$ region because that is where the dynamics of our massless scalar modes will be studied. The probability of crossing the mode across the null surface will be our main quantity to find out. As we have stated earlier that to study such quantity in this region one of the well-known techniques is tunneling formalism. The principal way of implementing the tunneling formalism is the HJ method [140]. In order to apply this idea, we need to identify the ingoing and the outgoing modes near the null hypersurface region. The outgoing mode is moving from $r < 0$ region (call as "*inside*") to $r > 0$ region (call as "*outside*") and vice versa for the ingoing one. Now, applying $\hat{p} \equiv -i\hbar\partial/\partial r$ on (7.4) we shall have the momentum eigenvalue as $-\partial S_0/\partial r$ in the semi-classical limit. For the outgoing case we have the positive momentum eigenvalue, which means one must have $\partial S_0/\partial r < 0$. Similarly, for the ingoing case, we have the negative momentum eigenvalue, i.e. $\partial S_0/\partial r > 0$. After this identification, we need to calculate the HJ actions for both outgoing and the ingoing modes and implement these expressions to calculate the tunneling probability to cross the null hypersurface.

In the semi-classical limit (i.e. $\hbar \to 0$), keeping only the leading order terms, we obtain the following form of the Eq. (7.3):

$$2(\partial_v S_0)(\partial_r S_0)+(2r\alpha+r^2\beta^2)(\partial_r S_0)^2+2r\beta^A(\partial_A S_0)(\partial_r S_0)+\mu^{AB}(\partial_B S_0)(\partial_A S_0)=0\,. \tag{7.7}$$

Here we see from Eq. (7.7) that $\partial_r S_0$ has two solutions which are

$$\partial_r S_0 = -\frac{\partial_v S_0+r\beta^A(\partial_A S_0)}{2r\alpha+r^2\beta^2} \pm \left[\left(\frac{\partial_v S_0+r\beta^A(\partial_A S_0)}{2r\alpha+r^2\beta^2}\right)^2 - \frac{\mu^{AB}(\partial_A S_0)(\partial_B S_0)}{2r\alpha+r^2\beta^2}\right]^{\frac{1}{2}}. \tag{7.8}$$

Among these two solutions, one corresponds to the outgoing mode, and the other one corresponds to the ingoing one. Let us get going to identify them.

First, we need to find out the leading order solutions of $\partial_r S_0$ in the near null hypersurface region. Considering the negative sign of Eq. (7.8), we obtain the leading order term in $r \to 0$ limit as (for details please see Appendix 7.A)

$$\partial_r S_0\Big|_- = -\frac{\partial_v S_0}{\alpha^{(0)}(v,x^A)r} \,. \tag{7.9}$$

According to our definition of the Hamiltonian of the system (which we have defined earlier below Eq. (7.6)) we can write Eq. (7.9) as

$$\partial_r S_0\Big|_- = \frac{H}{\alpha^{(0)}(v,x^A)r} \,. \tag{7.10}$$

For the initial position of the mode is at *'inside'*, we have $\partial_r S_0 < 0$ when $H > 0$. Therefore, as we mentioned earlier, the momentum direction is in the outward direction. Hence, the negative sign corresponds to the outgoing mode. So, we can write the Hamiltonian for the outgoing mode in the near null hypersurface region as

$$H = \alpha^{(0)}(v,x^A)r p_{r_{out}} \tag{7.11}$$

where $p_{r_{out}}$ is the outgoing momentum in r direction.

Similarly, considering the positive sign of Eq. (7.8) we obtain the leading order term that survives at $r \to 0$ limit is

$$\partial_r S_0\Big|_+ = -\frac{1}{2}\frac{\mu^{(0)AB}(\partial_A S_0)(\partial_B S_0)}{\partial_v S_0} \,, \tag{7.12}$$

where $\mu^{(0)AB}$ is the first term of the expansion of μ^{AB} about $r = 0$. Therefore, in terms of the Hamiltonian, we can write the above equation as

$$\partial_r S_0\Big|_+ = \frac{1}{2}\frac{\mu^{(0)AB}(\partial_A S_0)(\partial_B S_0)}{H} \,. \tag{7.13}$$

This implies for $H > 0$ we have $\partial_r S_0 > 0$. Therefore the momentum direction, in this case, is in the inward direction. So, it corresponds to the ingoing mode, and the expression of Hamiltonian in this case is

$$H = \frac{1}{2}\frac{\mu^{(0)AB}p_A p_B}{p_{r_{in}}} \,, \tag{7.14}$$

where $p_{r_{in}}$ is the ingoing momentum in r direction.

From the expression of the outgoing Hamiltonian (7.11) one can see that the outgoing mode suffers a singularity at $r = 0$. In contrast, the ingoing mode does not experience such

a thing (see Eq. (7.14)). This interesting observation has significant implications in the calculation of the tunneling probability, as we shall see in the later parts. Furthermore, in Appendix 7.B we also varified the form of the outgoing Hamiltonian (Eq. (7.11)) in the particle description through the Lagrangian formalism.

7.4 Transverse coordinate average of the Hamiltonian

Next, we want to explore the consequences of this classical Hamiltonian in the quantum tunnelling picture. It may be worth to point out here that in earlier calculations (chapter 5 and chapter 6) the spacetime metric was static or stationary and hence $\alpha^{(0)}$ was constant. However, this is not the case here.

However before proceeding for executing the tunneling formalism, let us prepare the stage for implementing it on our Hamiltonian. The structure of the Hamiltonian for the outgoing particle in the near null hypersurface region is multidimensional in this case due to the presence of $\alpha^{(0)}(v,x^A)$. Therefore, we have a situation where the case of a multidimensional tunneling has appeared. Multidimensional tunnelling event has been discussed in [334] for the usual physical systems. One of the proposals to calculate tunnelling probability is to do calculation on an average potential by considering averaging over directions except one. Hence following this idea and since tunnelling occurs radially just across the null surface, we read the transverse coordinates average of the Hamiltonian: $\bar{H} = \int H\sqrt{\mu}\ d^2x^A / \int \sqrt{\mu} d^2x^A$. This yields

$$\bar{H} = \bar{\alpha}(v) r p_{r_{out}} \equiv \bar{E}\ , \tag{7.15}$$

where $\bar{\alpha}(v)$ is defined as

$$\bar{\alpha}(v) = \frac{\int \alpha^{(0)}(v,x^A)\sqrt{\mu} d^2x^A}{\int \sqrt{\mu} d^2x^A}\ . \tag{7.16}$$

Here one thing is to be mentioned that during the consideration of the average of the Hamiltonian H, the integrating average applied only on $\alpha^{(0)}(v,x^A)$ because both r and $p_{r_{out}}$ are independent of x^A. We shall use this average Hamiltonian (7.15) in the next section in order to investigate the thermalization of our null surface through tunneling formalism.

7.5 Tunneling and Thermality

We start by calculating the HJ action for the outgoing object. Choosing the integration limit from $r = -\epsilon$ to $r = \epsilon$ for the outgoing object where $\epsilon > 0$ and is a very small number

suggests that the outgoing object crosses the null hypersurface from just *'inside'* to just *'outside'* in the vicinity of the null hypersurface. Therefore, we obtain the HJ action for the outgoing species (field mode or the particle) as

$$S_{out} = \frac{\bar{E}}{\bar{\alpha}(v)}\int_{-\epsilon}^{\epsilon}\frac{dr}{r} + \int p_{v_{out}}dv + \int p_{A_{out}}dx^A \ . \tag{7.17}$$

From the above integration it can be seen that the first integration term will contain the imaginary part as there exists a singularity at $r = 0$ and other two integrations will contribute in the real part of the total integration. Also in the first integration we have pulled out the term $\bar{E}/\bar{\alpha}(v)$ as it is constant of motion (please see Appendix 7.C). Hence, after performing the integration in Eq. (7.17) we obtain

$$S_{out} = -\frac{i\pi\bar{E}}{\bar{\alpha}(v)} + \text{Real part} \ . \tag{7.18}$$

In a similar way, we can calculate the HJ action for the ingoing species also. However, in this case, the action does not contain any singularity at $r = 0$ (see Eq. (7.14) and Eq. (7.B.5)); thus, it turns out to be

$$S_{in} = \text{Real quantity} \ . \tag{7.19}$$

Accordingly, the probability for the outgoing object crossing the null hypersurface turns out to be

$$P_{out} \propto \exp\left(-\tfrac{2\pi\bar{E}}{\hbar\bar{\alpha}(v)}\right) \ , \tag{7.20}$$

whereas the probability of crossing the null hypersurface for the ingoing one is $P_{in} \sim 1$. Therefore, the tunneling probability comes out to be

$$\Gamma(v) = \frac{P_{out}}{P_{in}} \sim \exp\left(-\frac{2\pi\bar{E}}{\hbar\bar{\alpha}(v)}\right) \ . \tag{7.21}$$

This particular expression of the tunneling probability is similar to Boltzmann factor. Therefore can be considered as thermal in nature with the temperature of the system is identified as

$$T(v) = \frac{\hbar\bar{\alpha}(v)}{2\pi} \ . \tag{7.22}$$

However, this very expression of the temperature is not a constant; instead, it is a function of v. It means at every other $v = constant$ null hypersurface near $r = 0$ region, the observer will feel different values of temperature of the system for every different value of v. This is a reflection of the evolving nature of our null surface which corresponds to a non-equilibrium situation. We will come back to this point again in the next section.

7.6 Summary and Discussions

Let us summarise the results obtained in the present chapter. We started by addressing the fact that gravitational field equations near any null surface in an arbitrary space-time reduce to a thermodynamic identity, and it generalises the results previously available in the context of the horizon. Our prime motive was to find out the underlying reason for this noticeable fact in order to convey the cause why thermodynamical attributions are associated with any arbitrary null hypersurface. We start our calculations using the KG equation in the field-theoretic approach, and in the semi-classical limit, we obtain that the system Hamiltonian for the outgoing mode in the near null hypersurface region comes out to be of xp kind. In the appendix, the same has been explored in the Lagrangian formalism for a massless outgoing particle as well. In the context of thermality, we proceed with the conventional idea of tunneling mechanism, and after implementing the tunneling formalism in the near null hypersurface region, we obtain that our system is thermal in nature. However, the system temperature we found, in this case, is not constant; rather, it is a function of the timelike coordinate, unlike the previous results of the black hole horizons (SSS BH and the Kerr one) (chapter 5 and chapter 6).

Now, let us discuss the key features of the present result in a more detailed manner. Our results justify the fact how temperature can be associated with any generic null hypersurface. In our earlier chapters we predicted that the emergence of thermality into the system has a tight connection with the *local* instability of the system in the context of horizon (chapter 5 and chapter 6). This connection previously showed that if the Hamiltonian of the system turns out to be an unstable one in the classical scale, this instability may lead to the thermality of the system in the quantum scale. Here, we came across such Hamiltonian, which consists of a probed massless and chargeless species near any generic null hypersurface and the structure of the outgoing Hamiltonian, in this case, turns out to be of xp kind (see Eq. (7.11)).

We have already learnt that such specific Hamiltonian turns out to be that of an inverted harmonic oscillator (IHO) in a new set of canonical variables (see Eq. (5.29) of chapter 5) [273] and IHO potential is inherently unstable. This implies that our present outgoing species locally feel an instability due to the presence of null surface at $r = 0$. This fact can also be realised through the divergence of radial momentum $p_{r_{out}}$ at $r = 0$ for a given value of $\bar{E}$ (see Eq. (7.15)). Such peculiar instability provides a noticeable feature in the quantum regime. To escape through the potential ($\sim xp$) the outgoing

object needs to tunnel through a complex path as it experiences a singularity exactly at $r = 0$. Moreover, as we noticed in the calculation, $r = 0$ singularity (which is also the key for aforesaid instability) led to our main expression of tunneling probability (7.21). Usually, the time-reversal invariance demands that the emission probability is equal to that for the absorption process proceeding backwards in time and vice versa. Whereas our present result is not consistent with this. Therefore the present observation shows that the probability of emission of particles through the null surface at a certain time is different from the probability of absorption of particles by the surface at that time. Hence it is more likely for a particular region to gain particles than lose them. Moreover, the exponential behaviour of our result portrays the thermal nature of the system. This thermality comes into the picture only because of this peculiar singularity at $r = 0$, which originates due to the specific structure of the outgoing Hamiltonian in the null surface regime. Therefore, we feel that the local instability in the near null hypersurface region may be the reason for making the system thermal at the quantum scale.

Previously, this connection between instability and thermality was established only in specific cases containing horizons (chapter 5 and chapter 6). Here we generalise the same for a generic null hypersurface. Therefore, we feel that the present discussion may unfold the deeper reason for having the thermodynamical quantities of not only horizon but also for any generic null surface at the quantum level. Moreover, in this chapter we have also represented one of the important applications of tunneling mechanism for more general background.

Finally, we make a comment on the conceptual aspect of defining thermodynamics on a generic null surface which is an evolving one. Thermodynamics for an equilibrium system is well established. In contrast, our null surface can not be considered as an equilibrium one. Therefore the concept of temperature and corresponding zeroth law etc., are not consistent with equilibrium thermodynamics. Instead, we need to invoke "non-equilibrium" definitions of these thermodynamic quantities. This subject is not fully established, but there are a few suggestions and advancements. A point to be noted is that if the system is in non-equilibrium steady states, different thermometers, sensitive to different degrees of freedom (DOF), will show different temperature readings, which lead to the difficulty of defining only one temperature for these systems [335]. Hence, the equilibrium version of the zeroth law does not work in its full glory. However, a restricted validation of zeroth law can be considered here, and in that case, the temperature must be defined with respect to some specified DOF. For instance, if a system is composed of two subsystems and they have different DOF, then corresponding to each DOF one can

define a temperature. Consequently, the zeroth law is valid within that particular DOF. This, in turn, gives rise to different "local" temperatures in the system as it consists of different degrees of freedom. In this local sense, the law of thermodynamics and the thermodynamics parameters can be defined, but that will be accompanied by heat flux, temperature gradient etc., among different DOF (see discussion in Section 4.1 of [335] for details). Of course, for the "global" equilibrium, this wipeout. Now, comparing with that situation, we see our system also obeys the characteristics of the non-equilibrium steady-state situation where our null hypersurface is evolving with the changing value of v. Therefore, we expect that the temperature of our system will be defined following the same concept as it is defined in non-equilibrium situations. A proposal for defining the effective temperature was suggessted by S. Weinberg in the case of a non-equilibrium system of photons by relating absorption rate coefficient Λ and the stimulated emission coefficient Ω (see discussion in Section 6.2 of [335] for details):

$$\frac{\Omega}{\Lambda} = e^{-\frac{E}{T_{\text{eff}}}} \,. \tag{7.23}$$

In the present discussion, we have adopted the same spirit in order to identify the temperature of the null surface. However, the status of the zeroth law for our system is still an open question as the complete knowledge of the degrees of freedom for our system is yet to be explored and therefore needs further investigation. However, we feel that the lack of a complete theory of non-equilibrium thermodynamics at present will keep us at bay to get full justification of thermodynamics of a null surface. On the other hand, if we consider that the evolution of the null hypersurface is quasi-static in nature, then our temperature can be justified through equilibrium thermodynamics by considering that the surface is at equilibrium at each instant.

Appendices

7.A Derivation of Eq. (7.9) and Eq. (7.12)

In the near null hypersurface region, i.e. $r \to 0$ limit, $\alpha(v,r,x^A)$ can be expanded (using Taylor series expansion)

$$\alpha(v,r,x^A) = \alpha^{(0)}(v,x^A) + \alpha^{(1)}(v,x^A)r + \mathcal{O}(r^2)\,. \tag{7.A.1}$$

Now, looking back to Eq. (7.8) we can rewrite it as

$$\partial_r S = -\frac{\partial_v S + r\beta^A(\partial_A S)}{2r\alpha + r^2\beta^2} \pm \left(\frac{\partial_v S + r\beta^A(\partial_A S)}{2r\alpha + r^2\beta^2}\right)\left[1 - \frac{\mu^{AB}(\partial_A S)(\partial_B S)}{\left(\partial_v S + r\beta^A(\partial_A S)\right)^2}\left(2r\alpha + r^2\beta^2\right)\right]^{\frac{1}{2}}. \tag{7.A.2}$$

Now, at $r \to 0$ the above equation turns into

$$\begin{aligned}\partial_r S &\simeq -\frac{\partial_v S + r\beta^A(\partial_A S)}{2r\alpha + r^2\beta^2} \pm \left(\frac{\partial_v S + r\beta^A(\partial_A S)}{2r\alpha + r^2\beta^2}\right)\left[1 - \frac{1}{2}\frac{\mu^{AB}(\partial_A S)(\partial_B S)}{\left(\partial_v S + r\beta^A(\partial_A S)\right)^2}\left(2r\alpha + r^2\beta^2\right)\right] \\ &\simeq -\frac{\partial_v S + r\beta^A(\partial_A S)}{2r\alpha + r^2\beta^2} \pm \left[\left(\frac{\partial_v S + r\beta^A(\partial_A S)}{2r\alpha + r^2\beta^2}\right) - \frac{1}{2}\frac{\mu^{AB}(\partial_A S)(\partial_B S)}{\left(\partial_v S + r\beta^A(\partial_A S)\right)}\right].\end{aligned} \tag{7.A.3}$$

Considering the negative sign solution of $\partial_r S$ we obtain from Eq. (7.A.3)

$$\partial_r S\Big|_- = -2\frac{\partial_v S + r\beta^A(\partial_A S)}{2r\alpha + r^2\beta^2} + \frac{1}{2}\frac{\mu^{AB}(\partial_A S)(\partial_B S)}{\left(\partial_v S + r\beta^A(\partial_A S)\right)}\,. \tag{7.A.4}$$

The first term of Eq. (7.A.4), using the expansion of $\alpha(v,r,x^A)$, in the near null hypersurface region reduces to

$$\begin{aligned}\frac{\partial_v S + r\beta^A(\partial_A S)}{2r\alpha + r^2\beta^2} &\simeq \frac{\partial_v S + r\beta^A(\partial_A S)}{2r\alpha^{(0)}\left(1 + \frac{r\alpha^{(1)}}{\alpha^{(0)}} + \frac{r\beta^2}{2\alpha^{(0)}}\right)} \\ &= \frac{\partial_v S + r\beta^A(\partial_A S)}{2r\alpha^{(0)}}\left(1 - \frac{r\alpha^{(1)}}{\alpha^{(0)}} - \frac{r\beta^2}{2\alpha^{(0)}}\right).\end{aligned} \tag{7.A.5}$$

Similarly, from the second term of Eq. (7.A.4), in the near null hypersurface region we obtain

$$\frac{\mu^{AB}(\partial_A S)(\partial_B S)}{\left(\partial_v S + r\beta^A(\partial_A S)\right)} \simeq \frac{\mu^{AB}(\partial_A S)(\partial_B S)}{\partial_v S}\left(1 - \frac{r\beta^A(\partial_A S)}{\partial_v S}\right). \tag{7.A.6}$$

Hence, putting the approximated values of these two terms in Eq. (7.A.4) we obtain the only leading order term in the near null hypersurface region

$$\partial_r S\Big|_- = -\frac{\partial_v S}{2r\alpha^{(0)}(v,x^A)}, \tag{7.A.7}$$

i.e. Eq. (7.9) in our main text. In the similar manner we can also obtain the expression of $\partial_r S|_+$. Taking the positive sign solution in Eq. (7.A.3) and considering the leading order term at $r \to 0$ limit we end up getting Eq. (7.12).

7.B Hamiltonian: Particle description in Lagrangian formalism

In Section 7.3, using HJ formalism we land up to a particular Hamiltonian structure (Eq. (7.11)) of the outgoing scalar mode in the near null hypersurface region. Here we like to find out whether the same Hamiltonian structure can be obtained using the Lagrangian of a particle.

Consider the Lagrangian $L = \sqrt{-g_{ab}\dot{x}^a\dot{x}^b}$ where $\dot{x}^a = dx^a/dv$. Since we are considering a massless particle, for convenience v has been chosen here as the affine parameter for the geodesics of the particle. Therefore, under the background of metric (7.1) we obtain the form of the Lagrangian of the system as

$$L = \left[2r\alpha - 2\dot{r} + 2r\beta_A\dot{x}^A - \mu_{AB}\dot{x}^A\dot{x}^B\right]^{\frac{1}{2}} \tag{7.B.1}$$

where the expressions of the corresponding momentum components are

$$p_r = -\frac{1}{\left[2r\alpha - 2\dot{r} + 2r\beta_A\dot{x}^A - \mu_{AB}\dot{x}^A\dot{x}^B\right]^{\frac{1}{2}}}; \tag{7.B.2}$$

$$p_A = \frac{r\beta_A - \mu_{AB}\dot{x}^B}{\left[2r\alpha - 2\dot{r} + 2r\beta_A\dot{x}^A - \mu_{AB}\dot{x}^A\dot{x}^B\right]^{\frac{1}{2}}}\,. \tag{7.B.3}$$

Therefore, we obtain the Hamiltonian of the system as

$$H = \frac{1}{2p_r}\left[(2r\alpha + r^2\beta^2)p_r^2 + 2r\beta^A p_A p_r + (1 + p_A^2)\right]\,. \tag{7.B.4}$$

The above expression of the Hamiltonian (7.B.4) reveals that there are two solutions of p_r in trems of H and p_A. It is evident that one solution of p_r corresponds to the outgoing particle while the other one corresponds to the ingoing one. Now, in the near null hypersurface region ($r \to 0$) considering only the leading order terms in these two solutions of p_r, we obtain

$$p_r\Big|_- = \frac{H}{\alpha^{(0)}(v,x^A)r} \quad \text{and} \quad p_r\Big|_+ = \frac{1}{2}\left(\frac{1+p_A^2}{H}\right) \tag{7.B.5}$$

where (−) and (+) sign represents the -ve and the +ve sign solutions of p_r of the quadratic equation (7.B.4) respectively. Therefore, we can see that the expression of the -ve sign solution of p_r exactly matches with Eq. (7.10) which we identified as the momentum in r direction for the outgoing mode, i.e. $p_{r_{out}}$. So, it is evident that the -ve sign solution of p_r corresponds to the momentum of the outgoing particle and we obtain the similar structure of the outgoing Hamiltonian in the near null hypersurface region (see Eq. (7.11)).

Therefore, using the particle description in Lagrangian formalism we obtain the similar expression of the outgoing Hamiltonian in the near null hypersurface region as we obtained in the field mode description in Section 7.3. Whereas for the ingoing particle the Hamiltonian structure in the near null hypersurface region may differ in those two descriptions (see (7.14) and Eq. (7.B.5)) but their natures are same as the ingoing particle does not suffer any singularity at $r = 0$.

7.C Conserved quantity $\bar{H}/\bar{\alpha}(v)$

Now, we have the near null hypersurface Hamiltonian for the outgoing particle, i.e.

$$H = \alpha^{(0)}(v, x^A) r p_{r_{out}} \tag{7.C.1}$$

and after averaging out the transverse coordinates we have

$$\bar{H} = \bar{\alpha}(v) r p_{r_{out}} \ . \tag{7.C.2}$$

Now, let us check the variation of $\bar{H}/\bar{\alpha}(v)$ with respect to some affine parameter λ, i.e.

$$\begin{aligned} \frac{d}{d\lambda}\left(\frac{\bar{H}}{\bar{\alpha}(v)}\right) &= \frac{d}{d\lambda}\left(r p_{r_{out}}\right) \\ &= \dot{r} p_{r_{out}} + r \dot{p}_{r_{out}} \end{aligned} \tag{7.C.3}$$

where $\dot{} \equiv \frac{d}{d\lambda}$. Now, from the Hamilton's equations of motion we obtain

$$\dot{r} = \frac{\partial \bar{H}}{\partial p_{r_{out}}} = \bar{\alpha}(v) r \tag{7.C.4}$$

and the other one is

$$\dot{p}_{r_{out}} = \frac{\partial \bar{H}}{\partial r} = -\bar{\alpha}(v) p_{r_{out}} \ . \tag{7.C.5}$$

Now, putting the values of $\dot{r}$ and $\dot{p}_{r_{out}}$ in Eq. (7.C.3) we obtain

$$\begin{aligned} \frac{d}{d\lambda}\left(\frac{\bar{H}}{\bar{\alpha}(v)}\right) &= \bar{\alpha}(v) r p_{r_{out}} + \left(-\bar{\alpha}(v) r p_{r_{out}}\right) \\ &= 0 \,. \end{aligned} \tag{7.C.6}$$

It tells that the quantity $\bar{H}/\bar{\alpha}(v) = \bar{E}/\bar{\alpha}$ is conserved during the motion of the particle under the average Hamiltonian $\bar{H}$.

CHAPTER 8

CONCLUSIONS AND OUTLOOK

8.1 Conclusions

Over the last few years there has been a growing interest to study the thermal and geometrical properties of black hole horizon and its intimate connection with the dynamics of particle motion near it. It has been observed that the presence of a horizon introduces chaos in a system. The reason behind this fascinating feature of the horizon is not explained elaborately anywhere. Particle motion near the horizon has always been an interesting topic to the physicists. However, in the presence of any horizon, either static or stationary, why an integrable system starts to show chaotic dynamics has always been a mystery. In fact, why all the horizons (static or stationary) give the same feature is yet to be known completely.

On the other hand, black hole thermodynamics is a long-standing concept which originates through an analogy between the laws of Black holes and those of usual thermodynamical systems, but the reason why these thermodynamical quantities are associated with horizon has not been discussed properly anywhere. In fact, the underlying physical mechanism which provides temperature in the horizon system is still unclear to us. Consequently, which microscopic degrees of freedoms are responsible for such a feature is not known either. Though people have tried many attempts, there are no concrete explanations until now.

Therefore, in this thesis, for the first time, we have tried to give a unified reason for both the characteristics of horizon, i.e. the reason for chaotic influence on a system and

the thermal behaviour of it and have tried to find out if there is any connection between them. The chapter wise findings of the thesis are the followings;

Starting with the second chapter, in the present chapter we have studied the implications of the influence of an event horizon on an integrable system when the system comes under the influence of the horizon. The whole study has been done in the classical picture. The results that we found in this chapter can be summarized as follows;

- The trajectories of a massless and chargeless particle in a very near horizon region have been studied. The theoretical analysis showed that the radial motion is exponentially increasing function of time parameter which indicates that the horizon may influence chaotic behaviour in the motion of a particle in an integrable system when it interacts with the horizon of a black hole.
- With the application of the numerical simulations the situation in presence of harmonic potential, it has been observed that this is indeed the case. We found that the trajectories of the particle trapped in a Harmonic potential which is an integrable system, becomes chaotic in nature after a certain value of energy of the system. Here both SSS and Kerr black holes cases have been investigated.
- In the numerical simulations we particularly studied the Poincaré sections, largest Lyapunov exponents and Power spectral Density (PSD) of the composite system for confirming that the system undergoes chaotic dynamics whenever it reaches under the influence of the horizon. Interestingly, the breaking of Poincaré sections into different tori, the positive value of the largest Lyapunov exponent and the population of different frequencies in the PSD diagram under some particular values of the system parameters confirm our prediction that the system undergoes through chaos whenever it comes under the influence of the horizon.
- Moreover, we found out that the largest Lyaunov exponent values settle down to a positive value below the upper bound the of the system, i.e. the surface gravity of the BHs for both the cases (SSS and Kerr). Therefore, from that perspective we conclude that our system satisfies the MSS bound according to the SYK model. Furthermore, we obtained that in case of Kerr black hole the steady state Lyapunov exponent increases on increase of the rotation parameter which suggests that the rotation of the black hole may induce more chaotic fluctuations in the motion of the particles.

We learned in the second chapter that when an event horizon exists, a system begins to exhibit chaotic behaviour in the near-horizon region. As a result, the continuing hypothesis that *the presence of a horizon may produce chaos in an integrable system* is studied further in this chapter from the perspective of a uniformly accelerated frame. We create a model that consists of a massless and chargeless particle trapped in a harmonic oscillator in a uniformly accelerated frame (namely Rindler observer). Here the Rindler frame provides a Killing horizon without any intrinsic curvature to the system. This distinguishes the current findings from the earlier calculations. Now, let us summarise the results of this chapter.

- In this chapter also we obtained that with the increment of some system parameters, i.e. energy of the system (E) and the acceleration of the Rindler frame the system shows chaotic dynamics in the vicinity region of the horizon which is confirmed by performing the numerical analyses.

- In the numerical analyses we studied the Poincar*é* sections of the system, the largest Lyapunov exponent of the system and PSD just like the earlier analyses (in the previous chapter). In this case also we found out that as we increase some of the parameters of the system (E and a) the Poincar*é* sections break into different tori and the PSD diagrams get populated. Moreover, the largest Lyapunov exponent values settles down to a positive value which confirms the chaotic behaviour of the system in the near horizon region.

- We also found that the chaos of the particle probing the Rindler horizon has a universal upper bound on the Lyapunov exponent. In this regard, it may be mentioned that the upper bound is given by the acceleration of the particle and it is independent of the external potentials which prevents the particles falling into the horizon. This upper bound conjecture of the Lyapunov exponent coincides with the prediction of the SYK model, argumented by Maldacena, Shenkar and Stanford [226] and it is confirmed with the application of numerical simulations.

- Therefore, from this analysis, it is apparent that an integrable system, when it comes under the influence of horizon, its dynamics can be chaotic. Since, in the present case, the horizon is part of the flat background (vanishing Riemann curvature), the conjecture – horizon makes system chaotic – is further balustrade as the curvature does not play much role.

Our next goal was to investigate the fundamental cause of this fascinating horizon characteristic after identifying the chaotic behaviour in a system close to the horizon. We therefore tried to offer a cogent explanation for such exceptional horizon properties in the fourth chapter. The findings from the fourth chapter are listed below;

- To find out the concrete reason for chaotic dynamics in the near horizon region we argued that the near horizon instability is the main cause of it. In section (4.2) the static spherically symmetric black hole, Rindler case and very restrictive trajectories for Kerr black hole have been explored in Painleve coordinates. It is observed that such is due to the appearance of xp type Hamiltonian for a near horizon motion of a particle.

- In the later section (4.3) we investigated the whole phenomena in a more extensive way. We find that there is another set of coordinates, namely the Eddington-Finkelstein (EF) coordinates, in which the motion of the particle along the null trajectory also faces the instability in the near horizon region. Moreover, such instability is very much there for any observer when the particle is following the outgoing null path in that particular EF coordinates.

- Notably, again the instability factor is given by the surface gravity of the black hole. When the particle is following the outgoing null route in those precise EF coordinates, we find that the observer associated with the EF frame measures the radial momentum of the particle as $p \sim e^{-\kappa t}$ where t is the EF time coordinate and the corresponding Hamiltonian of the system comes out to be of xp structure again. Therefore, as in the near horizon limit, i.e. $t \to -\infty$ the radial momentum diverges and indicates the presence of instability just like the case of Painleve coordinate system. It suggests that although the instability is observer independent for our particle motion, the particular form of the Hamiltonian is observer dependent. The observer associated with this specific frame, either in Painleve or in EF coordinates will see this form of the near horizon Hamiltonian.

- Moreover, in our next investigation, using the Raychaudhuri equation, we have calculated the expansion parameter of the null geodesics, which are followed by our test particle in that particular EF coordinate. Here, we have found that the expansion parameter shows instability in the near-horizon region. It means that in the near-horizon region, instability in the particle motion is an observer independent phenomena for this particular motion of the particle.

In the previous chapter we found that the particular structure of the Hamiltonian (xp kind) is responsible for the unavoidable instability provided by the horizon on the particle's motion at classical level. Following this classical picture we next proceed for the quantum calculation in the fifth chapter. This analysis has been concluded with the following results;

- After obtaining a clear picture of instability in the classical scale in the previous chapter, we next targeted quantum calculations in order to see quantum consequences due to this unstable xp kind structure of the near horizon Hamiltonian. We started with the tunnelling approach, where we found that this near horizon Hamiltonian predicts a finite probability of escaping the particle from the horizon and thereby providing a temperature to the horizon. The expression came out to be as that of Hawking [113].

- The next approach was the detector response approach in order to get a distinct idea about the relevant vacuum state. The observer or rather the detector, in this case, is following the same null trajectory in EF coordinate in the near horizon regime, as we mentioned earlier. The vacuum was chosen to be that Boulware vacuum in this case. After evaluating the response function numerically, we have obtained that the transition probability of the detector of detecting a photon in the Boulware vacuum is similar to Planck distribution. It showed that the detector will see the Boulware vacuum as a thermal bath.

- Next, our aim was to show particularly the inherent thermal characteristics of the xp which may appear not only in black hole space time but also in other areas of physics. We started with by calculating the density of states (DOS) of the system. In this process we particularly used the Gutzwiller's trace formula because usual quantization rule normally not applicable in this case. First, we write down the xp Hamiltonian in another canonically rotated coordinates and it turns out to be the Hamiltonian of an inverse harmonic oscillator. However, the complexified version of the IHO Hamiltonian leads to a harmonic oscillator which helped us to calculate the DOS using Gutzwiller's trace formula. Interestingly, the expression of the DOS turns out to be thermal in nature and the temperature is identified as the Hawking temperature [113].

- The other feature of the unstable potential is, it shows scattering phenomena. Therefore, our next approach was to study the scattering phenomena in the pres-

ence of this unstable xp kind near horizon Hamiltonian. Identifying the "in" and "out" states we obtained the transition probability for the particle to jump from the initial to final energy state, which yielded the thermal nature again with the desired Hawking temperature. Moreover, we gained the information about the frequency of the quasinormal modes from this scattering which matches with the earlier findings [262, 299–301].

In the sixth chapter, the validity of our already proposed conjecture – *horizon creates a local instability which acts as the source of the quantum temperature of black hole* – is being tested here for Kerr black hole. Here briefly we have the following results;

- Like our earlier chapters, the main focus, in this chapter, was to inspect whether the presence of local instability in the near horizon region is responsible for providing the temperature for a particular set of observer but this time in Kerr spacetime. We finally found that this is indeed the case. Although near horizon instability is an observer independent phenomenon for our chosen null path, the specific feature of the radial motion of the outgoing particle is a coordinate dependent event. The radial contribution in corresponding Hamiltonian of the system comes out to be of xp kind, which is indeed an unstable Hamiltonian.

- In the quantum regime, using the tunneling approach we obtain that thermality emerges due to that instability and the temperature exactly matches with the Hawking temperature. Therefore, it turns out that the extension of our proposed conjecture is applicable to much more generic black holes also. Hence, the generality of this conjecture is evident here, and thereby providing a prospective to become one of the leading candidates to understand the underlying mystery of the horizon thermalization in the context of black holes.

Dynamical properties of a generic null surface are known to have a thermodynamic interpretation. Such an interpretation is completely based on an analogy between the usual law of thermodynamics and structure of gravitational field equation on the surface. In the seventh chapter we materialise this analogy and show that assigning a temperature on the null surface for a local observer is indeed physically relevant. Here are the following results of the present chapter;

- Our prime motive was to find out the underlying reason for this noticeable fact in order to convey the cause why thermodynamical attributions are associated with any arbitrary null hypersurface. We start our calculations using the KG equation in the field-theoretic approach, and in the semi-classical limit, we obtain that the system Hamiltonian for the outgoing mode in the near null hypersurface region comes out to be of xp kind.

- In the context of thermality, we proceed with the conventional idea of tunneling mechanism, and after implementing the tunneling formalism in the near null hypersurface region, we obtain that our system is thermal in nature. However, the system temperature we found, in this case, is not constant; rather, it is a function of the timelike coordinate, unlike the previous results of the black hole horizons (SSS BH and the Kerr one).

- Previously, this connection between instability and thermality was established only in specific cases containing horizons (chapter 5 and chapter 6). Here we generalise the same for a generic null hypersurface. Therefore, we feel that the present discussion may unfold the deeper reason for having the thermodynamical quantities of not only horizon but also for any generic null surface at the quantum level. Moreover, in this chapter we have also represented one of the important applications of tunneling mechanism for more general background.

In this scenario where researchers are seeking to resolve many riddles of the black hole horizons, we hope our work can shed some light in that direction. A significant amount of efforts have been put to uncover the universal behaviour of the Lyapunov exponent and relate it with the temperature of the chaotic system. Thus, the analysis presented in the thesis illuminates some of the gray areas of the horizon characteristics. In addition, it also resolves some of the major debates in this topic (horizon thermodynamics). Additionally, it also generalizes some of the features of horizon thermodynamics which is studied case by case in different spacetimes. The way we have studied here, this is a completely new idea and could be a new technique to uncover the several mysteries of not only event horizons, but also any general system which has direct connection with IHO. Therefore we feel that the results as well as the techniques, introduced here, will have significant impact in the area of black holes as well as systems which have connection to IHO. With the progress of these present investigations, we think that the enigma of near horizon

physics may be revealed, and further exploration of the behaviour of the universal chaos and thermality of the horizon will be beneficial. In the following, we provide the areas where people can explore further for the better understanding of the subject.

8.2 Scope for future works

8.2.1 Studying Chaos in Modified Theories of Gravity

"What happens when one studies the possible chaotic features of near horizon spacetime in a better-motivated modified theory gravity?" Recently, there have been some works in this direction where people investigated whether chaos is present in geodesics of a slowly-rotating BH of dynamical Chern-Simons (dCS) gravity [336]. People have also attempted to ascertain the same nature in the geodesics of spinning BHs in quadratic gravity also [337]. Therefore, there are several motivations for studying the chaotic motion in the near horizon region of BHs in various alternative theories of gravity such as $f(R)$ gravity, Lanczos-Lovelock gravity *etc.* These studies may reveal several aspects of alternative theories of gravity which are yet to be fully understood. Furthermore, these features are crucial for a clear comprehension of the chaotic feature in the vicinity of the horizon in those theories.

8.2.2 Understanding The Underlying reason Why Complexification of The Frequency Leads to Thermality in The Context of Horizon

It is generally known that when the time coordinate is complexified, the path integration can be understood as the partition function and the periodicity of the complex time is known as the inverse temperature. Using this concept, Hawking demonstrated how the partition function calculation gives us the right expression for the horizon's entropy by Euclideanising the black hole metric. In this instance, the Hawking temperature is defined as the inverse of the periodicity of complexified time around the horizon [295]. In chapter 5 we found the time period of the primitive orbit T_l as $T_l = 2i\pi/\kappa$ in our computation by complexifying the frequency. It's interesting to note that this figure fits the time period exactly that Hawking discovered by Euclideanising spacetime. We therefore believe that Hawking's claim and our complexification of the frequency may be closely related and further investigation may reveal the underlying physical reason behind that which may unveil some interesting facts about horizon thermalisation.

8.2.3 Understanding The Significances of DOS in The Context of xp And Near-Horizon Systems

We utilised the Gutzwiller trace formula in chapter 5 to determine the system's total density of states (DOS). The DOS contains two parts for an unstable system like xp (in our scenario); one is the mean part and the other is the oscillatory part. Depending on the value of the oscillatory term in it, the oscillatory component might be either positive or negative. Here, we would like to point out that negative DOS is not at all unexpected for near equilibrium systems. For instance, the negative value of DOS for quantum systems has been documented in the literature [296]. According to [297], DOS can have negative values if there is a quasi-probability distribution at the quantum level, such as the Wigner distribution function. This primarily relates to instances where the system is just slightly out of equilibrium. The Wigner function and DOS have a close relationship; the latter has negative values for states that are not typically permitted (see section 8.1.3 of [274])). These negative values must, however, disappear at the classical limit $\hbar \to 0$. It is possible to verify that this is precisely occurring for (5.32) as well. The mean value is always positive, whereas it is a pure quantum contribution and disappears for $\hbar \to 0$. This fact relates to the Hamiltonian's unstable behaviour. However, the significance of it has not yet been fully appreciated. So, further investigation may lead to some intriguing findings where we can learn more not only about the unstable systems but also about the near-horizon systems.

8.2.4 Understanding Thermality of The Horizon from The Perspective of Many-Body Systems

In the present thesis we have studied the horizon thermalisation from the perspective of a single particle system. However, the deeper comprehension of thermality in case of the horizon will be much more robust if we visualize it from the perspective of a many particle system, because thermalisation is always connected to the many particle system. Therefore, the natural issue that arises is *"what happens to a many particle system when it approaches towards an event horizon? Does this instability still persist in such cases? Will that instability still lead to the thermality in the similar way?"* As we have seen that the instability arises in case of a single particle system, so, we may anticipate that this would hold true for a non-interacting many particle system as well and it would be interesting if the similar way it leads to thermality in the near horizon region. However, that is an open question which needs to be explored to obtain the complete explanation

of thermalisation in the context of horizon.

8.2.5 Can ETH Explain The Thermal Nature of The Horizon?

In literature, there are different approaches to checking thermality in a many-particle system. One such procedure is the eigenstate thermalisation hypothesis (ETH) [231, 338–349] which is a generic mechanism of thermalisation under unitary dynamics of isolated quantum systems. The ETH has been numerically validated for a considerable number of many-body Hamiltonians [339–349]. Moreover, ETH works in the cases of Hamiltonians that are chaotic and devoid of time reversal symmetry [231, 338, 350]. Incidentally, our single particle xp kind Hamiltonian satisfies both these conditions [288]. Additionally, this xp Hamiltonian falls within the category of a random matrix and its eigenvalues adhere to the characteristics of *Gaussian Unitary Ensemble* (GUE). In this instance, the average value of an observable of the system is always close to the equilibrium microcanonical ensemble average value in the later time, leading to thermalization, which is basically the feature of ETH. Therefore, if we can demonstrate similar kinds of characteristics in the many-body Hamiltonian near horizon region, we may expect that the proper explanation of thermalisation can be delivered using ETH in the context of the horizon.

8.2.6 Explanation of Thermality From the Perspective of A Collection of Many-IHOs System

In the present thesis, using the single particle system, we have obtained that the near horizon Hamiltonian consisting of a massless and chargeless particle behaves like a particle present in the inverse harmonic potential. We have also shown that the system corresponding to the Hamiltonian of an IHO has an intimate connection with thermality. Now, if we can check whether there is any option that a many-body system can be thought of as a collection of IHOs, then that can be useful to explain the thermalisation of the horizon in a much more robust way from the perspective of a many-particle system. The single particle analysis revealed the direction for elucidating the fundamental cause of horizon thermalisation. However, the whole motivation of the thesis will be completed if one can demonstrate that thermality can be explained in the same way for a many-body system made up of a collection of non-interacting IHOs in the next stage.

BIBLIOGRAPHY

[1] A. Einstein, "Concerning an heuristic point of view toward the emission and transformation of light," *Annalen Phys.*, vol. 17, pp. 132–148, 1905.

[2] A. Einstein, "über die von der molekularkinetischen theorie der wärme geforderte bewegung von in ruhenden flüssigkeiten suspendierten teilchen," *Annalen der physik*, vol. 4, 1905.

[3] A. Einstein, "On the electrodynamics of moving bodies," *Annalen Phys.*, vol. 17, pp. 891–921, 1905.

[4] A. Einstein, "The Formal Foundation of the General Theory of Relativity," *Sitzungsber. Preuss. Akad. Wiss. Berlin (Math. Phys.)*, vol. 1914, pp. 1030–1085, 1914.

[5] A. Einstein, "Erklärung der perihelbewegung des merkur aus der allgemeinen relativitätstheorie," *Sitzungsberichte der Königlich Preussischen Akademie der Wissenschaften (Berlin)*, pp. 831–839, jan 1915.

[6] A. Einstein, "Die Feldgleichungen der Gravitation," *Sitzungsberichte der Königlich Preussischen Akademie der Wissenschaften (Berlin)*, pp. 844–847, jan 1915.

[7] S. B, *A first course in General Relativity*.
Cambridge UK: Cambridge University Press, 2009.

[8] S. Weinberg, *Gravitation and Cosmology: Principles and Applications of the General Theory of Relativity*.
John Wiley and Sons Inc, 1972.

[9] F. W. Dyson, A. S. Eddington, and C. Davidson, "A Determination of the Deflection of Light by the Sun's Gravitational Field, from Observations Made at the Total Eclipse of May 29, 1919," *Philosophical Transactions of the Royal Society of London Series A*, vol. 220, pp. 291–333, jan 1920.

[10] F. Zwicky, "On the probability of detecting nebulae which act as gravitational lenses," *Phys. Rev.*, vol. 51, pp. 679–679, Apr 1937.

[11] J. Renn, T. Sauer, and J. Stachel, "The origin of gravitational lensing: A postscript to einstein's 1936 science paper," *Science*, vol. 275, no. 5297, pp. 184–186, 1997.

[12] D. E. Lebach, B. E. Corey, I. I. Shapiro, M. I. Ratner, J. C. Webber, A. E. E. Rogers, J. L. Davis, and T. A. Herring, "Measurement of the solar gravitational deflection of radio waves using very-long-baseline interferometry," *Phys. Rev. Lett.*, vol. 75, pp. 1439–1442, Aug 1995.

[13] B. Bertotti, L. Iess, and P. Tortora, "A test of general relativity using radio links with the Cassini spacecraft," *nat*, vol. 425, pp. 374–376, sep 2003.

[14] B. P. Abbott *et al.*, "Observation of Gravitational Waves from a Binary Black Hole Merger," *Phys. Rev. Lett.*, vol. 116, no. 6, p. 061102, 2016.

[15] B. P. Abbott *et al.*, "GW151226: Observation of Gravitational Waves from a 22-Solar-Mass Binary Black Hole Coalescence," *Phys. Rev. Lett.*, vol. 116, no. 24, p. 241103, 2016.

[16] Peskin and Schroeder, *An Introduction to Quantum Field Theory*.
Westview Press, 1 ed., 2015.

[17] M. Kaku, *Quantum Field Theory: A Modern Introduction*.
Oxford University Press, 1993.

[18] A. Das, *Lectures on Quantum Field Theory*.
World Scientific Publishing Company, 2008.

[19] R. Oerter, *The Theory of Almost Everything: The Standard Model, the Unsung Triumph of Modern Physics*.
Penguin Publishing Group, 2006.

[20] C. Rovelli, *Quantum Gravity*.
Cambridge Monographs on Mathematical Physics, Cambridge University Press, 2004.

[21] R. M. Wald, *General relativity*.
University of Chicago Press, first edition ed., 1984.

[22] G. Hooft, *Introduction to General Relativity*.
Rinton Press, 2001.

[23] S. M. Carroll, "Lecture notes on general relativity," 1997.

[24] B. Zwiebach and C. U. Press, *A First Course in String Theory*.
A First Course in String Theory, Cambridge University Press, 2004.

[25] J. Polchinski, *String Theory: Volume 1, An Introduction to the Bosonic String*.
Cambridge Monographs on Mathematical Physics, Cambridge University Press, 1998.

[26] J. Polchinski, *String theory. Vol. 2: Superstring theory and beyond*.
Cambridge Monographs on Mathematical Physics, Cambridge University Press, 2007.

[27] T. Thiemann, "Modern canonical quantum general relativity," 2001.

[28] A. Ashtekar, "New variables for classical and quantum gravity," *Phys. Rev. Lett.*, vol. 57, pp. 2244–2247, Nov 1986.

[29] A. Ashtekar, "New Hamiltonian Formulation of General Relativity," *Phys. Rev.*, vol. D36, pp. 1587–1602, 1987.

[30] T. Thiemann, "Lectures on loop quantum gravity," *Lect. Notes Phys.*, vol. 631, pp. 41–135, 2003.
[,41(2002)].

[31] A. Ashtekar and J. Lewandowski, "Background independent quantum gravity: A Status report," *Class. Quant. Grav.*, vol. 21, p. R53, 2004.

[32] C. Rovelli, "Loop quantum gravity," *Living Reviews in Relativity*, vol. 1, p. 1, Jan 1998.

[33] T. Thiemann, "Loop Quantum Gravity: An Inside View," *Lect. Notes Phys.*, vol. 721, pp. 185–263, 2007.

[34] L. Smolin, "An Invitation to loop quantum gravity," in *Proceedings, 3rd International Symposium on Quantum theory and symmetries (QTS3): Cincinnati, USA, September 10-14, 2003*, pp. 655–682, 2004.
[Rev. Mod. Phys.(2004)].

[35] T. Padmanabhan, "Duality and zero point length of space-time," *Phys. Rev. Lett.*, vol. 78, pp. 1854–1857, 1997.

[36] D. Kothawala, L. Sriramkumar, S. Shankaranarayanan, and T. Padmanabhan, "Path integral duality modified propagators in spacetimes with constant curvature," *Phys. Rev.*, vol. D80, p. 044005, 2009.

[37] J. F. Donoghue, "Introduction to the effective field theory description of gravity," in *Advanced School on Effective Theories Almunecar, Spain, June 25-July 1, 1995*, 1995.

[38] J. Donoghue, "Perturbative dynamics of quantum general relativity," in *Recent developments in theoretical and experimental general relativity, gravitation, and relativistic field theories. Proceedings, 8th Marcel Grossmann meeting, MG8, Jerusalem, Israel, June 22-27, 1997. Pts. A, B*, pp. 26–39, 1997.

[39] L. Parker and D. Toms, *Quantum Field Theory in Curved Spacetime: Quantized Fields and Gravity*.
Cambridge Monographs on Mathematical Physics, Cambridge University Press, 1 ed., 2009.

[40] R. M. Wald, *Quantum field theory in curved spacetime and black hole thermodynamics*.
University of Chicago Press, 1994.

[41] S. A. Fulling, "Aspects of Quantum Field Theory in Curved Space-time," *London Math. Soc. Student Texts*, vol. 17, pp. 1–315, 1989.

[42] B. S. DeWitt, "Quantum field theory in curved spacetime," *Physics Reports*, vol. 19, no. 6, pp. 295 – 357, 1975.

[43] L. H. Ford, "Quantum field theory in curved space-time," in *Particles and fields. Proceedings, 9th Jorge Andre Swieca Summer School, Campos do Jordao, Brazil, February 16-28, 1997*, pp. 345–388, 1997.

[44] P.-H. Lambert, "Introduction to Black Hole Evaporation," *PoS*, Modave, 2013.

[45] T. Jacobson, "Black holes and Hawking radiation in spacetime and its analogues," *Lect. Notes Phys.*, vol. 870, pp. 1–29, 2013.

[46] C. Kiefer, "Quantum aspects of black holes," in *DPG School of Physics (Course 2): Galactic Black Hole 2001 Bad Honnef, Germany, August 26-31, 2001*, 2002.

[47] J. H. Traschen, "An Introduction to black hole evaporation," in *Mathematical methods in physics. Proceedings, Winter School, Londrina, Brazil, August 17-26, 1999*, 1999.

[48] S. Hollands and R. M. Wald, "Quantum fields in curved spacetime," *Phys. Rept.*, vol. 574, 2015.

[49] T. Padmanabhan, "Thermodynamical Aspects of Gravity: New insights," *Rept.Prog.Phys.*, vol. 73, p. 046901, 2010.

[50] S. Chakraborty, S. Singh, and T. Padmanabhan, "A quantum peek inside the black hole event horizon," *JHEP*, vol. 06, p. 192, 2015.

[51] S. Chakraborty and K. Lochan, "Black Holes: Eliminating Information or Illuminating New Physics?," 2017.

[52] A. D. Helfer, "Do black holes radiate?," *Rept. Prog. Phys.*, vol. 66, pp. 943–1008, 2003.

[53] K. J. Hinton, "Particle detectors in rindler and schwarzchild space-times," *Journal of Physics A: Mathematical and General*, vol. 16, no. 9, p. 1937, 1983.

[54] M. K. Parikh and F. Wilczek, "Hawking radiation as tunneling," *Phys. Rev. Lett.*, vol. 85, pp. 5042–5045, 2000.

[55] M. Visser, "Essential and inessential features of Hawking radiation," *Int. J. Mod. Phys.*, vol. D12, pp. 649–661, 2003.

[56] D. Singleton and S. Wilburn, "Hawking radiation, Unruh radiation and the equivalence principle," *Phys. Rev. Lett.*, vol. 107, p. 081102, 2011.

[57] S. Bhattacharya and A. Lahiri, "Mass function and particle creation in Schwarzschild-de Sitter spacetime," *Eur. Phys. J.*, vol. C73, p. 2673, 2013.

[58] S. Singh, C. Ganguly, and T. Padmanabhan, "Quantum field theory in de Sitter and quasi–de Sitter spacetimes revisited," *Phys. Rev.*, vol. D87, no. 10, p. 104004, 2013.

[59] A. S. Lapedes, "Bogolyubov Transformations, Propagators, and the Hawking Effect," *J. Math. Phys.*, vol. 19, p. 2289, 1978.

[60] P. C. W. Davies, "Scalar particle production in Schwarzschild and Rindler metrics," *J. Phys.*, vol. A8, pp. 609–616, 1975.

[61] R. M. Wald, "On particle creation by black holes," *Communications in Mathematical Physics*, vol. 45, no. 1, pp. 9–34, 1975.

[62] S. Singh and S. Chakraborty, "Black hole kinematics: The "in"-vacuum energy density and flux for different observers," *Phys. Rev.*, vol. D90, no. 2, p. 024011, 2014.

[63] T. Dray and G. 't Hooft, "The effect of spherical shells of matter on the schwarzschild black hole," *Communications in Mathematical Physics*, vol. 99, no. 4, pp. 613–625, 1985.

[64] H. Kawai, Y. Matsuo, and Y. Yokokura, "A Self-consistent Model of the Black Hole Evaporation," *Int. J. Mod. Phys.*, vol. A28, p. 1350050, 2013.

[65] P.-M. Ho, "Comment on Self-Consistent Model of Black Hole Formation and Evaporation," *JHEP*, vol. 08, p. 096, 2015.

[66] S. B. Giddings and W. M. Nelson, "Quantum emission from two-dimensional black holes," *Phys. Rev. D*, vol. 46, pp. 2486–2496, Sep 1992.

[67] J. B. Hartle and S. W. Hawking, "Path Integral Derivation of Black Hole Radiance," *Phys. Rev.*, vol. D13, pp. 2188–2203, 1976.

[68] S. W. Hawking, "Particle Creation by Black Holes," *Commun. Math. Phys.*, vol. 43, pp. 199–220, 1975.
[Erratum: Commun.Math.Phys. 46, 206 (1976)].

[69] K. Schwarzschild, "On the gravitational field of a mass point according to Einstein's theory," *Sitzungsber. Preuss. Akad. Wiss. Berlin (Math. Phys.)*, vol. 1916, pp. 189–196, 1916.

[70] J. Droste, "The field of a single centre in Einstein's theory of gravitation, and the motion of a particle in that field," *Koninklijke Nederlandse Akademie van Wetenschappen Proceedings Series B Physical Sciences*, vol. 19, pp. 197–215, Jan. 1917.

[71] H. Reissner, "über die eigengravitation des elektrischen feldes nach der einsteinschen theorie," *Annalen der Physik*, vol. 355, pp. 106–120, jan 1916.

[72] G. Nordström, "On the Energy of the Gravitation field in Einstein's Theory," *Koninklijke Nederlandse Akademie van Wetenschappen Proceedings Series B Physical Sciences*, vol. 20, pp. 1238–1245, jan 1918.

[73] A. S. Eddington, "A comparison of whitehead's and einstein's formulæ," *Nature*, vol. 113, no. 2832, pp. 192–192, 1924.

[74] G. Lemaître, "L'univers en expansion," in *Annales de la Société scientifique de Bruxelles*, vol. 53, p. 51, 1933.

[75] A. Einstein and N. Rosen, "The particle problem in the general theory of relativity," *Physical Review*, vol. 48, no. 1, p. 73, 1935.

[76] J. L. Synge, "The gravitational field of a particle," in *Proceedings of the Royal Irish Academy. Section A: Mathematical and Physical Sciences*, vol. 53, pp. 83–114, JSTOR, 1950.

[77] D. Finkelstein, "Past-future asymmetry of the gravitational field of a point particle," *Physical Review*, vol. 110, no. 4, p. 965, 1958.

[78] C. Fronsdal, "Completion and embedding of the schwarzschild solution," *Physical Review*, vol. 116, no. 3, p. 778, 1959.

[79] M. D. Kruskal, "Maximal extension of schwarzschild metric," *Physical review*, vol. 119, no. 5, p. 1743, 1960.

[80] G. Szekeres, "On the singularities of a riemannian manifold," *Publicationes Mathematicae Debrecen 7*, vol. 7, p. 285, 1960.

[81] I. Novikov, "On the evolution of a semiclosed world," *Astronomicheskii Zhurnal*, vol. 40, p. 772, 1963.

[82] I. Novikov, "R-and t-regions in space-time with spherically symmetric space," *General Relativity and Gravitation*, vol. 33, no. 12, pp. 2259–2295, 2001.

[83] R. P. Kerr, "Gravitational field of a spinning mass as an example of algebraically special metrics," *Phys. Rev. Lett.*, vol. 11, pp. 237–238, Sep 1963.

[84] K. Akiyama *et al.*, "First M87 Event Horizon Telescope Results. I. The Shadow of the Supermassive Black Hole," *Astrophys. J. Lett.*, vol. 875, p. L1, 2019.

[85] K. Akiyama *et al.*, "First M87 Event Horizon Telescope Results. V. Physical Origin of the Asymmetric Ring," *Astrophys. J. Lett.*, vol. 875, no. 1, p. L5, 2019.

[86] K. Akiyama *et al.*, "First M87 Event Horizon Telescope Results. VI. The Shadow and Mass of the Central Black Hole," *Astrophys. J. Lett.*, vol. 875, no. 1, p. L6, 2019.

[87] K. Hioki and K.-i. Maeda, "Measurement of the kerr spin parameter by observation of a compact object's shadow," *Phys. Rev. D*, vol. 80, p. 024042, Jul 2009.

[88] B. P. Abbott *et al.*, "Observation of Gravitational Waves from a Binary Black Hole Merger," *Phys. Rev. Lett.*, vol. 116, no. 6, p. 061102, 2016.

[89] B. P. Abbott *et al.*, "GW151226: Observation of Gravitational Waves from a 22-Solar-Mass Binary Black Hole Coalescence," *Phys. Rev. Lett.*, vol. 116, no. 24, p. 241103, 2016.

[90] B. P. Abbott *et al.*, "Binary Black Hole Mergers in the first Advanced LIGO Observing Run," *Phys. Rev.*, vol. X6, no. 4, p. 041015, 2016.

[91] B. P. Abbott *et al.*, "GW170104: Observation of a 50-Solar-Mass Binary Black Hole Coalescence at Redshift 0.2," *Phys. Rev. Lett.*, vol. 118, no. 22, p. 221101, 2017.

[92] S. W. Hawking and G. F. R. Ellis, *The Large Scale Structure of Space-Time*. Cambridge Monographs on Mathematical Physics, Cambridge University Press, 2 2011.

[93] R. Penrose, "Gravitational collapse: The role of general relativity," *Riv. Nuovo Cim.*, vol. 1, pp. 252–276, 1969.

[94] D. Christodoulou, "The Formation of Black Holes in General Relativity," in *12th Marcel Grossmann Meeting on General Relativity*, pp. 24–34, 5 2008.

[95] N. Stergioulas, "Numerical simulations of black hole formation," *Lect. Notes Phys.*, vol. 769, pp. 177–208, 2009.

[96] M. W. Choptuik and F. Pretorius, "Ultra Relativistic Particle Collisions," *Phys. Rev. Lett.*, vol. 104, p. 111101, 2010.

[97] C. Misner, "Magic without magic: John archibald wheeler, a collection of essays in honor of his 60th birthday," *Freeman, San Francisco*, 1972.

[98] E. T. Newman, E. Couch, K. Chinnapared, A. Exton, A. Prakash, and R. Torrence, "Metric of a rotating, charged mass," *Journal of mathematical physics*, vol. 6, no. 6, pp. 918–919, 1965.

[99] M. Heusler, *Black Hole Uniqueness Theorems*.
Cambridge Lecture Notes in Physics, Cambridge University Press, 1996.

[100] M. REES, R. RUFFINI, and J. WHEELER, "Black holes, gravitational waves and cosmology: An introduction to current research(book)," *New York, Gordon and Breach, Science Publishers, Inc.(Topics in Astrophysics and Space Physics.*, vol. 10, 1974.

[101] W. Israel, "Event horizons in static vacuum space-times," *Physical review*, vol. 164, no. 5, p. 1776, 1967.

[102] B. Carter, "Axisymmetric Black Hole Has Only Two Degrees of Freedom," *Phys. Rev. Lett.*, vol. 26, pp. 331–333, 1971.

[103] D. C. Robinson, "Uniqueness of the Kerr black hole," *Phys. Rev. Lett.*, vol. 34, pp. 905–906, 1975.

[104] P. O. Mazur, "PROOF OF UNIQUENESS OF THE KERR-NEWMAN BLACK HOLE SOLUTION," *J. Phys. A*, vol. 15, pp. 3173–3180, 1982.

[105] J. D. Bekenstein, "Nonexistence of baryon number for black holes. ii," *Phys. Rev. D*, vol. 5, pp. 2403–2412, 1972.

[106] C. Teitelboim, "Nonmeasurability of the quantum numbers of a black hole," *Phys. Rev. D*, vol. 5, pp. 2941–2954, 1972.

[107] S. W. Hawking, "Black holes in general relativity," *Communications in Mathematical Physics*, vol. 25, no. 2, pp. 152–166, 1972.

[108] J. M. Bardeen, B. Carter, and S. W. Hawking, "The Four laws of black hole mechanics," *Commun. Math. Phys.*, vol. 31, pp. 161–170, 1973.

[109] R. M. Wald, *Quantum Field Theory in Curved Space-Time and Black Hole Thermodynamics*.
Chicago Lectures in Physics, Chicago, IL: University of Chicago Press, 1995.

[110] D. Sudarsky and R. M. Wald, "Extrema of mass, stationarity, and staticity, and solutions to the einstein-yang-mills equations," *Phys. Rev. D*, vol. 46, pp. 1453–1474, Aug 1992.

[111] V. Iyer and R. M. Wald, "Some properties of Noether charge and a proposal for dynamical black hole entropy," *Phys. Rev. D*, vol. 50, pp. 846–864, 1994.

[112] C. W. Misner, K. S. Thorne, and J. A. Wheeler, *Gravitation*. Macmillan, 1973.

[113] S. W. Hawking, "Black hole explosions," *Nature*, vol. 248, pp. 30–31, 1974.

[114] J. D. Bekenstein, "Black holes and entropy," *Phys. Rev. D*, vol. 7, pp. 2333–2346, 1973.

[115] J. D. Bekenstein, "Black holes and the second law," *Lett. Nuovo Cim.*, vol. 4, pp. 737–740, 1972.

[116] N. D. Birrell and P. C. W. Davies, *Quantum Fields in Curved Space*. Cambridge Monographs on Mathematical Physics, Cambridge, UK: Cambridge Univ. Press, 2 1984.

[117] G. W. Gibbons and S. W. Hawking, "Action Integrals and Partition Functions in Quantum Gravity," *Phys. Rev. D*, vol. 15, pp. 2752–2756, 1977.

[118] G. W. Gibbons and S. W. Hawking, "Cosmological Event Horizons, Thermodynamics, and Particle Creation," *Phys. Rev. D*, vol. 15, pp. 2738–2751, 1977.

[119] S. M. Christensen and S. A. Fulling, "Trace Anomalies and the Hawking Effect," *Phys. Rev. D*, vol. 15, pp. 2088–2104, 1977.

[120] S. P. Robinson and F. Wilczek, "A Relationship between Hawking radiation and gravitational anomalies," *Phys. Rev. Lett.*, vol. 95, p. 011303, 2005.

[121] S. Iso, H. Umetsu, and F. Wilczek, "Hawking radiation from charged black holes via gauge and gravitational anomalies," *Phys. Rev. Lett.*, vol. 96, p. 151302, 2006.

[122] S. Iso, H. Umetsu, and F. Wilczek, "Anomalies, Hawking radiations and regularity in rotating black holes," *Phys. Rev. D*, vol. 74, p. 044017, 2006.

[123] L. Alvarez-Gaume and E. Witten, "Gravitational Anomalies," *Nucl. Phys. B*, vol. 234, p. 269, 1984.

[124] R. Banerjee and S. Kulkarni, "Hawking radiation and covariant anomalies," *Phys. Rev. D*, vol. 77, p. 024018, 2008.

[125] K. S. Gajanan, "Field theory aspects of cosmology and black holes," other thesis, 11 2010.

[126] R. Banerjee, "Covariant Anomalies, Horizons and Hawking Radiation," *Int. J. Mod. Phys. D*, vol. 17, pp. 2539–2542, 2009.

[127] R. Banerjee and S. Kulkarni, "Hawking radiation, effective actions and covariant boundary conditions," *Phys. Lett. B*, vol. 659, pp. 827–831, 2008.

[128] R. Banerjee and S. Kulkarni, "Hawking Radiation, Covariant Boundary Conditions and Vacuum States," *Phys. Rev. D*, vol. 79, p. 084035, 2009.

[129] B. R. Majhi, "Thermodynamics of Sultana-Dyer Black Hole," *JCAP*, vol. 05, p. 014, 2014.

[130] P. Kraus and F. Wilczek, "Some applications of a simple stationary line element for the Schwarzschild geometry," *Mod. Phys. Lett. A*, vol. 9, pp. 3713–3719, 1994.

[131] P. Kraus and F. Wilczek, "Selfinteraction correction to black hole radiance," *Nucl. Phys. B*, vol. 433, pp. 403–420, 1995.

[132] P. Kraus and F. Wilczek, "Effect of selfinteraction on charged black hole radiance," *Nucl. Phys. B*, vol. 437, pp. 231–242, 1995.

[133] E. Keski-Vakkuri and P. Kraus, "Microcanonical D-branes and back reaction," *Nucl. Phys. B*, vol. 491, pp. 249–262, 1997.

[134] V. A. Berezin, A. Boyarsky, and A. Y. Neronov, "On the Mechanism of Hawking radiation," *Grav. Cosmol.*, vol. 5, pp. 16–22, 1999.

[135] G. E. Volovik, "Simulation of Painleve-Gullstrand black hole in thin He-3 - A film," *JETP Lett.*, vol. 69, pp. 705–713, 1999.

[136] A. Calogeracos and G. E. Volovik, "Rotational quantum friction in superfluids: Radiation from object rotating in superfluid vacuum," *JETP Lett.*, vol. 69, pp. 281–287, 1999.

[137] M. K. Parikh, "New coordinates for de Sitter space and de Sitter radiation," *Phys. Lett. B*, vol. 546, pp. 189–195, 2002.

[138] M. K. Parikh, "A Secret tunnel through the horizon," *Int. J. Mod. Phys. D*, vol. 13, pp. 2351–2354, 2004.

[139] M. K. Parikh, "Energy conservation and Hawking radiation," in *10th Marcel Grossmann Meeting on Recent Developments in Theoretical and Experimental General Relativity, Gravitation and Relativistic Field Theories (MG X MMIII)*, pp. 1585–1590, 2 2004.

[140] K. Srinivasan and T. Padmanabhan, "Particle production and complex path analysis," *Phys. Rev. D*, vol. 60, p. 024007, 1999.

[141] S. Shankaranarayanan, K. Srinivasan, and T. Padmanabhan, "Method of complex paths and general covariance of Hawking radiation," *Mod. Phys. Lett. A*, vol. 16, pp. 571–578, 2001.

[142] S. Shankaranarayanan, T. Padmanabhan, and K. Srinivasan, "Hawking radiation in different coordinate settings: Complex paths approach," *Class. Quant. Grav.*, vol. 19, pp. 2671–2688, 2002.

[143] T. Padmanabhan, "Entropy of horizons, complex paths and quantum tunneling," *Mod. Phys. Lett. A*, vol. 19, pp. 2637–2643, 2004.

[144] E. C. Vagenas, "Are extremal 2-D black holes really frozen?," *Phys. Lett. B*, vol. 503, pp. 399–403, 2001.

[145] A. J. M. Medved, "Radiation via tunneling from a de Sitter cosmological horizon," *Phys. Rev. D*, vol. 66, p. 124009, 2002.

[146] S. Shankaranarayanan, "Temperature and entropy of Schwarzschild-de Sitter space-time," *Phys. Rev. D*, vol. 67, p. 084026, 2003.

[147] A. J. M. Medved and E. C. Vagenas, "On Hawking radiation as tunneling with back-reaction," *Mod. Phys. Lett. A*, vol. 20, pp. 2449–2454, 2005.

[148] M. Arzano, A. J. M. Medved, and E. C. Vagenas, "Hawking radiation as tunneling through the quantum horizon," *JHEP*, vol. 09, p. 037, 2005.

[149] M. Angheben, M. Nadalini, L. Vanzo, and S. Zerbini, "Hawking radiation as tunneling for extremal and rotating black holes," *JHEP*, vol. 05, p. 014, 2005.

[150] Q.-Q. Jiang and S.-Q. Wu, "Hawking radiation of charged particles as tunneling from Reissner-Nordström-de Sitter black holes with a global monopole," *Phys. Lett. B*, vol. 635, pp. 151–155, 2006.
[Erratum: Phys.Lett.B 639, 684–684 (2006)].

[151] Q.-Q. Jiang, S.-Q. Wu, and X. Cai, "Hawking radiation as tunneling from the Kerr and Kerr-Newman black holes," *Phys. Rev. D*, vol. 73, p. 064003, 2006.
[Erratum: Phys.Rev.D 73, 069902 (2006)].

[152] J.-Y. Zhang and Z. Zhao, "Hawking radiation of charged particles via tunneling from the Reissner-Nordstroem black hole," *JHEP*, vol. 10, p. 055, 2005.

[153] J. Zhang and Z. Zhao, "Charged particles' tunnelling from the Kerr-Newman black hole," *Phys. Lett. B*, vol. 638, pp. 110–113, 2006.

[154] Y.-p. Hu, J.-y. Zhang, and Z. Zhao, "The Relation between Hawking radiation via tunnelling and the laws of black hole thermodynamics," 1 2006.

[155] R. Zhao, H.-F. Li, and S.-L. Zhang, "Canonical Entropy of charged black hole," 8 2006.

[156] L. Zhao, "Tunnelling through black rings," *Commun. Theor. Phys.*, vol. 47, pp. 835–842, 2007.

[157] S.-Q. Wu and Q.-Q. Jiang, "Remarks on Hawking radiation as tunneling from the BTZ black holes," *JHEP*, vol. 03, p. 079, 2006.

[158] R. Kerner and R. B. Mann, "Tunnelling, temperature and Taub-NUT black holes," *Phys. Rev. D*, vol. 73, p. 104010, 2006.

[159] S.-Q. Wu and Q.-Q. Jiang, "Hawking radiation of charged particles as tunneling from higher dimensional Reissner-Nordstrom-de Sitter black holes," 3 2006.

[160] B. D. Chowdhury, "Problems with Tunneling of Thin Shells from Black Holes," *Pramana*, vol. 70, pp. 593–612, 2008.

[161] E. T. Akhmedov, V. Akhmedova, T. Pilling, and D. Singleton, "Thermal radiation of various gravitational backgrounds," *Int. J. Mod. Phys. A*, vol. 22, pp. 1705–1715, 2007.

[162] E. T. Akhmedov, V. Akhmedova, and D. Singleton, "Hawking temperature in the tunneling picture," *Phys. Lett. B*, vol. 642, pp. 124–128, 2006.

[163] V. Akhmedova, T. Pilling, A. de Gill, and D. Singleton, "Temporal contribution to gravitational WKB-like calculations," *Phys. Lett. B*, vol. 666, pp. 269–271, 2008.

[164] J. Ren, J. Zhang, and Z. Zhao, "Tunnelling Effect and Hawking Radiation from a Vaidya Black Hole," *Chin. Phys. Lett.*, vol. 23, pp. 2019–2022, 2006.

[165] P. Mitra, "Hawking temperature from tunnelling formalism," *Phys. Lett. B*, vol. 648, pp. 240–242, 2007.

[166] S. Yang and D. Chen, "A new method to study hawking tunneling radiation of the charged particles from ressiner-nordström black hole," *International Journal of Theoretical Physics*, vol. 46, no. 7, pp. 1747–1752, 2007.

[167] B. Chatterjee, A. Ghosh, and P. Mitra, "Tunnelling from black holes in the Hamilton Jacobi approach," *Phys. Lett. B*, vol. 661, pp. 307–311, 2008.

[168] R. Di Criscienzo, M. Nadalini, L. Vanzo, S. Zerbini, and G. Zoccatelli, "On the Hawking radiation as tunneling for a class of dynamical black holes," *Phys. Lett. B*, vol. 657, pp. 107–111, 2007.

[169] R. Kerner and R. B. Mann, "Tunnelling from Godel black holes," *Phys. Rev. D*, vol. 75, p. 084022, 2007.

[170] R. Banerjee and B. R. Majhi, "Quantum Tunneling and Back Reaction," *Phys. Lett. B*, vol. 662, pp. 62–65, 2008.

[171] R. Banerjee, B. R. Majhi, and S. Samanta, "Noncommutative Black Hole Thermodynamics," *Phys. Rev. D*, vol. 77, p. 124035, 2008.

[172] R. Banerjee and B. R. Majhi, "Quantum Tunneling Beyond Semiclassical Approximation," *JHEP*, vol. 06, p. 095, 2008.

[173] R. Banerjee and B. R. Majhi, "Connecting anomaly and tunneling methods for Hawking effect through chirality," *Phys. Rev. D*, vol. 79, p. 064024, 2009.

[174] R. Banerjee and B. R. Majhi, "Hawking black body spectrum from tunneling mechanism," *Phys. Lett. B*, vol. 675, pp. 243–245, 2009.

[175] B. R. Majhi, *Quantum Tunneling in Black Holes*.
PhD thesis, Calcutta U., 2010.

[176] R. Banerjee, B. R. Majhi, and E. C. Vagenas, "Quantum tunneling and black hole spectroscopy," *Phys. Lett. B*, vol. 686, pp. 279–282, 2010.

[177] B. R. Majhi, "Hawking radiation and black hole spectroscopy in Horava-Lifshitz gravity," *Phys. Lett. B*, vol. 686, pp. 49–54, 2010.

[178] R. Banerjee, B. R. Majhi, and E. C. Vagenas, "A Note on the Lower Bound of Black Hole Area Change in Tunneling Formalism," *EPL*, vol. 92, no. 2, p. 20001, 2010.

[179] B. R. Majhi, "Emergent gravity: From statistical point of view," *J. Phys. Conf. Ser.*, vol. 405, p. 012020, 2012.

[180] K. Bhattacharya and B. R. Majhi, "Temperature and thermodynamic structure of Einstein's equations for a cosmological black hole," *Phys. Rev. D*, vol. 94, no. 2, p. 024033, 2016.

[181] R. Kerner and R. B. Mann, "Fermions tunnelling from black holes," *Class. Quant. Grav.*, vol. 25, p. 095014, 2008.

[182] Y. Sekiwa, "Decay of the cosmological constant by Hawking radiation as quantum tunneling," 2 2008.

[183] A. J. M. Medved, "A Brief Editorial on de Sitter Radiation via Tunneling," 2 2008.

[184] G. E. Volovik, "On de Sitter radiation via quantum tunneling," *Int. J. Mod. Phys. D*, vol. 18, p. 1227, 2009.

[185] R. Li and J.-R. Ren, "Dirac particles tunneling from BTZ black hole," *Phys. Lett. B*, vol. 661, pp. 370–372, 2008.

[186] R. Di Criscienzo and L. Vanzo, "Fermion Tunneling from Dynamical Horizons," *EPL*, vol. 82, no. 6, p. 60001, 2008.

[187] R. Li, J.-R. Ren, and S.-W. Wei, "Hawking radiation of Dirac particles via tunneling from Kerr black hole," *Class. Quant. Grav.*, vol. 25, p. 125016, 2008.

[188] R. Kerner and R. B. Mann, "Charged Fermions Tunnelling from Kerr-Newman Black Holes," *Phys. Lett. B*, vol. 665, pp. 277–283, 2008.

[189] D.-Y. Chen, Q.-Q. Jiang, and X.-T. Zu, "Hawking radiation of Dirac particles via tunnelling from rotating black holes in de Sitter spaces," *Phys. Lett. B*, vol. 665, pp. 106–110, 2008.

[190] E. C. Vagenas, "Generalization of the KKW analysis for black hole radiation," *Phys. Lett. B*, vol. 559, pp. 65–73, 2003.

[191] E. C. Vagenas, "Complex paths and covariance of Hawking radiation in 2-D stringy black holes," *Nuovo Cim. B*, vol. 117, pp. 899–908, 2002.

[192] E. C. Vagenas, "Two-dimensional dilatonic black holes and Hawking radiation," *Mod. Phys. Lett. A*, vol. 17, pp. 609–618, 2002.

[193] Y.-P. Hu, J.-Y. Zhang, and Z. Zhao, "Massive particles-prime Hawking radiation via tunneling from the G.H. dilaton black hole," *Mod. Phys. Lett. A*, vol. 21, pp. 2143–2149, 2006.

[194] Z. Xu and B. Chen, "Hawking radiation from general Kerr-(anti)de Sitter black holes," *Phys. Rev. D*, vol. 75, p. 024041, 2007.

[195] C.-Z. Liu and J.-Y. Zhu, "Hawking radiation and black hole entropy in a gravity ' *s* rainbow," *Gen. Rel. Grav.*, vol. 40, pp. 1899–1911, 2008.

[196] A. Yale and R. B. Mann, "Gravitinos Tunneling from Black Holes," *Phys. Lett. B*, vol. 673, pp. 168–172, 2009.

[197] D.-Y. Chen, Q.-Q. Jiang, S.-Z. Yang, and X.-T. Zu, "Fermions tunnelling from the charged dilatonic black holes," *Class. Quant. Grav.*, vol. 25, p. 205022, 2008.

[198] E. T. Akhmedov, T. Pilling, and D. Singleton, "Subtleties in the quasi-classical calculation of Hawking radiation," *Int. J. Mod. Phys. D*, vol. 17, pp. 2453–2458, 2008.

[199] T. Pilling, "Tunneling derived from Black Hole Thermodynamics," *Phys. Lett. B*, vol. 660, pp. 402–406, 2008.

[200] T. K. Nakamura, "Factor two discrepancy of Hawking radiation temperature," 6 2007.

[201] R. Banerjee and B. R. Majhi, "Quantum Tunneling, Trace Anomaly and Effective Metric," *Phys. Lett. B*, vol. 674, pp. 218–222, 2009.

[202] B. R. Majhi, "Fermion Tunneling Beyond Semiclassical Approximation," *Phys. Rev. D*, vol. 79, p. 044005, 2009.

[203] B. R. Majhi and S. Samanta, "Hawking Radiation due to Photon and Gravitino Tunneling," *Annals Phys.*, vol. 325, pp. 2410–2424, 2010.

[204] S. K. Modak, "Corrected entropy of BTZ black hole in tunneling approach," *Phys. Lett. B*, vol. 671, pp. 167–173, 2009.

[205] R. Banerjee and S. K. Modak, "Exact Differential and Corrected Area Law for Stationary Black Holes in Tunneling Method," *JHEP*, vol. 05, p. 063, 2009.

[206] R. Banerjee and S. K. Modak, "Quantum Tunneling, Blackbody Spectrum and Non-Logarithmic Entropy Correction for Lovelock Black Holes," *JHEP*, vol. 11, p. 073, 2009.

[207] R. Banerjee, S. Gangopadhyay, and S. K. Modak, "Voros product, Noncommutative Schwarzschild Black Hole and Corrected Area Law," *Phys. Lett. B*, vol. 686, pp. 181–187, 2010.

[208] P. Painleve, "La mécanique classique et la théorie de la relativité," *Comptes Rendue de lÁcademie de Seances*, vol. 173, pp. 677–680, 1921.

[209] W. G. Unruh, "Notes on black hole evaporation," *Phys. Rev. D*, vol. 14, p. 870, 1976.

[210] S. D. Mathur, "The Information paradox: A Pedagogical introduction," *Class. Quant. Grav.*, vol. 26, p. 224001, 2009.

[211] R. Mann and T. Steele, "Thermodynamics and quantum aspects of black holes in (1+ 1) dimensions," *Classical and Quantum Gravity*, vol. 9, no. 2, p. 475, 1992.

[212] S. K. Modak, L. Ortíz, I. Peña, and D. Sudarsky, "Non-Paradoxical Loss of Information in Black Hole Evaporation in a Quantum Collapse Model," *Phys. Rev. D*, vol. 91, no. 12, p. 124009, 2015.

[213] S. L. Adler and A. C. Millard, "Generalized quantum dynamics as prequantum mechanics," *Nucl. Phys. B*, vol. 473, pp. 199–244, 1996.

[214] A. Bassi and G. C. Ghirardi, "Dynamical reduction models," *Phys. Rept.*, vol. 379, p. 257, 2003.

[215] A. Bassi, K. Lochan, S. Satin, T. P. Singh, and H. Ulbricht, "Models of Wave-function Collapse, Underlying Theories, and Experimental Tests," *Rev. Mod. Phys.*, vol. 85, pp. 471–527, 2013.

[216] S. W. Hawking, "Quantum Gravity and Path Integrals," *Phys. Rev. D*, vol. 18, pp. 1747–1753, 1978.

[217] R. P. Feynman, "Space-time approach to non-relativistic quantum mechanics," in *Feynman's Thesis—A New Approach To Quantum Theory*, pp. 71–109, World Scientific, 2005.

[218] J. D. Bekenstein, "Generalized second law of thermodynamics in black hole physics," *Phys. Rev. D*, vol. 9, pp. 3292–3300, 1974.

[219] V. Cardoso, A. S. Miranda, E. Berti, H. Witek, and V. T. Zanchin, "Geodesic stability, Lyapunov exponents and quasinormal modes," *Phys. Rev. D*, vol. 79, no. 6, p. 064016, 2009.

[220] K. Hashimoto and N. Tanahashi, "Universality in Chaos of Particle Motion near Black Hole Horizon," *Phys. Rev. D*, vol. 95, no. 2, p. 024007, 2017.

[221] K. Hashimoto, K. Murata, and N. Tanahashi, "Chaos of Wilson Loop from String Motion near Black Hole Horizon," *Phys. Rev. D*, vol. 98, no. 8, p. 086007, 2018.

[222] F. Lu, J. Tao, and P. Wang, "Minimal Length Effects on Chaotic Motion of Particles around Black Hole Horizon," *JCAP*, vol. 12, p. 036, 2018.

[223] M. Čubrović, "The bound on chaos for closed strings in Anti-de Sitter black hole backgrounds," *JHEP*, vol. 12, p. 150, 2019.

[224] P. Colangelo, F. De Fazio, and N. Losacco, "Chaos in a $Q\bar{Q}$ system at finite temperature and baryon density," *Phys. Rev. D*, vol. 102, no. 7, p. 074016, 2020.

[225] D.-Z. Ma, D. Zhang, G. Fu, and J.-P. Wu, "Chaotic dynamics of string around charged black brane with hyperscaling violation," *JHEP*, vol. 01, p. 103, 2020.

[226] J. Maldacena, S. H. Shenker, and D. Stanford, "A bound on chaos," *JHEP*, vol. 08, p. 106, 2016.

[227] K. Hashimoto, K. Murata, and R. Yoshii, "Out-of-time-order correlators in quantum mechanics," *JHEP*, vol. 10, p. 138, 2017.

[228] S. H. Strogatz, "Nonlinear dynamics and chaos: with applications to physics," *Biology, Chemistry and Engineering*, p. 1, 1994.

[229] S. H. Shenker and D. Stanford, "Black holes and the butterfly effect," *JHEP*, vol. 03, p. 067, 2014.

[230] Z. Tian, Y. Lin, U. R. Fischer, and J. Du, "Testing the upper bound on the speed of scrambling with an analogue of Hawking radiation using trapped ions," *Eur. Phys. J. C*, vol. 82, no. 3, p. 212, 2022.

[231] M. Srednicki, "Chaos and quantum thermalization," *Phys. Rev. E*, vol. 50, pp. 888–901, Aug 1994.

[232] T. Morita, "Thermal Emission from Semi-classical Dynamical Systems," *Phys. Rev. Lett.*, vol. 122, no. 10, p. 101603, 2019.

[233] S. S. Hegde, V. Subramanyan, B. Bradlyn, and S. Vishveshwara, "Quasinormal Modes and the Hawking-Unruh Effect in Quantum Hall Systems: Lessons from Black Hole Phenomena," *Phys. Rev. Lett.*, vol. 123, no. 15, p. 156802, 2019.

[234] J. M. Maldacena and N. Seiberg, "Flux-vacua in two dimensional string theory," *JHEP*, vol. 09, p. 077, 2005.

[235] P. Betzios, N. Gaddam, and O. Papadoulaki, "The Black Hole S-Matrix from Quantum Mechanics," *JHEP*, vol. 11, p. 131, 2016.

[236] S. Dalui, B. R. Majhi, and P. Mishra, "Presence of horizon makes particle motion chaotic," *Phys. Lett. B*, vol. 788, pp. 486–493, 2019.

[237] S. Dalui, B. R. Majhi, and P. Mishra, "Induction of chaotic fluctuations in particle dynamics in a uniformly accelerated frame," *Int. J. Mod. Phys. A*, vol. 35, no. 18, p. 2050081, 2020.

[238] S. Dalui, B. R. Majhi, and P. Mishra, "Horizon induces instability locally and creates quantum thermality," *Phys. Rev. D*, vol. 102, no. 4, p. 044006, 2020.

[239] S. Dalui and B. R. Majhi, "Near horizon local instability and quantum thermality," *Phys. Rev. D*, vol. 102, no. 12, p. 124047, 2020.

[240] S. Dalui and B. R. Majhi, "Horizon thermalization of Kerr black hole through local instability," *Phys. Lett. B*, vol. 826, p. 136899, 2022.

[241] S. Dalui, B. R. Majhi, and T. Padmanabhan, "Thermal nature of a generic null surface," *Phys. Rev. D*, vol. 104, no. 12, p. 124080, 2021.

[242] A. Adhikari, K. Bhattacharya, C. Chowdhury, and B. R. Majhi, "Fluctuation-dissipation relation in accelerated frames," *Phys. Rev. D*, vol. 97, no. 4, p. 045003, 2018.

[243] L. Bombelli and E. Calzetta, "Chaos around a black hole," *Class. Quant. Grav.*, vol. 9, pp. 2573–2599, 1992.

[244] Y. Sota, S. Suzuki, and K.-i. Maeda, "Chaos in static axisymmetric space-times. 1: Vacuum case," *Class. Quant. Grav.*, vol. 13, pp. 1241–1260, 1996.

[245] W. M. Vieira and P. S. Letelier, "Chaos around a Henon-Heiles inspired exact perturbation of a black hole," *Phys. Rev. Lett.*, vol. 76, pp. 1409–1412, 1996.

[246] S. Suzuki and K.-i. Maeda, "Chaos in Schwarzschild space-time: The motion of a spinning particle," *Phys. Rev. D*, vol. 55, pp. 4848–4859, 1997.

[247] N. J. Cornish and N. E. Frankel, "The Black hole and the pea," *Phys. Rev. D*, vol. 56, pp. 1903–1907, 1997.

[248] A. P. S. de Moura and P. S. Letelier, "Chaos and fractals in geodesic motions around a nonrotating black hole with an external halo," *Phys. Rev. E*, vol. 61, pp. 6506–6516, 2000.

[249] M. D. Hartl, "Dynamics of spinning test particles in Kerr space-time," *Phys. Rev. D*, vol. 67, p. 024005, 2003.

[250] W. Han, "Chaos and dynamics of spinning particles in Kerr spacetime," *Gen. Rel. Grav.*, vol. 40, pp. 1831–1847, 2008.

[251] M. Takahashi and H. Koyama, "Chaotic motion of Charged Particles in an Electromagnetic Field Surrounding a Rotating Black Hole," *Astrophys. J.*, vol. 693, pp. 472–485, 2009.

[252] D. Li and X. Wu, "Chaotic motion of neutral and charged particles in a magnetized Ernst-Schwarzschild spacetime," *Eur. Phys. J. Plus*, vol. 134, no. 3, p. 96, 2019.

[253] S. Carroll, *Spacetime and geometry. An introduction to general relativity*. Addison Wesley, 2004.

[254] Y. Zhang, X. Liu, M. R. Belić, W. Zhong, Y. Zhang, and M. Xiao, "Propagation dynamics of a light beam in a fractional schrödinger equation," *Phys. Rev. Lett.*, vol. 115, p. 180403, Oct 2015.

[255] K. Kowalski and J. Rembielinski, "The Relativistic massless harmonic oscillator," *Phys. Rev. A*, vol. 81, p. 012118, 2010.

[256] J. Guckenheimer and P. Holmes, *Nonlinear oscillations, dynamical systems, and bifurcations of vector fields*, vol. 42.
Springer Science and Business Media, 2013.

[257] M. Sandri, "Numerical calculation of lyapunov exponents," *Math. J.*, vol. 6, no. 3, p. 78 – 84, 1996.

[258] P. Stoica and R. Moses, "Spectral analysis of signals," 2005.

[259] E. E. Zotos, "Classifying orbits in the classical hénon–heiles hamiltonian system," *Nonlinear Dynamics*, vol. 79, no. 3, pp. 1665–1677, 2015.

[260] T. Stachowiak and T. Okada, "A numerical analysis of chaos in the double pendulum," *Chaos, Solitons and Fractals*, vol. 29, no. 2, pp. 417–422, 2006.

[261] I. Percival, "Chaos in hamiltonian systems," p. 131 – 143, 1987.

[262] T. Padmanabhan, *Gravitation: Foundations and frontiers*.
Cambridge University Press, 12 2014.

[263] N. J. Cornish and G. W. Gibbons, "The Tale of two centers," *Class. Quant. Grav.*, vol. 14, pp. 1865–1881, 1997.

[264] A. Das, S. Dalui, C. Chowdhury, and B. R. Majhi, "Conformal vacuum and the fluctuation-dissipation theorem in a de Sitter universe and black hole spacetimes," *Phys. Rev. D*, vol. 100, no. 8, p. 085002, 2019.

[265] P. K. Mishra, J. Herault, S. Fauve, and M. K. Verma, "Dynamics of reversals and condensates in two-dimensional kolmogorov flows," *Phys. Rev. E*, vol. 91, p. 053005, May 2015.

[266] Q.-Q. Zhao, Y.-Z. Li, and H. Lu, "Static Equilibria of Charged Particles Around Charged Black Holes: Chaos Bound and Its Violations," *Phys. Rev. D*, vol. 98, no. 12, p. 124001, 2018.

[267] V. Kaloshin and M. Levi, "Geometry of arnold diffusion," *SIAM Review*, vol. 50, no. 4, pp. 702–720, 2008.

[268] X. Guo, K. Liang, B. Mu, P. Wang, and M. Yang, "Minimal Length Effects on Motion of a Particle in Rindler Space," *Chin. Phys. C*, vol. 45, no. 2, p. 023115, 2021.

[269] C. Doran, "A New form of the Kerr solution," *Phys. Rev. D*, vol. 61, p. 067503, 2000.

[270] K. Chakraborty and B. R. Majhi, "Detector response along null geodesics in black hole spacetimes and in a Friedmann-Lemaitre-Robertson-Walker Universe," *Phys. Rev. D*, vol. 100, no. 4, p. 045004, 2019.

[271] R. Banerjee and B. R. Majhi, "Fluctuation–dissipation relation from anomalous stress tensor and Hawking effect," *Eur. Phys. J. C*, vol. 80, no. 5, p. 435, 2020.

[272] A. Bakshi, B. R. Majhi, and S. Samanta, "Gravitational surface Hamiltonian and entropy quantization," *Phys. Lett. B*, vol. 765, pp. 334–338, 2017.

[273] M. V. Berry and J. P. Keating, *H=xp and the Riemann Zeros*, pp. 355–367. Boston, MA: Springer US, 1999.

[274] H.-J. Stöckmann, *Quantum Chaos, an introduction*. Cambridge University Press, 1999.

[275] E. Gourgoulhon and J. L. Jaramillo, "A 3+1 perspective on null hypersurfaces and isolated horizons," *Phys. Rept.*, vol. 423, pp. 159–294, 2006.

[276] E. Poisson, *A Relativist's Toolkit: The Mathematics of Black-Hole Mechanics*. Cambridge University Press, 12 2009.

[277] M. Maitra, D. Maity, and B. R. Majhi, "Near horizon symmetries, emergence of Goldstone modes and thermality," *Eur. Phys. J. Plus*, vol. 135, no. 6, p. 483, 2020.

[278] P. C. W. Davies, S. A. Fulling, and W. G. Unruh, "Energy Momentum Tensor Near an Evaporating Black Hole," *Phys. Rev. D*, vol. 13, pp. 2720–2723, 1976.

[279] R. M. Wald, "The thermodynamics of black holes," *Living Rev. Rel.*, vol. 4, p. 6, 2001.

[280] S. Carlip, "Black Hole Thermodynamics," *Int. J. Mod. Phys. D*, vol. 23, p. 1430023, 2014.

[281] W. G. Unruh, "Particle detectors and black holes," *Proceedings of the 1st Marcel Grossmann Meeting on General Relativity, edited by R. Ruffini*, pp. 527–536, 1977.

[282] B. S. Dewitt, "Particle detectors and black holes," *General relativity: An Einstein centenary survey, edited by S. W. Hawking and W. Israel*, pp. 680–745, 1979.

[283] L. C. B. Crispino, A. Higuchi, and G. E. A. Matsas, "The Unruh effect and its applications," *Rev. Mod. Phys.*, vol. 80, pp. 787–838, 2008.

[284] M. O. Scully, S. Fulling, D. Lee, D. N. Page, W. Schleich, and A. Svidzinsky, "Quantum optics approach to radiation from atoms falling into a black hole," *Proc. Nat. Acad. Sci.*, vol. 115, no. 32, pp. 8131–8136, 2018.

[285] G. B. Arfken and H. J. Weber, *Mathematical Methods for Physicists*. New York, USA: Academic Press, sixth ed., 2012.

[286] M. V. Berry, "Riemann's Zeta function: A model for quantum chaos?," *Lect. Notes Phys.*, vol. 263, pp. 1–17, 1986.

[287] M. Berry and J. Keating, *$H = xp$ and the Riemann zeros*, pp. 355 – 367. United States: Plenum Press, 1999.

[288] M. V. Berry and J. P. Keating, "The riemann zeros and eigenvalue asymptotics," *SIAM Review*, vol. 41, no. 2, pp. 236–266, 1999.

[289] R. K. Bhaduri, A. Khare, S. M. Reimann, and E. L. Tomusiak, "The Riemann Zeta Function and the Inverted Harmonic Oscillator," *Annals of Physics*, vol. 254, pp. 25–40, Feb. 1997.

[290] M. C. Gutzwiller, *Chaos in classical and quantum mechanics*, vol. 1. Springer Science and Business Media, 2013.

[291] G. Sierra, "A quantum mechanical model of the Riemann zeros," *New J. Phys.*, vol. 10, p. 033016, 2008.

[292] M. V. Berry, "Private communication,"

[293] G. Barton, "Quantum Mechanics of the Inverted Oscillator Potential," *Annals Phys.*, vol. 166, p. 322, 1986.

[294] S. Gentilini, M. C. Braidotti, G. Marcucci, E. DelRe, and C. Conti, "Physical realization of the glauber quantum oscillator," *Scientific Reports*, vol. 5, no. 1, pp. 1–6, 2015.

[295] S. W. Hawking, "The path integral approach to quantum gravity," *General Relativity: An Einstein Centenary Survey, eds. S. W. Hawking and W. Israel*, 1979.

[296] O. Scarlatella, A. A. Clerk, and M. Schiro, "Spectral functions and negative density of states of a driven-dissipative nonlinear quantum resonator," *New Journal of Physics*, vol. 21, no. 4, p. 043040, 2019.

[297] I. S. Gomez, M. Losada, and O. Lombardi, "About the concept of quantum chaos," *Entropy*, vol. 19, no. 5, 2017.

[298] B. Yan, L. Cincio, and W. H. Zurek, "Information Scrambling and Loschmidt Echo," *Phys. Rev. Lett.*, vol. 124, no. 16, p. 160603, 2020.

[299] K. D. Kokkotas and B. G. Schmidt, "Quasinormal modes of stars and black holes," *Living Rev. Rel.*, vol. 2, p. 2, 1999.

[300] E. Berti, V. Cardoso, and A. O. Starinets, "Quasinormal modes of black holes and black branes," *Class. Quant. Grav.*, vol. 26, p. 163001, 2009.

[301] R. A. Konoplya and A. Zhidenko, "Quasinormal modes of black holes: From astrophysics to string theory," *Rev. Mod. Phys.*, vol. 83, pp. 793–836, 2011.

[302] A. Das, *Field Theory*.
World Scientific, 2nd ed., 2006.

[303] M. R. Setare, A. Jalali, and B. R. Majhi, "Thermalization of horizon through asymptotic symmetry in three-dimensional massive gravity," *Phys. Lett. B*, vol. 818, p. 136350, 2021.

[304] B. R. Majhi, "Is instability near a black hole key for "thermalization" of its horizon?," *Gen. Rel. Grav.*, vol. 54, no. 8, p. 90, 2022.

[305] V. Subramanyan, S. S. Hegde, S. Vishveshwara, and B. Bradlyn, "Physics of the Inverted Harmonic Oscillator: From the lowest Landau level to event horizons," *Annals Phys.*, vol. 435, p. 168470, 2021.

[306] H. E. Camblong, A. Chakraborty, and C. R. Ordonez, "Near-horizon aspects of acceleration radiation by free fall of an atom into a black hole," *Phys. Rev. D*, vol. 102, no. 8, p. 085010, 2020.

[307] A. Azizi, H. E. Camblong, A. Chakraborty, C. R. Ordonez, and M. O. Scully, "Acceleration radiation of an atom freely falling into a Kerr black hole and near-horizon conformal quantum mechanics," *Phys. Rev. D*, vol. 104, no. 6, p. 065006, 2021.

[308] Y. Wang, C. Sheng, Y.-H. Lu, J. Gao, Y.-J. Chang, X.-L. Pang, T.-H. Yang, S.-N. Zhu, H. Liu, and X.-M. Jin, "Quantum simulation of particle pair creation near the event horizon," *National Science Review*, vol. 7, pp. 1476–1484, 05 2020.

[309] M. Blau, "Lecture notes on general relativity," 2022.

[310] B. R. Majhi and T. Padmanabhan, "Noether current from the surface term of gravitational action, Virasoro algebra and horizon entropy," *Phys. Rev. D*, vol. 86, p. 101501, 2012.

[311] B. R. Majhi, "Noether current of the surface term of Einstein-Hilbert action, Virasoro algebra and entropy," *Adv. High Energy Phys.*, vol. 2013, p. 386342, 2013.

[312] B. R. Majhi, "Noncommutativity in near horizon symmetries in gravity," *Phys. Rev. D*, vol. 95, no. 4, p. 044020, 2017.

[313] M. Parikh, S. Sarkar, and A. Svesko, "Local first law of gravity," *Phys. Rev. D*, vol. 101, no. 10, p. 104043, 2020.

[314] T. Padmanabhan, "A Dialogue on the Nature of Gravity," in *Foundations of Space and Time: Reflections on Quantum Gravity*, pp. 8–49, 10 2009.

[315] T. Jacobson, "Thermodynamics of space-time: The Einstein equation of state," *Phys. Rev. Lett.*, vol. 75, pp. 1260–1263, 1995.

[316] D. Kothawala, S. Sarkar, and T. Padmanabhan, "Einstein's equations as a thermodynamic identity: The Cases of stationary axisymmetric horizons and evolving spherically symmetric horizons," *Phys. Lett. B*, vol. 652, pp. 338–342, 2007.

[317] A. Paranjape, S. Sarkar, and T. Padmanabhan, "Thermodynamic route to field equations in Lancos-Lovelock gravity," *Phys. Rev. D*, vol. 74, p. 104015, 2006.

[318] R.-G. Cai, L.-M. Cao, Y.-P. Hu, and S. P. Kim, "Generalized Vaidya Spacetime in Lovelock Gravity and Thermodynamics on Apparent Horizon," *Phys. Rev. D*, vol. 78, p. 124012, 2008.

[319] D. Kothawala and T. Padmanabhan, "Thermodynamic structure of Lanczos-Lovelock field equations from near-horizon symmetries," *Phys. Rev. D*, vol. 79, p. 104020, 2009.

[320] A. Mohd and S. Sarkar, "Thermodynamics of Local Causal Horizons," *Phys. Rev. D*, vol. 88, no. 2, p. 024026, 2013.

[321] K. Parattu, B. R. Majhi, and T. Padmanabhan, "Structure of the gravitational action and its relation with horizon thermodynamics and emergent gravity paradigm," *Phys. Rev. D*, vol. 87, no. 12, p. 124011, 2013.

[322] S. Chakraborty, K. Parattu, and T. Padmanabhan, "Gravitational field equations near an arbitrary null surface expressed as a thermodynamic identity," *JHEP*, vol. 10, p. 097, 2015.

[323] S. Chakraborty and T. Padmanabhan, "Thermodynamical interpretation of the geometrical variables associated with null surfaces," *Phys. Rev. D*, vol. 92, no. 10, p. 104011, 2015.

[324] S. Dey and B. R. Majhi, "Covariant approach to the thermodynamic structure of a generic null surface," *Phys. Rev. D*, vol. 102, no. 12, p. 124044, 2020.

[325] S. Chakraborty, S. Bhattacharya, and T. Padmanabhan, "Entropy of a generic null surface from its associated Virasoro algebra," *Phys. Lett. B*, vol. 763, pp. 347–351, 2016.

[326] K. Bhattacharya and B. R. Majhi, "Noncommutative Heisenberg algebra in the neighbourhood of a generic null surface," *Nucl. Phys. B*, vol. 934, pp. 557–577, 2018.

[327] H. Adami, M. M. Sheikh-Jabbari, V. Taghiloo, and H. Yavartanoo, "Null surface thermodynamics," *Phys. Rev. D*, vol. 105, no. 6, p. 066004, 2022.

[328] S. Chakraborty, "Lanczos-Lovelock gravity from a thermodynamic perspective," *JHEP*, vol. 08, p. 029, 2015.

[329] S. Dey, K. Bhattacharya, and B. R. Majhi, "Thermodynamic structure of a generic null surface and the zeroth law in scalar-tensor theory," *Phys. Rev. D*, vol. 104, no. 12, p. 124038, 2021.

[330] V. Moncrief and J. Isenberg, "Symmetries of cosmological Cauchy horizons," *Commun. Math. Phys.*, vol. 89, no. 3, pp. 387–413, 1983.

[331] S. Hollands, A. Ishibashi, and R. M. Wald, "A Higher dimensional stationary rotating black hole must be axisymmetric," *Commun. Math. Phys.*, vol. 271, pp. 699–722, 2007.

[332] E. M. Morales, "On a second law of black hole mechanics in a higher derivative theory of gravity," 2008.

[333] K. Parattu, S. Chakraborty, B. R. Majhi, and T. Padmanabhan, "A Boundary Term for the Gravitational Action with Null Boundaries," *Gen. Rel. Grav.*, vol. 48, no. 7, p. 94, 2016.

[334] M. Razavy, *Quantum theory of tunneling*.
World Scientific, 2013.

[335] J. Casas-Vazquez and D. Jou, "Temperature in non-equilibrium states: a review of open problems and current proposals," *Rep. Prog. Phys.*, vol. 66, 2003.

[336] A. Cárdenas-Avendaño, A. F. Gutierrez, L. A. Pachón, and N. Yunes, "The exact dynamical Chern–Simons metric for a spinning black hole possesses a fourth constant of motion: A dynamical-systems-based conjecture," *Class. Quant. Grav.*, vol. 35, no. 16, p. 165010, 2018.

[337] A. Deich, A. Cárdenas-Avendaño, and N. Yunes, "Chaos in quadratic gravity," *Phys. Rev. D*, vol. 106, no. 2, p. 024040, 2022.

[338] J. M. Deutsch, "Quantum statistical mechanics in a closed system," *Phys. Rev. A*, vol. 43, pp. 2046–2049, Feb 1991.

[339] M. Rigol, V. Dunjko, and M. Olshanii, "Thermalization and its mechanism for generic isolated quantum systems," *Nature*, vol. 452, no. 7189, pp. 854–858, 2008.

[340] M. Rigol, "Breakdown of thermalization in finite one-dimensional systems," *Phys. Rev. Lett.*, vol. 103, p. 100403, Sep 2009.

[341] G. Biroli, C. Kollath, and A. M. Läuchli, "Effect of rare fluctuations on the thermalization of isolated quantum systems," *Phys. Rev. Lett.*, vol. 105, p. 250401, Dec 2010.

[342] R. Steinigeweg, J. Herbrych, and P. Prelovšek, "Eigenstate thermalization within isolated spin-chain systems," *Phys. Rev. E*, vol. 87, p. 012118, Jan 2013.

[343] R. Steinigeweg, A. Khodja, H. Niemeyer, C. Gogolin, and J. Gemmer, "Pushing the limits of the eigenstate thermalization hypothesis towards mesoscopic quantum systems," *Phys. Rev. Lett.*, vol. 112, p. 130403, Apr 2014.

[344] H. Kim, T. N. Ikeda, and D. A. Huse, "Testing whether all eigenstates obey the eigenstate thermalization hypothesis," *Phys. Rev. E*, vol. 90, p. 052105, Nov 2014.

[345] W. Beugeling, R. Moessner, and M. Haque, "Finite-size scaling of eigenstate thermalization," *Phys. Rev. E*, vol. 89, p. 042112, Apr 2014.

[346] A. Khodja, R. Steinigeweg, and J. Gemmer, "Relevance of the eigenstate thermalization hypothesis for thermal relaxation," *Phys. Rev. E*, vol. 91, p. 012120, Jan 2015.

[347] L. D'Alessio, Y. Kafri, A. Polkovnikov, and M. Rigol, "From quantum chaos and eigenstate thermalization to statistical mechanics and thermodynamics," *Advances in Physics*, vol. 65, no. 3, pp. 239–362, 2016.

[348] J. R. Garrison and T. Grover, "Does a single eigenstate encode the full hamiltonian?," *Phys. Rev. X*, vol. 8, p. 021026, Apr 2018.

[349] T. Yoshizawa, E. Iyoda, and T. Sagawa, "Numerical large deviation analysis of the eigenstate thermalization hypothesis," *Phys. Rev. Lett.*, vol. 120, p. 200604, May 2018.

[350] M. Srednicki, "The approach to thermal equilibrium in quantized chaotic systems," *Journal of Physics A: Mathematical and General*, vol. 32, no. 7, p. 1163, 1999.